Study of the termination factor like Dom34-Hbs1 complex : functional analysis of their roles in RNA quality control and in stimulating translation by dissociating inactive ribosomes

Antonia van den Elzen

UNIVERSITÉ DE STRASBOURG

ÉCOLE DOCTORALE DES SCIENCES DE LA VIE ET DE LA SANTÉ

Institut de Génétique et de Biologie Moléculaire et Cellulaire

THÈSE présentée par :

Antonia VAN DEN ELZEN

soutenue le : **13 septembre 2013**

pour obtenir le grade de : **Docteur de l'université de Strasbourg**

Discipline/ Spécialité : Aspects moléculaires et cellulaires de la biologie

Étude du complexe Dom34-Hbs1 ressemblant aux facteurs de terminaison: analyse fonctionnelle de ses rôles dans le contrôle qualité des ARN et dans la stimulation de la traduction par dissociation des ribosomes inactifs.

Study of the termination factor like Dom34-Hbs1 complex: functional analysis of their roles in RNA quality control and in stimulating translation by dissociating inactive ribosomes.

THÈSE dirigée par :

Dr. SERAPHIN Bertrand	Directeur de recherche, Université de Strasbourg

RAPPORTEURS :

Dr. MOUGIN Annie	Chargée de recherche, Université Paul Sabatier Toulouse III
Dr. LE HIR Hervé	Directeur de recherche, Ecole Normale Supérieure

---

AUTRES MEMBRES DU JURY :

Prof. Dr. Alan Hinnebusch	National Institutes of Health
Dr. Marat Yusupov	Directeur de recherche, Université de Strasbourg

ACKNOWLEDGEMENTS

I would like to start by thanking Bertrand, for giving me the opportunity to work in his lab. I very much enjoyed working with you and learning from you. As a relatively inexperienced master student, you gave me the possibility to work on a very exciting project with a lot of potential, which motivated me to stay for a PhD. Especially after the first year of my PhD, you gave me a lot of freedom in exploring different directions, which gave me the opportunity to learn a lot of different techniques and evolve my ability to pose interesting scientific questions and develop ways to address them. I thank you for your mentorship and for always being available for questions, discussions or for giving advice, at the same time letting me work in a relatively independent way, which for me was a great way to learn.

I am also very grateful to all members of the Seraphin lab, with whom I had the pleasure to work during my PhD. I had a great time working with you and I learned a lot from all of you.
Maria, we arrived at the same time, we'll leave at the same time. We shared a lot of good, but also bad times in and outside the lab. It was great to explore first Gif and Paris and then Strasbourg and the area around it with you, not to mention our Friday (or Saturday) night movies (or dinners, or other occasions..). I admire your hard work, your collegiality, your great kindness and your perseverance. Thank you for your friendship, your listening ear, your support and your advice. I hope you'll soon be able to continue your career in Spain.
I am very happy to have spent much of my time in the Seraphin lab in the presence of the incredible Vova, a personality once met, one will never forget. We shared many lunches and our appreciation of CROUS food. Thank you for many discussions about science and lab life, some of which were quite inspirational. But at least as important: thank you for your infectious laugh, sharing your incredible adventures (if ever published, I hope to receive a copy), anecdotes, your great company and your friendship. I admire your bright, quick and original mind and hope you'll have a great future in science.
Also with Delphine I shared several years in and outside the lab. In my first months, arriving as the only non-French speaking person in a French lab, your open and warm personality has helped me feel welcome and at ease, and encouraged me to start practicing my French. I very much enjoyed our biking trips (to Paris, to McDonalds, to the dechetterie..), our sing star and karaoke experiences, dancing on the tables German style..

Many thanks to Céline, managing the lab during almost my entire PhD with your great organizational skills, for protocols, for advice, for many delicious cakes and your cheerful and social presence.
Valerio, I enjoyed your very cheerful and open character, your sense of humour, and of course your great talent for cooking, the results of which we had the pleasure to taste both inside and outside the lab. I'm sure you'll do a great post doc and I wish you all the best for your future career.
Claudine, it has been a pleasure to work with a person friendly and funny as you are. Thank you for advice, and, especially in the beginning, sharing your knowledge about the complicated IGBMC organization with us.
Fabienne, it was a pleasure to have you as a colleague during all my time in the Séraphin lab. Thank you for advice and constructive remarks.
Olga, Natacha, I enjoyed working with you and admire how you combine your passion for scientific research with raising your young families.
I would also like to thank many other people with whom I shared some time in the lab. In Strasbourg: Benjamin (AKTA man), Ola, Santiago, Sandrea, Brigitte, Nicolas, Grégoire, Aurélie, Marine. And in Gif sur Yvette: Charlotte, Ysaline, Juliette, Sabine, Margot, Emilie, Alice, Marie-Claire, Jérôme, Manoël, François.

I would like the members of the jury Dr. Alan Hinnebusch, Dr. Marat Yusupov and especially the rapporteurs Dr. Annie Mougin and Dr. Hervé Le Hir, for reading my thesis, coming to my defense and for an interesting, challenging discussion.

I would also like to mention all the people I collaborated with. Thank you to Marc Graille and Julien Henri, who initiated the Dom34-Hbs1 project. I very much appreciate to have had the opportunity to join you on this project, even if when I started I was a relatively inexperienced master student. Thank you for your confidence, for everything that I learned about the structural side of our story, and for having me contribute to the functional side of it.
I am also grateful to Rachel Green, who welcomed me in her lab and contributed a lot to the writing of an exciting manuscript. A lot of thanks to Anthony Schuller, for your enthusiasm and hard work which turned my stay in the Green lab into a very productive period, and for all the work you did afterwards, the results of which were of great importance for my project. I am also grateful to you for your warm welcome and all your help in organizing my stay in the Green lab.

I would like to thank my family, especially my parents. I am very grateful for your constant support, even when I decided to rigorously change plans for my future career. Thanks to you I am now doing something that I am very passionate about. Your support has also made it relatively easy for me to decide on moving to another country, and yet another country even further away in the future, because I know that a geographical distance will never come between the close family that we are.

Finally I would like to thank Sergey. For all your support, in every possible way. For always believing in me, giving me pep talks when needed. For sharing your great scientific knowledge with me and inspiring me with your creativity, your original way of thinking, your motivation and your eagerness to learn. For teaching me never to limit myself by self-imposed boundaries. I thank you for all the adventures we shared in and around Strasbourg, and I am looking forward very much to the great adventure that lies ahead of us, and many more to come.

ABSTRACT

Translation is a cyclic process, consisting of four stages: initiation, elongation, termination and recycling. Recycling is important, as it ensures that ribosomal subunits become available for new rounds of translation. It is tightly coupled to termination: in eukaryotes termination factors eRF1 and eRF3 together with ATPase Rli1 induce peptide release and subsequent ribosome dissociation.If during translation elongation a ribosome stalls it will be unable to terminate and cannot be recycled via the canonical pathway.

The highly conserved factors Dom34 and Hbs1 form a complex structurally similar to the eRF1-eRF3 complex that, together with Rli1, dissociates eukaryotic ribosomes stalled on a messenger RNA (mRNA) as well as vacant ribosomes *in vitro*. Dom34 and Hbs1 are also known to function in RNA quality control pathways that target mRNAs (No-go decay or NGD) and ribosomal RNAs (Non-functional 18S rRNA decay or 18S NRD) that cause inefficient translation. NGD and 18S NRD share several characteristics, including the mechanism that triggers these pathways (ribosomal stalling) and the involvement of Dom34 and Hbs1. It has therefore been proposed that they may reflect one single pathway, in which ribosomal stalling induces ribosome dissociation and degradation of mRNA and rRNA.

In the first part of my PhD work I tried to obtain more insight into the functional requirements of Dom34 and Hbs1 for RNA quality control. In addition I studied how NGD and 18S NRD relate and what other factors play a role in these pathways. I performed, together with our collaborators, a structure-function analysis of the Dom34-Hbs1 complex in the yeast *Saccharomyces cerevisiae*. I found that the GTPase activity of Hbs1 is required for both NGD and 18S NRD. However, disruption of Dom34-Hbs1 interaction affected the complex's function in NGD but not in 18S NRD, showing that the role of Dom34-Hbs1 in the two pathways can be genetically separated. My results could suggest that mRNA and rRNA in a stalled translational complex may not always be simultaneously degraded upon ribosomal stalling. To further examine whether mRNAs that cause NGD may induce degradation of ribosomal RNA or protein, NGD substrates were translated *in vitro* in *S. cerevisiae* extract. No indications of ribosomal RNA or protein degradation were found. To identify factors other than Dom34 and Hbs1 that are involved in NGD and 18S NRD, I developed methods to specifically purify stalled ribosomes No new interacting partners could be identified.

The second part of my PhD work focused on identifying roles of Dom34-Hbs1 mediated ribosome dissociation beyond RNA quality control. This resulted in finding a role of Dom34-

Hbs1 and Rli1 dissociating inactive ribosomes that accumulate, due to a global inhibition of translation, during glucose starvation stress in *S. cerevisiae*. By making the ribosomal subunits of these inactive ribosomes available for initiation, the Dom34-Hbs1 complex stimulates restart of translation upon stress relief. Finally a combination of *in vitro* and *in vivo* data indicated that the role of Dom34-Hbs1 to make subunits available from inactive ribosomes is also required in non-stressed cells to allow optimal translation. These findings indicate that, upon ribosome recycling after translation termination, ribosomal subunits do not always immediately engage in a new round of translation. Instead they can form inactive ribosomes, that need to be dissociated by the Dom34-Hbs1 complex and Rli1 for their subunits to become available for translation. This could provide a new level of regulation of eukaryotic translation initiation.

RÉSUMÉ

L'expression des gènes eucaryotes est un processus complexe se déroulant en plusieurs étapes. Un transcrit primaire, produit dans le noyau par la transcription de l'ADN, est transformé en un ARN messager (ARNm) mature par une succession de modifications. Il s'agit notamment de l'ajout d'une structure de coiffe en 5', de l'épissage et de l'ajout d'une queue polyadénine (poly (A)) en 3'. Après export dans le cytoplasme, l'ARNm est généralement traduit en une protéine, avant d'être dégradé. La plupart de ces étapes sont soumises à des régulations, selon le type de cellule, le stade de développement et les conditions environnementales. Dans le cytoplasme, l'expression de la protéine est affectée par régulation de la traduction ainsi que par la dégradation de l'ARNm.

La dégradation de l'ARNm sert au moins deux fonctions. Tout d'abord, le métabolisme des ARNm «normaux» permet une régulation quantitative et contribue à la régulation de l'expression des gènes au niveau post-transcriptionnel. Deuxièmement, les voies de contrôle qualité des ARN détectent et éliminent les ARNm défectueux, ce qui empêche la production de protéines aberrantes et potentiellement dangereuses.

La traduction est effectuée par les ribosomes: de grands complexes composés d'ARN et de protéines assemblées sous la forme de deux sous-unités. La traduction est un processus cyclique qui se divise en quatre étapes. Dans la phase d'initiation, les ribosomes et d'autres facteurs nécessaires pour la traduction s'assemblent sur l'ARNm et se localisent sur le site d'initiation de la traduction (codon d'initiation). La régulation de la traduction se produit surtout au niveau de cette étape. Au cours de l'élongation, le ribosome produit une protéine en liant des acides aminés sous la forme d'un polypeptide. La séquence d'acides aminés est codée par la séquence des triplets de nucléotides (codons) présent dans l'ARNm. Les étapes de terminaison et le recyclage sont couplés étroitement. Quand le ribosome rencontre un codon stop, les facteurs de terminaison eRF1 et eRF3 sont recrutés. En collaboration avec l'ATPase Rli1, ils induisent la libération de la protéine alors complète et la dissociation subséquente du complexe traductionnel. Les sous-unités ribosomiques ainsi libérées deviennent disponibles pour des nouveaux cycles de traduction.

Si lors de la traduction, le ribosome pause à cause d'une structure secondaire, une séquence particulière, ou un défaut de l'ARNm, il ne pourra pas terminer la traduction et être recyclé par la voie classique. Un mécanisme de recyclage alternatif a évolué pour dissocier de tels complexes arrêtés. Les facteurs Dom34 et Hbs1, conservés chez les eucaryotes et, au moins

pour Dom34, chez les archées, forment un complexe structurellement similaire au complexe formé par les facteurs de terminaison eRF1 et eRF3. Des expériences biochimiques ont montré que Dom34 et Hbs1 s'insèrent dans le site A du ribosome (le même site auquel eRF1 et eRF3 se lient) et dissocient des ribosomes qui sont bloqués sur un ARNm, quel que soit le codon sur lequel le ribosome se trouve. En outre, Dom34 et Hbs1 dissocient des ribosomes qui ne sont pas liés à un ARNm. En dehors de la dissociation des ribosomes « pausés », Dom34 et Hbs1 sont impliqués dans des voies de contrôle qualité des ARN qui ciblent des ARNm et/ou des ARN ribosomiques (ARNr) engagés dans un complexe de traduction inefficace. Dans le No-go decay (NGD), un ARNm qui cause une pause traductionnelle lors de l'élongation est ciblé vers la dégradation. Ce processus est initié par un clivage endonucléolytique près du site de pause. L'accumulation des produits de clivage, visibles quand ils sont stabilisés artificiellement, dépend de Dom34 et Hbs1. Le Non-Functional 18S rRNA decay (18S NRD) cible les ARNr 18S fonctionnellement défectueux. Les ARNr 18S sont les ARNr qui composent une grande partie de la petite sous-unité ribosomique. Lorsque de tels ARNs défectueux sont présents dans des ribosomes conduisant à une traduction inefficace, ils sont éliminés et leurs dégradations dépendent de Dom34 et Hbs1. Le NGD et le 18S NRD partagent plusieurs caractéristiques, y compris le mécanisme qui initie ces processus (traduction inefficace), la participation des facteurs Dom34 et Hbs1 et leur localisation. Il a donc été proposé qu'ils pourraient représenter une voie unique, au cours de laquelle une pause traductionnelle induit la dissociation du ribosome, et la dégradation de l'ARNm et de l'ARNr.

Dans la première partie de mon travail de thèse, j'ai essayé de définir les caractéristiques fonctionnelles de Dom34 et Hbs1 requises pour le contrôle qualité des ARN. De plus, j'ai étudié la relation entre le NGD et le 18S NRD et j'ai essayé d'identifier des nouveaux facteurs qui jouent un rôle dans ces deux voies. J'ai réalisé, en collaboration avec une équipe de biologie structurale, une analyse structure-fonction du complexe Dom34-Hbs1 de la levure *Saccharomyces cerevisiae*. Basé sur un modèle structural obtenu par nos collaborateurs, j'ai construit des mutants qui bloquent liaison du GTP sur la GTPase Hbs1 ainsi que des mutants qui perturbent l'interaction entre Dom34 et Hbs1. En étudiant l'effet de ces mutations sur le NGD et le 18S NRD, j'ai observé que l'activité GTPase de Hbs1 est nécessaire pour le NGD et le 18S NRD. Cependant, la perturbation de l'interaction entre Dom34 et Hbs1 empêche la fonction du complexe dans le NGD mais pas dans le 18S NRD, montrant que les roles de Dom34-Hbs1 dans ces voies peuvent être séparés génétiquement. Mes résultats pourraient suggerer que l'ARNm et l'ARNr dans un complexe de traduction « pausé » ne sont pas

toujours dégradés simultanément. Afin de savoir si, lors du NGD, il y a dégradation de l'ARNr ou des protéines ribosomiques, des substrats ARNm qui causent le NGD ont été traduits dans un extrait cellulaire de *S. cerevisiae*. Aucune indication de dégradation des ARNr ou des protéines ribosomiques n'a été obtenue.

Pour identifier les facteurs autres que Dom34 et Hbs1 qui sont impliqués dans le NGD et le 18S NRD, j'ai essayé de purifier des ribosomes « pausés » pendant la traduction et les partenaires associés. J'ai mis au point une méthode pour la purification spécifique de ribosomes contenant un ARNr 18S défectueux. Cependant, aucun nouveau facteur associé à ces complexes n'a été identifié.

La deuxième partie de mon travail de thèse s'est concentrée sur le rôle de Dom34-Hbs1 dans la dissociation des ribosomes en dehors du contrôle de qualité des ARN. Ces expériences m'ont permis de mettre en évidence un role de Dom34 et Hbs1 dans la sortie de stress.

Beaucoup de conditions de stress provoquent un arrêt global de la traduction. Cela permet aux cellules d'utiliser économiquement des ressources limitées pour la production de protéines nécessaires pour s'adapter à l'état de stress. Lorsque le stress est terminé, la traduction redémarre rapidement. Ceci est possible car pendant le stress, les ribosomes inactifs sont stockés et peuvent être remobilisé rapidement. Au cours du stress resultant de la déplétion de glucose chez la levure, les ribosomes inactifs contiennent la protéine Stm1 dans une conformation qui maintient les deux sous-unités ribosomiques associées et empêche le recrutement d'un ARNm. Le redémarrage rapide de la traduction après l'arrêt du stress exige la dissociation des ribosomes inactifs pour rendre leurs sous-unités disponibles pour de nouveaux cycles d'initiation de la traduction.

Je me suis demandé si Dom34 et Hbs1 pouvaient être responsables de la dissociation des ribosomes inactifs, stimulant ainsi le redémarrage de la traduction. A cette fin, j'ai analysé le rôle du complexe Dom34-Hbs1 dans le redémarrage de la traduction après déplétion de glucose chez *S. cerevisiae*. J'ai observé qu'en absence de Dom34 ou Hbs1, la reprise de la traduction après réadition de glucose est beaucoup plus lente que dans les cellules sauvages. Mes résultats montrent aussi que les ribosomes inactifs qui s'accumulent pendant la déplétion de glucose sont des substrats de protéines Dom34, Hbs1 et Rli1 recombinantes in vitro. De plus, l'affaiblissement de l'interaction entre les sous-unités ribosomiques par la suppression de Stm1 réduit le besoin de Dom34 pour la reprise de la traduction. Cela confirme que la stimulation par Dom34-Hbs1 de la reprise de la traduction dépend de leur activité de dissociation de ribosomes inactifs. Alors que Dom34 et Hbs1, ainsi que l'activité GTPase de Hbs1, sont nécessaires pour le redémarrage efficace de la traduction, l'interaction entre

Dom34 et Hbs1 ne l'est pas. Ces exigences sont similaires à celles requises pour le 18S NRD. Finalement, j'ai trouvé que le rôle du complexe Dom34-Hbs1 dans la dissociation des ribosomes inactifs et la stimulation de la traduction ne se limite pas aux conditions de stress. En effet, dans les cellules en croissance, des ribosomes inactifs sont produits, quoiqu'à un niveau moindre que lors d'un stress. J'ai constaté que, en absence de Dom34, ces ribosomes inactifs s'accumulent dans les cellules en croissance. Aussi, le complexe Dom34-Hbs1 est capable de stimuler la traduction effectuée par des ribosomes qui n'ont pas été exposés au stress Ces résultats suggèrent que, lors du cycle de traduction, après la terminaison, il est possible que des sous-unités ribosomiques ne s'engagent pas immédiatement dans un nouveau cycle de traduction. Ces sous-unités peuvent former des ribosomes inactifs qui doivent être dissociée par le complexe Dom34-Hbs1, en présence de Rli1 pour les rendre disponibles pour de nouveaux cycles de traduction. Cela pourrait créer un nouveau niveau de régulation de l'initiation de la traduction.

TABLE OF CONTENTS

LIST OF FIGURES

LIST OF TABLES

LIST OF ABBREVIATIONS

18S NRD	Non-functional 18S ribosomal RNA decay
25S NRD	Non-functional 25S ribosomal RNA decay
3’ UTR	3’ untranslated region
5’ UTR	5’ untranslated region
CBP	Calmodulin binding protein
GFP	Green fluorescent protein
IRES	Internal ribosome entry site
ITAF	IRES transacting factor
Met-tRNA$_i$	Methionine bound initiator tRNA
mRNA	Messenger RNA
NGD	No-go decay
NRD	Non-functional ribosomal RNA decay
NS	Non-stop
NSD	Non-stop decay
ORF	Open reading frame
PAP	Peroxidase anti-peroxidase
PCI	Phenol:chloroform:isoamyl alcohol 25:24:1
PCR	Polymerase chain reaction
rRNA	Ribosomal RNA
RQC	Ribosome Quality Control complex
Rz	Ribozyme
SDS-PAGE	SDS polyacylamide gel
SL	Stem loop
TAP	Tandem affinity purification
tRNA	Transfer RNA
uORF	Upstream open reading frame

1. INTRODUCTION

1.1 EUKARYOTIC GENE EXPRESSION: LIFE AND DEATH OF A MESSENGER RNA

The central dogma of molecular biology resumes gene expression: DNA makes RNA makes protein. In eukaryotes this sequence of events is complicated by the fact that the transcription of a DNA sequence into an RNA sequence and the translation of RNA sequence into protein is spatially separated, the first occurring in the nucleus, the latter in the cytoplasm. Therefore the RNA needs to be exported from the nucleus into the cytoplasm before it can be translated. Apart from this, primary transcripts are extensively processed, before a mature messenger RNA (mRNA) is produced that can be translated.

Gene expression is heavily regulated, which gives cells the opportunity to vary their content and function according to cell type, developmental stage and environmental conditions. Regulation occurs at practically all stages of gene expression: at the level of transcription, processing and export of the resulting RNA as well as localization, translation and stability of the RNA and localization and activity of the protein.

This thesis focuses on the role of two protein factors in translation dependent detection and degradation of faulty RNAs and in regulation of translation, studied in the eukaryotic model system yeast (*Saccharomyces cerevisiae*). Therefore this first paragraph will, after a brief introduction of RNA production, processing and export, specifically focus on translation and RNA degradation in eukaryotes.

1.1.1 Transcription, processing and export

A gene can be defined as a DNA sequence that holds the information to produce a protein or a functional RNA. Transcription of a gene is mediated by RNA polymerases that incorporate nucleotides into an RNA molecule using a DNA strand as a template. RNA polymerases are recruited to the 5' end of a gene, the promoter region. This requires the assembly of various proteins, the general transcription factors, at the promoter. The promoter contains sequence elements that influence the rate of transcription of a gene, mostly by binding regulatory factors. The expression of a gene is also affected by regulatory sequence at a larger distance. Three different types of RNA polymerases each transcribe different classes of genes. mRNAs transcribed from protein encoding genes, are produced by RNA polymerase II.

Eukaryotic transcripts are extensively processed (Figure 1). Much of this processing occurs or initiates while transcription is still ongoing. A cap structure is added to the 5' end of transcripts produced by RNA polymerase II. This cap consists of a guanine nucleotide that is

linked to the 5'end of the transcript via a 5' to 5' tri-phosphate linkage. The cap protects the mRNA from degradation and is important for translation (see paragraph 1.1.2.2). The protein coding sequence on DNA, and therefore also on a primary transcript, is interrupted by stretches of non-coding sequence, called introns. These are removed during by a large, dynamic assembly of RNA and proteins in a process called splicing. The use of splice sites can be regulated, which results in the potential to produce multiple, different mRNAs from a single gene. At their 3' end mRNAs are polyadenylated. The site of polyadenylation is determined by the recognition of a specific sequence, that recruits protein factors responsible for cleavage of the RNA and subsequent addition of the poly(A) tail.

During transcription and processing the mRNA associates with a variety of proteins. Some of these proteins serve as signals needed for active export of the mRNA through the nuclear pore complex, a large multi-protein structure that forms a channel through the nuclear envelope. Once the mRNA is exported into the cytoplasm, it may be transported to a certain cellular location and it can be translated (Alberts et al, 2008).

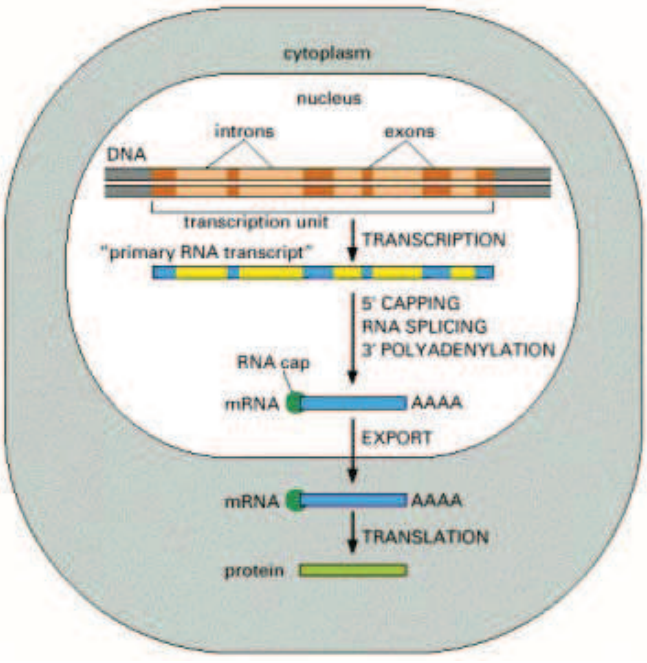

(Alberts et al, 2008)

Figure 1 Transcription and mRNA processing in eukaryotic cells.

1.1.2 Translation

The nucleotide sequence of a mRNA is translated into a chain of amino acids, called a polypeptide, that will eventually fold into a protein. Translation is mediated by large, highly

conserved complexes, the ribosomes, that operate in a four stage cyclic process (Figure 2). During translation initiation a ribosome assembles on a mRNA to form a functional ribosome. In the elongation stage the ribosome mediates incorporation of amino acids into a growing polypeptide chain, according to the nucleotide sequence of the mRNA. During the termination phase, the now completed polypeptide is released. In the ensuing recycling phase the post-termination ribosome is released from the mRNA, making it available for new rounds of translation. In the following paragraphs the actors and stages of the translation cycle will be described in more detail.

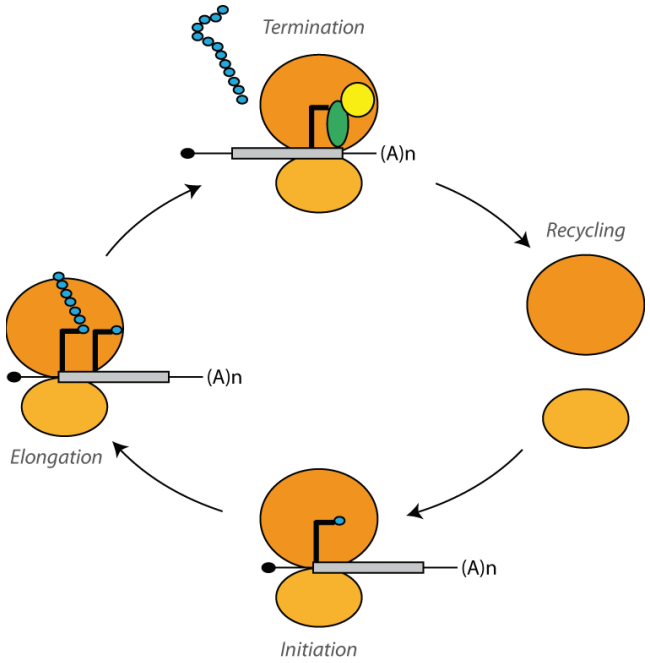

Figure 2 Translation is a cyclic, four stage process.

1.1.2.1 The principle actors in translation

1.1.2.1.1 The messenger RNA

After export from the nucleus into the cytoplasm a mRNA can be translated. The amino acid sequence of the peptide to be produced derives from the mRNA nucleotide sequence. Each group of three consecutive nucleotides, which is called a codon, corresponds to a specific amino acid (see the genetic code in Figure 3). Translation starts at a start codon, which always consists of an AUG triplet, encoding the amino acid methionine. The codons downstream of the start codon then dictate the order of the following amino acids to be incorporated in the

growing polypeptide. The polypeptide is completed when one out of three stop codons (UAA, UAG or UGA) is encountered.

(Alberts et al, 2008)

Figure 3 The genetic code.
Each nucleotide triplet, or codon, encodes an amino acid.

The sequence between a start codon and the first stop codon found within the same reading frame is called an open reading frame (ORF). The non-coding sequences up- and downstream of an ORF, present in the mRNA, are called 5' and 3' untranslated regions (UTR) (Figure 4A). mRNAs can circularize through interaction of cap-associated proteins with the poly(A) binding protein, called Pab1 in yeast (Alberts et al, 2008) (Figure 4B).

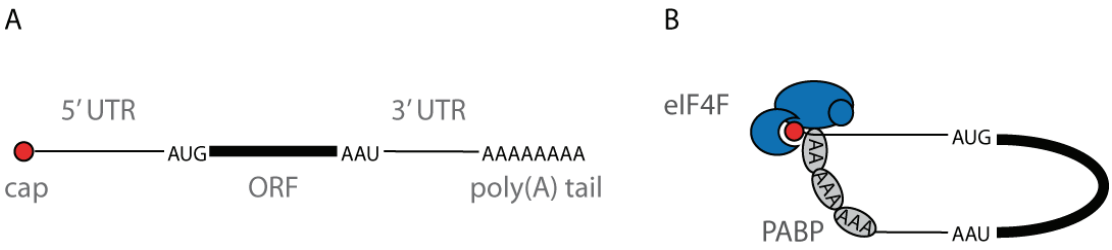

Figure 4 Messenger RNA.
A: Open reading frame (ORF) and untranslated regions (UTR) in a mRNA.
B: mRNA circularization through the interaction of cap-binding proteins with the poly(A) binding protein Pab1.

1.1.2.1.2 The transfer RNA

Translation of a mRNA nucleotide sequence into a amino acid sequence requires adapter molecules: the transfer RNAs (tRNA). This adapter function is mediated by two functional sites of the tRNA. First, it contains an anticodon loop that basepairs specifically with a codon on the mRNA. Second, it can be charged with a specific amino acid, according to the identity of the anticodon loop and other features. Sequence complementarity between various regions in the tRNA molecule results in a cloverleaf-like arrangement, when drawn in 2D. In 3D the tRNA molecule adopts an L-shaped structure (Alberts et al, 2008) (Figure 5).

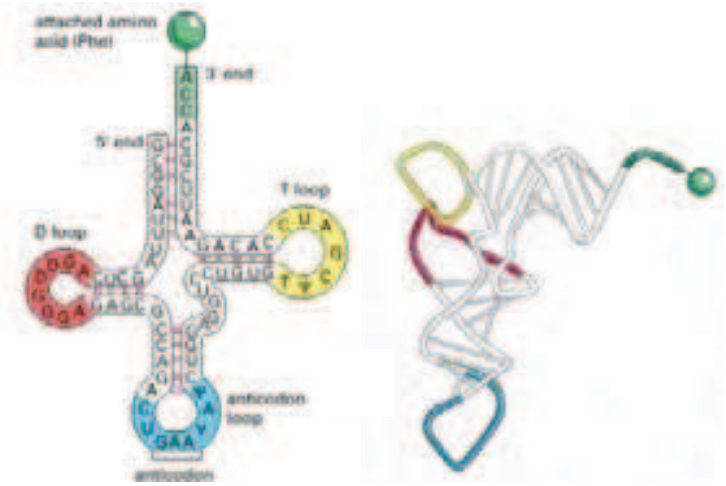

(Alberts et al, 2008)

Figure 5 Transfer RNA.
2D (left) and 3D (right) structure an aminoacyl-tRNA molecule.

1.1.2.1.3 The ribosome

The translation of a mRNA into an amino acid sequence is catalyzed by ribosomes. These are large RNA protein complexes, varying in size from 2.3 MDa in bacteria to 4.3 MDa in higher eukaryotes (Figure 6). Ribosomes consist of a small and a large subunit, which are often named after their sedimentation rate (in bacteria: 30S and 50S subunit, in eukaryotes: 40S and 60S subunit respectively). Together the subunits form the 70S (in bacteria) or 80S (in eukaryotes) ribosome (Alberts et al, 2008). Each subunit contains ribosomal RNA (rRNA) in complex with an array of ribosomal proteins. In the bacterial small ribosomal subunit a 16S rRNA is complexed with 21 proteins. In yeast or higher eukaryotes an 18S rRNA is complexed with 33 proteins. The bacterial large ribosomal subunit is composed of a 23S and a 5S rRNA and 33 proteins. In yeast the large ribosomal subunit contains a 25S, a 5S and a 5.8S complexed with 46 proteins, whereas higher eukaryotes contain a 28S, a 5S and a 5.8S rRNA and 47 proteins (Melnikov et al, 2012).

The core of the ribosome is, both in structure and function, highly conserved between all three domains of life. Since the early 2000s high resolution X-ray structures of bacterial and archaeal ribosomes have contributed immensely to our functional understanding of ribosomes from all domains of life (Schmeing & Ramakrishnan, 2009). In recent years X-ray structures of eukaryotic ribosomes have become available (Ben-Shem et al, 2011; Ben-Shem et al, 2010; Rabl et al), shedding light on the function related structural differences between ribosomes from different domains, including the eukaryote-specific expansions that cause eukaryotic ribosomes to be significantly larger in size (Melnikov et al, 2012).

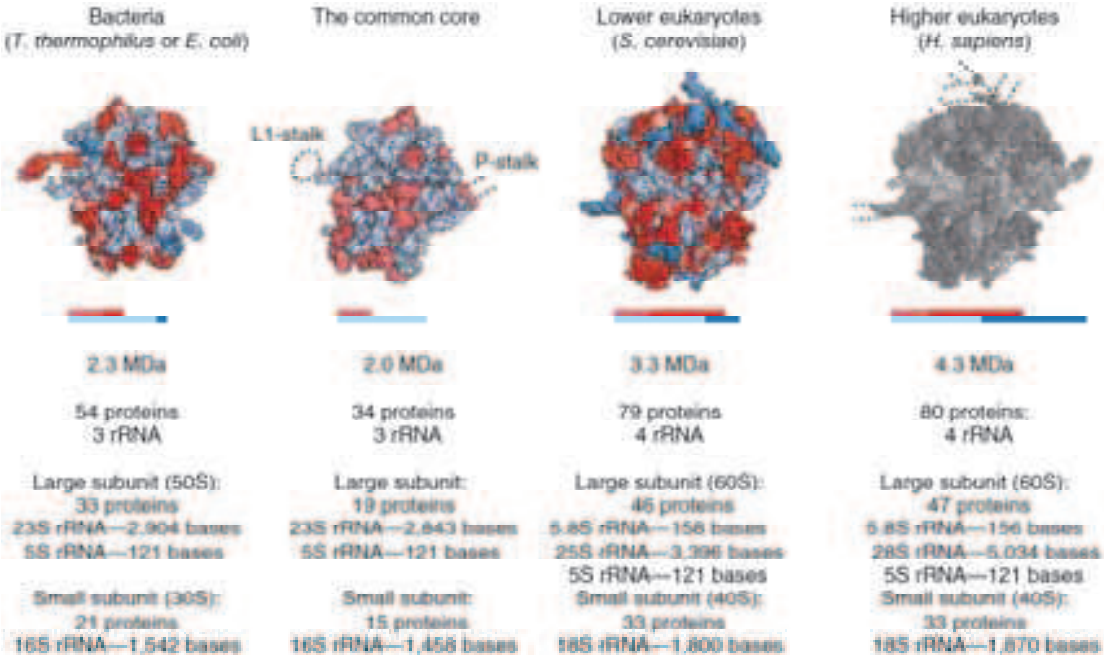

(Melnikov et al, 2012)

Figure 6 Bacterial and eukaryotic ribosomes

Composition of bacterial (*E. coli*) and eukaryotic (*S. cerevisae* and *H. sapiens*) ribosomes, as well as their conserved core. Ribosomal RNA is indicated in blue, ribosomal proteins in red. RNA and protein conserved in all domains of life is indicated in light blue and light red respectively.

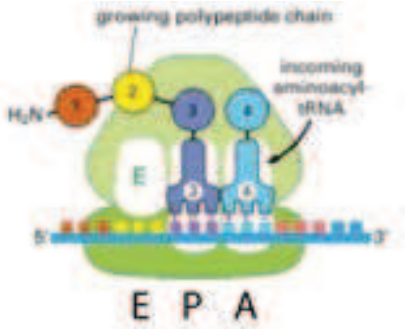

Figure 7 tRNA binding sites in the ribosome. An aminoacyl-tRNA binds to the A-site, the P-site contains a peptidyl-tRNA and in the E-site a deaminoacylated tRNA leaves the ribosome.

(Alberts et al, 2008)

A translating ribosome is bound to a mRNA that threads through the 40S ribosomal subunit. The ribosome contains three binding sites for tRNAs : the A, P and E site (Figure 7). The tRNAs binding to these adjacent sites basepair with adjacent codons. The A-site (aminoacyl site) binds incoming aminoacyl-tRNAs. If their anticodons pair correctly with the A-site codon, the amino acid will be incorporated into the growing peptide chain. The P-site

(peptidyl site) contains the growing peptide chain associated to a tRNA. The E-site (exit site) is the site where a tRNA leaves the ribosome (Alberts et al, 2008).

Two important functional sites are the decoding center in the small ribosomal subunit and the peptidyl transferase center in the large ribosomal subunit. The decoding center monitors correct codon and anti-codon base pairing in the ribosomal A-site. The highly conserved nucleotides G530, A1492 and A1493 (E. coli numbering) of the 16S rRNA are important. They interact directly with the codon-anticodon duplex in the A-site and form a static part of the decoding center, defining its spatial and stereo chemical properties. By forcing mismatching codon-anticodon duplexes into a specific, energetically unfavourable geometry, this is thought to cause their dissociation of the mismatching tRNA from the ribosome (Demeshkina et al, 2012; Ogle et al, 2001).

The peptidyl transferase center catalyzes the formation of a covalent peptide bond between the peptide in the P-site and the amino acid in the A-site. No ionizing groups of the ribosome have been found to directly take part in this reaction. The center catalyzes the reaction by providing a network of interactions, thereby precisely orienting the two reactants, changing the transition state and lowering the activation entropy of the reaction (Alberts et al, 2008; Rodnina).

1.1.2.2 Initiation

All of the steps in eukaryotic translation initiation described below are depicted in Figure 8. Eukaryotic translation initiation starts with the formation of a 43S pre-initiation complex (PIC). The methionine bound initiator tRNA (Met-tRNA$_i$), the anticodon of which is complementary to the AUG start codon, forms a complex with GTP-bound initiation factor eIF2, to form a ternary complex (TC) (1). The ternary complex binds to the P-site of a 40S ribosomal subunit, which is complexed with initiation factors eIF1, eIF1A, eIF3, to form the 43S PIC that also contains eIF5 (2). eIF1, eIF1A, eIF3 and eIF5 all contribute to efficient binding of the ternary complex to the 40S subunit. Binding of eIF1 and eIF1A to the 40S subunit induce an “open” conformation, which may facilitate ternary complex binding

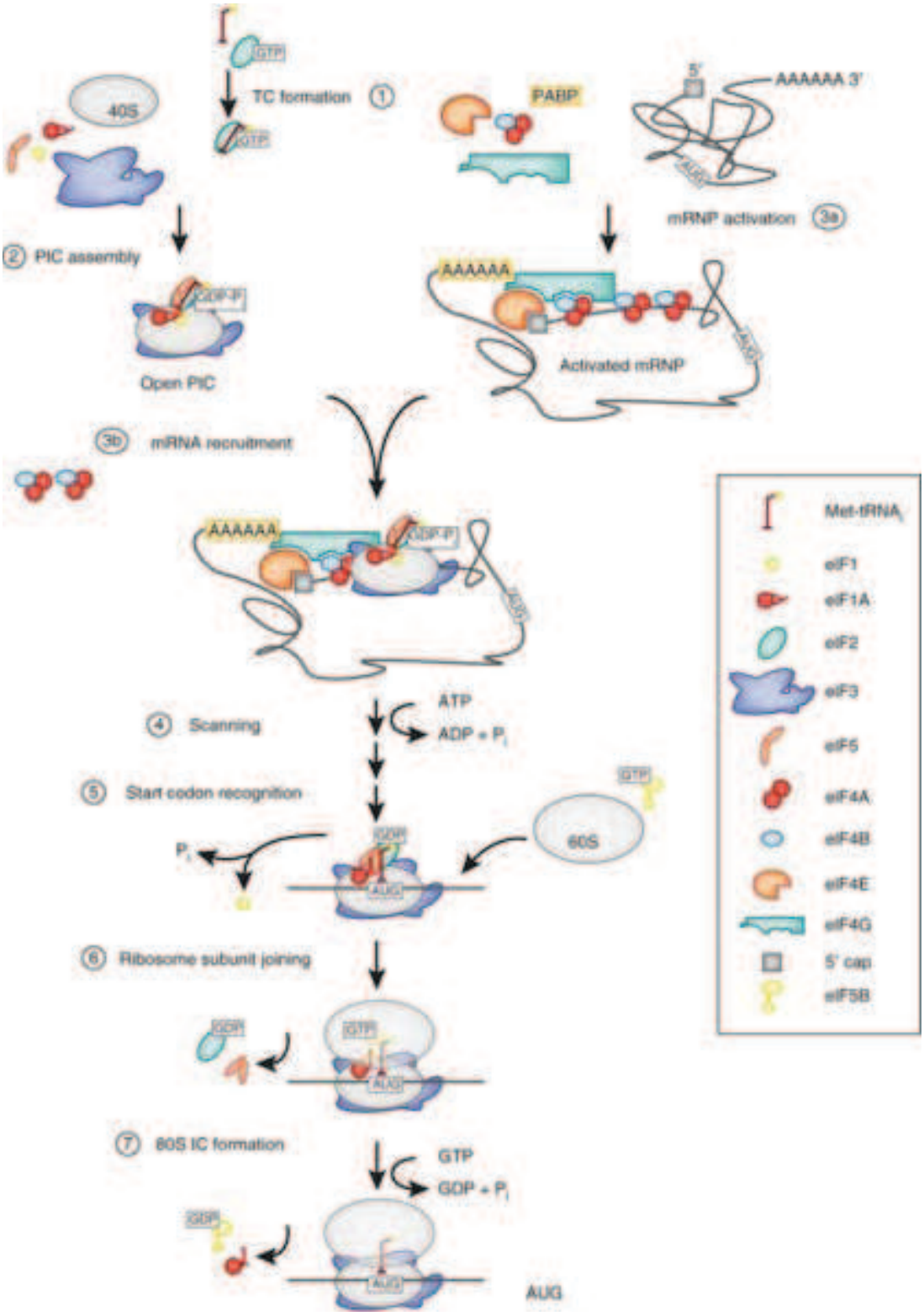

(Aitken & Lorsch, 2012)

Figure 8 Eukaryotic translation initiation
For further details see text

(Aitken & Lorsch, 2012; Hinnebusch & Lorsch, 2012; Jackson et al, 2010). eIFs 1, 3, 5 and the ternary complex can also form a multifactor complex in absence of the ribosome (Asano et al, 2000), which opens the possibility that they can be recruited to the 40S subunit as one complex.

The 43S PIC is recruited to the 5'end of a mRNA (3b). This is facilitated by additional initiation factors bound to the 5' end of the mRNA and the poly(A) tail bound factor Pab1 (3a). At the 5' end of the mRNA an eIF4F complex is bound. This consists of the cap-binding factor eIF4E, eIF4G that acts as a scaffold and the helicase eIF4A. Stimulated by eIF4G and one of the homologous factors eIF4B or eIF4H, eIF4A unwinds the often structured 5' UTR of the mRNA. eIF4G also binds the poly(A) tail associated Pab1, thereby circularizing the mRNA, which may couple termination events to subsequent initiation on the same mRNA. For recruitment of the 43S PIC to the mRNA eIF3 appears to play an important stimulatory role. In higher eukaryotes it may do so by interacting with eIF4G. However, in yeast these two factors do not interact directly. eIF5 and eIF4B may also play a role in 43S recruitment to the mRNA. The 43S complex then starts scanning the 5'UTR (4), unwound by eIF4A, until it encounters the start codon. Other helicases, such as the essential Ded1 helicase in yeast and Dhx29 in mammals, were also found to be important for enabling scanning through structured 5' UTRs. The eIF1 and eIF1A induced open conformation is essential for scanning and start codon localization.

eIF1 functions as a gate keeper in start codon recognition. It is ejected from the scanning 43S complex upon the encounter of an AUG codon, which subsequently triggers the release of the inorganic phosphate that results from GTP hydrolysis by eIF2, and closing of the PIC. This results in a 48S complex (5). The ejection of eIF1 may be the consequence of the formation of a codon-anticodon helix between $tRNA_i$ and mRNA, which is sterically incompatible with eIF1 binding (Rabl et al, 2011). eIF1 release is stimulated by eIF5. After AUG recognition and the resulting conformational changes, GDP bound eIF2 and eIF5 dissociate. Then the 60S subunit joins, which is facilitated by the GTPase eIF5B (6). Subunit joining causes GTP hydrolysis by eIF5B, which leads to conformational changes in the 80S complex and the dissociation of eIF5B. Finally eIF1A is the last initiation factor to dissociate before translation elongation can start (7) (Aitken & Lorsch, 2012; Hinnebusch & Lorsch, 2012; Jackson et al, 2010).

The ribosome then starts translating the sequence of codons downstream the start codons. Once a ribosome has moved away from the start codon, a new ribosome can initiate. This

results in one mRNA being translated by multiple ribosomes simultaneously. Together they form a polysome.

1.1.2.2.1 Cap-independent translation initiation

In several conditions, such as viral infection and stress, cap-dependent initiation is down regulated. Cap-independent pathways circumvent this down-regulation by using internal ribosome entry sites (IRES) in the 5'UTR. These IRES were first described in viral mRNAs. Several endogenous, eukaryotic mRNAs have since been identified to be capable of initiating translation by both cap-dependent and IRES dependent mechanisms. Viral IRESs are grouped into different types, depending on initiation factor requirements, the need for additional factors (IRES transacting factors or ITAFs) and whether the ribosome is recruited directly to the translation start site or not (Thompson, 2012). Further details for all categories are described in Figure 9.

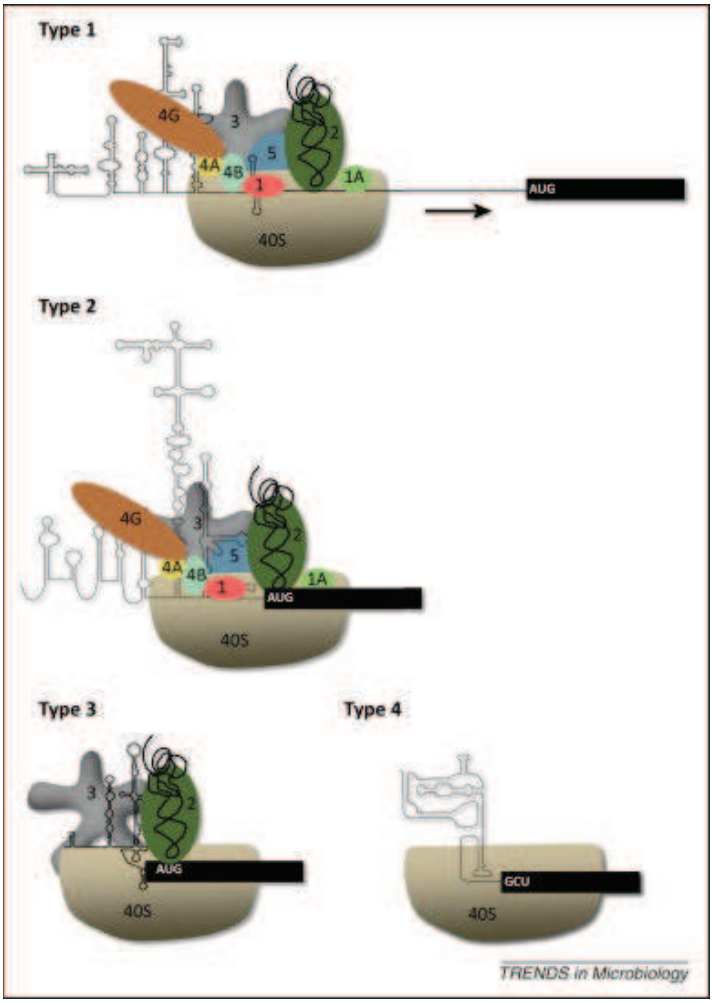

Figure 9 Classificiation of internal ribosomal entry sites
Type 1 and 2 IRESs recruit 43S PICs using eIF4G, eIF4A and eIF4B. Type 1 IRESs require additional ITAFs, and the 43S complex scans the mRNA from the IRES in 3' direction until it encounters a start codon. Type 3 IRESs can bind to a 40S subunit without additional factors. To bind Met-tRNAi eIF3 and eIF2 or a functional analog (ligatin, eIF2A) are needed. At type 2 and 3 IRESs 40S subunits initiate directly at the site to which they are recruited. Type 4 IRESs do not require any initiation factors. 40S subunits initiate directly at the site to which they are recruited, on a non-AUG codon positioned in the A-site. Therefore the initiator Met-tRNAi is not required.

(Thompson, 2012)

1.1.2.3 Elongation

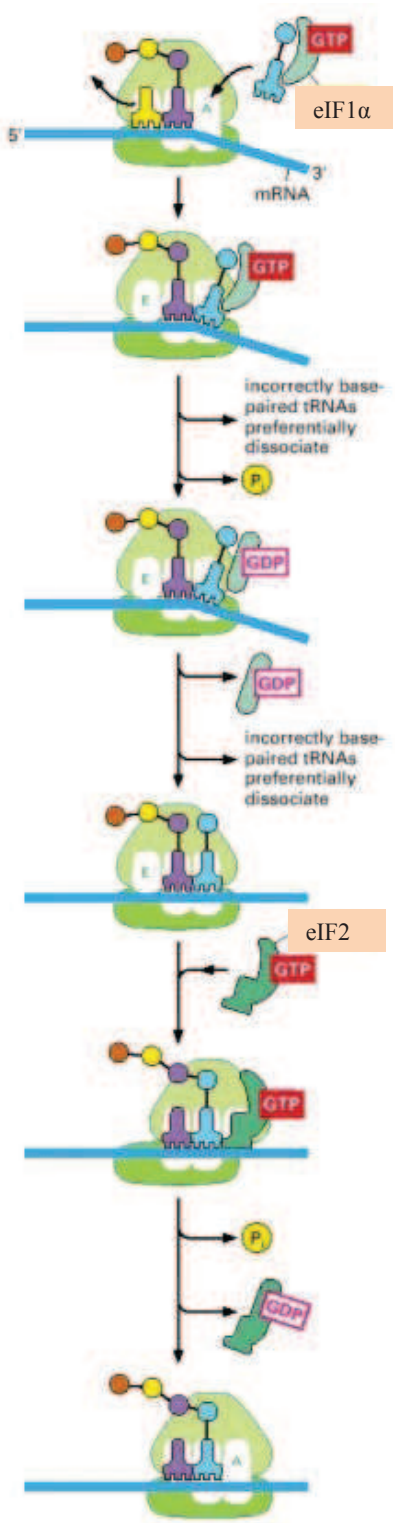

(Alberts et al., 2008)

Figure 10 Translation elongation

Following canonical translation initiation, an 80S ribosome is positioned over the start codon, with the Met-tRNA$_i$ bound in its P-site. Now an aminoacyl-tRNA can bind, that matches the codon present in the A-site. The aminoacyl-tRNA is escorted by the GTP bound elongation factor eIF1α. Correct basepairing between the codon and the anticodon is monitored during several proofreading steps and involves GTP hydrolysis. Correct basepairing results in accommodation of the amino acid bound end of the tRNA in the PTC of the 60S subunit. The PTC then catalyzes the transfer of the amino acid (or in later cycles, the peptide) from the P-site tRNA onto the amino acid bound to the A-site tRNA. This results in a now one amino acid longer peptidyl-tRNA in the A-site.

Then a translocation takes place. This starts with the translocation of the large subunit, leaving the tRNAs in a so-called hybrid state. Whereas the deaminoacylated tRNA and the newly formed peptidyl tRNA are still in P and A-site position on the small subunit, they are now in E and P-site position in the large ribosomal subunit respectively. Subsequently, the small subunit translocates as well, moving three nucleotide (one codon) positions on the mRNA. This results in the deaminoacylated tRNA and the peptidyl tRNA ending up fully in E and P-site respectively. The E-site tRNA can then leave the ribosome. Translocation is highly stimulated by GTP hydrolysis by elongation factor eEF2. After translocation the A-site is vacant, a new aminoacyl-tRNA complementary to the new A-site codon can bind. The described process is repeated for all codons downstream the start codon, elongating the

peptide in production, until the ribosome reaches a stop codon.

1.1.2.4 Termination

Termination occurs when a stop codon enters the ribosomal A-site. Stop codon recognition by termination factors results in the hydrolysis of the ester bond between the P-site tRNA and the now completed polypeptide, the latter being released. There are three stop codons (UAA, UAG and UGA). A single termination factor, eRF1, recognizes all three of them (Ito et al, 2002; Kervestin et al, 2001) and induces peptidyl-tRNA hydrolysis by the ribosomal peptidyl transferase center. Although eRF1 can induce peptidyl-tRNA hydrolysis by itself, it acts quite inefficiently. The GTPase eRF3 greatly stimulates eRF1 mediated peptide release, in a GTP dependent manner (Alkalaeva et al, 2006).

eRF1 is composed of three domains and structurally resembles a tRNA molecule (Song et al, 2000). It interacts with stop codons in the ribosomal A-site through its N-terminal domain. Various biochemical and *in vivo* studies together with bioinformatical analysis (e.g. Chavatte et al, 2002; Frolova et al, 2002; Liang et al, 2005; Seit-Nebi et al, 2002) have implicated several (groups of) conserved residues, among which the NIKS motif, in stop codon recognition. The central domain contains a highly conserved GGQ motif that is essential for triggering peptidyl-tRNA hydrolysis (Frolova et al, 1999; Song et al, 2000). Based on homologous bacterial processes, the GGQ motif is thought to locate in the peptidyl transferase center. This positioning causes rRNA rearrangements, making the ester bond of the peptidyl-tRNA accessible for nucleophylic attack by a water molecule (Jin et al, 2010).

eRF3 belongs to the same family of GTPase as eEF1α (Atkinson et al, 2008). Members of this family are highly similar with regard to their C-terminal domains (GTPase or G domain, domains II and III) , but differ in their N-terminal length and amino acid sequence (Inagaki & Ford Doolittle, 2000). eRF3 by itself has weak GTPase activity, which is greatly stimulated by the combined presence of eRF1 and the ribosome (Frolova et al, 1996).

eRF1 and eRF3 stably interact mainly through their C-terminal domains (Cheng et al, 2009; Ebihara & Nakamura, 1999; Ito et al, 1998; Merkulova et al, 1999). Structural and biochemical data suggest additional interactions between the central domain of eRF1 and domains G, II and III of eRF3 (Cheng et al, 2009; Kononenko et al, 2008). Especially the interaction of eRF1 with the G domain of eRF3 may explain how eRF1 stimulates GTP binding (Hauryliuk et al, 2006; Mitkevich et al, 2006; Pisareva et al, 2006) and hydrolysis by eRF3. In yeast GTP binding is required for stable eRF1-eRF3 interaction (Kobayashi et al, 2004).

Translation termination and subsequent recycling of the post-termination complex are tightly coupled. The key factor in ribosome recycling, the ATPase Rli1 (see next paragraph), was found to stimulate eRF1-eRF3 mediated peptide release four-fold, in a manner independent of its ATPase activity (Shoemaker & Green, 2011).

The information above in combination with additional findings have led to a model of eukaryotic translation termination, which is depicted in Figure 11. It starts with the eRF1-eRF3-GTP complex binding the stop-codon containing A-site of a ribosome (1). In its GTP bound form the complex adopts a conformation in which the GGQ motif of eRF1 is far away from the peptidyl transferase center (Taylor et al, 2012). Upon stop codon recognition by eRF1 the eRF3 bound GTP will be hydrolyzed (2). In its GDP bound form eRF3 will dissociate from the ribosome (3). ATP bound Rli1 will then bind at a site overlapping the one recognized by eRF3 (Becker et al, 2012). As a consequence of the last three processes, eRF1 will accommodate, positioning its GGQ motif in the peptidyl transferase center (4). This leads to peptidyl-tRNA hydrolysis and the peptide being released from the ribosome (5). Rli1 binding may stimulate peptide release by accelerating eRF1 accommodation (Shoemaker & Green, 2011), perhaps by facilitating eRF3 dissociation.

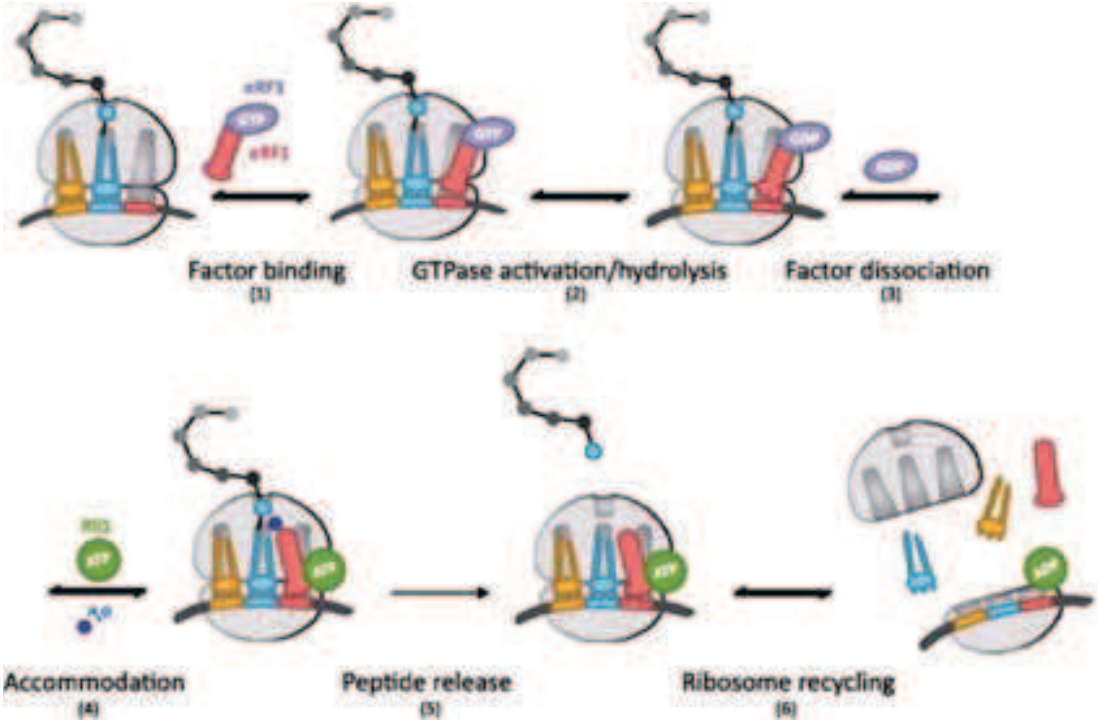

(Shoemaker & Green, 2011)

Figure 11 Eukaryotic translation termination and recycling.
Steps 1 to 6 are discussed in the text.

1.1.2.5 Recycling

After peptide release, a post-termination complex containing a ribosome, mRNA, P-site tRNA, eRF1 and probably Rli1 needs to be dissociated to make its components available for new rounds of translation. Biochemical experiments have shown that Rli1, also known as ABCE1 in some organisms, mediates recycling of human, yeast and archaeal ribosomal subunits after translation termination (Barthelme et al, 2011; Pisarev et al, 2010; Shoemaker & Green, 2011) (step 6 in Figure 11). For convenience, this factor will from here on be referred to as Rli1.

Susceptibility of post-termination complexes for Rli1 induced ribosome recycling does not depend on peptide release, but appears to require the presence of eRF1 (or a paralog, see paragraph 1.3.3) in the ribosomal A-site. Following puromycin caused peptide release the human Rli1 homolog cannot induce ribosome recycling. However, in presence of a catalytically inactive eRF1 mutant Rli1 mediated ribosomal subunit dissociation does occur (Pisarev et al, 2010). Consistently, archaeal Rli1 recycles post-termination complexes cooperatively with the archaeal eRF1 ortholog aRF1 (Barthelme et al, 2011). The affinity of Rli1 for the post-termination complex increases greatly in presence of a non-hydrolysable ATP analog, indicating that it binds in complex with an ATP molecule (Pisarev et al, 2010).

Rli1 is an ABC (ATPase binding cassette) family ATPase, that is highly conserved in eukaryotes and archaea (Figure 12). Like in other members of its family, two nucleotide binding domains in a head to tail orientation create two composite nucleotide binding sites. Rli1 also contains a highly conserved iron-sulfur cluster domain containing two $[4Fe\text{-}4S]^{2+}$ clusters (Barthelme et al, 2007; Karcher et al, 2008).

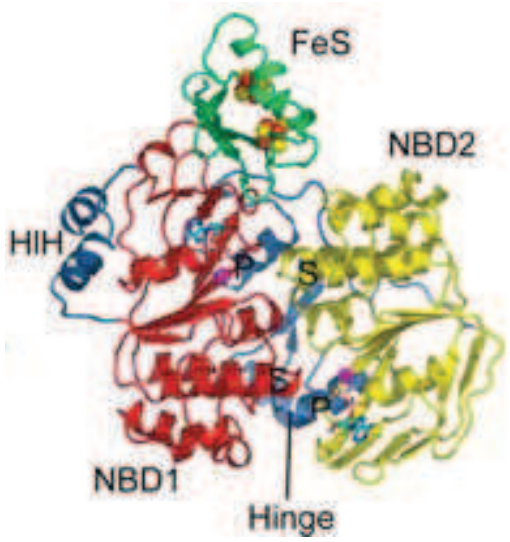

Figure 12 Structure of Rli1
Structural model of the *Pyrococcus abyssi* ortholog of Rli1, ABCE1. The iron-sulfur domain, depicted in green, contains two [4Fe-4S]2+ clusters (Fe in red, S in yellow). The two nucleotide binding domains NBD1 (yellow) and NBD2 (orange) are oriented in a head-to-tail orientation, separated by a hinge domain (light blue). The NBDs together form two composite nucleotide binding sites, which here contain ADP molecules.

(Karcher et al, 2008)

The nucleotide binding domain of Rli1 is essential for ribosome recycling (Barthelme et al, 2011) and in human and yeast *in vitro* systems ATP hydrolysis is needed for ribosome dissociation (Pisarev et al, 2010; Shoemaker & Green, 2011). Although the intrinsic ATPase activity of Rli1 is quite low, it is strongly enhanced by eRF1 bound post-termination complexes (Pisarev et al, 2010), indicating that ATP hydrolysis is induced in the ribosomal context.

These findings led to a model for human and yeast Rli1, in which ATP hydrolysis causes conformational changes that lead to ribosomal subunit dissociation (Figure 13). However, Rli1 mediated ribosome recycling in archaea might be mechanistically different. Here ATP hydrolysis is not required for Rli1 and aRF1 induced splitting of vacant 70S ribosomes. Instead Rli1 dissociation from the ribosome requires ATP hydrolysis. A model has been proposed in which Rli1 binds to post-termination complexes, then acquires ATP which induces a change in conformation resulting in ribosome splitting. This is followed by ATP hydrolysis leading to dissociation of Rli1 and aRF1 (Barthelme et al, 2011). However, the different observations in eukaryotic and archaeal systems might be explained by a difference in experimental set up (the use of post-termination complexes in eukaryotic systems versus vacant 70S ribosomes in archaeal systems).

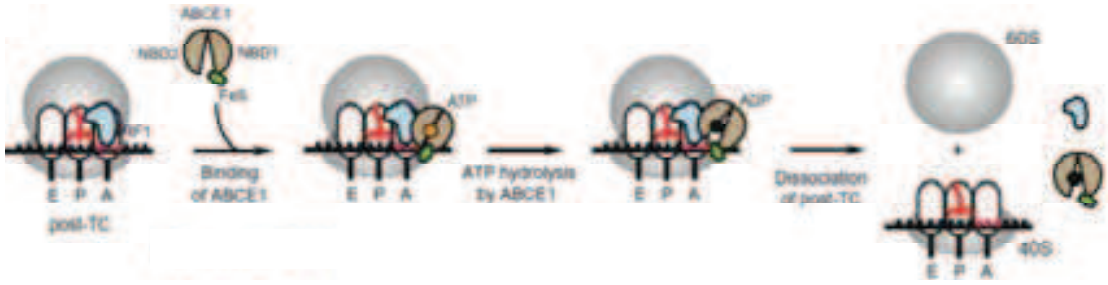

(Jackson et al, 2012)

Figure 13 Eukaryotic ribosome recycling
Rli1 binds to an eRF1 bound post-termination complex. ATP hydrolysis induces a conformational change that leads to dissociation of the ribosomal subunits.

The iron-sulfur cluster domain of Rli1 is also needed for recycling and its absence impedes binding of the archaeal Rli1 homolog to small ribosomal subunits (Barthelme et al, 2011). Together with the presence of a conserved positively charged patch on its surface, hypothetically interacting with negatively charged rRNA (Karcher et al, 2008), this suggests a role in ribosome binding.

Structural models of yeast and archaeal Rli1 in complex with a ribosome and eRF1 paralog Dom34 (Becker et al, 2012, see paragraph 1.3.3.2) have given additional insight into the mechanism of ribosome dissociation. Further mechanistical details about how ATP hydrolysis by Rli1 may cause ribosome dissociation will be discussed in paragraph 1.3.3.2.

After human Rli1 induced ribosomal subunit dissociation, mRNA and P-site tRNA remain bound to the 40S subunit. Biochemical experiment using human factors have shown that their dissociation is mediated by initiation factors eIF1, 1A, 3 and the latter's loosely associated subunit eIF3j (Pisarev et al, 2010). Whereas tRNA dissociation depends mainly on eIF1 and 1A, in agreement with their binding close to the P-site (Lomakin et al, 2003; Rabl et al, 2011), mRNA dissociation requires all factors (Pisarev et al, 2010). The requirement of these factors binding to a 40S subunit during translation initiation suggests that they may directly connect ribosome recycling with a new round of translation (Aitken & Lorsch, 2012; Jackson et al, 2010; Nurenberg & Tampe, 2013).

1.1.3 Messenger RNA degradation

Ultimately all mRNAs will be degraded. Cytoplasmic mRNA degradation in eukaryotes serves several functions. First, "regular" mRNA turnover determines, together with the rate of production, the level of a certain mRNA in the cell. Continuous mRNA degradation allows changing rates of transcription to regulate cellular mRNA concentrations. Second, mRNA turnover itself can be regulated. For example, the binding of certain transacting protein and/or RNA factors to regulatory elements in the mRNA can induce rapid degradation of a mRNA in conditions in which this is necessary. Finally, RNA quality control pathways detect and degrade faulty RNAs that may result from aberrant RNA production of processing.

RNA decay mechanisms have been extensively studied in yeast. Considering the topic of my PhD work and the model organism used, this paragraph will introduce the major cytoplasmic degradation pathways with an emphasis on yeast. All data referred to are obtained with yeast systems, unless mentioned otherwise. In large part, cytoplasmic RNA quality control pathways make use of these pathways. The quality control pathways I studied during my PhD will be introduced in further detail in paragraph 1.4.

1.1.3.1 The major cytoplasmic RNA decay pathways

In yeast cytoplasmic RNA decay occurs via two general pathways: one that degrades mRNAs in 5' to 3' direction and one that operates in 3' to 5' direction (Figure 14). Both pathways start with a deadenylation step, which is often rate limiting.

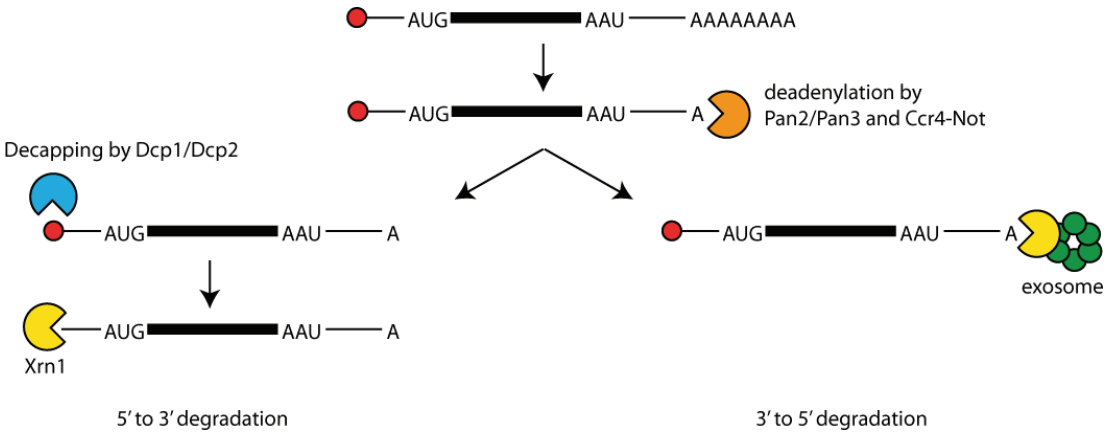

Figure 14 The major cytoplasmic mRNA decay pathways in yeast

1.1.3.1.1 Deadenylation

Two deadenylase complexes mediate this step: the Ccr4-Not complex (Daugeron et al, 2001; Tucker et al, 2001) and the Pan2/Pan3 complex (Boeck et al, 1996). In both mammalian and yeast cells, deadenylation appears to be biphasic. First the poly(A) tail is shortened by the Pan2/Pan3 complex. This can be followed by a more rapid Ccr4-Not mediated deadenylation step (Brown & Sachs, 1998; Yamashita et al, 2005). Deadenylation in general as well as deadenylation of specific mRNAs is controlled by several factors. An example is the poly(A) binding protein Pab1, which stimulates Pan2/Pan3 activity and inhibits Ccr4-Not activity *in vitro* (Brown & Sachs, 1998; Tucker et al, 2002). Consistent with Pab1 affecting deadenylation, a mutation in its C-terminus was found to inhibit mRNA decay *in vivo*, probably by interfering with Pab1 release from the poly(A) tail to be degraded (Simon & Seraphin, 2007). An example of factors that regulate deadenylation of specific mRNAs is the proteins of the Puf family, which bind to elements in the 3'UTR of mRNA subsets (Hook et al, 2007; Olivas & Parker, 2000).

Importantly, in several stress conditions deadenylation of certain mRNAs is inhibited, due to inhibition of both Pan2/Pan3 and Ccr4-Not action (Hilgers et al, 2006). This may promote the preservation of these mRNAs during stress, when there is a general shut down of translation and many mRNAs are degraded (Arribere et al, 2011; see paragraph 1.2).

1.1.3.1.2 Decapping and 5' to 3' decay

The 5' to 3' degradation pathway is the predominant pathway in general mRNA turnover. Following deadenylation, the 5' cap structure is removed. This is mediated by a complex formed by the catalytic subunit Dcp2 (van Dijk et al, 2002) and Dcp1, that stimulates Dcp2 activity by promoting an active conformation (She et al, 2008). The resulting 5'-monophosporylated mRNA is a substrate for rapid and processive degradation by the exonuclease Xrn1 (Hsu & Stevens, 1993). A structural study indicates that Xrn1 can unwind structured RNA, which explains the enzymes high processivity without the requirement of a helicase (Jinek et al, 2011).

Dcp1/Dcp2 needs additional factors for maximum activity. These function to enhance decapping through different mechanisms. While some factors act by directly stimulating decapping, others appear to stimulate decapping by inhibiting translation. Several observations indicate that decapping is in competition with translation initiation. This may seem easy to understand from the fact that initiation factor eIF4E, required for translation initiation, is bound to the cap and may interfere with accessibility for Dcp1/Dcp2. Indeed the eIF4E cap-binding protein inhibits decapping *in vitro* (Schwartz & Parker, 2000). Consistently, mutating initiation factors increases the rate of decapping (Schwartz & Parker, 1999). The factors Dhh1 and Pat1 are examples of enhancers of decapping that act through repressing translation (Coller & Parker, 2005). The exact mechanism by which this repression of translation leads to decapping is not known. Other factors enhance decapping by directly stimulation Dcp1/Dcp2. Pat1 also stimulates decapping by this mechanism. Similarly to another factor, Edc3, it acts by directly binding to Dcp2 (Nissan et al, 2010). Pat1 acts in a complex with a ring of seven Sm-like proteins, Lsm1-7, typically know to bind RNA (Salgado-Garrido et al, 1999). Edc1 and Edc2 stimulate decapping by binding to Dcp1, using a proline rich motif (Borja et al, 2011).

1.1.3.1.3 3' to 5' decay by the exosome

Following deadenylation a mRNA can be further digested by a large exonuclease complex that degrades in 3' to 5' direction: the exosome (Anderson & Parker, 1998). The exosome has multiple functions. Not only does it degrade mRNAs in the cytoplasm, it is also present in the nucleus. Here it functions in the maturation of several types of stable RNAs, including rRNAs, and in the degradation of aberrantly processed RNAs and various types of unstable, non-coding RNAs. The composition of the exosome as well as the cofactors it uses to be

recruited to its substrates differs depending on subcellular localization and type of substrate (Lykke-Andersen et al, 2011).

The exosome is composed of a catalytically inactive core, composed of a ring formed by six subunits with similarity to bacterial RNase PH, flanked on the top by three RNA binding domain containing proteins (Figure 15). The inactive core is associated with one or two catalytically active subunits. In yeast the cytoplasmic exosome is bound to a single catalytic subunit: Dis3 (Dziembowski et al, 2007; Liu et al, 2006). Dis3 possesses both exo- and endonucleolytic activity, the first located in its RNB domain, the latter in its PIN domain (Dziembowski et al, 2007; Lebreton et al, 2008). Regular mRNA turnover depends mainly on Dis3 exonuclease activity. However, for the degradation of some aberrant RNAs known to be substrates for RNA quality control either exo- or endonuclease activity is sufficient (Schaeffer & van Hoof, 2011; see paragraph 1.4.3.2). Although catalytically inactive, the core, which forms a channel, is important for RNA degradation. Probably the RNA substrate is threaded through the channel before it reaches the catalytic subunit (Bonneau et al, 2009). Occlusion of the channel impairs exo- and endonucleolytic function *in vitro* and *in vivo* (Drazkowska et al, 2013; Wasmuth & Lima, 2012).

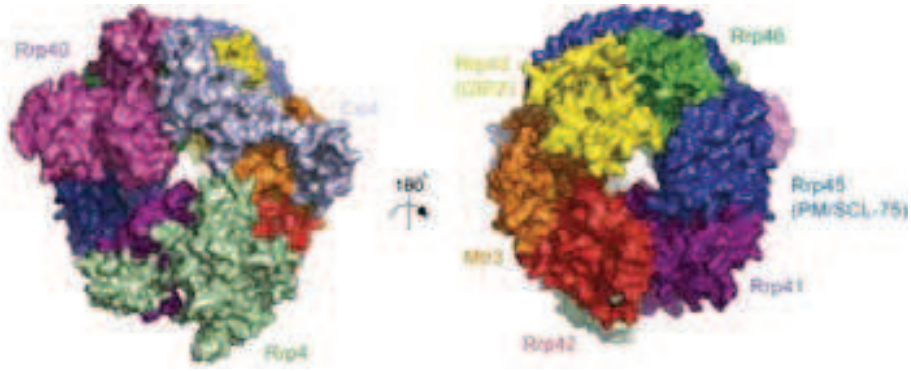

(Liu et al, 2006)

Figure 15 Inactive core of the exosome from *S. cerevisiae*.
On the left : top view, showing the three RNA binding domain containing proteins. On the right : bottom view, showing the six proteins similar to bacterial RNase PH.

Cytoplasmic mRNA decay by the exosome also requires the GTPase Ski7 and the Ski complex (Anderson & Parker, 1998; van Hoof et al, 2000). The Ski complex (Figure 16) consists of Ski2, a helicase, Ski3 and two copies of Ski8 (Brown et al, 2000). Ski7 belongs to the same family of GTPases as eIF1α, the C-terminal domain being homologous to other GTPases in this family. The N-terminal domain of Ski7, that lacks sequence similarity within this family, is sufficient for general RNA turnover. This domain interacts with both the

exosome and the Ski complex (Figure 16) and breaking these interactions inhibits RNA decay (Araki et al, 2001). Both the N and the C-terminal domain of Ski7 play a role in the degradation of certain RNAs that lack a stop codon and are substrates for RNA quality control (van Hoof et al, 2002).

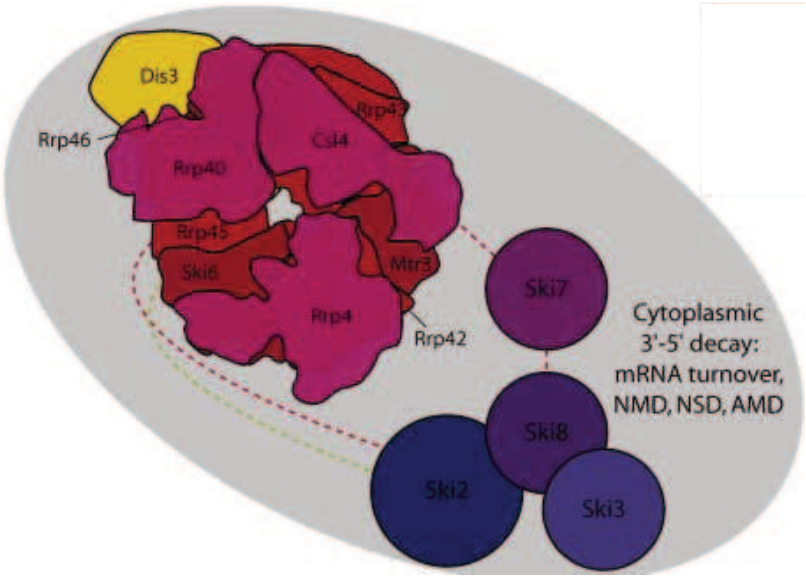

(Lebreton & Seraphin, 2008)

Figure 16 Cytoplasmic mRNA degradation by the exosome requires Ski7 and the Ski complex

1.1.3.1.4 P-bodies

In yeast and mammalian cells, factors involved in decapping and downstream 5' to 3' mRNA degradation co-localize in cytoplasmic granules, called processing bodies or P-bodies. These include Ccr4-Not, Dcp1-Dcp2, Pat1, Lsm1-7, Edc3, Dhh1 and the exonuclease Xrn1. P-bodies were found to be sites of active mRNA degradation (Cougot et al, 2004; Sheth & Parker, 2003; van Dijk et al, 2002). Ribosomal proteins and most translational factors are absent from P-bodies in yeast (Teixeira et al, 2005). It may therefore seem contradictory that for some mRNAs polyadenylation and decapping were found to occur on polysomal mRNA (Hu et al, 2009). However, most factors found in P-bodies are also found diffusely distributed in the cytoplasm (Eulalio et al, 2007). Some RNA degradation may therefore initiate or occur entirely outside P-bodies.

Apart from mRNA decay factors, P-bodies also contain factors involved in translational repression, RNA quality control and, in metazoan cells, factors involved in miRNA mediated silencing, with silenced mRNAs accumulating in P-bodies (Eulalio et al, 2007). Importantly, P-bodies increase in number and size during stress (Brengues et al, 2005; Kedersha et al, 2005; Teixeira et al, 2005). This will be discussed further in paragraph 1.2.3.

1.1.3.2 Cytoplasmic RNA quality control

Aberrant mRNAs can be be the result of errors in mRNA production and processing. When translated they may produce defective, potentially toxic proteins. Cells have mechanisms to detect and degrade these faulty mRNAs in pathways collectively referred to as RNA quality control. In several cytoplasmic RNA quality control pathways aberrant mRNAs are detected during translation. mRNAs containing premature stop codons are detected and degraded in the Nonsense mediated decay (NMD) pathway, mRNAs without stop codon in Non-stop decay (NSD) and mRNAs that contain sites causing ribosomes to stall during elongation in No-go decay (NGD). Related to the latter is a pathway that targets defective rRNAs causing inefficient translation: Non-functional rRNA decay acting on 18S rRNA substrates (18S NRD).

RNA degradation in NMD requires the formation of a surveillance complex, which forms as a consequence of premature termination. This complex includes the helicase Upf1 as well as Upf2 and Upf3. Depending on the organism, a combination of additional factors participates in premature stop codon recognition and downstream events. In multicellular organisms proteins of the SMG family are required, whereas in mammalian cells the exon junction complex plays a role in NMD (Kervestin & Jacobson, 2012). The latter complex is deposited near many but not all exon-exon junctions during splicing (Le Hir et al, 2000; Sauliere et al, 2010; Sauliere et al, 2012) and is displaced by ribosomes during translation. The presence of an exon junction complex 3' of a terminating ribosome plays a role in mammalian NMD (Kervestin & Jacobson, 2012). In yeast NMD substrates are degraded by the major cytoplasmic degradation pathways. In *Drosophila melanogaster*, degradation is initiated by an endonucleolytic cleavage. In mammalian cells NMD substrates can be degraded by the major degradation pathways as well as by the endonucleolytic cleavage mechanism (Nicholson & Mühlemann, 2010). NMD endonucleolytic cleavage was found to be mediated by the SMG factor SMG6 (Eberle et al, 2009; Huntzinger et al, 2008).

The other RNA quality control pathways will be introduced in detail in paragraph 1.4.

1.2 TRANSLATION INHIBITION IN STRESS CONDITIONS

Cells encounter many stress conditions that require changes in gene expression to adapt to the change in environment. Exposure to stress induces a variety of adaptive responses, both at the transcriptional and the post-transcriptional level. During my PhD work I studied a role of the

Dom34-Hbs1 complex in translation initation, in cells recovering from stress. This paragraph will therefore focus on stress related changes at the level of translation.

During many types of stress a global shut down of translation occurs. As translation is a energy consuming process, this has the advantage that the cells save vastly on their energy expenditure. In addition, it causes a reduction in the levels of proteins that might interfere with the stress response. At the same time a subset of genes, required for cell survival during stress, is selectively translated (Holcik & Sonenberg, 2005).

1.2.1 Mechanisms of general translation inhibition

A global shutdown of translation during stress is mostly mediated by a general inhibition of translation initiation. The mechanistic details of this inhibition differ per type of stress. Many stress induced translation inhibiting mechanisms involve altered concentrations or activities of translation initiation factors. Two important mechanisms will be described below. This is by no means an exhaustive overview of all mechanism of stress related translation inhibition described in literature (see also Figure 17).

1.2.1.1 The TOR pathway and 4E-BPs

The target of rapamycin (TOR) pathway is the major nutrient sensing pathway in cells. TOR interacts with other factors to form two distinct complexes. These complexes integrate information coming from at least five major signaling pathways that indicate energy status, stress, concentrations of oxygen, amino acids and growth factors. According to these signals the TOR pathway regulates major cellular processes, including translation. Growth permitting conditions (nutrient availability, absence of stress etc.) stimulate translation via this pathway. In mammalian cells the major effector proteins of the TOR pathway that affect translation are the 4E binding protein 4E-BP1, which prevents eIF4E from interacting with eIF4G, and the S6 kinases 1 and 2 (S6K1 and 2) (Ma & Blenis, 2009).

Upon stress, inactivation of the TOR pathway results in hypophosphorylation of 4E-BP1, which then tightly binds and sequesters eIF4E, thereby preventing the recruitment of other initiation factors and the 43S PIC to the caps of mRNAs. Inhibition of the TOR pathways also results in dephosphorylation and inactivation of S6K1. This results in reduced activity of the RNA helicase eIF4A and also affects eIF3 function. Apart from direct effects on translation initiation factors, S6Ks also control ribosome biogenesis (Ma & Blenis, 2009). An example of 4E-BP mediated translation inhibition in stress is the response to heat shock in mammalian

cells (Vries et al, 1997). The 4E-BP Eap1 may also play a role in heat shock associated translation inhibition in yeast (Meier et al, 2006). Eap1 also plays a role in cadmium and diamide induced oxidative stress (Mascarenhas et al, 2008). In mammalian cells 4E-BP1was mediates translation inhibition in response to DNA damage induced by ionizing radation (Braunstein et al, 2009) or hypoxia (Connolly et al, 2006).

1.2.1.2 eIF2α phosphorylation

Many types of stress induce phosphorylation of the α subunit of initiation factor eIF2 at serine 51. eIF2, in its GTP bound form binds methionyl initiator tRNA to form a ternary complex, required for translation initiation. During initiation the eIF2 bound GTP is hydrolyzed (see paragraph 1.1.2.2). The guanine-nucleotide exchange factor eIF2B is responsible for replacing the resulting GDP with GTP, thereby making eIF2 competent for tRNA binding and participation in translation initiation again. Phosphorylated eIF2 acts as an inhibitor of eIF2B, which causes the levels of GTP bound eIF2 and ternary complex to drop, resulting in a reduced rate of translation initiation (Safer, 1983).

Several kinases have been described to phosphorylate eIF2α. Amino acid starvation stress causes an increase in the level of uncharched tRNAs. In yeast and mammalian cells this causes activation of the kinase Gcn2, which targets eIF2α (Dever et al, 1992; Harding et al, 2000). Gcn2 dependent phosphorylation of eIF2α also mediates translation inhibition in yeast exposed to oxidative stress (Mascarenhas et al, 2008; Shenton et al, 2006) and high NaCl concentrations (Goossens et al, 2001) and in UV irradiated mammalian cells (Deng et al, 2002). Translation inhibition upon membrane stress in mammalian cells and yeast (De Filippi et al, 2007) and upon cold shock in mammalian cells (Underhill et al, 2006) also depends on eIF2α phosphorylation. Other kinases that induce translation inhibition by phosphorylating eIF2α include PERK, HRI and PKR. They play a role in translation inhibition due to elevated levels of reactive oxygen species in hypoxia (Koritzinsky et al, 2007; Liu et al, 2008), hemin depletion and virus infection respectively (Hinnebusch, 2005), in mammalian cells.

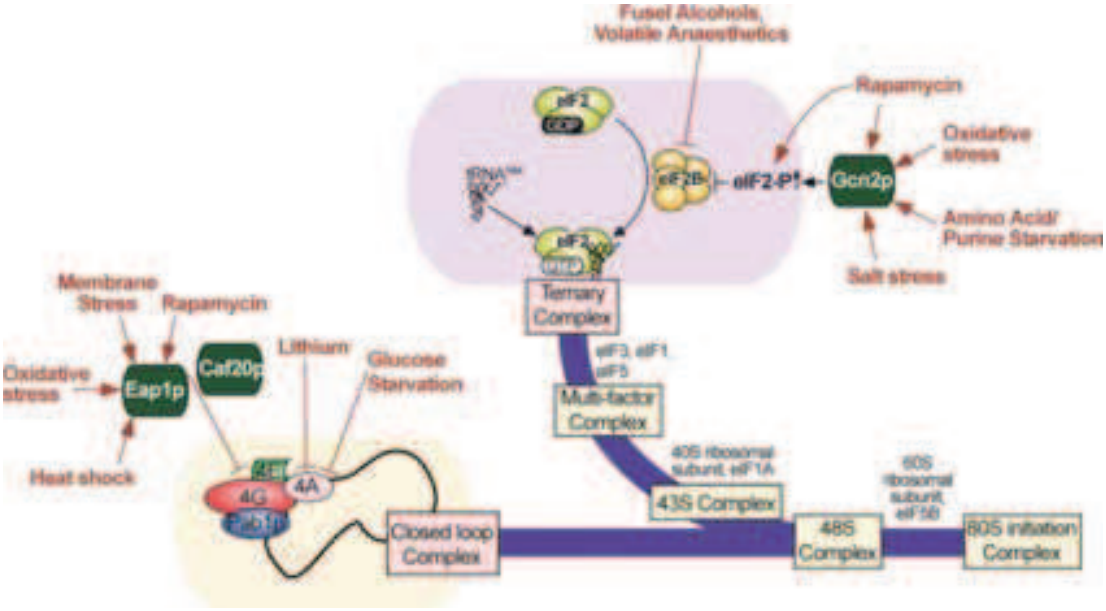

(Simpson & Ashe, 2012)

Figure 17 Mechanisms of inhibition of translation initiation during stress in *S. cerevisiae*.

1.2.1.3 Translation during stress

Apart from a global repression of translation, the translation of stress-specific subsets of mRNAs is specifically upregulated. Therefore these mRNAs should evade the generally targeting inhibitory mechanisms described above. One way to escape translation inhibitory mechanisms that target cap-dependent translation, is the use of cap-independent mechanisms, such as IRES. It was shown that in yeast starved of a carbon source, translation of mRNAs containing IRESs is upregulated (Paz et al, 1999). IRES dependent translation of several genes is required for invasive growth, important for yeast survival in nutrient deplete conditions, during starvation (Gilbert et al, 2007). It has been estimated that up to 10% of cellular mRNAs contain IRESs (Mitchell et al, 2005).

A more specific, well described example of upregulated translation during stress concerns the yeast mRNA *GCN4* (Figure 18). The resulting protein promotes the expression of stress-related genes. The *GCN4* mRNA contains four upstream ORFs (uORFs). The level of ternary complex regulates whether a uORF or the actual GCN4 ORF is translated. In mammalian cells translation of the stress response gene *ATF4* is regulated in a similar way (Harding et al, 2000).

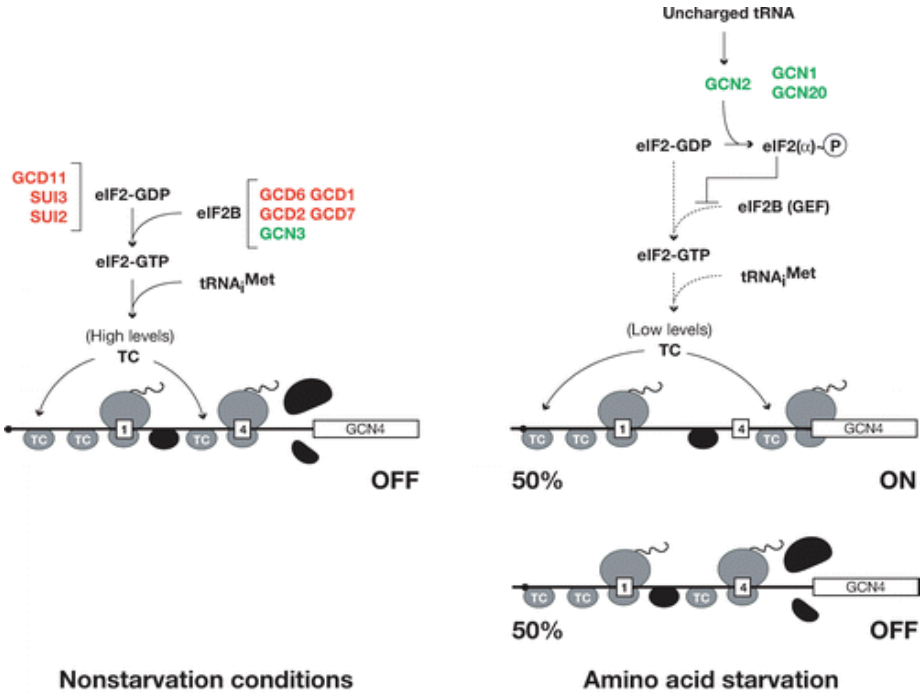

(Hinnebusch, 2005)

Figure 18 Gcn4 translation during stress

The GCN4 mRNA contains 4 upstream ORFs (uORFs). After translating uORF1, the context of termination is such that a proportion of 40S subunits stays associated to the mRNA, resumes scanning and reinitiates at a downstream ORF. When ternary complex (TC) is available, it is likely to bind the 40S subunit before it reaches the AUG of uORF2, 3 or 4. This results in translation of the uORFs, followed by termination and dissociation of the ribosome. During stress conditions in which TC levels are low, e.g. amino acid starvation, a TC will more frequently bind to the scanning 40S subunit only after it has passed the other uORFs but before reaching the AUG of the actual GCN4 ORF. This results in translation of the GCN4 ORF.

1.2.2 Translation inhibition in glucose depletion

Part of the work reported in this thesis describes a role of the factors Dom34 and Hbs1 in restart of translation after glucose starvation stress. Mechanisms controlling the translational response to this stress are described in more detail in this paragraph.

Glucose depletion causes a strong, rapid inhibition of translation (within 10 minutes), that is readily reversed upon glucose addition in yeast (Ashe et al, 2000). This rapid inhibition is not a general reaction to depletion of a carbon source, as translation inhibition does not occur or occurs after a longer delay upon starvation of cells grown on several other carbon sources (sucrose, raffinose, maltose, galactose) (Ashe et al, 2000). After ~60 minutes of starvation, global translation partly recovers. This probably reflects the translation of genes induced by the glucose starvation stress response, which are required for surviving the glucose depleted condition (Arribere et al, 2011).

The mechanism that causes translation inhibition in glucose depleted cells is not completely understood. In yeast translation inhibition does not depend on phosphorylation of eIF2α. In presence of a non-phosphorylatable eIF2α mutant inhibition of translation still occurs, the level of phosphorylated eIF2α does not increase and GCN4 translation does not increase (Ashe et al, 2000; Castelli et al). Translation inhibition does not depend on 4E-BPs Eap1 and Caf20 either (Castelli et al). It was observed in *S. cerevisiae* that during glucose depletion initiation factor eIF4A disappears from ribosomal fractions. At the same time the level of interaction between eIF3 and eIF4G increases. This suggests that due to a problem in 5'UTR scanning because of the absence of the helicase eIF4A in the PIC, initiation is blocked and 43S complexes accumulate (Castelli et al).

Glucose depleted yeast is completely or partially resistant to translation inhibition when it lacks factors involved in decapping and 5' to 3' mRNA degradation, such as Dcp1, Dcp2, or Lsm1 and Pat1. These mutant strains are also resistant to translation inhibition caused by other stresses, including amino acid starvation, addition of lithium, rapamycin (inhibitor of the TOR pathway) or the fusel alcohol butanol (Holmes et al, 2004). This suggests that translation inhibition may be affected by the total level of mRNAs available for translation. Interestingly it was found by genome wide analysis of mRNA abundance that upon glucose starvation in yeast changes in mRNA abundance in polysomes mirror changes in the total level of that mRNA, without any large changes in polysome occupancy (the ratio of the level of a particular mRNA in polysomal fractions and of its total level) (Arribere et al, 2011). Based on the combination of these results it has been suggested that the rapid inhibition of translation upon glucose depletion could be caused by rapid degradation of mRNAs (Arribere et al, 2011).

An alternative explanation suggested that interfering with mRNA degradation could overcome translation inhibition due to increased mRNA levels. The increased amount of mRNAs overwhelms the translation control mechanism acting by mass action (Holmes et al, 2004). Supporting this hypothesis it was found that accumulation of other factors needed for translation initiation (increased levels of free 40S accumulating due to defects in 60S biogenesis, eIF4G overexpression) also suppress glucose depletion induced translation inhibition (Holmes et al, 2004). However, neither one of the aforementioned hypotheses can explain why also strains lacking Xrn1, in which decapped and therefore translationally uncompetent mRNAs accumulate, are resistant to translation inhibition and why strains defective in deadenylation (*ccr4*Δ, *pan2*Δ*pan3*Δ), in which translation competent mRNAs are expected to accumulate, are not resistant to translation inhibition (Holmes et al, 2004).

1.2.3 P-bodies and stress granules

What happens to the large amount of mRNAs that is no longer translated when translation is inhibited during stress? Several reports indicate that they localize to specific granules that assemble in the cytoplasm upon stress, where they may be degraded or stored.

In yeast and mammalian cells several stress conditions cause an increase in size and number of P-bodies (Brengues et al, 2005; Kedersha et al, 2005; Teixeira et al, 2005). It is thought that during translation inhibition mRNAs can accumulate in P-bodies. This is supported by the finding that reporter mRNAs localize to P-bodies upon glucose depletion (Brengues et al, 2005). During stress the mRNAs in P-bodies may be degraded or stored in a translationally repressed condition, to reenter the translation cycle upon stress relief. While the first idea is supported by the observation that the levels of many mRNAs decrease upon glucose starvation stress (Arribere et al, 2011),the latter is supported by the finding that upon restoring non-stressed conditions after glucose starvation reporter mRNAs disappear from P-bodies, but only if translation initiation can occur (Brengues et al, 2005).

In mammalian cells a second type of cytoplasmic granules accumulates as a consequence of defective or inhibited translation initiation. These granules are named stress granules. They contain non-translating mRNAs as well as initiation factors eIF4E, eIF4G, eIF4A, eIF3, eIF2, 40S ribosomal subunits and Pab1. Stress granules are therefore thought to be places where mRNAs associated with stalled 48S complexes, which may accumulate as a consequence of translation inhibition, initially localize during stress (Anderson & Kedersha, 2008). Stress granules and P bodies have different dynamics, but they share several components and P bodies can transiently dock on stress granules, suggesting movement of factors and mRNAs between the two types of granules. Moreover, overexpression of factors that promote mRNA decay induce fusion of stress granules and P bodies (Kedersha et al, 2005). The highly dynamic nature and the composition of stress granules together with stress granule and P body dynamics have led to the idea that in stress granules a process of mRNA triage takes place (Figure 19). Some mRNAs will bind to factors promoting degradation and move to P bodies for decay. Others will associate to stabilizing factors and be exported or stored (in or outside stress granules or P bodies). Alternatively mRNAs can reenter the translation cycle (Anderson & Kedersha, 2008). In yeast heat shock causes the appearance of granules very similar in composition to mammalian stress granules (Grousl et al, 2009).

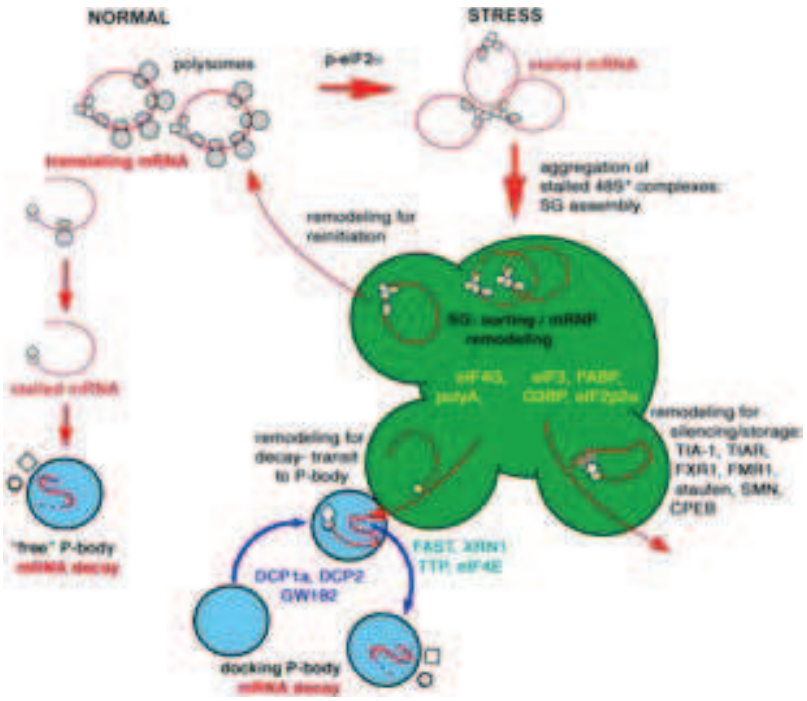

(Kedersha et al, 2005)

Figure 19 Model of the relationship between stress granules and P-bodies.
Stress granules are thought to be sites of mRNA triage. While some are stabilized and stored, others are targeted for degradation and directed to P-bodies. A third category reenters the translation cycle.

In glucose starved yeast a third type of granules form, called EGP bodies. They differ in composition from stress granules: whereas initiation factors eIF4E and eIF4G, Pab1 and reporter mRNAs accumulate in EGP bodies like in stress granules, eIF4AI and eIF3b do not (Hoyle et al, 2007). Therefore EGP bodies may contain circularized mRNAs but cannot be viewed as places where mRNAs associated with stalled 48S complexes localize upon stress. Whereas this may reflect a difference in translation inhibiting mechanism, the EGP bodies also differ from stress granules in their dynamics. EGP granules only form upon prolonged glucose starvation (20-25 minutes), long after the appearance of P-bodies (Hoyle et al, 2007) and mutations inhibiting P-body formation also inhibit EGP body assembly (Buchan et al, 2008). This chronology and dependence suggests that mRNAs first localize to P-bodies, to then move to EGP bodies which might serve as sites of long term storage of mRNAs during glucose depletion stress (Lui et al, 2010). Genome wide data indicate that the population of mRNAs stored during glucose starvation consists mainly of those encoding ribosomal proteins. These mRNAs reenter the translation cycle when after a brief period of starvation glucose is added (Arribere et al, 2011).

1.2.4 Ribosome hibernation

In many translation inhibiting stress conditions ribosomes that can no longer initiate new rounds of translation accumulate as inactive, "hibernating" ribosomes. Storing ribosomes in an inactive state may protect them from damage and ensures that upon stress relief translation can quickly recover without the energy and time consuming need for extensive ribosome biogenesis. For example in yeast, inactive ribosomes that accumulate during glucose starvation stress rapidly redistribute into polysomes upon glucose addition (Ashe et al, 2000).

In bacteria hibernating ribosomes have been well studied. In *Eschericia coli* stress induced factors bind to ribosomes in a translation inhibiting conformation. One of these factors, RMF, has been found to be induced in at least ten different stress conditions (Moen et al, 2009). Binding of RMF to inactive ribosomses causes 70S ribosomes to dimerize into 90S complexes. The binding of a second factor, HPF, further stabilizes the dimer, and converts it into a 100S particle (Ueta et al, 2008). Alternatively, a factor, Yfi1, may bind and stabilize the formation of inactive, monomeric 70S ribosomes (Agafonov et al, 1999). Structural studies have shown that binding of RMF interferes with binding of the small ribosomal subunit to a mRNA, whereas association of ribosomes with HPF or Yfi1 is incompatible with mRNA and tRNA binding (Polikanov et al, 2012). This provides an explanation for the translation inhibitory effect of these factors.

In eukaryotic cells inactive ribosomes also accumulate during stress. Although in rat cells inactive ribosome dimers have been observed in amino acid starved conditions, these have not been observed in any other eukaryotic organism so far (Krokowski et al, 2011). In many cell types 80S ribosomes accumulate during a wide variety of stress conditions. This was shown for example to occur in mammalian cells upon serum-depletion (Nielsen et al, 1981), in yeast and mammalian cells after amino acid shortage (Krokowski et al, 2011; Tzamarias et al, 1989) and in yeast during osmotic stress (Uesono & Toh, 2002), lithium induced stress (Montero-Lomeli et al, 2002), and after exposure to fusel alcohols (Ashe et al, 2001). The 80S ribosomes that accumulate in *S. cerevisiae* during glucose starvation stress (Ashe et al, 2000) contain the protein Stm1 in a conformation that is incompatible with translation and that stabilizes the inactive 80S monomers (Ben-Shem et al, 2011). This factor and its role in translation inhibiting stress will be discussed in further detail in the paragraphs below.

1.2.5 Stm1

In *S. cerevisiae* the Stm1 protein was originally identified as a factor binding specific DNA structural elements: G4 quadruplexes (Frantz & Gilbert, 1995) and purine motif triple helical DNA (Nelson et al, 2000). It was implicated in several processes including promotion of apoptosis-like cell death (Kazemzadeh et al, 2012; Ligr et al, 2001) and telomere replication (Hayashi & Murakami, 2002).

1.2.5.1 Stm1 and translation

Although, in agreement with a function in telomere replication, a fraction of Stm1 localizes to the nucleus, a much larger amount is found in the cytoplasm (Van Dyke et al, 2004). Here it binds to ribosomes (Inada et al, 2002; Van Dyke et al, 2004). Whereas Stm1 was found in fractions of the cell lysate, obtained from growing yeast, that contain 80S ribosomes or polysomes, none could be detected in fractions not containing any ribosomes (Van Dyke et al, 2004). In high speed sedimentation complexes Stm1 is found to be present in similar quantities as several ribosomal proteins (Van Dyke et al, 2006). Together these findings suggest that a large majority of Stm1 is bound to ribosomes, and that nearly all ribosomes, including the translating ones, are bound to Stm1.

Several effects of deletion or overexpression of Stm1 have been reported. In *S. cerevisiae* deletion of *STM1* causes a reduction in overall protein synthesis. Overexpression of Stm1 causes a reduction of protein synthesis as well, but only in the first hour of overexpression, accompanied by an increase in polysome/80S ratio (Van Dyke et al, 2009). The latter suggests that Stm1 negatively affects elongation, termination or recycling. It should be noted that these overexpression experiments were performed in yeast in which protein degradation by the proteasome was inhibited. Stm1 overexpression caused the accumulation of an ubiquitylated form, whereas the level of unubiquitylated Stm1 was essentially unaffected (Van Dyke et al, 2009). This suggests that the protein level of Stm1 is tightly controlled and that the effects observed in these overexpression conditions might be due to the accumulation of ubiquitylated Stm1. On the other hand, in support of the effects being due to Stm1 overdosage, in yeast lysate and rabbit reticulocyte lysate addition of Stm1 also inhibits translation in a manner independent of the presence of a cap or poly(A) tail on the translated mRNA. Moreover, in yeast lysate Stm1 addition causes trapping of a reporter mRNA in 80S ribosomes, in a way that is dependent on translation initiation (Balagopal & Parker, 2011).

These findings support a negative effect of an excess of Stm1 on translation by affecting a step downstream of translation initiation.

1.2.5.2 Stm1 and recovery from translation inhibiting conditions

Stm1 appears to be important for recovery of growth after certain growth limiting conditions. Absence of Stm1 reduces the amount of *S. cerevisiae* cells recovering from nitrogen starvation (Van Dyke et al, 2006). *S. cerevisiae* lacking Stm1 also takes more time to recover growth upon glucose addition, after spending several days in stationary phase. This coincides with a strong reduction in the reappearance of polysomes (Van Dyke et al, 2013), indicating that Stm1 is needed for restart of translation when cells shift from growth inhibiting to growth permitting conditions. Several observations indicate that the importance of Stm1 for recovery of growth and translation depends on a role of the protein promoting the preservation of ribosomes during stress or other situations that reduce the rate of translation in a cell. First of all it was observed that deletion of Stm1 leads to a decrease in the 80S ribosome peak in polysome profiles during stationary phase as well as a reduction in the level of 60S subunit protein L3 (Van Dyke et al, 2013). Second, Stm1 was found to be bound to inactive ribosomes accumulating during glucose starvation stress in *S. cerevisiae*, in a conformation that clamps the subunits together. X-ray crystallography studies on ribosomes purified from glucose starved *S. cerevisiae* (Ben-Shem et al, 2011) demonstrate that the protein follows the path of the mRNA from the ribosomal mRNA entry tunnel to the P-site (Figure 20). It contacts several conserved 40S subunit residues important in mRNA and tRNA binding in both A and P-site. This conformation of Stm1 therefore prevents mRNA and tRNA binding. From the P-site it crosses to the 60S subunit, where it contacts 60S rRNA and protein. This conformation of Stm1, interacting with both subunits, clamps them together, preventing subunit dissociation (Ben-Shem et al, 2011). A similar conformation of Stm1 homologs was observed recently in human and *Drosophila* ribosomes (Anger et al, 2013). A function of Stm1 stabilizing ribosomal subunit association is further supported by the observation that adding Stm1 to ribosomal subunits *in vitro* induces subunit joining into an 80S ribosome (Correia et al, 2004).

The stabilizing, translation inhibiting conformation of Stm1 during stress suggests a function analogous to RMF, HPF and YfiA in bacteria. A major difference, however, is that Stm1 is not induced in stress conditions and also binds to polysomal, and therefore translating ribosomes in non-stress conditions (see above). This suggests that ribosome bound Stm1 can

adopt at least two conformations: one that is compatible and one that is incompatible with translation.

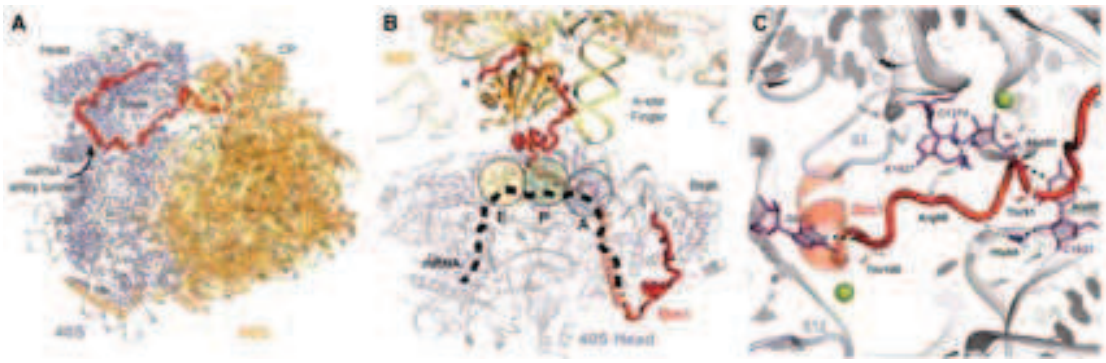

(Ben-Shem et al, 2011)

Figure 20 Stm1 in a ribosome from glucose starved *S. cerevisiae.*
Stm1 interacts with both ribosomal subunits and partly occupies the mRNA tunnel. It interacts with conserved rRNA residues known to interact with mRNA and tRNA (magenta). Stm1: red, 40S subunit: grey, 60S subunit: orange.

1.3 THE TERMINATION FACTOR-LIKE COMPLEX DOM34-HBS1

Central to my PhD work are the factors Dom34 and Hbs1, which form a complex with ribosome dissociating activity, acting on both RNA bound and RNA free ribosomes. The complex has been implicated in various RNA quality control pathways that act on stalled translational complexes. The Dom34-Hbs1 complex will be introduced in this paragraph.

Dom34 (also known as Pelota in many organisms) and Hbs1 are two factors with sequence similarity to translation termination factors eRF1 and eRF3 respectively. Hbs1 is a GTPase belonging to the family of eEF1α-like GTPases, like termination factor eRF3 and elongation factor eEF1α (Atkinson et al, 2008; Wallrapp et al, 1998). For convenience all Dom34-Pelota orthologs will be refered to as Dom34 from here on.

Dom34 and Hbs1 have been shown to interact *in vivo* by yeast two hybrid and GST pull down experiments (Carr-Schmid et al, 2002), as well as *in vitro* (Graille et al, 2008). Dom34 and Hbs1 are conserved proteins. Dom34 has orthologs in eukaryotes and archaea (Eberhart & Wasserman, 1995; Ragan et al, 1996). Whereas Hbs1 has orthologs only in eukaryotes (Inagaki & Ford Doolittle, 2000; Wallrapp et al, 1998), the function of an archaeal Dom34 GTPase partner appears to be filled by aEF1α. Archaeal Dom34 and aEF1α interact as shown by yeast two hybrid experiments, co-immunoprecipitation of recombinant proteins, and co-crystalization experiments (Kobayashi et al, 2010; Saito et al, 2010).

Structural resemblance of the Dom34-Hbs1 complex to the eRF1-eRF3 complex and other ribosome binding complexes (see 1.3.2.1) suggests that the Dom34-Hbs1 complex can bind the ribosomal A-site. This was further confirmed by cryo-EM studies on ribosome bound Dom34-Hbs1 complex (Becker et al, 2011) and biochemical competition experiments, in which the presence of inactive eRF1 reduced Dom34-Hbs1 activity (Shoemaker et al, 2010). Interaction with Dom34 increases the affinity of Hbs1 for GTP 5 to 12-fold (Chen et al, 2010; Graille et al, 2008), whereas GTP binding by Hbs1 increases its affinity for Dom34 9-fold (Chen et al, 2010). Interaction with both Dom34 and a ribosome stimulates GTP hydrolysis by Hbs1 maximally (Pisareva et al, 2011; Shoemaker et al, 2010).

Dom34 and Hbs1 are cytoplasmic proteins (Huh et al, 2003; Xi et al, 2005). In *Drosophila* Dom34 mRNA is expressed at various stages of development and in adults (Eberhart & Wasserman, 1995). Hbs1 is expressed during early mouse embryonic development and in various tissues in adult mice (Wallrapp et al, 1998). In subcellular fractionation experiments

on human Hep2G cells Dom34 co-localizes with actin microfilaments and it is found near the nuclear envelope, presumably at the endoplasmic reticulum (Burnicka-Turek et al, 2010).

1.3.1 Phenotypical analysis

In the yeast *S. cerevisiae* deletion of *DOM34* was reported to cause slow growth, exhibit a G1 delay and to be defective in meiotic division, sporulation and in pseudohyphal growth (Davis & Engebrecht, 1998). However, the growth defect might be dependent on the genetic background of the strain (see also paragraph 1.3.1.1), as it was not reproduced in other reports (Carr-Schmid et al, 2002), see also result section). In higher eukaryotes absence of Dom34 appears to have a more severe impact. In *Drosophila* males homozygous for *dom34* mutations are sterile due to a defect in spermatogenesis. The cell cycle arrests early in the first meiotic division, where no breakdown of the nuclear envelope or spindle formation occurs. In addition *dom34* mutants have eye defects, with the eyes of homozygous mutants being 30 % smaller than those of heterozygous siblings (Eberhart & Wasserman, 1995). It was also found that Dom34 controls self-renewal of germline stem cells by repressing differentiation (Xi et al, 2005). Mouse embryos lacking Dom34 do not develop past day 7.5 of embryogenesis, due to a defect in proliferation after formation of the three germ layers (Adham et al, 2003). In human Hep2G cells overexpression of Dom34, which is physically associated with the actin cytoskeleton, disrupts actin stress fibers and negatively affects cell growth (Burnicka-Turek et al, 2010).

Hbs1 was identified as a multicopy suppressor of a slow growth phenotype in strains that lack cytosolic Hsp70 proteins Ssb1 and Ssb2 (Nelson et al, 1992). The Ssb proteins are chaperones that prevent newly produced polypeptides from aggregating, aiding their correct folding (Willmund et al, 2013). It has been suggested that Hbs1 might function to catalyze stop-codon independent peptide release from ribosomes stalled due to nascent peptide aggregation (Inagaki & Ford Doolittle, 2000). Although Hbs1 is similar in structure to termination factor eRF3 (see paragraph 1.3.2.1), it cannot complement its absence, nor does it interact with the binding partner of eRF3, eRF1 (Wallrapp et al, 1998).

1.3.1.1 Dom34 and Hbs1 are important in strains with 40S subunit deficiency

In *S. cerevisiae* deletion of either *DOM34* or *HBS1* results in synthetic slow growth defects with deletion of genes encoding a copy of a 40S ribosomal subunit protein. This effect is most pronounced at low temperatures (Bhattacharya et al, 2010; Carr-Schmid et al, 2002). Because

most ribosomal proteins are encoded by two gene copies (e.g. ribosomal protein S28 by *RPS28A* and *RPS28B*), these strains have reduced levels of a particular 40S subunit protein, which results in 40S subunit deficiency (Bhattacharya et al, 2010; Carr-Schmid et al, 2002). This is accompanied by a reduction in the number of polysomes and protein production, indicating that the decreased number of 40S subunits available result in reduced translation initiation (Figure 21). Deletion of *DOM34* or *HBS1* causes an increase in the amount of 80S ribosomes and, especially at lower temperatures, a slight reduction in the number of polysomes. The slowly growing double mutants (*rpsX*Δ*dom34*Δ or *rpsX*Δ*hbs1*Δ, in which X can represent various numbers corresponding to different 40S subunit proteins) combine the 40S subunit deficiency with the increase in 80S ribosomes of the two single mutants. The number of polysomes and protein production are further reduced, most likely explaining the growth defect (Bhattacharya et al, 2010; Carr-Schmid et al, 2002).

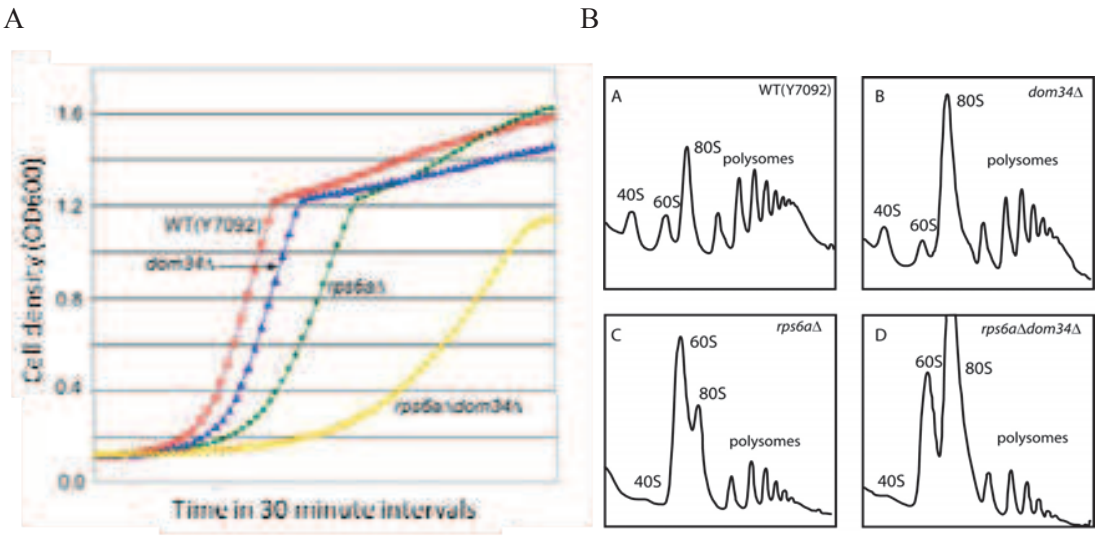

(Bhattacharya et al, 2010)

Figure 21 Deletion of Dom34 causes growth defect in 40S subunit deficient yeast.
Growth curves (A) and polysome profiles (B) of wild type (WT), *dom34*Δ, *rps6a*Δ and *rps6a*Δ*dom34*Δ S. cerevisae. A. Deletion of Dom34 does not affect growth in a wild type strain, but severly slows growth in a strain lacking one copy of the two genes encoding ribosomal protein S6. B. In absence of Dom34 causes an increase in 80S ribosomes and a slight reduction in polysomes, both in wild type and in 40S subunit deficient *rps6a*Δ yeast.

Further supporting a critical role of Dom34 and Hbs1 in conditions where translation initiation is reduced is the observation that deletion of *DOM34* or *HBS1* causes slow growth in yeast in which translation is inhibited by constitutive phosporylation, and thereby inhibition of initiation factor eIF2 (Carr-Schmid et al, 2002). Interestingly, the yeast strain in which

single deletion of *DOM34* causes a slow growth phenotype has relatively low levels of free 40S subunits and high levels of 60S subunits (Davis & Engebrecht, 1998), suggesting that the strain has a pre-existing 40S subunit deficiency, making Dom34 and Hbs1 important for growth. In this strain overexpression of *RPS30A*, encoding 40S subunit protein S30, rescues the *dom34*Δ slow growth phenotype (Davis & Engebrecht, 1998).

1.3.2 Structural models of Dom34 and Hbs1

Structural information on Dom34 and Hbs1 is available from X-ray crystallography studies on Dom34 from *S. cerevisiae* (Graille et al, 2008), its archaeal paralogs from *Thermoplasma acidphilum* (Lee et al, 2007), *Archaeoglobus fulgidus* and *Sulfolobus solfataricus* (Lee et al, 2010), on Dom34 in complex with Hbs1 from *S. pombe* (Chen et al, 2010) and on the archaeal Dom34 in complex with its partner aEF1α from *Aeropyrum pernix* (Kobayashi et al, 2010). In addition a cryo-EM study on the *S. cerevisiae* Dom34-Hbs1 complex bound to a ribosome has been published (Becker et al, 2011).

Dom34 is composed of three domains (Figure 22). The individual domains are highly similar between structures obtained from different orthologs, but the relative positions of the domains with respect to each other differ. This indicates flexibility of the linker regions connecting the domains and suggests that large conformational changes are essential for the function of Dom34 (Graille et al, 2008; Lee et al, 2010; Lee et al, 2007).

Whereas the central and C-terminal domains of Dom34 are similar in sequence and structure to those of translation termination factor eRF1, the N-terminal domain is not (Figure 22). It adopts a highly divergent Sm-fold (Graille et al., 2008; Lee et al., 2007). The Sm-fold is found in the Lsm family of proteins, which form RNA binding hexa- or heptemers (Khusial et al, 2005). However the N-terminal domain of Dom34 lacks the Sm1 and Sm2 motifs implicated in RNA binding and has structural impairments preventing oligomerization (Graille et al, 2008). Because of its difference from eRF1, the Dom34 N-terminal domain lacks conserved residues essential for stop codon recognition in eRF1, such as the NIKS loop (Frolova et al, 2002).

The central domain of Dom34 is structurally similar to that of eRF1. A major difference resides in the absence of the GGQ motif and the length of the α-helix following it (Graille et al, 2008; Lee et al, 2007) (Figure 22). In eRF1 the GGQ motif is essential for triggering peptidyl-tRNA hydrolysis, thereby releasing the peptide (Frolova et al, 1999). It is therefore unlikely that Dom34 can induce peptidyl-tRNA hydrolysis.

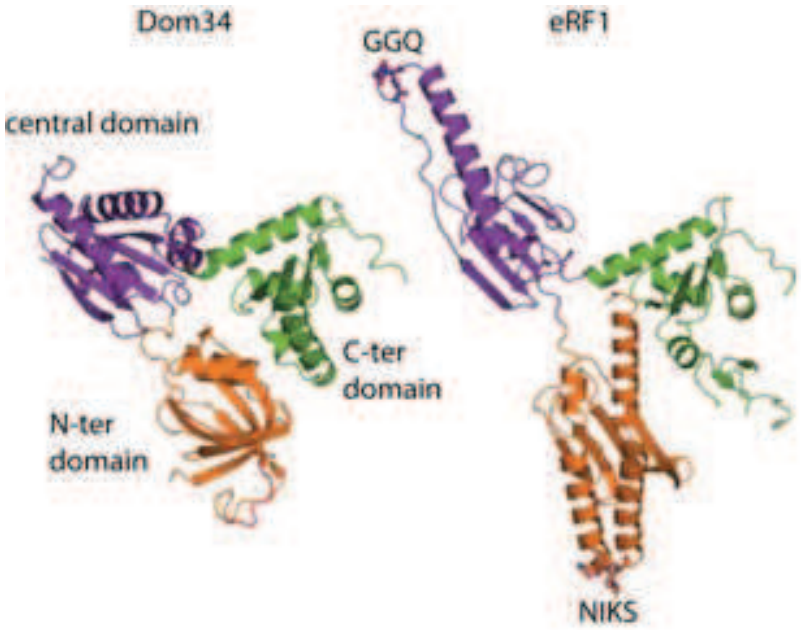

(Graille & Seraphin, 2012)

Figure 22 Dom34 versus eRF1

Crystal structures of *S. cerevisiae* Dom34 (Graille et al, 2008) and human eRF1 (Song et al, 2000). The positions of the highly conserved GGQ and NIKS motifs in eRF1, important for peptidyl-tRNA hydrolysis and stop codon recognition respectively, are indicated.

Hbs1 consists of three structured domains, the domains G, II and III, preceded by an unstructured N-terminus (Chen et al, 2010). The three structured domains resemble those of EF-Tu, the related bacterial GTPase responsible for bringing tRNAs to the ribosomal A-site (Chen et al, 2010). The G domain harbors the GTP binding and hydrolysis activity of Hbs1, as in other GTPases. G domains have a universal structure and contain several highly conserved elements important for its activity. These include the P-loop - a phosphate binding loop – and two switch regions I and II, which change conformation between GTP and GDP bound state (Vetter & Wittinghofer, 2001).

1.3.2.1 The Dom34-Hbs1 complex

Three sets of structural data are available on Dom34 in complex with a GTPase partner. In case of archaeal Dom34, this binding partner is not Hbs1 but aEF1α (Saito et al, 2010). All complexes structurally resemble other complexes that bind the ribosomal A-site, such as the bacterial EF-Tu-tRNA complex (Chen et al, 2010; Kobayashi et al, 2010).

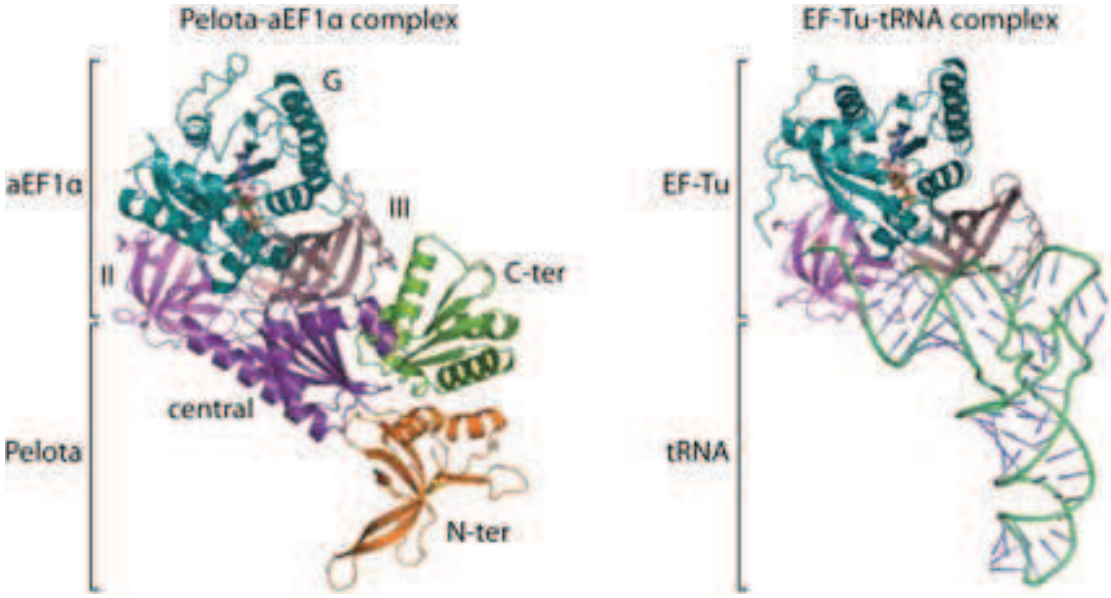

(Graille & Seraphin, 2012)

Figure 23 The archaeal Pelota-aEF1α complex structurally resembles the bacterial EF-Tu complex
Crystal structures of the Aeropyrum pernix Pelota-aEF1α complex (Kobayashi et al, 2010) and the *E. coli* EF-Tu-tRNA complex. Domains are depicted in different colours.

A major difference between the Dom34-Hbs1/aEF1α complexes is found in the orientation of the G domain. In the *S. pombe* complex it rotates away from domains II and III and does not interact with Dom34 (Chen et al, 2010). In the archaeal complex and the ribosome bound *S. cerevisiae* complex it rotates towards domains II and III and participates in interaction with Dom34 (Becker et al, 2011; Kobayashi et al, 2010). Whereas the latter two structures are obtained from complexes containing GTP and the GTP analog GDPNP respectively, the *S. pombe* structure was obtained from a complex not binding any nucleotide (Becker et al, 2011; Chen et al, 2010; Kobayashi et al, 2010). This might suggest that the orientation of the G domain depends on whether a GTP molecule is bound or not. However, this is not in line with the observations of our collaborators Julien Henri and Marc Graille, who found Hbs1, without nucleotide or bound to GDP, to be in a similar conformation as Hbs1 in the archaeal and the *S. cerevisiae* ribosome bound complexes (see result section). Alternatively, the deviating orientation of the G domain in the *S. pombe* model could be due to crystal packing. Clearly the conformation in which the G-domain rotates towards II and III is the one that is adopted when binding the ribosomal A-site.

The interface between Dom34 and Hbs1 or Dom34 and aEF1α involves multiple domains of both proteins. In all three models the C-terminal domain of Dom34 interacts with domain III of Hbs1 and the central domain of Dom34 interacts with domains II and III of Hbs1. In the

archaeal and the *S. cerevisiae* ribosome bound model the central domain of Dom34 also interact with the G domain of Hbs1. The molecular details of the interactions differ between the models. Notably a conserved positively charged loop in the central domain of Dom34 is participating in Dom34-Hbs1/aEF1α interaction in all models: in the *S. pombe* model it contacts Hbs1 domain II and III, whereas in the other two models it interacts with switch I in the G domain. Another highly conserved Dom34 central domain motif, PGF, interacts with switch I and II of the Hbs1 G domain in the archaeal model.

1.3.2.2 Interaction of the Dom34-Hbs1 complex with the ribosome

The cryo-EM model of *S. cerevisiae* Dom34 and Hbs1 bound to a ribosome shows that two loops in the N-terminal domain of Dom34 reach deep into the decoding center of the ribosomal A-site. Here they interact with rRNA and with ribosomal proteins that contact residues important in decoding. Binding of Dom34-Hbs1 to a ribosome stalled on an mRNA causes the densities that represent mRNA in the ribosomal P-site to disappear. This suggests that Dom34-Hbs1 binding induces destabilization of mRNA-ribosome interaction. The model identified a structured part of the N-terminus of Hbs1, located at the mRNA entry site of the ribosome (Figure 24). In the ribosome bound model switch I of Hbs1 is resolved, whereas in the non-ribosome bound models it was not completely resolved (Becker et al, 2011). This, and the observation described above that Dom34 directly interacts with the switch regions, may provide a structural explanation on how interaction with Dom34 and the ribosome promote GTP binding and/or hydrolysis by Hbs1 (Chen et al, 2010; Graille et al, 2008; Shoemaker et al, 2010).

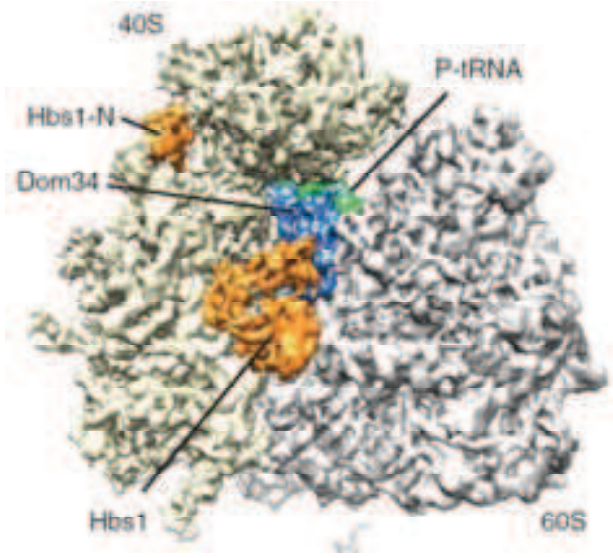

Figure 24 Cryo-EM model of ribosome bound Dom34-Hbs1.

(Becker et al, 2011)

1.3.3 The Dom34-Hbs1 complex dissociates ribosomes

Dom34 and Hbs1 can dissociate the subunits of ribosomes that are stalled on mRNAs as well as vacant, mRNA-free ribosomes. For efficient dissociation the ATPase Rli1 is required as well.

1.3.3.1 *In vitro* dissociation of stalled and vacant ribosomes

The first evidence that the Dom34-Hbs1 complex can dissociate stalled ribosomes came from biochemical experiments, in which *in vitro* assembled translational complexes, stalled on either a sense or a stop codon, were incubated with *S. cerevisiae* Dom34 and Hbs1. This resulted in ribosome dissociation and the release of a peptidyl-tRNA, with the rate of dissociation being independent on the codon type (Shoemaker et al, 2010). In contrast incubation with termination factors eRF1 and eRF3 causes peptide release only from ribosomes with a stop codon in their A site. Dom34-Hbs1 mediated peptidyl-tRNA release is a factor 15 slower than eRF1-eRF3 mediated peptide release. (Shoemaker et al, 2010). Further biochemical experiments reported that human Dom34 and Hbs1 can dissociate not only ribosomes stalled on a mRNA, but also *in vitro* assembled 80S ribosomes that are not associated with mRNA or translation factors. In both cases the human ortholog of Rli1 is required as well (Pisareva et al, 2011). In agreement with this Rli1 was also found to stimulate the rate of yeast Dom34-Hbs1 mediated dissociation of ribosomes stalled on a mRNA more than ten-fold (Shoemaker & Green, 2011). These biochemical studies, together with structural studies on Dom34 and Rli1 bound to a ribosome have given insight into the mechanistic details of Dom34-Hbs1 mediated ribosome dissociation.

1.3.3.2 Mechanistic details of Dom34-Hbs1 and Rli1 mediated ribosome dissociation

Whereas both Dom34 and Rli1 strongly contribute to the rate of ribosome dissociation, Hbs1 is less required. The incubation of vacant or stalled ribosomes with all three human factors for 10 minutes results in complete dissociation. Whereas absence of Rli1 blocks dissociation completely, absence of Hbs1 merely leads to a reduction in the fraction of ribosome dissociated (Pisareva et al, 2011). Kinetic analysis of the contribution of the yeast factors in dissociating stalled ribosomes indicates that whereas absence of Rli1 slowed dissociation more than 10-fold, absence of Hbs1 reduced the dissociation rate only 2,5-fold (Shoemaker & Green, 2011). On the other hand, adding Hbs1 but blocking its GTPase activity, either by addition of the non-hydrolyzable GTP analog GDPNP or by mutating the Hbs1 G domain,

causes a large reduction in dissociation of both vacant and stalled ribosomes (Pisareva et al, 2011; Shoemaker et al, 2010; Shoemaker & Green, 2011). For example, a yeast Hbs1 GTPase mutant slows dissociation of stalled ribosomes more than 20-fold (Shoemaker & Green, 2011). These observations indicate that Hbs1 is not absolutely required for Dom34 to bind the ribosomal A-site and induce ribosome dissociation. However, when Hbs1 complexes with Dom34, its GTPase activity is essential for binding of the complex to the ribosome and/or inducing ribosome dissociation.

Cryo-EM studies of *S. cerevisiae* Dom34 and Rli1, as well as their archaeal (*Pyrococcus furiosus*) orthologs bound to a ribosome stalled on a mRNA in presence of non-hydrolysable ATP analog ADPNP show that Rli1 occupies the same place as Hbs1 in the ribosomal A-site, where it interacts with the C-terminal domain of Dom34. Therefore Hbs1 and Rli1 cannot bind the ribosome or Dom34 simultaneously and should bind sequentially (Becker et al, 2012). The presence of a non-hydrolysable GTP analog prevents Hbs1 from dissociating from the ribosome (Shoemaker & Green, 2011). This may explain why the GTPase activity of Hbs1 is important for ribosome dissociation, by allowing Rli1 to bind after GTP hydrolysis dependent Hbs1 release.

Like other members of the ABC protein family, Rli1 contains a twin nucleotide binding domain, in a head to tail orientation (see paragraph 1.1.2.5). These nucleotide binding domains change from a closed conformation to an open conformation upon ATP hydrolysis. This causes a tweezer-like power stroke, which causes conformational changes in other domains of the protein itself as well as associated proteins (Hopfner & Tainer, 2003). Rli1 ATPase activity is essential for inducing ribosome dissociation, as the presence of non-hydrolysable ADPNP was shown to strongly inhibit yeast Dom34 and Rli1 mediated dissociation of stalled ribosomes (Shoemaker & Green, 2011). It has been proposed, based on structural models, that the conformational change in Rli1 induced by ATP hydrolysis is transmitted to Dom34, via the interaction between the iron-sulfur domain of Rli1 and the C-terminal domain of Dom34. The change in conformation of Dom34 may then induce separation of the ribosomal subunits (Becker et al, 2012).

Based on these structural and biochemical observations a model of Dom34, Hbs1 and Rli1 mediated ribosome dissociation can be proposed, that is depicted in Figure 26 (Becker et al, 2012; Shoemaker & Green, 2011). Dom34 in complex with GTP bound Hbs1 binds to a ribosome stalled on a mRNA or a vacant ribosome (1). An unknown signal induces GTP hydrolysis (2), which causes Hbs1 to dissociate (3) and makes the complex competent for recycling. ATP bound Rli1 can then bind (4). ATP hydrolysis causes conformational changes

in Rli1 and Dom34, which result in destabilization of ribosomal subunit interaction and, in case of a stalled ribosome, release of the peptidyl-tRNA (5).

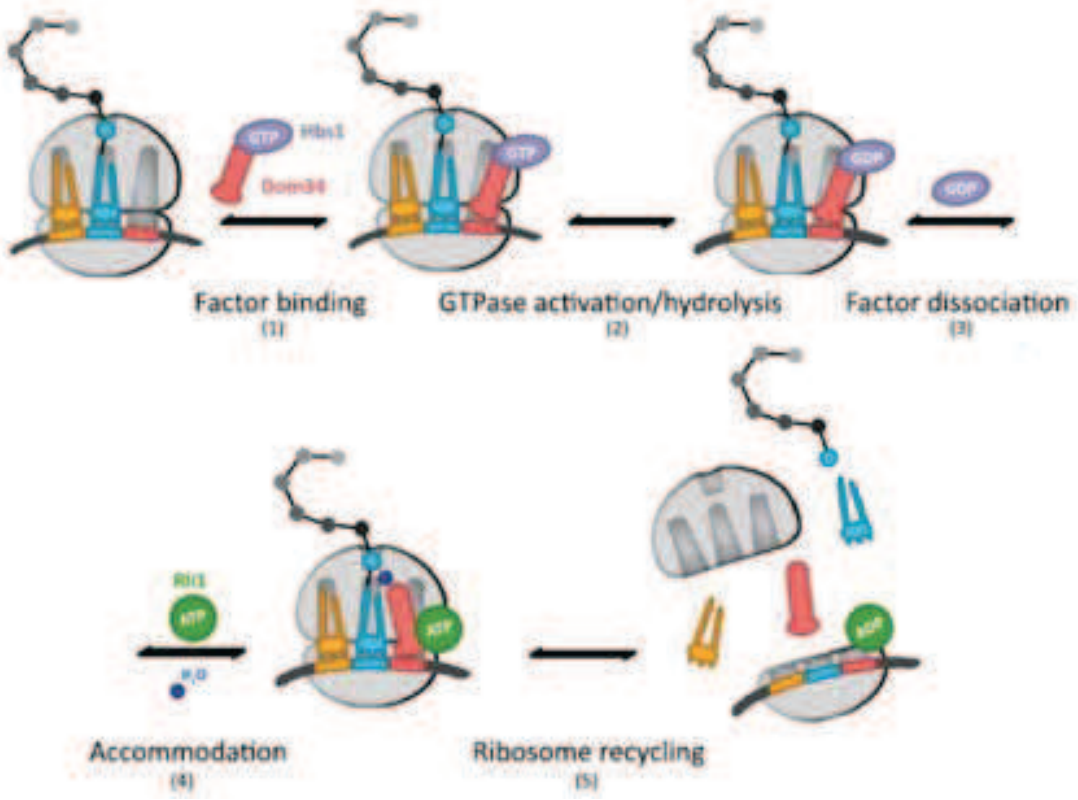

Adapted from (Shoemaker & Green, 2011)

Figure 25 Ribosome recycling by Dom34, Hbs1 and Rli1.
For further details see text.

It is unclear what happens to the mRNA, in case of mRNA bound ribosomes. Following dissociation of stalled yeast ribosomes it stays associated to the 40S subunit (Shoemaker et al, 2010), but after dissociation of stalled human ribosomes it was found to be not ribosome bound (Pisareva et al, 2011). This difference may depend on the length of the part of the mRNA that is interacting with the ribosome (see below).

Human orthologs of Dom34, Hbs1 and Rli1 only dissociate stalled ribosomes efficiently if the length of the mRNA extending 3' of the ribosomal P-site is shorter than 13 nucleotides (Pisareva et al, 2011). Yeast Dom34-Hbs1 and Rli1 dependent dissociation of stalled ribosomes also exhibits a dependence on the length of the mRNA 3' of the ribosome, although to a lesser extent than the human factors. In the yeast system, ribosomes stalled on mRNAs with a length up to 23 nucleotides downstream the P-site are dissociated with equal

efficiency. Beyond 23 nucleotides the length of the mRNA downstream of the P-site negatively correlates with the dissociation rate. In the yeast system the mRNA length dependence depends on the presence of Hbs1. It has been speculated that the N-terminus of Hbs1 is involved in monitoring mRNA length downstream of the ribosome, as it is located near the mRNA entry site (see paragraph 1.3.2.2) (Shoemaker & Green, 2011). The mRNA length dependence *in vitro* suggests that *in vivo* Dom34-Hbs1 and Rli1 mediated dissociation of ribosomes stalled in the middle of a mRNA might be preceded by a step shortening the mRNA downstream of the stalled ribosome, e.g. by endonuclease cleavage (see paragraph 1.4.1).

1.3.3.3 Dom34-Hbs1 mediated ribosome dissociation *in vivo*

Two reports have been published that describe situations in which Dom34, Hbs1 and Rli1 mediated ribosome dissociation may play a role. When mRNAs do not have a termination codon the ribosomes that translate them cannot terminate and recycle via the canonical route. This causes stalling of ribosomes at the 3' end or, in case the mRNA has a poly(A)tail, on the poly(A)tail of the mRNA. This, as well as the pathway that rapidly degrades these non-stop mRNAs will be described in further detail in paragraph 1.4.3. The ribosomes stalled on non-stop mRNAs may block passage of the degradation machinery responsible for rapid decay of the mRNA. It was found that in absence of Dom34 or Hbs1 non-stop mRNAs are stabilized, suggesting that these factors are needed for removing the stalled ribosomes. Moreover it was found that absence of functional Dom34 or Hbs1 caused accumulation of ribosome associated peptidyl-tRNAs, further supporting this hypothesis (Tsuboi et al, 2012).

Dom34-Hbs1 and Rli1 mediated ribosome dissociation may also be important for ribosome biogenesis. It was shown that during ribosome maturation 60S subunits associate with immature pre-40S subunits (Lebaron et al, 2012; Strunk et al, 2012). This is thought to serve as a quality control step. In absence of Dom34, or when Rli1 is depleted, ribosome assembly factors, which normally co-sediment mainly with pre-40S subunits, were found to co-sediment with 80S ribosomes. This was interpreted as an accumulation of pre-40S – 60S complexes, indicating that Dom34 and Rli1 are involved in their dissociation (Strunk et al, 2012). However, a wild type control strain was missing in these experiments. In another strain with a wild type-like genotype but grown in other conditions (with galactose as a carbon source instead of glucose), a similar set of assembly factors was found to co-sediment with 80S ribosomes, making it questionable whether Dom34 and Rli1 are really involved in dissociating immature ribosomes.

1.4 CO-TRANSLATIONAL RNA QUALITY CONTROL ON INEFFICIENTLY TRANSLATING COMPLEXES

Stalling of ribosomes during translation elongation makes a cell face two problems. First, an incomplete peptide is produced that is potentially toxic. Second, depending on the strength and cause of stalling a ribosome may not be able to terminate and therefore canonical peptide release and recycling cannot occur. Stalling can lead to queuing of ribosomes upstream of the primary stalled ribosome resulting in a large reduction in the rate of translation of the affected mRNA and, if stalling occurs with high frequency, potential sequestration of translation factors.

Cells have acquired pathways to deal with the causes and results of inefficient translation. In eukaryotes three pathways have been described that detect and degrade RNAs that cause ribosome stalling. These are No-go decay (NGD), Non-functional rRNA decay (NRD) and Non-stop decay (NSD). Although identified as separate pathways that target RNAs, they have many characteristics in common and are tightly associated with mechanisms that deal with the consequences of ribosome stalling. The three pathways will be introduced in the following paragraphs. While I did not study NSD during my PhD, it will be introduced in detail because of its mechanistic overlap with the other two pathways.

1.4.1 No-go decay

In NGD stalling of a ribosome during elongation causes the degradation of the mRNA on which it is stalled.

1.4.1.1 Mechanism of No-go decay

NGD was first described by Doma & Parker in the yeast *S. cerevisiae*. They found that the insertion of a stem-loop, which was known to block the passage of elongating ribosomes (Hosoda et al, 2003), causes the destabilization of a PGK1 reporter mRNA. Its half life decreases two-fold compared to a reporter without stem-loop. This destabilization does not depend on the major 5’ to 3’ or 3’ to 5’ cytoplasmic degradation pathways or on NMD as absence of functional Dcp2, Ski7 or Upf1 does not affect the stability of the reporter. Insertion of a stem-loop in the 3’UTR, blocking ribosome scanning and thereby initiation, or insertion of a termination codon upstream of the stem loop prevented degradation. This

supports the idea that translation of the NGD reporter and subsequent ribosome stalling is required for substrate detection.

In strains in which 5' to 3' degradation is blocked (*xrn1*Δ) a degradation intermediate accumulates that corresponds in size to a fragment covering all nucleotides between stem-loop and 3' end. When 3' to 5' degradation is blocked (in absence of functional Ski complex or Ski7) an intermediate accumulates that corresponds in size to a fragment covering all nucleotides between 5' end and stem-loop. This indicates that degradation of the mRNA is initiated by an endonucleolytic cleavage in the vicinity of the ribosome stall site, and that the resulting decay intermediates are substrates of Xrn1 and the cytoplasmic exosome (Doma & Parker, 2006) (Figure 26). The accumulation of at least the 5' cleavage products was found to be dependent on the presence of the factors Dom34 and Hbs1 (Doma & Parker, 2006), which was interpreted as Dom34 and Hbs1 stimulating mRNA cleavage.

When Xrn1 mediated degradation is blocked, a stemloop containing PGK1 mRNA, or a product containing its 3' end, accumulates in P-bodies. This suggests that NGD 3' cleavage products are degraded in P-bodies (Cole et al, 2009). A NGD intermediate resulting from a stem-loop containing PGK1 reporter mRNA was also shown to accumulate in *Drosophila* S2 cells (Passos et al, 2009), indicating that the pathway is conserved in higher eukaryotes. This intermediate accumulation is dependent on the presence of the Dom34 ortholog in *Drosophila*.

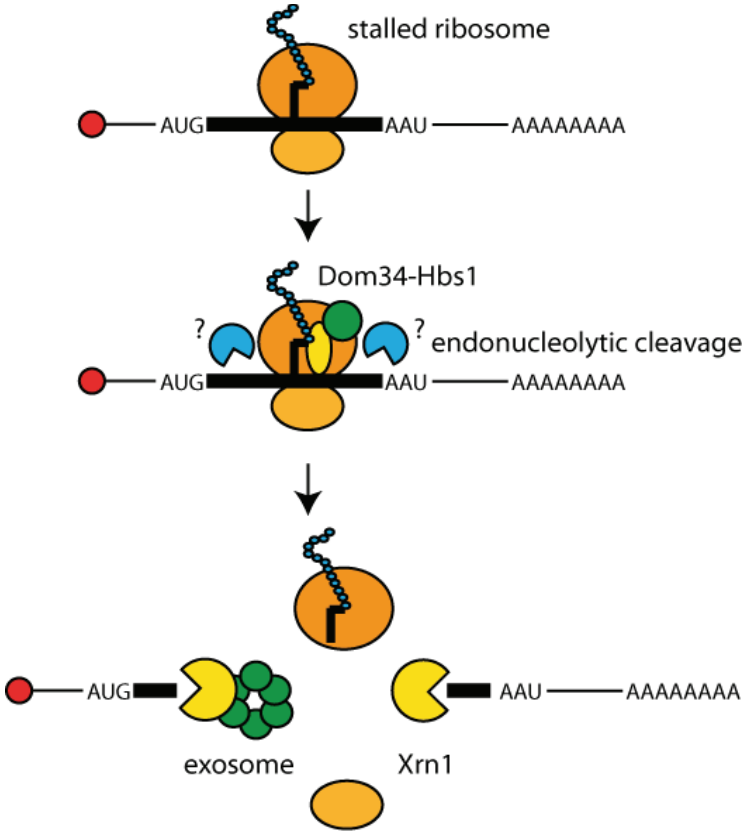

Figure 26 No-go decay model.

1.4.1.2 Stall sites that cause NGD

Apart from a stem-loop, other sites that cause ribosomal stalling were shown to induce NGD in *S. cerevisiae*. These include pseudoknots, rare codons and premature termination codons, although NGD efficiency is low when compared to a stem-loop (Doma & Parker, 2006). Also RNA damage causes mRNA destabilization that may be related to NGD. The Pokeweed antiviral protein (PAP) is normally expressed in the pokeweed plant (*Phytolacca americana*) and is known to depurinate viral RNAs. When the Brome mosaic viral RNA3 is co-expressed in *S. cerevisiae* with PAP, causing depurination at specific sites, this leads to destabilization of the RNA. In analogy with NGD substrates, blocking the major cytoplasmic RNA degradation pathways caused the Dom34-Hbs1 dependent accumulation of RNA degradation intermediates (Gandhi et al, 2008). This suggests that depurinated RNA might cause ribosome stalling and induce NGD. However, the mechanistic characteristics of RNA degradation differ from NGD as described above. Instead of accumulation of a 5' intermediate in a strain in which 3' to 5' degradation was blocked and accumulation of a 3'

intermediate in a strain in which 5' to 3' degradation was blocked, the authors observed the accumulation of a 3' intermediate in the first strain and a 5' intermediate in the second strain. This does not correspond to the results of an NGD endonucleolytic cleavage, but could instead be the consequence of the depurination site blocking progress of the exonucleases that might start degrading the RNA from its ends.

An mRNA that contains a sequence encoding multiple consecutive basic amino acids induces NGD. The production of a stretch of positively charged amino acids causes ribosomes to pause due to interaction of the positively charged nascent peptide with the negatively charged ribosomal tunnel *in vitro* (Lu & Deutsch, 2008; Lu et al, 2007). *In vivo* positively charged amino acids have been shown to locally slow down translating ribosomes (Charneski & Hurst, 2013). Similar to stem-loop induced NGD, stretches of 12 arginines (R12) or lysines (K12) cause the accumulation of a 5' degradation intermediate in a *ski2*Δ strain and a 3' intermediate in a *xrn1*Δ strain, when inserted between GFP and FLAG in a GFP-FLAG-HIS3 reporter gene, indicating endonucleolytic cleavage. The level of the 5' intermediate is at least partly dependent on the presence of Dom34 (Kuroha et al, 2010).

A quadruple repeat of the very inefficiently translated arginine codon CGA (Letzring et al, 2010) appeared particularly efficient in triggering NGD. It causes a 5-fold decrease in the half life of a reporter PGK1 mRNA (Chen et al, 2010). Whereas for other stall sites either translational stalling or RNA degradation appear thus inefficient that steady state levels of full length mRNAs are not visibly affected (Kuroha et al, 2010), see results section), a CGA repeat reduces them by 75%. The CGA repeat causes the accumulation of NGD intermediates when Xrn1 or exosome-mediated degradation is defective. In contrast to other stall sites, deletion of Dom34 or Hbs1 does not lead to reduced accumulation of the intermediates, indicating that their production and decay are Dom34-Hbs1 independent (Chen et al, 2010).

Finally G-rich nucleotide sequences have been shown to cause the accumulation of expected NGD intermediates in strains defective for Xrn1 or exosome-mediated degradation, when inserted in a GFP-FLAG-HIS3 reporter mRNA. It was proposed that these G-rich sequences form a stable quadruplex structure that does not allow ribosomes to pass. The accumulation of NGD intermediates is Dom34-Hbs1 dependent (Tsuboi et al, 2012).

In summary various stall sites can induce NGD. The efficiency of mRNA degradation and the Dom34-Hbs1 dependence of NGD intermediate accumulation vary per type of stall site.

1.4.1.3 Endonucleolytic cleavage

NGD starts with an endonucleolytic cleavage. The identity of the endonuclease has not been identified so far. The N-terminal domain of Dom34 from *S. cerevisiae* and an archaeal paralog has been reported to have ribonuclease activity in *in vitro* experiments(Lee et al, 2007). However, these observations could not be reproduced with *S. cerevisiae* Dom34 (Passos et al, 2009). That Dom34 is not the endonuclease is further supported by many *in vivo* studies in which reporter mRNAs were still cleaved in absence of Dom34, even though in most cases with less efficiency (Chen et al, 2010; Kuroha et al, 2010; Passos et al, 2009). It has also been excluded that the endonuclease activity of the exosome is responsible for NGD cleavage (Schaeffer & van Hoof, 2011).

Several attempts have been made to map the exact sites of cleavage induced by various stall sites, using methods like analysis of the resulting fragments on gel or by northern blotting, 5'-RACE and primer extension experiments. In most cases cleavage sites were identified at one or multiple locations upstream of the site where a ribosome was expected to stall (Chen et al, 2010; Doma & Parker, 2006; Tsuboi et al, 2012). At least in case of a stem loop, some cleavage sites were identified downstream of the stall site as well (Doma & Parker, 2006).

If stalling is strong and certainly if stalled ribosomes cannot be released, one would expect that additional ribosomes queue up upstream of the primarily stalled ribosome. These secondarily stalled ribosomes may also induce mRNA cleavage. Indeed there is evidence that multiple cleavages can occur due to queuing of ribosomes (Tsuboi et al, 2012) (see paragraphs 1.4.4.1 and 1.4.5).

1.4.2 Non-functional ribosomal RNA decay

In NRD rRNAs that are defective in translation are degraded. The pathway was first described by LaRiviere et al. in 2006 and has only been studied in *S. cerevisiae*. It was found that specific mutations in rRNAs that make them functionally defective do not affect their maturation, but the resulting mature rRNAs are rapidly degraded. This leads to a 5 to 10-fold decrease in their steady state level. The mutants studied affected either positions G530 or A1492 (*E. coli* numbering system) of the 18S rRNA, which are important nucleotides in the decoding center, and positions A2451 or U2585 of the 25S rRNA, located in the peptidyl transferase center (LaRiviere et al, 2006).

1.4.2.1 Non-functional ribosomal RNA decay on defective 18S rRNAs

Mutant 18S rRNAs localize in the cytoplasm, with the same diffuse distribution as wild type 18S rRNAs. Their degradation is inhibited by the translation elongation inhibiting antibiotic cycloheximide (Cole et al, 2009) and they are found in both 40S and 80S peak of polysome profiles obtained by sucrose density sedimentation (LaRiviere et al, 2006). This suggests that 40S subunits containing defective 18S rRNAs can associate with 60S subunits, that the affected 40S subunits participate in (inefficient) translation and that this participation in translation is required for the detection and degradation of the defective 18S rRNA.

The mechanism of defective 18S rRNA degradation and the machinery involved is not completely known (Figure 27). Although mutant 18S rRNAs are partly stabilized (2-fold) in strains defective for recruitment of the cytoplasmic exosome (*ski7*Δ), a mutation in the exosome's catalytic subunit Dis3 does not affect their stability. In some genetic backgrounds, but not in others, mutant 18S rRNAs are partly stabilized (3-fold) in strains lacking Xrn1. 18S NRD targets co-localize with NGD targets in P-bodies when Xrn1 mediated degradation is blocked. Importantly, mutant 18S rRNAs are stabilized 2-fold in absence of Dom34 or Hbs1, with deletion of Dom34 or Hbs1 in combination with deletion of Xrn1 or Ski7 resulting in a dramatic, synergistic stabilization (Cole et al, 2009). Possibly, Dom34-Hbs1 mediated ribosome dissociation is required to make the defective 18S rRNA in the 40S subunit accessible for the degradation machinery.

The 18S NRD pathway may target 18S rRNAs other than those with defects in the decoding center. In yeast with reduced activity of the Rio1 protein, a factor involved in 40S ribosomal subunit maturation, 40S particles containing 20S precursors of the 18S rRNA were found to accumulate and 18S rRNA levels were dramatically decreased. These immature 40S subunits are capable of binding 60S subunits and mRNA. The levels of 18S and 20S rRNAs suggested that large part of the accumulating 20S rRNAs are rapidly degraded. These findings, indicating degradation of immature rRNAs, that are part of ribosomes that may initiate translation but are probably defective in translation elongation, resemble the characteristics of 18S NRD. Moreover it was found that deletion of *DOM34* or *HBS1* causes a restoration of 18S rRNA levels accompanied by a decrease in 20S rRNA levels and it rescues the strain's growth defect. The authors' interpretation suggested that in absence of Dom34 or Hbs1 less efficient 20S rRNA degradation causes more pre-40S subunits to be available as substrates for the partially defective Rio1 to complete 40S subunit maturation (Soudet et al, 2010).

In summary, 18S NRD is a second pathway in which RNAs that cause inefficient translation are targeted for degradation and in which the Dom34-Hbs1 complex plays a role.

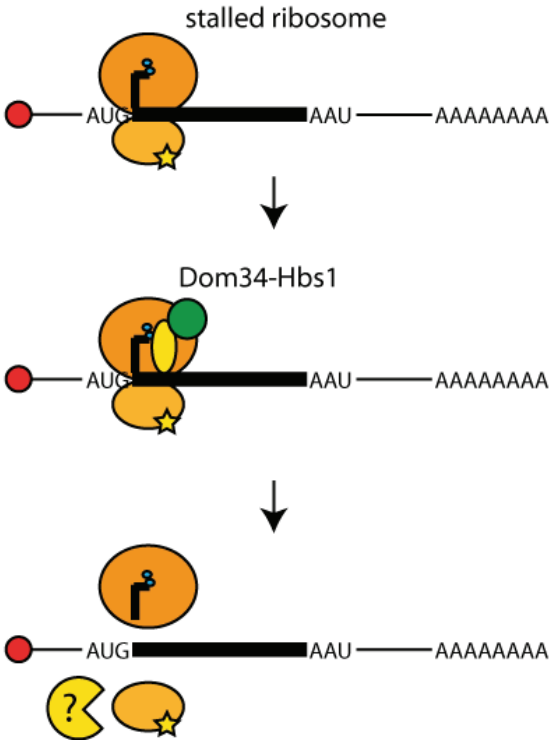

Figure 27 Non-functional 18S rRNA decay model.

1.4.2.2 Non-functional ribosomal RNA decay on defective 25S rRNAs

25S NRD differs from 18S NRD in several mechanistical aspects. In contrast to mutant 18S rRNAs, degradation of mutant 25S rRNAs is not inhibited by cycloheximide and is therefore not translation dependent. The RNA degradation machinery involved differs as well: no nucleases destabilizing defective 25S rRNAs have been identified so far. In particular Xrn1 and the exosome or the factors Dom34 or Hbs1 do not affect mutant 25S rRNA stability (Cole et al, 2009). Although deletion of Xrn1 does not affect the rate of degradation of a defective 25S rRNA, it results in the appearance of a shorter fragment (Cole et al, 2009) suggesting that the exonuclease might be involved in the degradation of decay intermediates produced from defective 25S rRNAs. Mutant 25S rRNAs localize at different sites than 18S rRNAs. They have been found in perinuclear foci, contrasting with the diffuse localization of mutant 18S rRNAs (Cole et al, 2009). 25S NRD was found to depend on several factors involved in protein degradation. This suggests that degradation of ribosomal proteins or ribosome associated proteins precedes and is required for the degradation of defective 25S rRNAs. 18S NRD does not depend on these factors (Fujii et al, 2009; Fujii et al, 2012).

1.4.3 Non-stop decay

In NSD mRNAs that lack a termination codon are rapidly degraded. Translation of these non-stop (NS) mRNAs results in stalled ribosomes, as in absence of a stop codon no canonical termination is possible. The term NSD has been used to describe the rapid decay of two types of non-stop mRNAs that mechanistically share some characteristics but differ on other points (Figure 28).

1.4.3.1 NSD substrates

The first type of these NS messages are polyadenylated mRNAs of which the ORF lacks an in frame termination codon. Poly(A)+ NS messages can result from the use of polyadenylation signals in an ORF or from point mutations that change a stop codon into a sense codon. Whereas translation of the first type results in the production of a truncated protein, the second type produces a longer protein consisting of a translated ORF and 3'UTR. In both cases the C-terminus of the protein contains a stretch of lysines resulting from translation of the poly(A) tail. As described in paragraph 1.4.1.2, a stretch of lysines causes ribosomes to stall. It is therefore not surprising that NSD and NGD share several mechanistic characteristics.

Genome wide analyses of mutations and SNPs in humans have identified over 100 mutations that change a stop codon into a sense codon {(Hamby et al, 2011; Yamaguchi-Kabata et al, 2008). Several diseases have been described to be caused by mutations turning stop codons into sense codons (Klauer & van Hoof, 2012). In some of these cases the affected mRNAs do not contain stop codons in the 3'UTR, downstream of the mutated stop codon, turning them into NS mRNAs (e.g.(Seminara et al, 2003; Taniguchi et al, 1998). The pathological effect of these mutations may result from the low protein levels produced from the NS transcripts. Therefore, if protein products from the NS mRNAs are not toxic the NSD mechanism contributes to pathology instead of preventing it.

The biological relevance of the NSD pathway is more likely to result from reducing levels of proteins produced from mRNAs that are prematurely polyadenylated. Premature polyadenylation is likely to occur with a certain frequency: many ORFs identified in human and yeast contain a consensus sequence for 3' cleavage and polyadenylation in their coding region (Frischmeyer et al, 2002). Moreover, it was found in HeLa cells that introns frequently contain cryptic polyadenylation signals (Kaida et al, 2010). Although premature cleavage and

polyadenylation at these sites is suppressed in a U1-dependent manner, NSD could provide a mechanism to prevent protein production from mis-spliced mRNAs.

A second type of NS mRNAs lacks both a stop codon and a poly(A) tail. These poly(A)- NS mRNAs may result from endonucleolytic cleavage in the ORF of an mRNA, such as occurs during NGD (Doma & Parker, 2006) or during NMD in some species (Eberle et al, 2009; Gatfield & Izaurralde, 2004). Translation of poly(A)- mRNAs would result in the production of a truncated protein. To study the fate of poly(A)- NS mRNAs, constructs have been used in which a hammerhead ribozyme (Rz) sequence was inserted in an ORF (Kobayashi et al, 2010; Meaux & Van Hoof, 2006; Schaeffer & van Hoof, 2011). The Rz cleaves the mRNA, and therefore transcription of these genes results in a capped mRNA sequence that lacks stop codon and poly(A) tail but contains instead an unconventional 2'-3' cyclic phosphate at its 3' end.

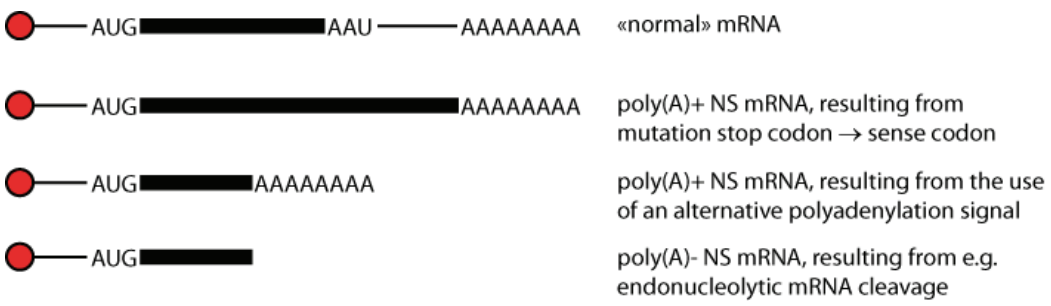

Figure 28 NSD substrates

1.4.3.2 Mechanism of non-stop mRNA degradation

Poly(A)+ NS mRNAs are unstable compared to their stop codon containing counterparts. This destabilization has been described for various mRNAs in *S. cerevisiae*, human and mouse cells (Frischmeyer et al, 2002; Inada & Aiba, 2005; Ito-Harashima et al, 2007; Kong & Liebhaber, 2007; Saito et al, 2013). The reduction in stability varies between different mRNAs, ranging from a reduction in half life that is 1.7-fold for a GFP-2A-HIS3-NS mRNA (Ito-Harashima et al, 2007) to 6.5 fold for a PGK1-NS mRNA (Frischmeyer et al, 2002) in *S. cerevisiae*. This indicates that the efficiency of NSD may depend on the type of mRNA or genetic background. In mammalian cells, variation in NSD efficiency appears even larger, with some NS mRNAs not being targeted for degradation at all. In HeLa cells the RNA level of GFP-NS was found to be similar to the mRNA level of its stop codon containing counterpart (Akimitsu et al, 2007) and in a mitochondrial neurogastrointestinal

encephalomyopathy patient a TYMP-NS mRNA was present at the same level as wild type TYMP mRNA (Torres-Torronteras et al, 2011).

Addition of cycloheximide stabilizes PGK1-NS mRNAs in *S. cerevisiae* and RPS19-NS mRNAs in human cells (Chatr-Aryamontri et al, 2004; Frischmeyer et al, 2002). In HeLa cells decay of a Flag-β-globin-NS mRNA was inhibited by cycloheximide and stimulated by specific translational activation (Saito et al, 2013). These observations indicate that NSD of poly(A)+ substrates is translation dependent.

Rapid degradation of both poly(A)+ and poly(A)- NS mRNAs is mediated by the cytoplasmic exosome and requires Ski7 and the Ski complex in *S. cerevisiae* (Figure 29). Absence of either one of the latter factors increases PGK1-NS stability to almost the same level as that of PGK1. (Frischmeyer et al, 2002; van Hoof et al, 2002). Absence of Ski7 leads to increased stability of the the poly(A)- NS mRNAs ProteinA-Rz (Meaux & Van Hoof, 2006) and GFP-Rz (Tsuboi et al, 2012) and Ski2 deletion causes increased levels of GFP-Rz mRNA (Kobayashi et al, 2010).

NSD of poly(A)+ substrates, of poly(A)- substrates and normal cytoplasmic mRNA turnover by the exosome differ in at least three aspects. Whereas for normal turnover and poly(A)-NSD only the N-terminal part of Ski7 is needed, poly(A)+ NSD requires both the N-terminal and the C-terminal parts of Ski7 (Tsuboi et al, 2012; van Hoof et al, 2002). Together with the fact that the C-terminal part of Ski7 resembles the C-terminal parts of other translational GTPases that bind the ribosome (see paragraph 1.1.3.1.3) and the finding that Ski7 physically interacts with the exosome (Araki et al, 2001; van Hoof et al, 2002), this suggests that Ski7 recruits the exosome to ribosomes stalled on poly(A)+ NS mRNAs. A second difference is that either the exo- or the endonuclease activity of the exosome's catalytic subunit Dis3 is sufficient for both poly(A)+ and poly(A)- NSD, whereas normal turnover is mediated by the exonuclease activity only (Schaeffer & van Hoof, 2011). Finally, whereas normal mRNA turnover by the exosome is preceded by a rate-limiting deadenylation step (see paragraph 1.1.3.1.1), in *S. cerevisiae* as well as mouse MEL/tTA cells the rapid decay of poly(A)+ NS mRNAs does not involve or depend on deadenylation by the deadenylases that act in regular RNA decay (Kong & Liebhaber, 2007; van Hoof et al, 2002).

As Ski7 is present only in a subset of *Saccharomycete* yeasts (Atkinson et al, 2008), NSD in all other eukaryotic cells should differ in mechanistic details. In HeLa cells it was found that the rapid degradation of the poly(A)+ Flag-β-globin-NS mRNA requires the two human Ski2 homologs Ski2 and Mtr4 and exosome subunit Dis3. Moreover it was found that also Hbs1, which is the protein most closely related to Ski7 in mammalian cells, and its partner Dom34

are required for efficient NSD. As these factors were observed to physically interact with the exosome and Ski complex, it was suggested that in mammalian cells they might replace Ski7 function and recruit the exosome to ribosomes on a poly(A)+ NS mRNA (Saito et al, 2013). On the other hand, the requirement of the Dom34-Hbs1 complex for NSD can be explained by its function to dissociate ribosomes stalled on the NS-mRNA. When not removed these ribosomes may block passage of the exosome (see paragraph 1.4.4.1).

It has been reported that the 5' to 3' degradation pathway also plays a role in poly(A)+ NSD. A *dcp1-2* mutant causes further stabilization of NS mRNAs in a *ski7*Δ background (Inada & Aiba, 2005). However, from the presented data it cannot be excluded that this is only because the (partly stabilized) NS mRNAs are substrates of "normal" cytoplasmic mRNA turnover.

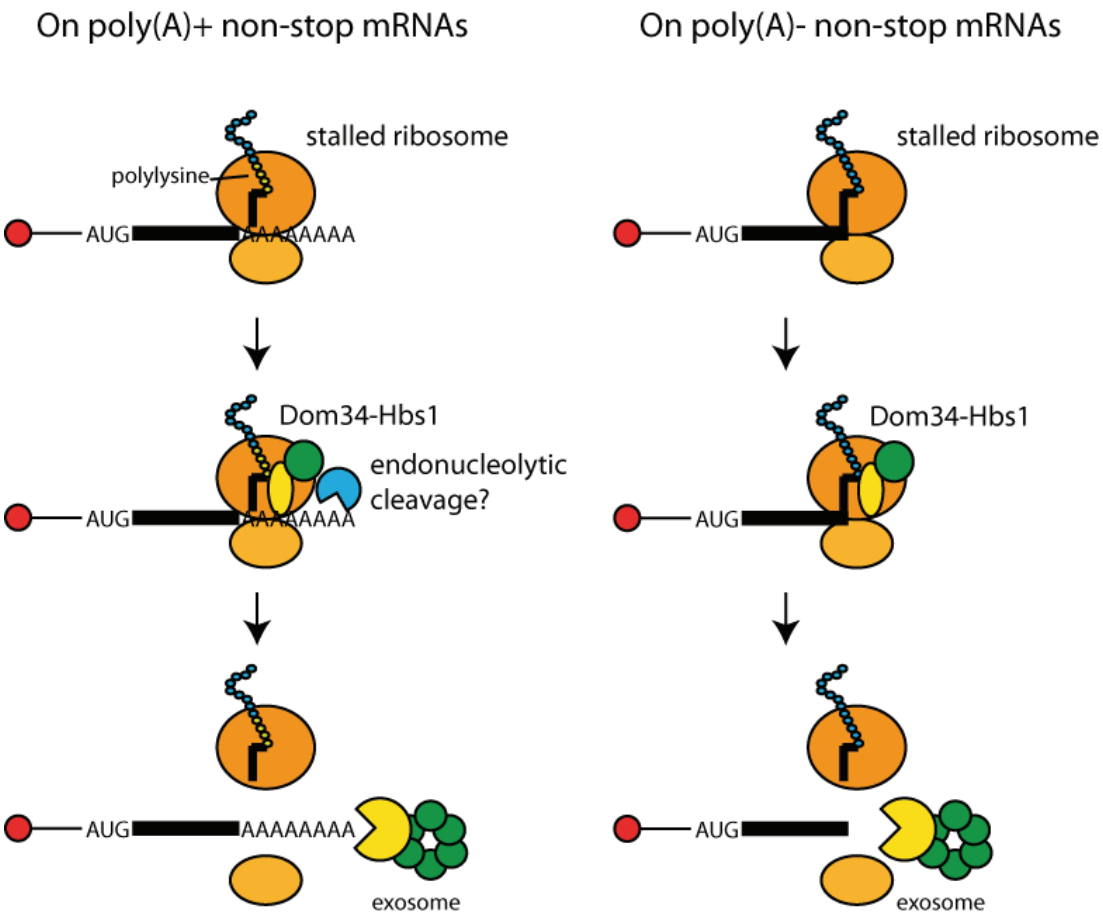

Figure 29 Non-stop decay model

1.4.4 The fate of stalled ribosomes and their nascent peptides

The detection of NGD, NSD and 18S NRD substrates all depend on translation that results in stalling of a ribosome at a site where it cannot terminate. Whereas in 18S NRD, a defective ribosome may not translate far enough into the ORF to produce peptides of biological significance, in NGD and NSD this may lead to the production of potentially harmful protein products. Another problem is that translation cannot terminate properly and without alternative recycling mechanisms peptidyl-tRNA containing ribosomes get stuck on the mRNA. To deal with these problems, cells have mechanisms to degrade the produced peptide and to release the ribosomes that cannot terminate. These mechanisms were all studied in *S. cerevisiae*.

1.4.4.1 Recycling of stalled ribosomes

Translation of NGD and NSD substrates, or by defective ribosomes result in stalling of ribosomes on sense codons or without any codon in their A-sites. The latter occurs on poly(A)- NS mRNA and on NGD substrates after cleavage, which results in a ribosome associated stop codon-less 5' fragment similar to a poly(A)- NS mRNA. These ribosomes cannot terminate or recycle via the canonical pathway. Impaired recycling is expected to cause queuing of upstream ribosomes and a decreased rate of translation. Indeed a HIS3-NS mRNA is associated with higher polysome fractions than its stop codon containing counterpart in *S. cerevisiae* (Inada & Aiba, 2005) and both in *S. cerevisiae* and in HeLa cells initiation-independent repression of translation of poly(A)+ NS mRNAs has been described (Akimitsu et al, 2007; Ito-Harashima et al, 2007). Dom34, Hbs1 and Rli1 provide a rescue mechanism that allows the recycling of stalled ribosomes, independent of the codon in the A-site.

Together with Rli1, Dom34 and Hbs1 can induce the dissociation of ribosomes stalled on mRNAs *in vitro* (Pisareva et al, 2011; Shoemaker et al, 2010; Shoemaker & Green, 2011). Several lines of *in vivo* evidence, in *S. cerevisiae*, support that these factors dissociate peptidyl-tRNA associated ribosomes stuck on poly(A)+ and poly(A)- NS mRNAs.

First, in absence of Dom34 peptidyl-tRNA produced from the poly(A)- NS mRNA GFP-Rz remains ribosome bound, which is not the case when Dom34 is present, supporting the idea of Dom34 dependent dissociation of the stalled complex. Second, deletion of *DOM34* stabilizes GFP-Rz, HIS3-NS and RNA14-NS mRNAs in wild type or *xrn1*Δ but not in *ski2*Δ background. This suggests that in absence of functional Dom34-Hbs1 complex, a non-

dissociated ribosome at the 3' end of these mRNAs blocks degradation by the exosome (Tsuboi et al, 2012). On the other hand, it could also be interpreted as Dom34 being needed for exosome recruitment (Saito et al, 2013). Third, in a *ski2*Δ context, in which poly(A)- NS mRNAs are stabilized, deletion of Dom34 causes a large reduction in the level of protein produced from a GFP-Rz mRNA (Kobayashi et al, 2010; Tsuboi et al, 2012). This can be interpreted as inhibited recycling of stalled ribosomes severely reducing translation rates.

Finally, deletion of Dom34 in a *ski2*Δ or *xrn1*Δ background leads to the appearance of a ladder of stabilized mRNA fragments resulting from a GFP-Rz mRNA and a HIS3-NS mRNA, that differ in size by the space a ribosome would occupy on the mRNA (Tsuboi et al, 2012). This was interpreted to reflect queuing of stalled ribosomes on a poly(A)+ NS mRNA when their dissociation is inhibited, with endonucleolytic cleavages being induced at different places between stalled ribosomes, reminiscent of the cleavages observed in NGD.

In vitro Dom34-Hbs1-Rli1 mediated dissociation of stalled ribosomes was efficient only when the RNA downstream of the A-site was of small length (Pisareva et al, 2011; Shoemaker & Green, 2011). This suggests that during NGD mRNA cleavage precedes ribosome recycling. The fact that the 5' cleavage product is similar to a poly(A)- NS mRNA suggests that recycling of ribosomes stalled on NGD substrates follows a mechanism similar to recycling of ribosomes on poly(A)- NS mRNAs. Indeed, deletion of Dom34 in a wild type background, causes accumulation of 5' cleavage products from mRNAs containing G-rich sequences, K12 or a stretch of rare (mostly arginine) codons, suggesting that stalled ribosomes block passage of the exosome (Tsuboi et al, 2012).

1.4.4.2 Nascent peptide degradation

The peptides produced from mRNAs containing a stall site are actively degraded. This was first described for truncated proteins produced from a GFP-HIS3-K12 reporter, which were found to be highly unstable (Ito-Harashima et al, 2007). Incomplete proteins produced from K12 or R12 containing mRNAs were found to be degraded by the proteasome, a large protein complex that is responsible for the majority of protein degradation in the eukaryotic cell. Inhibition of the proteasome leads to the accumulation of a truncated protein product from GFP-K12-FLAG-HIS3 and GFP-R12-FLAG-HIS3 reporters and from similar reporters containing insertions of endogenously occurring sequences that encode K/R rich peptides (Dimitrova et al, 2009). The accumulation of these truncated proteins depends on the presence of Rack1. Absence of this ribosome associated factor results in increased levels of full length

proteins and in a slight reduction in NGD efficiency. It is therefore proposed that Rack1 is required for ribosome stalling on stretches of basic amino acids (Kuroha et al, 2010).

Proteins are targeted for proteosomal degradation by polyubiquitination. Two E3 ubiquitin ligases were found to be responsible for targeting incomplete proteins produced from mRNAs containing K12 or R12 stall sites for degradation. These factors are Ltn1 and Not4. Deletion of Not4 inhibits the degradation of truncated proteins produced from GFP-K12-FLAG-HIS3 and GFP-R12-FLAG-HIS3 mRNAs (Dimitrova et al, 2009). Ltn1 is responsible for polyubiquitination and degradation of a GFP-FLAG-HIS3-K12 protein product, the stability of which is not affected by Not4 (Bengtson & Joazeiro, 2010). This suggests that the targets of Not4 and Ltn1, although both characterized by basic amino acid dependent ribosome stalling, may not overlap and depend on other factors than the stall site itself. Interestingly no truncated protein product resulting from a stem loop containing GFP-SL-FLAG-HIS3 mRNA was detected upon proteasome inhibition (Dimitrova et al, 2009). As stem loop containing NGD substrates are polyubiquitinated in rabbit reticulocyte lysates (Shao et al, 2013), this probably reflects the weakness of stem loop induced stalling in yeast.

Proteins produced from poly(A)+ NS mRNAs are also rapidly degraded: in *S. cerevisiae* their half lives are reduced compared to those of proteins translated from their stop codon containing counterparts (Bengtson & Joazeiro, 2010; Ito-Harashima et al, 2007). Similarly to truncated peptides produced from mRNAs containing a K12 stall site in their ORF, NS-proteins are degraded by the proteasome (Bengtson & Joazeiro, 2010; Ito-Harashima et al, 2007). Their degradation requires ubiquitination by Ltn1 (Bengtson & Joazeiro, 2010; Wilson et al, 2007). Polyubiquitination of the peptide by Ltn1 occurs at least partly while it is still associated with the ribosome as a peptidyl-tRNA: in a *ltn1*Δ strain the poly(A)+ NS protein accumulates in the 80S fraction (Bengtson & Joazeiro, 2010). The degradation mechanism of NS proteins strongly resembles that of peptides produced from some mRNAs containing K12 or R12 stall sites. Since the poly(A) tail translates into a stretch of polylysines, it is conceivable that stalling of a ribosome translating the poly(A) tail plays an important role in triggering the degradation of the peptide produced.

In rabbit reticulocyte lysate it was found that peptides produced from poly(A)+ NS mRNAs, poly(A)- NS mRNAs, and mRNAs containing a K12 or stem loop stall site are polyubiquitinated while still linked to the tRNA and bound to the ribosome. For a poly(A)-NS protein it was specified further that efficient ubiquitation requires dissociation of the stalled ribosome (see below) and that it depends on the Ltn1 homolog Listerin, which binds mainly to the ribosomal 60S subunit (Shao et al, 2013). Studies in *S. cerevisiae* showed that

ubiquitination of poly(A)+ NS-peptides by Ltn1 can start on 80S ribosomes, but that larger ubiquitin chains are found associated to ribosomes. Together these findings suggest that ubiquitination may start on 80S ribosomes, but, at least in mammalian systems, requires ribosomal subunit dissociation to produce larger chains.

Recent studies in *S. cerevisiae* found Ltn1 to be part of a Ribosome Quality Control complex (RQC) that also comprises the factors Tae2, Rqc1 and the hexamer forming protein Cdc48 with its cofactors (Figure 30). The whole RQC associates with 60S ribosomal subunits and its factors are needed for the degradation of peptides produced from poly(A)+ NS mRNAs and mRNAs containing an R12 stall site (Brandman et al, 2012; Defenouillere et al, 2013; Verma et al, 2013). Cdc48 is a force generator that in several of its functions extracts proteins or peptides from protein complexes or through pores across membranes (Stolz et al, 2011). It was therefore hypothesized that Cdc48 may extract the peptide from the 60S subunit's peptide tunnel and escort it to the proteasome (Brandman et al, 2012; Defenouillere et al, 2013; Verma et al, 2013).

Together these observations indicate that stalled ribosomes bind the RQC, possibly already when ribosomal subunits are still associated, but more so after subunit dissociation (see below). Ltn1 in the RQC ubiquitinates the 60S bound peptidyl-tRNA. Then Cdc48 and its cofactors can extract the peptide and guide it to the proteasome.

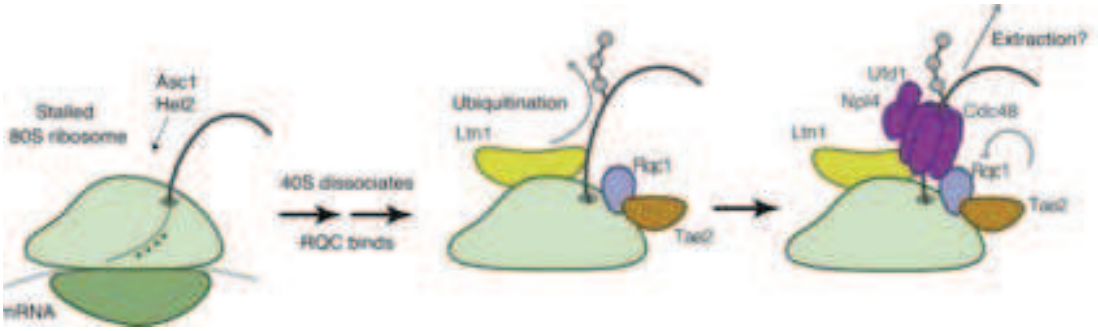

(Brandman et al, 2012)

Figure 30 Model of RQC mediated degradation of nascent peptides produced by stalled ribosomes.

1.4.5 Multiple roles for the Dom34-Hbs1 complex?

The Dom34-Hbs1 complex has been interpreted to play two separate roles in quality control pathways acting on stalled translational complexes. First, their absence was observed to cause a reduction in the accumulation of mainly the 5' NGD cleavage product, in strains deficient for exosome mediated degradation (see paragraph 1.4.1.1). This was interpreted to reflect

stimulation of the endonucleolytic cleavage by the Dom34-Hbs1 complex (Doma & Parker, 2006; Tsuboi et al, 2012). Second, the complex dissociates stalled ribosomes, which is thought to make ribosomal subunits and other translational factors available for new rounds of translation, and promotes the degradation of no-go and non-stop mRNAs (Pisareva et al, 2011; Shoemaker et al, 2010; Shoemaker & Green, 2011; Tsuboi et al, 2012) (see paragraph 1.4.4.1). However, one could argue that the dependence of NGD cleavage product accumulation on the Dom34-Hbs1 complex can be attributed to its ribosome dissociating activity too.

As described in paragraph 1.4.4.1, absence of Dom34 stabilizes poly(A)- NS mRNAs, which mimic 5' NGD intermediates, in wild type and *xrn1*Δ background, suggesting that non-recycled ribosomes block passage of the exosome. In contrast, in a *ski2*Δ strain, in which the NS mRNA is stabilized, absence of Dom34 causes destabilization of poly(A)- NS mRNAs. This was interpreted to be the result of multiple endonucleolytic cleavages induced by the queue of ribosomes stalled in absence of Dom34-Hbs1 mediated release (Tsuboi et al, 2012). By the same mechanism absence of functional Dom34-Hbs1 could cause destabilization of 5' NGD cleavage products, in strains defective for cytoplasmic exosomal degradation. Following this explanation, the lower level of 5' NMD cleavage products in absence of Dom34 or Hbs1 is not due to Dom34-Hbs1 being required for their production, but because in absence of Dom34-Hbs1 the fragments are destabilized.

1.5 PROJECT OUTLINE

In my PhD work I studied the function of the complex formed by Dom34 and Hbs1. In the first part of my work I focused on RNA quality control pathways the Dom34-Hbs1 complex functions in. In the second part I studied the biological relevance of Dom34-Hbs1 mediated ribosome dissociation. This included a search for roles of the complex beyond RNA quality control.

1.5.1 The Dom34-Hbs1 complex and RNA quality control

NGD, 18S NRD and NSD share several characteristics, including inefficient translation or ribosomal stalling as a trigger for RNA degradation and the involvement of Dom34 and Hbs1. At the moment my work on this project started, the involvement of Dom34 and Hbs1 in NSD was not yet defined, therefore my work focuses on NGD and 18S NRD. Because of the similarities between these pathways it has been hypothesized that they may reflect one single pathway, in which the recruitment of Dom34 and Hbs1 to stalled ribosomes induces degradation of mRNA and 18S rRNA and induces ribosome dissociation (Cole et al, 2009; Soudet et al, 2010).

During my thesis I tried to obtain more insight into the function Dom34, Hbs1 and other factors in NGD and 18S NRD. Questions I addressed were:

- What are the functional requirements of the Dom34-Hbs1 complex in NGD and 18S NRD? More specifically I addressed the importance of the GTPase activity of Hbs1 and the interaction between Dom34 and Hbs1.
- How do NGD and 18S NRD relate? Do they represent one single pathway in which stalled ribosomes induce degradation of both mRNA and 18S RNA, or do they occur independently?
- What is the endonuclease responsible for mRNA cleavage in NGD?
- Are there other, thus far unidentified factors acting on stalled ribosomes?

To address these questions various approaches were used, using the yeast *S. cerevisiae* as an experimental system. These include a structure-function analysis on the Dom34-Hbs1 complex, in collaboration with Dr. Julien Henri and Dr. Marc Graille, *in vitro* translation experiments, the development of protocols to specifically purify stalled ribosomes with their associated factors and the analysis of the effect of several gene deletions on NGD and 18S NRD.

1.5.2 Biological relevance of Dom34-Hbs1 mediated ribosome dissociation

So far *in vivo* experiments have concentrated mainly on the role of the Dom34-Hbs1 complex in RNA quality control (Tsuboi et al, 2012). Defective RNAs that cause ribosomes to stall are expected to occur with low frequency and may therefore have relatively small consequences for the viability of individual cells, cell populations, or an entire organism. This is consistent with Dom34 being non-essential for viability in yeast, but contrasts with the more severe phenotypes of *DOM34* deletion in higher organisms. For example, in mice Dom34 deficient zygotes do not develop past a stage several days post-fertilization (Adham et al, 2003). I therefore tried to identify other situations in which Dom34-Hbs1 mediated ribosome dissociation is required. More specifically I addressed the following questions:

- Can the Dom34-Hbs1 complex dissociate inactive ribosomes, not associated with mRNA or translation factors, that accumulate during stress conditions, and thereby stimulate recovery of translation upon stress relief?
- Can the Dom34-Hbs1 complex act on post-termination complexes, and thereby replace eRF1-eRF3?
- Is Dom34-Hbs1 mediated removal of ribosomes from mRNAs needed for efficient degradation by Xrn1 or the exosome in general?

These questions where addressed using *S. cerevisiae*. The action of Dom34-Hbs1 on inactive ribosomes was studied in and after glucose depletion stress. Translation was monitored using polysome profiles obtained on sucrose density gradients and by measuring protein production. In collaboration with Anthony Schuller and Dr. Rachel Green (Johns Hopkins University, USA) biochemical ribosome recycling experiments were performed. Other experiments included the analysis of genetic interactions of Dom34 and Hbs1 with termination factors and RNA degradation factors.

The results of my work will be presented in the next section and include one paper published in Nature Structural and Molecular Biology in 2010 and one manuscript that is currently submitted for publication.

2. RESULTS

2.1 STUDY OF THE ROLE OF DOM34-HBS1 IN RNA QUALITY CONTROL

The RNA quality control pathways NGD and 18S NRD have several features in common. In both pathways the recognition of RNA targets depends on inefficient translation and in both pathways Dom34 and Hbs1 affect RNA degradation. In 18S NRD the factors stimulate the degradation of defective 18S rRNAs. In NGD, accumulation of at least the 5' degradation intermediate that results from mRNA cleavage, depends on Dom34 and Hbs1. It has been hypothesized that NGD and 18S NRD may represent one single pathway, in which ribosomal stalling causes Dom34-Hbs1 recruitment, which leads to ribosome dissociation and degradation of at least the mRNA and 18S rRNA (Cole et al, 2009; Soudet et al, 2010). Because Dom34 and Hbs1 are central players in both pathways, we performed a structure-function study on the complex they form. This study resulted in a publication in Nature Structural and Molecular Biology. A summary of this work together with the published article will be presented in the next paragraph. Supplementary data of the publication can be found in the supplementary information of this thesis.

2.1.1 A structure-function study of the Dom34-Hbs1 complex

Our collaborators, Dr. Julien Henri and Dr. Marc Graille, obtained X-ray crystallographic structures of *S. cerevisiae* Hbs1, in apo and GDP bound form. They also made a structural model of the Dom34-Hbs1 complex, based on superposition of Hbs1 and Dom34 crystal structures (Graille et al, 2008; Lee et al, 2007) on eRF1-eRF3 interacting domains (Cheng et al, 2009) and optimization based on comparison of calculated curves with small angle X-ray scattering data obtained from a yeast Dom34-Hbs1 complex. The Dom34-Hbs1 model overall resembled the structural models obtained from archaeal Dom34-aEF1α (Kobayashi et al, 2010) and ribosome bound Dom34-Hbs1 from *S. cerevisiae* (Becker et al, 2011) and differed from the *S. pombe* Dom34-Hbs1 crystallographic structure (Chen et al, 2010) in the orientation of the Hbs1 G domain (see paragraph 1.3.2.1). Similarly to the first two structures, this domain packs against domains II and III of Hbs1. This observation invalidates the hypothesis that the conformation in which the G domain packs against domains II and III is induced by GTP binding (see paragraph 1.3.2.1). In addition to the contacts between the C-terminal domain of Dom34 and domain III of Hbs1, similar to the interaction between the corresponding domains in eRF1-eRF3, the model of the complex predicts a second interface between the central domain of Dom34 and the G domain of Hbs1.

Based on these structural data I studied the importance of the GTPase activity of Hbs1 and of the interaction between Dom34 and Hbs1 for Dom34-Hbs1 function in *S. cerevisiae*. I produced mutants targeting the GTP binding site of Hbs1 as well as Dom34 and Hbs1 mutants that disrupt the interaction between the two factors. The effect of these mutations on Dom34 and Hbs1 function was studied. NGD was assayed by monitoring the Dom34-Hbs1 dependent accumulation of a degradation intermediate (see Figure 31). The effect of the Dom34-Hbs1 mutations on 18S NRD was analyzed by monitoring the steady levels of an 18S rRNA with a defect in the decoding center. In absence of Dom34 or Hbs1 the level of this 18S rRNA increases due to inefficient NRD. Finally, the effect of the Dom34-Hbs1 mutations on growth of yeast strains with a 40S subunit deficiency was studied. As described in paragraph 1.3.1.1, in these strains the absence of functional Dom34 or Hbs1 causes growth defects.

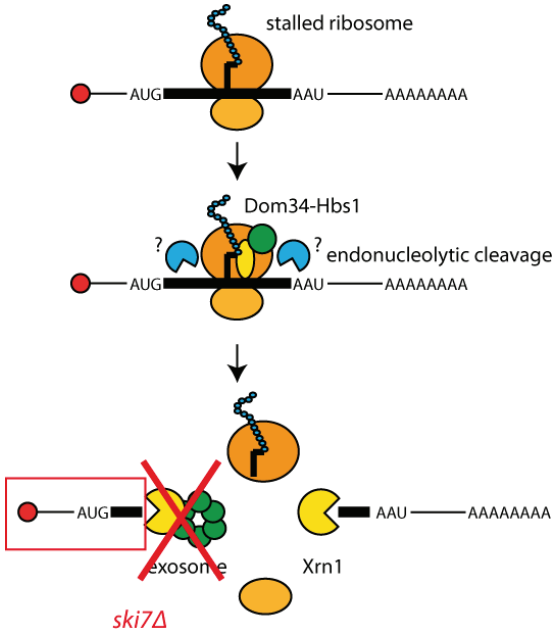

Figure 31 No-go decay assay
In a ski7Δ strain the 5' intermediate (in red rectangle) resulting from mRNA cleavage accumulates. This accumulation is dependent on the presence of functional Dom34 and Hbs1.

I found that GTP binding by Hbs1 is required for all functions tested. A stable interaction between Dom34 and Hbs1 was also required for their function in NGD. However, Dom34-Hbs1 interaction was not or much less important for the complex's function in 18S NRD. Mutations that disrupt Dom34-Hbs1 interaction had no or hardly any effect on growth in a strain with 40S subunit deficiency either. Moreover, an asymmetry was observed between the

effect of mutating Dom34 and mutating Hbs1 residues involved in the interaction. Whereas mutating Dom34 residues important for interaction with Hbs1 had a small effect on 18S NRD and growth in 40S subunit deficient strains, Hbs1 mutations affecting the other side of the interface had no effect at all.

In the paper these results were interpreted as Dom34 and Hbs1 interaction being required for efficient NGD endonucleolytic cleavage, but not for efficient 18S NRD or growth in a 40S subunit deficient strain. The ability to genetically separate these pathways would then indicate that upon recruitment of Dom34-Hbs1 to stalled ribosomes, mRNA and rRNA may not always be degraded simultaneously. However, as described in paragraph 1.4.5, the Dom34-Hbs1 dependence of NGD intermediate accumulation may not represent Dom34-Hbs1 dependent mRNA cleavage but could instead be caused by destabilization of the 5' NGD intermediate in absence of Dom34-Hbs1. This hypothesis would need a different interpretation of these data. This will be addressed further in the discussion section of this thesis.

nature
structural &
molecular biology

Dissection of Dom34–Hbs1 reveals independent functions in two RNA quality control pathways

Antonia M G van den Elzen[1,2,4], Julien Henri[3,4], Noureddine Lazar[3], María Eugenia Gas[1,2], Dominique Durand[3], François Lacroute[2], Magali Nicaise[3], Herman van Tilbeurgh[3], Bertrand Séraphin[1,2] & Marc Graille[3]

Eukaryotic cells have several quality control pathways that rely on translation to detect and degrade defective RNAs. Dom34 and Hbs1 are two proteins that are related to translation termination factors and are involved in no-go decay (NGD) and nonfunctional 18S ribosomal RNA (rRNA) decay (18S NRD) pathways that eliminate RNAs that cause strong ribosomal stalls. Here we present the structure of Hbs1 with and without GDP and a low-resolution model of the Dom34–Hbs1 complex. This complex mimics complexes of the elongation factor and transfer RNA or of the translation termination factors eRF1 and eRF3, supporting the idea that it binds to the ribosomal A-site. We show that nucleotide binding by Hbs1 is essential for NGD and 18S NRD. Mutations in Hbs1 that disrupted the interaction between Dom34 and Hbs1 strongly impaired NGD but had almost no effect on 18S NRD. Hence, NGD and 18S NRD could be genetically uncoupled, suggesting that mRNA and rRNA in a stalled translation complex may not always be degraded simultaneously.

The transfer of genetic information from DNA to RNA in eukaryotes requires a multistep combination of transcription and processing. These processes are sources of errors in which nonfunctional RNAs can affect the accuracy of gene expression. Such mistakes can lead to cell death or disease, and so cells have developed several quality control mechanisms to detect and degrade these nonfunctional RNAs[1,2]. For example, mRNAs containing a premature stop codon or lacking an in-frame stop codon are degraded by the nonsense-mediated decay (NMD)[2,3] and non-stop decay (NSD)[4,5] pathways, respectively. These targets are recognized and degraded through interactions among the translational apparatus, pathway-specific factors and mRNA degradation machineries. These processes prevent the accumulation of aberrant, potentially deleterious proteins while facilitating ribosome recycling.

Recently, two RNA surveillance pathways that involve identical factors have been described in *Saccharomyces cerevisiae*. First, an engineered stable stem-loop that forces the ribosome to pause during elongation was shown to induce rapid mRNA degradation[6]. This was initiated by endonuclease cleavage close to the stem-loop and was followed by 5′→3′ degradation of the 3′ cleavage product by the exonuclease Xrn1 and 3′→5′ degradation of the 5′ cleavage product mediated by the exosome, which was recruited by Ski7 and the Ski complex[6]. This pathway, named no-go decay, or NGD, also targets depurinated mRNAs, which induce stalling of ribosomes[7]. NGD involves the proteins Dom34 and Hbs1 (ref. 6), which are related to the translation termination factors eRF1 and eRF3, respectively.

Dom34 and Hbs1 have also been implicated in the 18S NRD pathway[8,9], which degrades nonfunctional 18S rRNAs that have been associated into ribosomal subunits but cannot support efficient translation. This pathway also targets some immature ribosomes that engage in translation[10]. Neither Dom34 nor Hbs1 is required for efficient growth in *S. cerevisiae*. However, deletion of *HBS1* or *DOM34* causes severe growth defects in strains that contain a null allele for one out of several genes that encode proteins of the small ribosomal subunit (*RPS30A*, *RPS30B*, *RPS14A*)[11]. These strains are still viable, as pairs of genes encode the corresponding ribosomal proteins. However, in such strains the remaining gene copy is probably insufficient to maintain a proper balance of the corresponding protein, leading to the accumulation of incomplete or unstable small ribosomal subunits that are predisposed to stalling. Hence, there is growing evidence that Dom34 and Hbs1 are involved in clearing RNAs that induce translational stalls from cells.

Studies in yeast, *Drosophila* and mouse have shown that Dom34 (known as Pelota in higher eukaryotes) is required for correct cell divisions[12–15]. Dom34 is structurally related to the translation termination factor eRF1 except for its N-terminal domain, which adopts an Sm-fold that is commonly found in RNA recognition or degradation factors[16,17]. This domain has been reported to have an *in vitro* divalent

[1]Equipe Labellisée La Ligue, Institut de Génétique et de Biologie Moléculaire et Cellulaire (IGMBC), Illkirch, France; Centre National de la Recherche Scientifique (CNRS) UMR7104, Illkirch, France; Inserm, U964, Illkirch, France; Université de Strasbourg, Strasbourg, France. [2]Centre de Génétique Moléculaire (CGM), CNRS FRE3144, Gif-sur-Yvette, France. [3]Institut de Biochimie et Biophysique Moléculaire et Cellulaire (IBBMC), CNRS UMR8619 Bat 430 Université Paris-Sud, Orsay, France. [4]These authors contributed equally to this work. Correspondence should be addressed to B.S. (seraphin@igbmc.fr) or M.G. (marc.graille@u-psud.fr).

Received 23 April; accepted 29 October; published online 21 November 2010; doi:10.1038/nsmb.1963

metal ion–dependent endonuclease activity[17]. However, this finding has been challenged[18] because the *in vitro* nuclease activity could not be reproduced and overexpression of Rps30a was sufficient to restore some mRNA cleavage in the absence of Dom34.

Dom34 associates with Hbs1, a member of the family of eEF-1A-like GTPases. This family includes the translation elongation factors eEF-1A and EF-Tu, which deliver amino acyl-transfer RNAs (tRNAs) to the ribosomal A-site, eRF3 and Ski7 (refs. 11,16,19,20). Initially, Hbs1 was identified as a suppressor of Hsp70 subfamily B. In yeast, deletion of both *SSB1* and *SSB2* (which encode Hsp70 chaperones that interact with nascent polypeptide chains as they exit the ribosome) results in slower cell growth, a reduced number of translating ribosomes and slower translation[21]. These phenotypes are suppressed by overexpression of Hbs1, which suggests that Hbs1 helps to mediate stop codon–independent peptide release from ribosomes that are stalled by the absence of Hsp70-mediated nascent polypeptide channeling. This function is related to the one proposed for Hbs1 and Dom34 in both NGD and 18S NRD[22]. Hbs1 is a GTP-binding protein whose affinity for GTP but not GDP is enhanced by Dom34, in a similar way to how eRF1 enhances the ability of eRF3 to bind to GTP[11,16,23].

To gain insight into the mechanisms by which the Dom34–Hbs1 complex takes part in these quality control pathways, we have solved the crystal structure of *S. cerevisiae* Hbs1 and obtained a low-resolution model of the Dom34–Hbs1complex by small-angle X-ray scattering (SAXS). This allowed us to study the precise role of the Hbs1 nucleotide-binding site and its interaction with Dom34 in NGD and 18S NRD, and this revealed that these two processes can be genetically uncoupled.

RESULTS

Overall structure

As the N terminus of *S. cerevisiae* Hbs1 is predicted to be poorly folded, we purified several Hbs1 fragments starting at different positions and obtained diffracting crystals for the construct that encompassed residues 135–610 (hereafter referred to as Hbs1dN134). We solved the structure of this construct using the single-wavelength anomalous dispersion (SAD) method (see **Supplementary Fig. 1** for experimental electron density maps). The structures of the apo and GDP-bound forms were further refined to resolutions of 2.5 Å and 2.95 Å, respectively (**Table 1**). We found that Hbs1dN134 comprised an N-terminal GTPase domain (residues 165–398) and two six-stranded β-barrel domains (domain II, residues 399–498 and domain III, residues 499–610; **Fig. 1a**). The GTPase domain was preceded by a long N-terminal loop (residues 140–164) that was partially folded as an α-helix (αA), which packed against domain II. The GTPase domain adopted the classical α/β structure that is common to GTPases such as EF-Tu, eRF3 and Ras[24,25]. It comprised a central six-stranded β-sheet (strand order β6, β5, β4, β1, β3 and β2, which is antiparallel to the others) flanked by seven α-helices (α1, α2, α6 and α7 on one side of the sheet and α3–α5 on the other). This domain was connected to domain II by a long α-helix (α7; residues 376–398). Domains II and III adopted a fold similar to the corresponding domains from EF-Tu and eRF3 (refs. 24,26). In all structures of members of the eEF-1A superfamily, domains II and III are held in the same relative orientation, but this is not true for the GTPase domain. In the structure of *Schizosaccharomyces pombe* eRF3, there are no contacts between the GTPase domain and domains II and III[24] (**Supplementary Fig. 2a**). In Hbs1dN134, the GTPase domain packed against domains II and III in a manner reminiscent of the EF-Tu–GDPNP complex. SAXS experiments in solution on Hbs1dN134 showed that the conformation observed in our crystal structure fully agrees with the conformation of the protein in solution and hence is not induced by crystal packing (see **Supplementary Data** and **Supplementary Fig. 2**).

Table 1 Data collection and refinement statistics

	Native	SeMet	GDP form
Data collection			
Space group	$P4_22_12$	$P4_22_12$	$P4_22_12$
Cell dimensions			
a, *b*, *c* (Å)	110.6, 110.6, 188.1	110.6, 110.6, 188.1	110.6, 110.6, 188.1
α, β, γ (°)	90, 90, 120	90, 90, 120	90, 90, 120
Resolution (Å)	30–2.5 (2.54–2.5)	30–3.2 (3.39–3.2)	20–2.95 (3.13–2.95)
R_{sym}	0.076 (0.486)	0.087 (0.472)	0.097 (0.491)
$I/\sigma I$	26 (3.7)	12.5 (2.9)	8.5 (2.2)
Completeness (%)	96 (97.3)	99.6 (99.1)	97.9 (98.2)
Redundancy	3.5 (3.7)	3.7 (3.7)	2.6 (2.6)
Refinement			
Resolution (Å)	30–2.5		20–2.95
No. reflections	39,338		45,371
R_{work}/R_{free}	0.216/0.271		0.214/0.277
No. atoms			
Protein	6,887		6,922
Ligand/ion	–		54
Water	275		65
B-factors			
Protein	46.1		52.5
Ligand/ion	–		76.5
Water	45.6		41
R.m.s. deviations			
Bond lengths (Å)	0.006		0.011
Bond angles (°)	1.020		1.358

Values in parentheses are for highest-resolution shell.

The nucleotide-binding site

We have solved the structure of Hbs1dN134 in its apo form and in the presence of GDP. As observed for the archaeal SelB elongation factor and the eukaryotic release factor eRF3 (refs. 24,27), we saw no large-scale domain movements between the apo and GDP-bound forms of Hbs1dN134 (r.m.s. deviation of 0.4 Å over 430 Cα atoms).

GTPases are characterized by the presence of a P-loop and two highly flexible and conserved segments called switch regions I and II that are involved in nucleotide binding. These regions adopt radically different conformations depending on whether GDP or GTP is bound. The structure of the switch regions is highly variable for the GDP forms but invariant for the GTP forms[25]. In the Hbs1dN134 apo form, switch I (residues 194–234) was mostly disordered (absence of electron density for region 205–228), although its N-terminal part folded as a helix (α2). When GDP was bound, a portion from this switch (residues 217–228) folded as a small α-helix (α2′, residues 217–223) antiparallel to helix α2 (**Fig. 1b**). Switch II (residues 251–268) formed an α-helix (α3) that was connected to strand β3 by a loop. The orientation of helix α3 remained constant between the apo and GDP-bound forms, but the β3–α3 loop (residues 251–258) showed some flexibility (**Fig. 1b**). Most of the Hbs1 residues that contacted GDP structurally matched with the corresponding residues in the *Escherichia coli* EF-Tu–GDP complex[28] (**Fig. 1c**). The P-loop coordinated the GDP phosphate groups through the main chain atoms of Val176–Thr182 and side chains from the polar residues Asp177, Ser181 and Thr182.

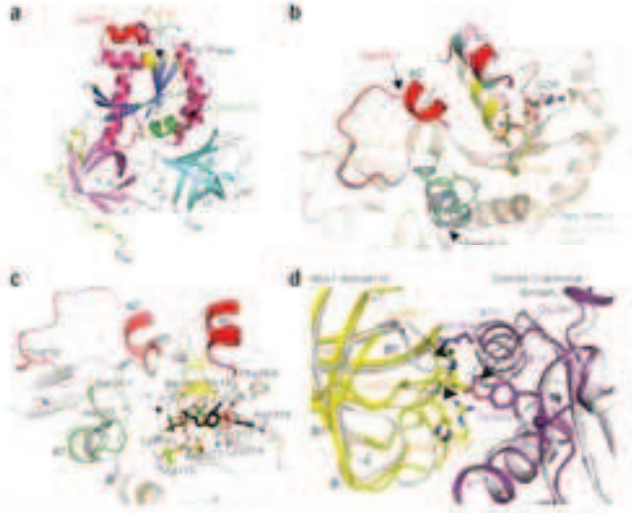

Lys314 and Phe354. In the EF-Tu–GDP complex, switch II contacted the Mg^{2+} ion. This was not the case for the Hbs1dN134–GDP complex as Mg^{2+} was omitted in our experiments owing to its inhibitory effect on binding of GDP to Hbs1 (data not shown).

Two point mutants of the nucleotide binding region have been described[11]: Val176 is part of the P-loop and is involved in phosphate binding (see above), whereas His255 of the switch II region is not directly in contact with GDP in the Hbs1dN134–GDP complex but is probably crucial for GTP binding, hydrolysis or both. To characterize the effect of these mutations on nucleotide binding, we produced three single-point mutants (V176G, H255E and K180A in the P-loop). Isothermal titration calorimetry (ITC) analyses showed that, unlike the wild-type protein, these mutants did not bind guanine nucleotides (**Supplementary Fig. 3a,b**). Circular dichroism (data not shown) and differential scanning calorimetry (DSC) measurements on these mutants suggested that they were correctly folded (**Supplementary Fig. 3**). We conclude that the substitutions that we introduced completely abolished nucleotide binding.

Low-resolution model of the Dom34–Hbs1 complex

Like eRF3 and eRF1, Hbs1 and Dom34 physically interact[11,16]. The eRF1–eRF3 interface is located between the eRF1 C-terminal domain and the domain III of eRF3 (ref. 29), which suggests that the Hbs1–Dom34 complex might be formed through the corresponding domains. Superimposition of these Dom34 and Hbs1 domains onto the eRF1–eRF3 structure provided evidence that this process involves residues from loops connecting strands βA′ to βB′ and βC′ to βD′ of Hbs1 (**Fig. 1d**). In this model, these loops face residues from the C-terminal part of helix α7, from α11 and from β13 of Dom34. This possibility was further supported by *in vitro* interaction data that showed that the Dom34 C-terminal domain, but not its N-terminal or central domains, was crucial for interaction with Hbs1 (data not shown).

To gain further insight into this issue, we performed SAXS measurements on the Dom34–Hbs1dN134 complex (**Fig. 2a** and **Supplementary Fig. 4**). From the crystal structures of yeast and archaeal Dom34 (comparison of these structures revealed large conformational changes), and of yeast Hbs1dN134 and the eRF1–eRF3 complex[16,17,29], we generated two initial models (yeast- and archaea-like) for the Dom34–Hbs1dN134 complex. We then compared the corresponding experimental and calculated scattering curves (see **Supplementary Data** and **Supplementary Fig. 4b,c**). The best agreement with the experimental scattering curve was obtained for the archaea-like model (**Fig. 2a**; χ-value of 5.9 versus 13.4 for the yeast-like model). In addition to the contacts between the Dom34 C-terminal domain and domain III of Hbs1, this model highlights contacts between the Dom34 central domain and the Hbs1 GTPase domain. We performed rigid-body modeling with SASREF[30] to improve the fit between calculated and experimental curves (**Fig. 2a,b**, χ-values ≤ 1.7; see **Supplementary Data** and **Supplementary Fig. 4**). In the resulting Dom34–Hbs1 model, Dom34 adopts a tRNA shape with its N-terminal and central domains matching the anticodon and amino acyl acceptor arms of a tRNA molecule, respectively, as observed in the EF-Tu–tRNA complex[26] (**Fig. 2b,c**). This suggested that Dom34–Hbs1 binds into the ribosomal A site. While this work was in progress, the crystal structures of the Hbs1–Dom34 complex from *S. pombe* (in the absence of nucleotide) and the EF1α–Dom34 complex from the archaea *Aeropyrum pernyx* (in the presence of GTP and Mg^{2+}) were reported[31,32]. In both structures, domain III from Hbs1 or EF1α interacts with the C-terminal domain of Dom34, but these complexes differ in the orientation of the GTPase domain relative to domains II and III. For *S. pombe*, this domain does not interact with Dom34, whereas for *A. pernyx*, this domain rotates by 180° and contacts the central domain from Dom34 as proposed in our model of the *S. cerevisiae* Dom34–Hbs1dN134 complex.

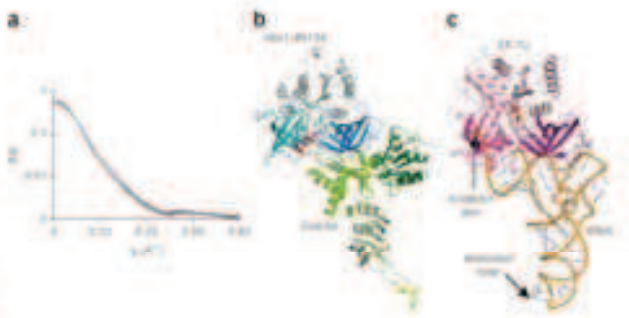

Our model is very similar to the *S. pombe* structure (r.m.s. deviation of 3.3 Å over 540 Cα atoms versus an r.m.s. deviation of 5 Å over 460 Cα atoms for *S. pombe*).

Nucleotide binding by Hbs1 is crucial for 18S NRD and NGD

Binding of GDP and GTP by members of the eEF-1A family is essential for their function. Consistently, two point mutations in the GDP binding site of Hbs1 (V176G and H255E), which abolish nucleotide binding (**Supplementary Fig. 3**), do not complement a deletion of *HBS1* (ref. 11). To investigate the physiological importance of nucleotide binding by Hbs1, we tested the effect of mutations that affect nucleotide binding (V176G, H255E and K180A) on NGD (**Fig. 3**), 18S NRD and growth in strains deleted for a small ribosomal subunit gene in *S. cerevisiae* (**Fig. 4**).

We first constructed a protein A–tagged version of Hbs1 that allowed us to follow its expression. The wild-type Hbs1–protein A fusion protein was indistinguishable from the wild-type non-fusion protein in all assays (see below). Mutants V176G, K180A and H255E accumulated normally in yeast cells (**Supplementary Fig. 5a**) and their DSC measurements were characteristic of well-folded proteins with a peak centered at a melting temperature (T_m) of 47 °C (6.8 °C lower than that of wild-type Hbs1; **Supplementary Fig. 5c**). We investigated the effect of these mutants on NGD as described[3]. Briefly, we monitored the Hbs1 (and Dom34)-dependent accumulation of the 5′ fragment that results from endonucleolytic cleavage of the NGD substrate PGK1-SL (PGK1 containing a stem–loop) in a *ski7*Δ strain[3–5]. Thus, we assayed whether Hbs1 mutants that abolished nucleotide binding could restore the accumulation of this degradation intermediate in a *ski7*Δ*hbs1*Δ strain. In the presence of our mutants, the ratio of degradation intermediate to full-length reporter mRNA was reduced to 30% of the ratio observed in the presence of wild-type Hbs1, a level similar to that detected in the absence of Hbs1 (**Fig. 3a** (lanes 4–6) and **c**).

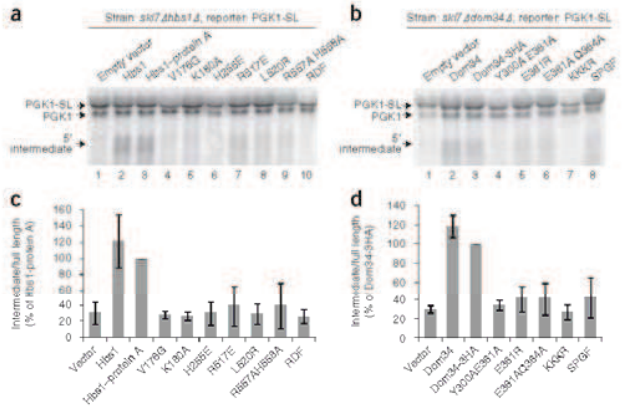

Figure 3 Effects of Hbs1 and Dom34 mutations on NGD. (**a**) Northern blot analysis of the steady-state levels of degradation intermediates of the NGD substrate PGK1-SL in a *ski7*Δ*hbs1*Δ *S. cerevisiae* strain transformed with Hbs1 mutants. The PGK1-SL reporter was expressed from plasmid pRP1251 and detected with oligonucleotide oRP132 (ref. 6). (**b**) Northern blot analysis of the steady state levels of PGK1-SL degradation intermediates in a *ski7*Δ*dom34*Δ *S. cerevisiae* strain transformed with Dom34 mutants. (**c**,**d**) Quantification of **a** and **b**, respectively. For each mutant the ratio of 5′ intermediate over full length PGK1-SL reporter was calculated and then standardized for the ratios calculated for Hbs1-proteinA or Dom34-3HA. Mean ± s.d. of three biological replicates is shown.

The rapid degradation of the 18S NRD substrate 18S A1492C depends at least partly on the presence of both Dom34 and Hbs1 (ref. 9). In the absence of either of these factors, steady-state levels of 18S A1492C RNA increased (**Fig. 4a**; compare lanes 1–3). We tested whether the Hbs1 mutants that were unable to bind nucleotide could restore degradation of 18S A1492C in an *hbs1*Δ strain and found that they could not (**Fig. 4a** (lanes 4–6) and **c**), leading to steady-state levels 3–4-fold higher than in the presence of wild-type Hbs1 (lanes 2 and 3) and similar to the level observed in the absence of Hbs1 (lane 1).

We screened for mutations that generated a synthetic growth phenotype in a *dom34*Δ background and identified mutations in genes that encoded the Rps28 proteins of the small ribosomal subunit (data not shown). This finding is consistent with previous results obtained with genes that encode other 40S subunit proteins[11]. Also consistent with these data, the V176G and H255E mutants could not complement the slow growth of an *rps28A*Δ*hbs1*Δ strain (**Fig. 4e**, compare with wild-type Hbs1). The K180A mutant was also inactive in this assay (**Fig. 4e**).

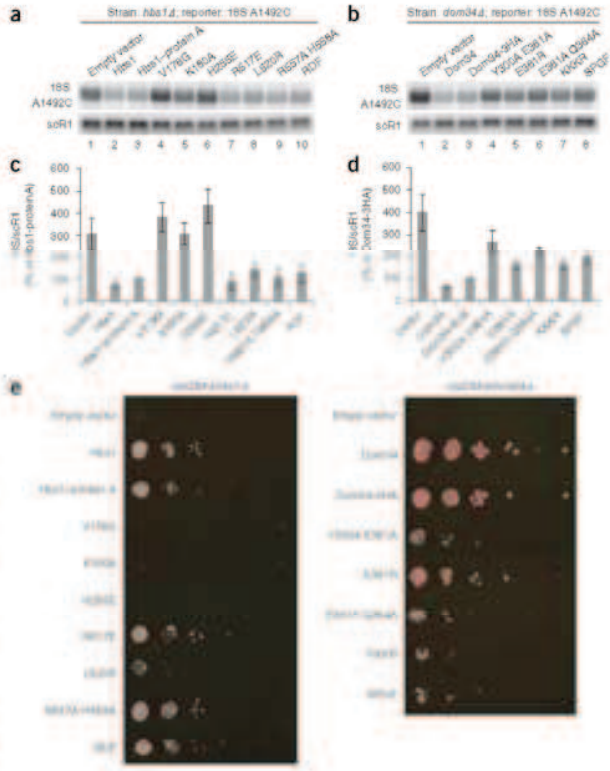

Figure 4 Effects of Hbs1 and Dom34 mutants on 18S NRD and growth in ribosomal protein deletion context. (**a**) Northern blot analysis of the steady-state levels of 18S A1492C NRD substrate in a *hbs1*Δ strain transformed with Hbs1 mutants. ScR1 RNAs were used as loading controls. The 18S A1492C reporter was expressed from plasmid pWL160-A1492C and detected by oligonucleotide FL125[6]. (**b**) Analysis of the steady-state levels of 18S A1492C NRD substrate in a *dom34*Δ strain transformed with Dom34 mutants. ScR1 RNAs are presented as loading controls. (**c**,**d**) Quantification of **a** and **b**, respectively. For each mutant, the ratio of 18S A1492C over scR1 signal was calculated and then manipulated for the ratio calculated for Hbs1-protein A or Dom34-3HA. Mean ± s.d. of three biological replicates is shown. (**e**) Strains deleted for both yeast ribosomal subunit protein Rps28A and Hbs1 (*rps28A*Δ*hbs1*Δ, left) or Dom34 (*rps28A*Δ*dom34*Δ, right) transformed with Hbs1 mutants or Dom34 mutants were spotted in six-ten-fold dilutions on YPDA plates and grown at 16 °C (6 days).

We conclude that nucleotide binding by Hbs1 is essential for NGD endonucleolytic cleavage, 18S rRNA NRD and for the function of Hbs1 that is required in strains that lack a gene encoding a ribosomal protein of the small subunit.

Role of the Dom34–Hbs1 interaction in NGD and 18S NRD

To test the functional importance of the Dom34–Hbs1 interaction, we tested several mutants that targeted residues of the main proposed interaction surface between the C-terminal domain of Dom34 and domain III of Hbs1 (Y300A-E361A, E361R and E361R-Q364A in Dom34 and R517E, L520R and R557A-H558A in Hbs1; **Fig. 1d**) for their effects on NGD, NRD and growth in an *rps28a*Δ strain.

According to the Dom34–Hbs1 model that we derived from SAXS measurements, the Dom34 central domain also contacts the GTPase domain of Hbs1. To investigate the functional importance of this interaction we also mutated this predicted interaction surface. In the Dom34 central domain, we mutated a conserved loop rich in basic residues (^{174}KKKR^{177}) into alanines (KKKR mutant), which has been shown to reduce NGD[18]. Mutations of similarly positioned basic residues in eRF1 affect the GTPase activity of eRF3, the interaction between eRF1 and eRF3 and their function[29]. In our model this loop could contact the γ-phosphate of a GTP molecule bound to Hbs1. We also mutated a highly conserved ^{222}SPGF^{225} motif in the central domain of Dom34 into AAGA (SPGF mutant). Mutation of the PGF peptide or of the proline alone has been shown to reduce NGD[18]. In our model the SPGF motif faces a conserved ^{179}RDF^{181} motif from the GTPase domain of Hbs1, which we also mutated into alanines (RDF mutant; **Supplementary Fig. 4g**). Using a yeast two-hybrid approach, we confirmed that these mutants had greatly reduced interactions with their wild-type partners (**Supplementary Fig. 5b,c**).

To confirm that mutants were expressed in *S. cerevisiae*, we introduced Dom34 mutants in a construct that carried a C-terminal 3HA tag and Hbs1 mutants in a construct that contained a C-terminal protein A tag. For each mutant, we measured protein expression in yeast by western blotting and measured protein stability by DSC analysis. All Hbs1 mutants as well as the E361R and to a lesser extent KKKR and SPGF Dom34 mutants were expressed in yeast (**Supplementary Fig. 5a**), whereas we detected smaller amounts of the Y300A-E361A and E361R-Q364A mutants of Dom34. Microcalorimetric experiments confirmed that all Hbs1 mutants behaved similarly to the wild-type protein (**Supplementary Fig. 3**). For Dom34, we could not obtain sufficient quantities of recombinant SPGF mutant to analyze its stability by DSC. All other Dom34 constructs were very similar, with the Y300A-E361A, E361A-Q364R and E361R mutants being only slightly less stable than the KKKR mutant and wild-type proteins (**Supplementary Fig. 3d**).

All mutations of the interaction surfaces caused a reduction in NGD (**Fig. 3a** (lanes 7–10) and **b**–**d**). The ratio of degradation intermediate to full-length reporter mRNA was decreased to the same extent as it was in strains that lacked Hbs1 or Dom34 (**Fig. 3a,b** (lane 1)). However, none of the Hbs1 mutants affected 18S NRD, as the level of 18S A1492C was identical to that seen in the presence of wild-type Hbs1 (**Fig. 4a** (lanes 7–10) and **c**). By contrast, all

Dom34 mutants caused some stabilization of the 18S A1492C NRD substrate (**Fig. 4b,d**), although not to the same extent as in the absence of Dom34. Although we cannot exclude the possibility that stabilization of the 18S A1492C NRD substrate in Dom34 Y300A-E361A and E361R-Q364A mutants results from decreased protein in cells, the effect of the E361R mutant, which is found at similar levels as wild-type Dom34, suggests that a functional Dom34–Hbs1 interaction surface is required for optimal 18S NRD. All mutations that affected interaction complemented the slow growth defect in *dom34Δrps28AΔ* or *hbs1Δrps28AΔ* strains (**Fig. 4e**), although the Hbs1 L520R mutant and all Dom34 mutants except E361R did not restore growth to the same extent as their wild-type counterparts.

These results indicate that the interaction between Dom34 and Hbs1 is crucial for efficient NGD but is less essential for 18S NRD and growth in the context of a strain lacking a gene encoding a ribosomal protein of the small subunit.

DISCUSSION

Eukaryotes have developed sophisticated surveillance pathways to detect nonfunctional or damaged DNA, RNA and proteins, thereby leading to their repair or rapid degradation. In this study, we focused on Hbs1 and Dom34, two interacting proteins that have been implicated in two RNA quality control pathways: NGD and 18S NRD[6,7,9,10]. Both pathways lead to the degradation of mRNAs or rRNAs that cannot undergo translation elongation, but their mechanisms remain unclear.

The domain organization of Hbs1dN134 is similar to those of other members of the eEF-1A family. As for EF-Tu, the Hbs1 GTPase domain is tightly packed onto domains II and III (**Fig. 1a**), by contrast with the 'open' structure observed for eRF3 (ref. 24). Our SAXS data (**Supplementary Fig. 2**) for Hbs1 as well as mutant analysis of *S. pombe* eRF3 (ref. 24) support the existence of a conserved 'closed' conformation that corresponds with our crystal structure and is likely to be necessary for the function of eEF-1A family members.

Like other eEF-1A factors, Hbs1 is likely to cycle between GTP-bound, GDP-bound and free forms. Nucleotide binding was essential for all the Hbs1 functions we tested, namely NGD, 18S NRD and growth complementation. In eRF3, GTP binding (stimulated by eRF1) promotes a rearrangement of the termination complex that leads to GTP hydrolysis followed by rapid hydrolysis of peptidyl-tRNA, peptide release, tRNA liberation and subunit dissociation[23,33–37]. Similarly, association of GTP with Hbs1, but not of non-hydrolyzable GDPNP, promotes ribosome dissociation and the release of peptidyl-tRNA[38]. Our mutants of Hbs1 that impaired nucleotide binding and thereby also prevented GTP hydrolysis are thus likely to impede this process, suggesting that such rearrangements are a prerequisite for initiating the degradation of the small ribosomal subunit or bound mRNA.

In our model of the Hbs1–Dom34 complex (**Fig. 2**), which is most likely to represent the solution structure, yeast Dom34 adopts the conformation that has been observed for its archaeal counterpart[17], rather than the cognate structure[16]. Our model is also more similar to the Dom34–EF1α from *A. pernyx* than to the *S. pombe* Dom34–Hbs1 structure[31,32]. Our Dom34–Hbs1 model is also strongly analogous to the bacterial EF-Tu–tRNA complex that is involved in translation elongation[26]. Comparison of our Hbs1–Dom34 model and the EF-Tu–tRNA complex (**Fig. 2b,c**) shows that Dom34 and the tRNA have similar shape and localization relative to the GTPase domains of their respective partners. The N-terminal, central and C-terminal domains of Dom34 occupy similar positions to the anticodon stem, amino acyl acceptor arm and T stem of tRNA, respectively. Thus, the N-terminal domain of Dom34 is likely to bind close to the mRNA codon in the A-site of the stalled ribosome. This domain is structurally unrelated to the eRF1 N-terminal domain and adopts an Sm-fold[39,40]. Two loops (residues 49–53 and 87–92) from this Dom34 domain that are functionally important for the NGD pathway in yeast[18] occupy approximately the same position as the tRNA anticodon loop in our model and hence could directly contact the mRNA codon, probably in a sequence-independent manner. Consistently, functional assays have shown that Dom34–Hbs1 induces ribosome dissociation independent of the sequence in the ribosome A site[38].

Binding data indicate that the interface between Hbs1 domain III and the C-terminal domain of Dom34 is essential for interaction, whereas contacts between the Hbs1 GTPase domain and the Dom34 central domain probably have regulatory functions (data not shown). In humans, binding of the central domain of eRF1 to eRF3 stimulates GTP binding and GTPase activity of the latter[33]. This may involve stabilization of the eRF3 switch region by Arg192 of eRF1 (ref. 29), which explains how eRF1 might stimulate the affinity of eRF3 for GTP[23,35]. The association of GTP with Hbs1 is similarly stimulated by Dom34 (ref. 16). The residues from *S. cerevisiae* Hbs1 domain III and the C-terminal domain of Dom34 that were involved in complex formation in our model do interact in the crystal structures of the Hbs1(EF1α)–Dom34 complexes[31,32]. However, the second interaction that was proposed in our study, involving residues SPGF of Dom34 and ^{256}RDF^{258} of Hbs1, is conserved in the *A. pernyx* structure but not in the *S. pombe* complex, owing to the 180° rotation of the GTPase domain of Hbs1.

Our results indicate that the interaction between Dom34 and Hbs1 is essential for NGD but is less crucial for 18S NRD or growth in an *rps28aΔ* strain. This suggests that a function of Hbs1 is required for NGD that is not essential for 18S NRD. Moreover, the interaction surface in Dom34 seems to be more essential for 18S NRD than the interaction surface in Hbs1. As both Dom34 and Hbs1 are essential for both NGD and 18S NRD, a possible explanation for our results is that an additional factor stabilizes the Dom34–Hbs1 interaction during 18S NRD but not during NGD. Alternatively, NGD may require a tighter interaction between Dom34 and Hbs1 than 18S NRD and might therefore be more affected by a weakening of the interaction of Hbs1. It is also possible that Dom34 interacts with another factor that is specifically required for NGD through the interaction surface that is used by Hbs1, explaining the asymmetry of our mutant phenotypes.

Although the corresponding mechanistic details remain to be elucidated, our data indicate that NGD and 18S NRD can be genetically uncoupled. Given that NGD and 18S NRD share several factors (Hbs1, Dom34 and components of the degradation machinery) and target substrates with similar characteristics, it has been proposed that these processes occur in parallel as a consequence of inappropriate stalling of a ribosome[9]. However, our results suggest that mRNA and rRNA in a stalled translation complex may not always be simultaneously degraded. Notably, the observation that the growth phenotype assayed in the absence of Rps28a correlates with their effects on 18S NRD, but not on NGD, indicates that in these cells 18S NRD has become crucial. The absence of 18S NRD might be quantitatively more detrimental to cells than defective NGD: in the former, a small fraction of stalled ribosomes might quickly have a general impact on translation by sequestering functional ribosomes in dead polysomes, whereas in the latter, only a few mRNAs and ribosomes would be affected.

Overall, our data show that eukaryotic cells use the Hbs1–Dom34 complex as a tRNA–elongation factor complex mimic to carry out RNA quality control mechanisms. Entry of the Dom34–Hbs1 complex to the A-site of stalled ribosomes contributes to NGD and 18S NRD, but the rules that govern its specific recruitment are unknown. However, our data indicate that these two processes can

be functionally separated. The mechanisms that control the outcome of binding of Dom34–Hbs1 to a stalled ribosome—degradation of the substrate mRNA, destruction of the small ribosomal subunit or both—remain to be deciphered.

METHODS

Methods and any associated references are available in the online version of the paper at http://www.nature.com/nsmb/.

Accession codes. Protein Data Bank: 3P26 for apo-Hbs1 and 3P27 for Hbs1-GDP.

Note: Supplementary information is available on the Nature Structural & Molecular Biology website.

ACKNOWLEDGMENTS

We thank K. Blondeau, B. Faivre, J. Cicolari, D. Lebert, Y. Billier, B. Bonneau and D. Rentz for technical assistance; M. Moore (U. Mass. Medical School) and R. Parker (University of Arizona) for plasmid gifts; and P. Vachette for discussions. Supported by the Agence Nationale pour la Recherche (ANR-06-BLAN-0075-02 and ANR-07-BLAN-0093), the Association Française contre les Myopathies (AFM), La Ligue contre le Cancer Equipe Labellisée 2008, CNRS, the ESF EUROCORES RNA Quality and the EU '3D-Repertoire' program (LSHG-CT-2005-512028). J.H. and A.M.G.v.d.E. hold predoctoral grants from the Université Paris-Sud 11 and Université de Strasbourg, respectively. M.E.G. is supported by the Spanish Ministry of Science and Innovation. We acknowledge SOLEIL for provision of synchrotron radiation facilities and thank A. Thompson and J. Perez for assistance with beamlines Proxima-1 and SWING, respectively.

AUTHOR CONTRIBUTIONS

J.H., A.M.G.v.d.E., M.G. and B.S. designed experiments. J.H., A.M.G.v.d.E., N.L., D.D., F.L., M.N. and M.E.G. performed experiments. J.H., A.M.G.v.d.E., D.D., H.v.T., M.G. and B.S. analyzed data and wrote the paper.

COMPETING FINANCIAL INTERESTS

The authors declare no competing financial interests.

Published online at http://www.nature.com/nsmb/.
Reprints and permissions information is available online at http://npg.nature.com/reprintsandpermissions/.

1. Doma, M.K. & Parker, R. RNA quality control in eukaryotes. *Cell* **131**, 660–668 (2007).
2. Isken, O. & Maquat, L.E. Quality control of eukaryotic mRNA: safeguarding cells from abnormal mRNA function. *Genes Dev.* **21**, 1833–1856 (2007).
3. Amrani, N., Sachs, M.S. & Jacobson, A. Early nonsense: mRNA decay solves a translational problem. *Nat. Rev. Mol. Cell Biol.* **7**, 415–425 (2006).
4. Frischmeyer, P.A. *et al.* An mRNA surveillance mechanism that eliminates transcripts lacking termination codons. *Science* **295**, 2258–2261 (2002).
5. van Hoof, A., Frischmeyer, P.A., Dietz, H.C. & Parker, R. Exosome-mediated recognition and degradation of mRNAs lacking a termination codon. *Science* **295**, 2262–2264 (2002).
6. Doma, M.K. & Parker, R. Endonucleolytic cleavage of eukaryotic mRNAs with stalls in translation elongation. *Nature* **440**, 561–564 (2006).
7. Gandhi, R., Manzoor, M. & Hudak, K.A. Depurination of Brome mosaic virus RNA3 in vivo results in translation-dependent accelerated degradation of the viral RNA. *J. Biol. Chem.* **283**, 32218–32228 (2008).
8. LaRiviere, F.J., Cole, S.E., Ferullo, D.J. & Moore, M.J. A late-acting quality control process for mature eukaryotic rRNAs. *Mol. Cell* **24**, 619–626 (2006).
9. Cole, S.E., LaRiviere, F.J., Merrikh, C.N. & Moore, M.J. A convergence of rRNA and mRNA quality control pathways revealed by mechanistic analysis of nonfunctional rRNA decay. *Mol. Cell* **34**, 440–450 (2009).
10. Soudet, J., Gelugne, J.P., Belhabich-Baumas, K., Caizergues-Ferrer, M. & Mougin, A. Immature small ribosomal subunits can engage in translation initiation in *Saccharomyces cerevisiae*. *EMBO J.* **29**, 80–92 (2010).
11. Carr-Schmid, A., Pfund, C., Craig, E.A. & Kinzy, T.G. Novel G-protein complex whose requirement is linked to the translational status of the cell. *Mol. Cell. Biol.* **22**, 2564–2574 (2002).
12. Adham, I.M. *et al.* Disruption of the pelota gene causes early embryonic lethality and defects in cell cycle progression. *Mol. Cell. Biol.* **23**, 1470–1476 (2003).
13. Davis, L. & Engebrecht, J. Yeast dom34 mutants are defective in multiple developmental pathways and exhibit decreased levels of polyribosomes. *Genetics* **149**, 45–56 (1998).
14. Eberhart, C.G. & Wasserman, S.A. The pelota locus encodes a protein required for meiotic cell division: an analysis of G2/M arrest in *Drosophila* spermatogenesis. *Development* **121**, 3477–3486 (1995).
15. Xi, R., Doan, C., Liu, D. & Xie, T. Pelota controls self-renewal of germline stem cells by repressing a Bam-independent differentiation pathway. *Development* **132**, 5365–5374 (2005).
16. Graille, M., Chaillet, M. & van Tilbeurgh, H. Structure of yeast Dom34: a protein related to translation termination factor Erf1 and involved in No-Go decay. *J. Biol. Chem.* **283**, 7145–7154 (2008).
17. Lee, H.H. *et al.* Structural and functional insights into Dom34, a key component of No-Go mRNA decay. *Mol. Cell* **27**, 938–950 (2007).
18. Passos, D.O. *et al.* Analysis of Dom34 and its function in no-go decay. *Mol. Biol. Cell* **20**, 3025–3032 (2009).
19. Atkinson, G.C., Baldauf, S.L. & Hauryliuk, V. Evolution of nonstop, no-go and nonsense-mediated mRNA decay and their termination factor-derived components. *BMC Evol. Biol.* **8**, 290 (2008).
20. Wallrapp, C. *et al.* The product of the mammalian orthologue of the *Saccharomyces cerevisiae HBS1* gene is phylogenetically related to eukaryotic release factor 3 (eRF3) but does not carry eRF3-like activity. *FEBS Lett.* **440**, 387–392 (1998).
21. Nelson, R.J., Ziegelhoffer, T., Nicolet, C., Werner-Washburne, M. & Craig, E.A. The translation machinery and 70 kd heat shock protein cooperate in protein synthesis. *Cell* **71**, 97–105 (1992).
22. Inagaki, Y., Blouin, C., Susko, E. & Roger, A.J. Assessing functional divergence in EF-1α and its paralogs in eukaryotes and archaebacteria. *Nucleic Acids Res.* **31**, 4227–4237 (2003).
23. Pisareva, V.P., Pisarev, A.V., Hellen, C.U., Rodnina, M.V. & Pestova, T.V. Kinetic analysis of interaction of eukaryotic release factor 3 with guanine nucleotides. *J. Biol. Chem.* **281**, 40224–40235 (2006).
24. Kong, C. *et al.* Crystal structure and functional analysis of the eukaryotic class II release factor eRF3 from *S. pombe*. *Mol. Cell* **14**, 233–245 (2004).
25. Vetter, I.R. & Wittinghofer, A. The guanine nucleotide-binding switch in three dimensions. *Science* **294**, 1299–1304 (2001).
26. Nissen, P. *et al.* Crystal structure of the ternary complex of Phe-tRNAPhe, EF-Tu, and a GTP analog. *Science* **270**, 1464–1472 (1995).
27. Leibundgut, M., Frick, C., Thanbichler, M., Bock, A. & Ban, N. Selenocysteine tRNA-specific elongation factor SelB is a structural chimaera of elongation and initiation factors. *EMBO J.* **24**, 11–22 (2005).
28. Song, H., Parsons, M.R., Rowsell, S., Leonard, G. & Phillips, S.E. Crystal structure of intact elongation factor EF-Tu from *Escherichia coli* in GDP conformation at 2.05 A resolution. *J. Mol. Biol.* **285**, 1245–1256 (1999).
29. Cheng, Z. *et al.* Structural insights into eRF3 and stop codon recognition by eRF1. *Genes Dev.* **23**, 1106–1118 (2009).
30. Petoukhov, M.V. & Svergun, D.I. Global rigid body modelling of macromolecular complexes against small-angle scattering data. *Biophys. J.* **89**, 1237–1250 (2005).
31. Chen, L. *et al.* Structure of the Dom34–Hbs1 complex and implications for no-go decay. *Nat. Struct. Mol. Biol.* **17**, 1233–1240 (2010).
32. Kobayashi, K. *et al.* Structural basis for mRNA surveillance by archaeal Pelota and GTP-bound EF1α complex. *Proc. Natl. Acad. Sci. USA* **107**, 17575–17579 (2010).
33. Kononenko, A.V. *et al.* Role of the individual domains of translation termination factor eRF1 in GTP binding to eRF3. *Proteins* **70**, 388–393 (2008).
34. Alkalaeva, E.Z., Pisarev, A.V., Frolova, L.Y., Kisselev, L.L. & Pestova, T.V. In vitro reconstitution of eukaryotic translation reveals cooperativity between release factors eRF1 and eRF3. *Cell* **125**, 1125–1136 (2006).
35. Hauryliuk, V., Zavialov, A., Kisselev, L. & Ehrenberg, M. Class-1 release factor eRF1 promotes GTP binding by class-2 release factor eRF3. *Biochimie* **88**, 747–757 (2006).
36. Pisarev, A.V. *et al.* The role of ABCE1 in eukaryotic posttermination ribosomal recycling. *Mol. Cell* **37**, 196–210 (2010).
37. Salas-Marco, J. & Bedwell, D.M. GTP hydrolysis by eRF3 facilitates stop codon decoding during eukaryotic translation termination. *Mol. Cell. Biol.* **24**, 7769–7778 (2004).
38. Shoemaker, C.J., Eyler, D.E. & Green, R. Dom34:Hbs1 promotes subunit dissociation and peptidyl-tRNA drop-off to initiate no-go decay. *Science* **330**, 369–372 (2010).
39. Séraphin, B. Sm and Sm-like proteins belong to a large family: identification of proteins of the U6 as well as the U1, U2, U4 and U5 snRNPs. *EMBO J.* **14**, 2089–2098 (1995).
40. Wilusz, C.J. & Wilusz, J. Eukaryotic Lsm proteins: lessons from bacteria. *Nat. Struct. Mol. Biol.* **12**, 1031–1036 (2005).

ONLINE METHODS

Cloning, expression and purification of Hbs1 proteins. The truncated version of the HBS1 gene (*YKR0084c*) with the first 134 residues deleted was amplified by PCR from *S. cerevisiae* S288C genomic DNA. An additional His_6 tag was introduced downstream of the 3′ coding sequence. The PCR products were cloned into a modified pET28 vector between EagI and NotI restriction sites. The protein was expressed and purified as described for the full-length protein[16]. A seleno-methionine (Se-Met) derivative of Hbs1dN134 was expressed in Se-Met-supplemented minimal medium using the same expression system as for the native protein. The Se-Met protein was purified with the same method as for the native protein.

The full-length mutated versions (V176G, H255E, K180A) of the HBS1 gene (*YKR0084c*) were amplified by PCR from *S. cerevisiae* expression plasmids and inserted in an ampicillin-resistant pET21a vector. An additional His_6 tag was introduced downstream of the coding sequence between BamHI and NotI restriction sites. The mutants were expressed and purified using the same protocol as the Hbs1dN134 protein. See further details in **Supplementary Methods**.

Yeast strains and plasmids. Yeast strains were constructed by standard methods and are derivatives of BMA64 except for Y190 (two hybrid). Strains and plasmids are listed in **Supplementary Table 1**.

Dom34 and the upstream flanking sequence were amplified from genomic DNA and cloned between the XhoI and XbaI sites of pRS415, giving pBS3217. Hbs1 with its flanking sequences was amplified from genomic DNA and cloned between the SmaI and HindIII sites of pRS415, generating pBS3611. C-terminal tags (3HA for Dom34 and protein A for Hbs1) were introduced by fusion PCR. The Dom34-3HA product digested by HindIII and NheI was cloned into pBS3217, generating pBS3685. The Hbs1–protein A product digested by NdeI and HindIII was cloned into pBS3611, generating pBS3614.

Dom34 and Hbs1 point mutations were introduced in pBS3685 or pBS3614 respectively by QuickChange mutagenesis, except for the KKKR mutant, which was produced by fusion PCR, digested by HindIII and XhoI, and cloned into pBS3685. All constructs were verified by sequencing.

RNA analysis. Yeast cultures were grown in CSM-Leu-Ura (NGD assay) or CSM-Leu-Trp (18S NRD assay) containing 2% (w/v) galactose at 30 °C until OD_{600} 0.6–1.2. Total RNA was obtained by hot phenol extraction, 10 µg RNA was separated on 1.5% (w/v) agarose- 6.3% (w/v) formaldehyde gel (18S NRD) or 15 µg on 1.25% agarose-6, 7% formaldehyde gel with bridges of Whatman paper separating gel from running buffer (NGD) and transferred to a Hybond-XL membrane (GE Healthcare) as described[41]. Probe FL125 was 5′ labeled with T4 polynucleotide kinase (Fermentas) and γ-32P ATP. For detection of endogenous scR1 and the PGK1-SL reporter, probes were made by a random priming reaction on a PCR products using the Neblot kit (New England Biolabs) and α-32P dCTP. Prehybridization and hybridization of the membranes with the labeled probes were performed in 5 M $NaPO_4$, pH 7.2, 1% (w/v) BSA, 1 mM EDTA, 2.8% SDS at 42 °C and 40 °C, respectively (NRD), 55 °C (scR1) or 65 °C (PGK1-SL). Signals were visualized with a Typhoon 8600 Variable Mode Imager and quantified using ImageQuant 5.2 software (Molecular Dynamics).

41. Prouteau, M., Daugeron, M.C. & Seraphin, B. Regulation of ARE transcript 3′ end processing by the yeast Cth2 mRNA decay factor. *EMBO J.* **27**, 2966–2976 (2008).

doi:10.1038/nsmb.1963

2.2 STUDY OF THE MECHANISTICAL DETAILS OF RNA QUALITY CONTROL ON STALLED TRANSLATIONAL COMPLEXES

2.2.1 The functional relationship between No-go decay and Non-functional 18S rRNA decay

The data presented above gave an indication that Dom34-Hbs1 dependent 18S rRNA degradation can occur independently of Dom34-Hbs1 dependent alteration in mRNA stability. I aimed to further study the relationship between NGD and 18S NRD. More specifically I analyzed whether the translation of a NGD substrate (a stall site containing mRNA) induces degradation of rRNAs or ribosomal proteins.

To address this question I used an *in vitro* translation method in *S. cerevisiae* extract, developed by Anne-Laure Finoux (Finoux, 2006). A yeast extract was obtained based on a method published by (Tuite & Plesset, 1986). In this extract, cellular mRNAs were still present, and needed to be removed to allow optimal translation of *in vitro* added mRNAs. Therefore the extract was first treated with micrococcal nuclease (MNase). The digestion time needed to be optimized: a treatment too short would not remove cellular mRNAs sufficiently, whereas a treatment too long would cause degradation of rRNA, thereby decreasing translation efficiency. To determine the optimal digestion time, aliquots of the yeast extract were incubated with 150 U/ml MNase for varying amounts of time. Then 500 ng mRNA encoding firefly luciferase (Gallie et al, 1991) was added to 15 µl translation reactions, to be

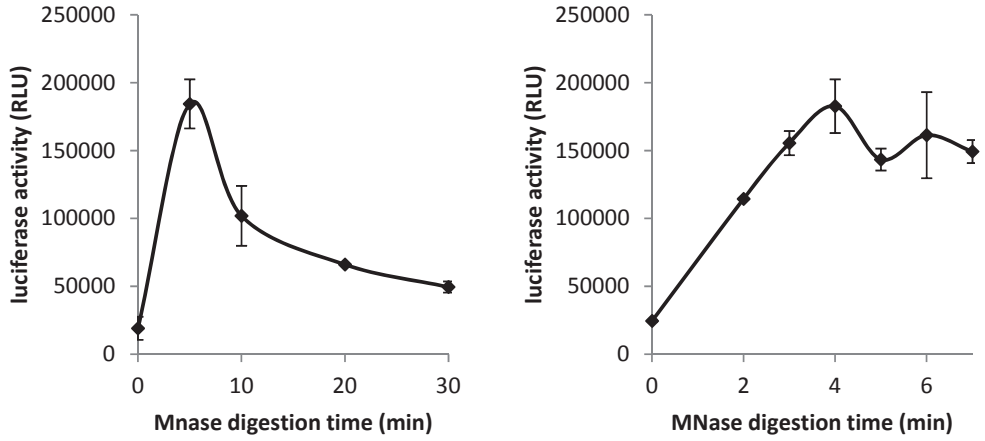

Figure 32 Optimization of micrococcal nuclease digestion time.
Translation efficiency, represented by the activity of luciferase produced after one hour of translation, is plotted against the time yeast extract was treated with MNase.

translated during one hour. Luciferase activity was determined, as a measure of protein production. Figure 32 shows that, using this quantity of enzyme, optimal translation occurred after 4 minutes of MNase treatment.

The yeast extract was used to translate a mRNA encoding a TAP tag, consisting of protein A and calmodulin binding peptide (CBP) (Rigaut et al, 1999) linked to a triple HA tag and green fluorescent protein (GFP). This mRNA contained a stem loop stall site (Doma & Parker, 2006) between the 3HA and GFP sequence (TAP-SL-GFP mRNA). A negative control did not contain the stem loop (TAP-GFP mRNA). The aim was to study whether translation of the stall site containing mRNA caused destabilization of the rRNA and proteins of the ribosomes translating it. For such a destabilization to be visible as a reduction in total rRNA or ribosomal protein level over time, it is important that a large part of the ribosomes present in the extract engage in translation of the stall site mRNA. The fraction of translating ribosomes is expected to depend on the concentration of the mRNA that is translated. To optimize the mRNA concentration, both TAP-SL-GFP and TAP-GFP were added in different amounts to 15 µl translation reactions, followed by translation for one hour. The amount of protein produced was then determined by western blot (Figure 33). Optimal protein production was achieved when between 600 and 1200 ng mRNA was added to the extract.

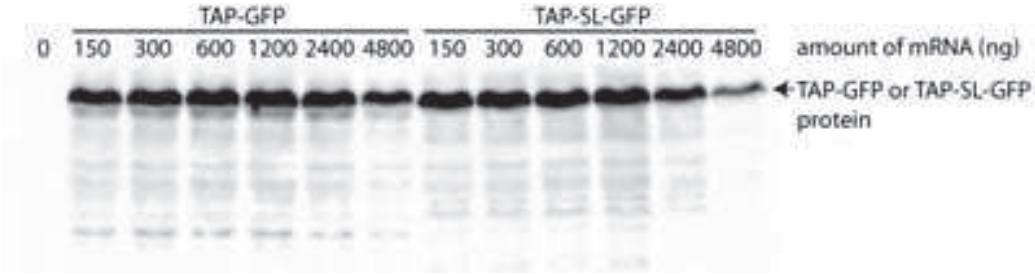

Figure 33 Optimization of the mRNA concentration.
Protein produced from the indicated quantities of TAP-GFP and TAP-SL-GFP mRNA after one hour of translation in yeast extract. Proteins were detected by western blot using peroxidase anti-peroxidase (PAP, Sigma).

600 ng of the stem loop or control mRNA was translated in 15µl translation reactions that were stopped at different time points. RNA and protein content were analyzed by northern blot and western blot respectively.

Figure 34 shows that the levels of 18S and 25S rRNAs do not decrease over time, during translation of a NGD substrate. Neither does the level of 60S subunit protein Rpl1A or the ribosome associated protein Stm1 change.

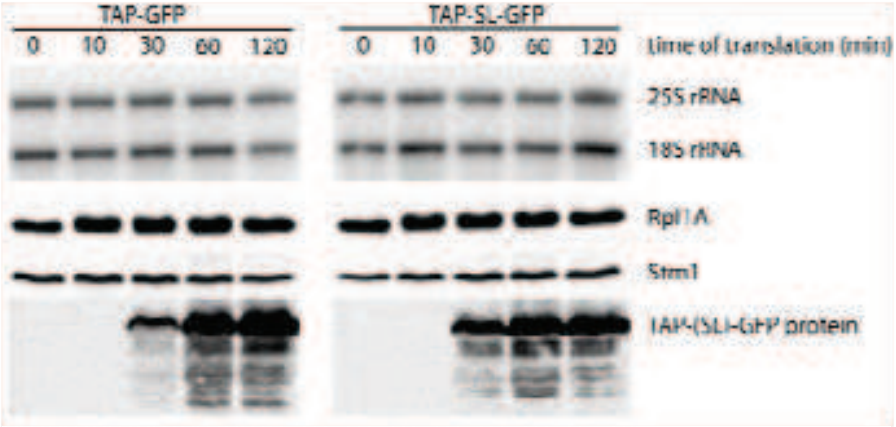

Figure 34 The effect of translating a stem loop containing mRNA on ribosomal RNA and protein stability. TAP-GFP and TAP-SL-GFP were translated for the indicated amounts of time in yeast extract. The levels of rRNAs and ribosomal or ribosome associated proteins were determined at the indicated timepoints. 18S rRNA and 25S rRNA were detected by northern blot using probes OBS4814 and OBS5408 respectively. Rpl1A and Stm1 were detected by western blot using polyclonal rabbit antibodies AbBS6 and AbBS8 respectively. TAP-GFP or TAP-SL-GFP protein was detected by PAP.

In summary no signs of ribosomal RNA or protein degradation as a consequence of ribosomal stalling induced by a mRNA stall site are visible. However, it cannot be excluded either. First of all because it is not clear what fraction of ribosomes in the extract is translating. If only a small fraction of ribosomes translates and stalls on the stem loop mRNA, their degradation will not be visible. Second, the stem loop appears to be a very inefficient stall site. The stem loop mRNA produces full-length protein at a level practically indistinguishable from the level of protein produced from the control mRNA (Figure 33 and
Figure 34). This indicates that, even if a high proportion of ribosomes may be translating, only a small fraction will stall and therefore stalling induced ribosome degradation may not be visible. The use of a stronger stall site, perhaps a CGA repeat (see paragraph 1.4.1.2) should improve the assay. Finally, the *in vitro* conditions may not be representative of the *in vivo* situation. It should be tested whether the extract contains the machinery necessary for stalling induced rRNA degradation. To get an indication it could be verified whether a mutant 18S rRNA is a subjected to NRD in yeast extract.

2.2.2 Search for the No-go decay endonuclease

The endonuclease responsible for endonucleolytic cleavage of the mRNA in NGD has not been identified so far. In humans and *Drosophila*, the NMD pathway involves an endonucleolytic cleavage of the mRNA that is mediated by the protein Smg6 (Eberle et al,

2009; Huntzinger et al, 2008). The yeast proteins Esl1 and Esl2 show sequence similarity to human Smg6. Moreover, Esl2 was reported to interact with ribosomes (Fleischer et al, 2006). I therefore tested whether one of these factors could be responsible for the mRNA cleavage in NGD. The NGD assay depicted in Figure 31 was used to test whether the absence of Esl1 or Esl2 resulted in reduced intermediate production. The reporter mRNA used contained a sequence encoding CBP linked to a 3HA tag, followed by the same stem loop as used in (Doma & Parker, 2006) (CBP-3HA-SL). A control reporter did not contain a stem loop (CBP-3HA). The CBP-3HA-SL reporter efficiently produced a 5' NGD intermediate in a *ski7*Δ background, indicating mRNA cleavage. The absence of Esl1 or Esl2 did not reduce the accumulation of this 5' intermediate (Figure 35). This suggests that Esl1 or Esl2 are not the endonucleases responsible for mRNA cleavage in NGD. However, it cannot be excluded that there is redundancy between these factors or between these factors and other unknown factors. A triple *ski7*Δ*esl1*Δ*esl2*Δ mutant would elucidate whether the first possibility is true.

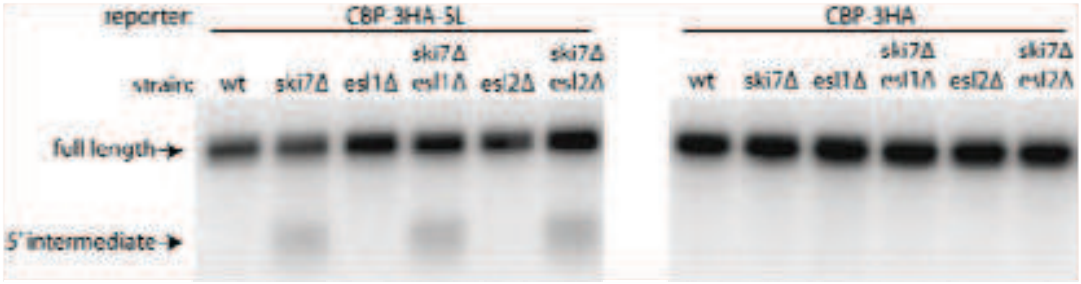

Figure 35 Esl1 and Esl2 are not required for No-go decay endonucleolytic cleavage.
Northern blot analysis of the steady state levels of a 5' degradation intermediate produced by endonucleolytic cleavage from the indicated mRNA reporters was used to determine the requirement of Esl1 and Esl2 for mRNA cleavage in NGD. mRNA was detected by probe OBS4671.

2.2.3 A method to purify ribosomes with a defective 18S rRNA

Questions remain about what factors are involved in RNA degradation in NGD and 18S NRD. As already indicated above, the endonuclease responsible for mRNA cleavage in NGD has not been identified. For 18S NRD, the mechanistic details of rRNA degradation are not clear. At the time this research was performed, little was known about what happened to the peptide produced by a stalled ribosome. In an attempt to obtain more insight into the mechanisms acting on stalled ribosomes, I designed a method to purify defective ribosomes.
The purpose of this method was to specifically purify ribosomes containing a mutation in the 18S rRNA, rendering them non-functional and therefore substrates for 18S NRD. By comparing the set of proteins that co-purify with mutant ribosomes with the set of proteins

that co-purify with wild type ribosomes, I hoped to identify proteins that specifically interact with defective ribosomes and that may act in 18S NRD and perhaps also in associated pathways.

2.2.3.1 Tandem affinity purification

The tandem affinity purification (TAP) method allows the purification of a protein and factors interacting with this protein under native conditions. When combined with mass spectrometry, it can be used to identify proteins interacting with a given target protein (Rigaut et al, 1999).

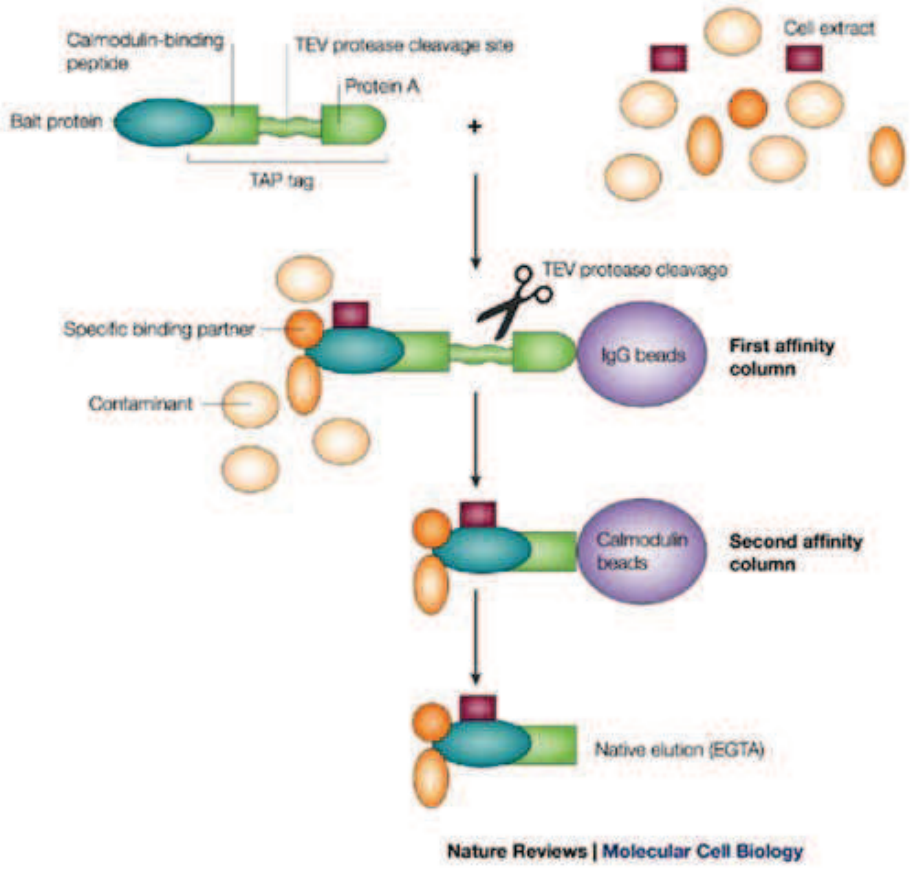

(Huber, 2003)

Figure 36 Tandem affinity purification.

The target protein is linked to a tag that consists of protein A and CBP, separated by a TEV protease recognition site. The method consists of two subsequent purification steps (see Figure 36). In the first step, cell lysate is incubated with IgG beads, to which protein A binds.

The target protein and associated factors are eluted from the IgG beads by the action of TEV protease, which cleaves the linkage between protein A and CBP. The eluate is then incubated with calmodulin beads, which binds the CBP-tagged complex. Elution occurs by the addition of EGTA, which chelates Ca^{2+} ions needed for CBP-calmodulin interaction.

2.2.3.2 Construct production and validation

Ribosomes in which residue A1492 (*E. coli* counting), an important residue in the decoding center, is mutated (A1492C) are known substrates for 18S NRD (Cole et al, 2009). To specifically purify mutant ribosomes, a human U1 stem loop was inserted in a mutant 18S A1492C rRNA construct, which was produced in the lab of Dr. Melissa Moore (LaRiviere et al, 2006). In this construct a rDNA gene is under the control of a promoter that is induced in presence of galactose but repressed in presence of glucose. This construct contains a tag inserted in the 18S rRNA sequence that allows its specific detection by probe FL125 in northern analysis, while it is co-expressed with endogenous rDNA genes.

A loop in helix 39 or helix 44 of the 18S rRNA sequence was replaced with the U1 stem loop. It had been shown before that yeast strains expressing only 18S rRNAs with tags inserted at these positions were viable (Petrov & Puglisi, 2010). In the crystal structure of the yeast 80S ribosome (Ben-Shem et al, 2011) these sites are exposed on the 40S subunit surface. The tagged mutant 18S rRNA was co-expressed with the RNA binding domain of human protein U1A, which interacts with the U1 stem loop (Nagai et al, 1995). This U1A RNA binding domain was linked to a TAP-tag at its C-terminus, resulting in a U1A-TAP construct. The TAP-tag allowed the purification of U1 containing mutant ribosomes. 18S rRNA constructs with a U1 stem loop inserted in antisense direction, which does not bind to U1A, served as a negative control. An overview of the construct is given in Figure 37.

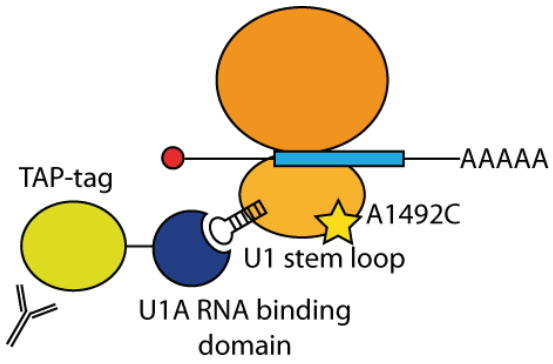

Figure 37 Method to purify a defective ribosome.

First, the expression of the tagged 18S rRNA and the U1A-TAP or TAP-U1A proteins was tested. Insertion of a U1 stem loop, in sense or antisense direction, in helix 39 caused a reduction in the steady state level of wild type 18S rRNA (Figure 38A). An explanation could be that the insertion causes the rRNA to be non-functional, making it a substrate for 18S NRD. Therefore this construct was not further analyzed. Insertion of the U1 stem loop in helix 44 did not affect the steady state level of either wild type or mutant 18S rRNA (Figure 38A). This indicates that insertion of the tag at this position is less likely to affect ribosome function and does not interfere with the 18S NRD process. The 18S rRNA with the U1 stem loop inserted in helix 44 will from here on be referred to as 18S-U1 rRNA. U1A-TAP protein was expressed equally well in yeast co-expressing tagged 18S rRNA constructs and yeast not expressing these constructs (Figure 38B).

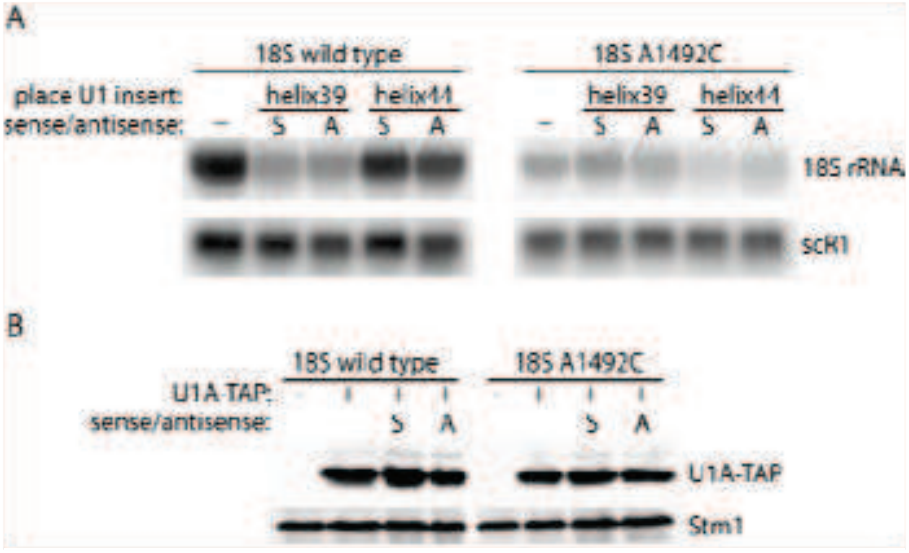

Figure 38 Steady state levels of tagged 18S rRNAs and U1A-TAP protein.
A: 18S rRNA (wild type or mutant) with a U1 stem loop (sense or antisense) inserted in helix 39 or helix 44 was expressed in *S. cerevisiae* grown in the presence of 2% galactose. 18S rRNA was detected by northern analysis using probe OBS3118. scR1 RNA was used as a loading control and detected by probes resulting from random priming of a scR1 PCR product. B: U1A-TAP protein was co-expressed with 18S rRNA (wild type or mutant) containing a U1 stem loop (sense or antisense) in helix 44 in *S. cerevisiae* grown in the presence of 2% galactose. Protein was extracted using a rapid protocol (Kushnirov, 2000) and U1A-TAP was detected by western analysis using PAP. Stm1 was used as a loading control and was detected by the antibody AbBS8.

I then tested whether U1A-TAP binds to translating ribosomes. Their sedimentation through sucrose density gradients was followed and compared with the sedimentation pattern of 18S-U1 rRNA and with the profile formed by (mainly ribosomal) RNA. First of all, this allowed

us to see whether U1A-TAP binds to ribosomes at all: if not it will be present on the top of the gradient only. Second, it gives an indication on whether U1A-TAP binds to ribosomes that participate in translation, depending on whether it co-sediments with polysomes.

Figure 39A shows that U1A-TAP binds translating ribosomes, as it was found in polysomal fractions when co-expressed with wild type 18S rRNA containing a sense U1 stem loop. As expected, U1A-TAP did not bind to ribosomes when the U1 stem loop was inserted in antisense direction (Figure 39B). The A1492C mutation caused 18S rRNAs to shift to lower density fractions (compare Figure 39C and D to A and B): the mutant 18S rRNA is less represented in polysomal fractions and more in 80S fractions compared to wild type 18S rRNA. As expected, the U1A-TAP distribution displays a similar shift to lighter fractions (compare Figure 39C and A).

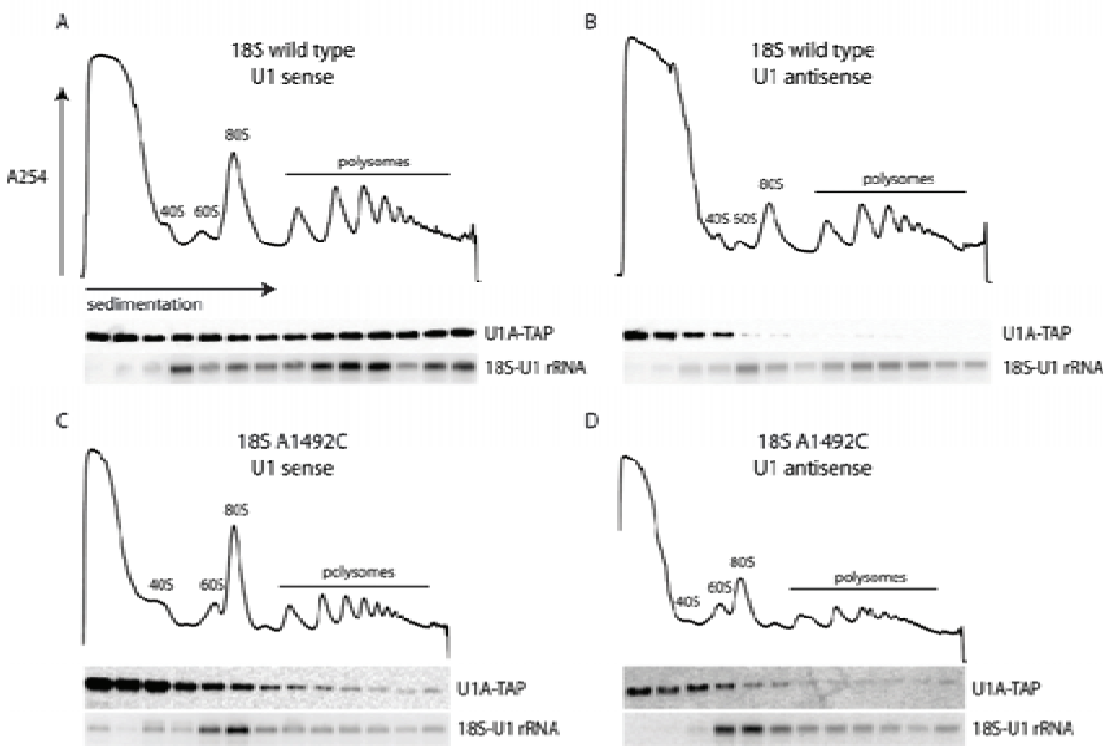

Figure 39 Sedimentation of 18S wild type and mutant rRNA and U1A-TAP.
Sucrose density sedimentation of the lysate obtained from *S. cerevisiae* co-expressing U1A-TAP and 18S rRNA (wild type or mutant) with a U1 stem loop (in sense or antisense direction) inserted in helix 44. Yeast was grown on medium containing 2% galactose. U1A-TAP was detected by western analysis on samples of equal size taken from gradient fractions produced by a gradient fractionator, using PAP. 18S rRNA was extracted from equal size samples taken from fractions produced by a gradient fractionator, and was detected by northern analysis, using probe OBS3118.

All together, these data show that insertion of the U1 stem loop does not interfere with ribosome function and that it efficiently binds U1A-TAP. In addition, as the antisense U1 stem loop does not bind U1A-TAP, this construct should be a valid negative control in ribosome purification experiments.

2.2.3.3 Optimization of the purification protocol

A purification protocol generally consists of a step in which cells are lysed, a step in which the lysate is cleared, often by high speed centrifugation, and finally the actual purification. The conditions for all these steps were optimized for purification of ribosomes and factors of which the binding to ribosomes may be sensitive to high salt concentrations.

First of all, cells were lysed by vortexing in presence of glass beads. This relatively gentle way of lysing cells has been shown before to be effective in ribosome purification methods (Ben-Shem et al, 2011; Ben-Shem et al, 2010) and was chosen to minimize the loss of interaction between ribosomes and associated proteins. It further has the advantage that this method does not disrupt mitochondria (Lang et al, 1977), which avoids contamination with mitochondrial ribosomes. Second, lysis and purification buffers were optimized for the purification of ribosomes and associated proteins. All buffers contained 10 mM Mg^{2+}, to stabilize ribosomal subunit interaction, and relatively low salt concentrations were used (a maximum of 100 mM NaCl). Third, clearing the lysate in a high speed centrifugation step may cause ribosomes to sediment and therefore be lost from the cleared lysate, due to their large size. Therefore the speed and time of centrifugation was optimized to end up with a maximum quantity of ribosomes in the cleared lysate (see below). Finally, the time between cell lysis and the final elution was kept as short as possible: cell lysis and purification steps were all performed in a single day.

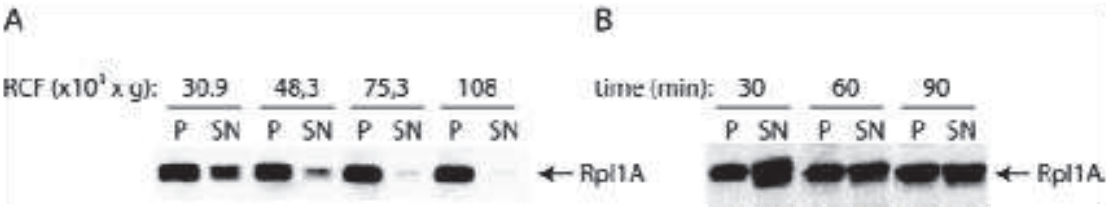

Figure 40 Optimization of centrifugation speed and time.

A: *S. cerevisiae* lysate was subjected to centrifugation at the indicated relative centrifugal forces (RCF) in a JA-25.50 ($30.9x10^3$ and $48.3x10^3$ x g) or a 50.2 Ti rotor ($75.3x10^3$ and $108x10^3$ x g) for 84 minutes. B: *S. cerevisiae* lysate was subjected to centrifugation at 30.8 x g for the indicated times in a JA-25.50 rotor. To determine the presence of ribosomes in pellet (P) and supernatant (SN), samples taken from supernatant and pellet, resuspended in the same volume as the supernatant, were analyzed by western blot. The ribosomal protein Rpl1A was detected using antibody AbBS6.

In search for optimal lysate clearance conditions, yeast lysate was subjected to centrifugation at four different speeds for 84 minutes. As shown in Figure 41A, the lowest centrifugal force ($30.9x10^3$ x g) resulted in the highest fraction of ribosomal protein in the supernatant. It was then tested if, at that speed, the centrifugation time affected the fraction of ribosomal protein in the supernatant. Figure 40B shows that a longer centrifugation time did not result in a higher fraction of ribosomal protein in the supernatant. Therefore I decided to apply a centrifugal force of 30.8 x g for 30 minutes in the purification protocol.

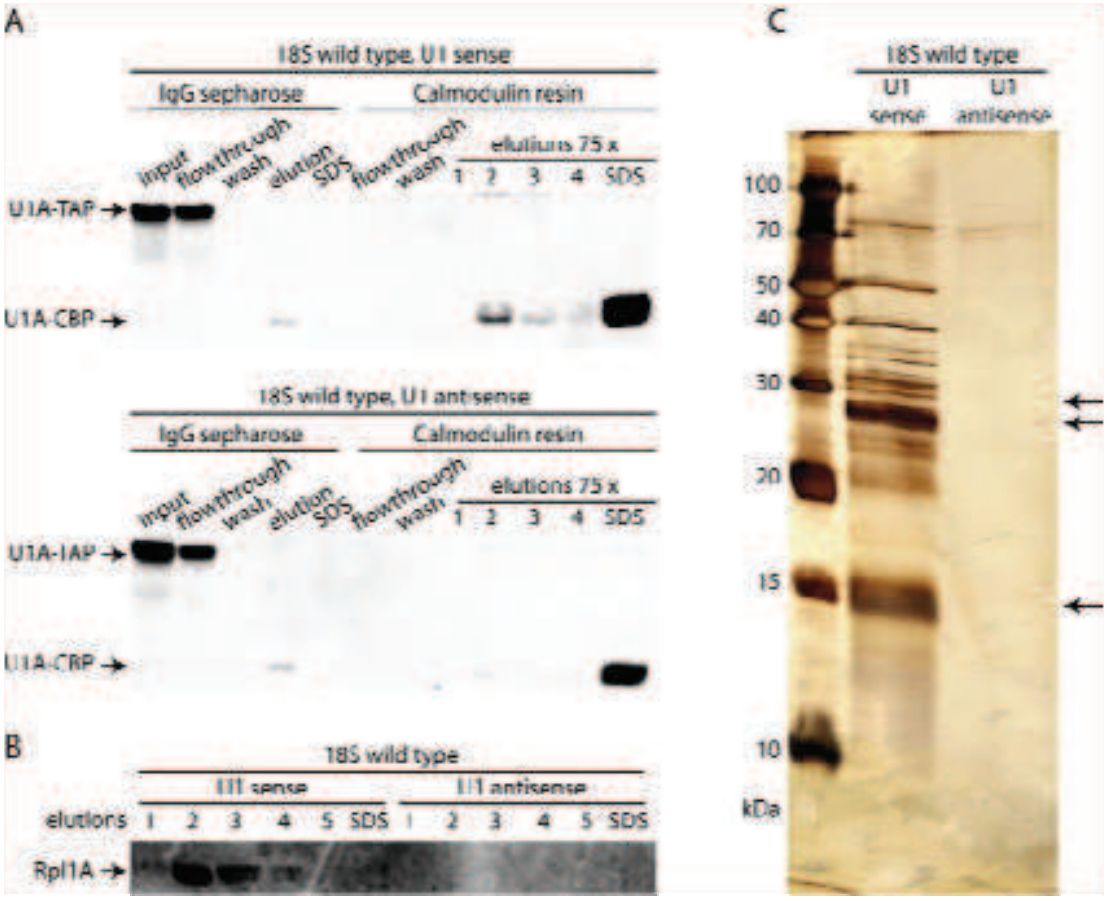

Figure 41 Purification of wild type ribosomes via U1 stem loop and U1A-TAP.
A tandem affinity purification was performed on lysate from yeast expressing 18S-U1 rRNA (sense or antisense) and U1A-TAP, grown in presence of 2% galactose. A: 3,3 x 10^{-6} fractions of each purification step (except for the elutions which are 75 x more concentrated) were analysed by western blot: the presence of U1A-TAP (after TEV cleavage U1A-CBP) was followed using peroxidase anti-peroxidase (Sigma). B: Elution fractions of a similar purification were analyzed by western blot for the presence or ribosomal protein Rpl1A, using antibody AbBS6. C: Elution fraction E2 of the purification shown in A was separated on a 15% SDS-PAGE and visualized by silver staining. The arrows indicate bands that were analyzed by mass spectrometry.

Purifications were then performed, using the optimized TAP method, on yeast co-expressing wild type 18S-U1 rRNA and U1A-TAP. The presence of U1A-TAP was followed throughout the purification. Figure 41A shows that, as expected, U1A-TAP was purified from yeast expressing 18S rRNA with the U1 stem loop inserted in sense direction, as well as from yeast expressing 18S rRNA with the U1 stem loop inserted in antisense direction. Most of the U1A-TAP stays bound to the calmodulin beads after elution, it only dissociates from the beads in presence of 1% SDS. However, when elution fractions were analyzed for the presence of ribosomal protein Rpl1A, most of this protein eluted in elution fractions E2 and E3 (Figure 41B). Elution fractions E2 were concentrated by lyophilisation and analyzed on a 15 % SDS-PAGE. Three of the bands that appeared after silver staining were analyzed by mass spectrometry (indicated by arrows in Fig. 42B). All bands contained a mixture of several 40S and 60S subunit proteins, confirming that the method I developed purifies ribosomes.

Finally, purifications were performed on yeast co-expressing wild type 18S-U1 rRNA and U1A-TAP and on yeast co-expressing mutant 18S-U1 rRNA and U1A-TAP. The culture volume used for purification was twice higher for strains containing mutant ribosome than for strains containing wild type ribosome, to approximately compensate for the reduced levels of mutant ribosomes as a consequence of 18S NRD. For each purification, elution fraction E2 was concentrated by lyophilization and analyzed on a 10-20 % gradient SDS-PAGE. To also compare large size proteins, a second elution fraction was analyzed on a 7% SDS-PAGE. The pattern of bands obtained from the purification of mutant 18S-U1 sense rRNA was compared with that obtained from the purification of wild type 18S-U1 sense rRNA (Figure 42). On the two gels, 11 bands were identified that were present in the elution of the mutant ribosome purification, but not in the elutions of the wild type ribosome purification. These bands were cut from the gels and analyzed by mass spectrometry. Bands cut from similar positions in the wild type elution were used as negative controls.

The low intensity of the bands cut, corresponding to low amounts of proteins, complicated reliable identification of the proteins they represented. Most proteins identified were represented by only few peptides. For many bands peptides were identified that corresponded to a mixture of proteins that were either ribosomal proteins, proteins commonly associated with translating ribosomes or highly abundant proteins like GAPDH. All of these were considered to either co-purify non-specifically with mutant ribosomes or to represent proteins associated with both the mutant and wild-type ribosomes. Also several factors involved in ribosome biogenesis were identified, such as Noc4, Nob1 (band 1), Krr1, Nop1 (band 3). This may be a consequence of overrepresentation of mutant 18S rRNA in pre-40S subunits, due to

their rapid degradation once they are mature. Although it has been excluded before that the mutation used here causes a problems in 18S rRNA processing (Cole et al, 2009), it is also possible that 18S A1492C ribosomes stay associated with ribosome assembly factors longer than their wild type counterparts. Finally, it cannot be excluded that in our strain background, the A1492C does inhibit pre-40S maturation.

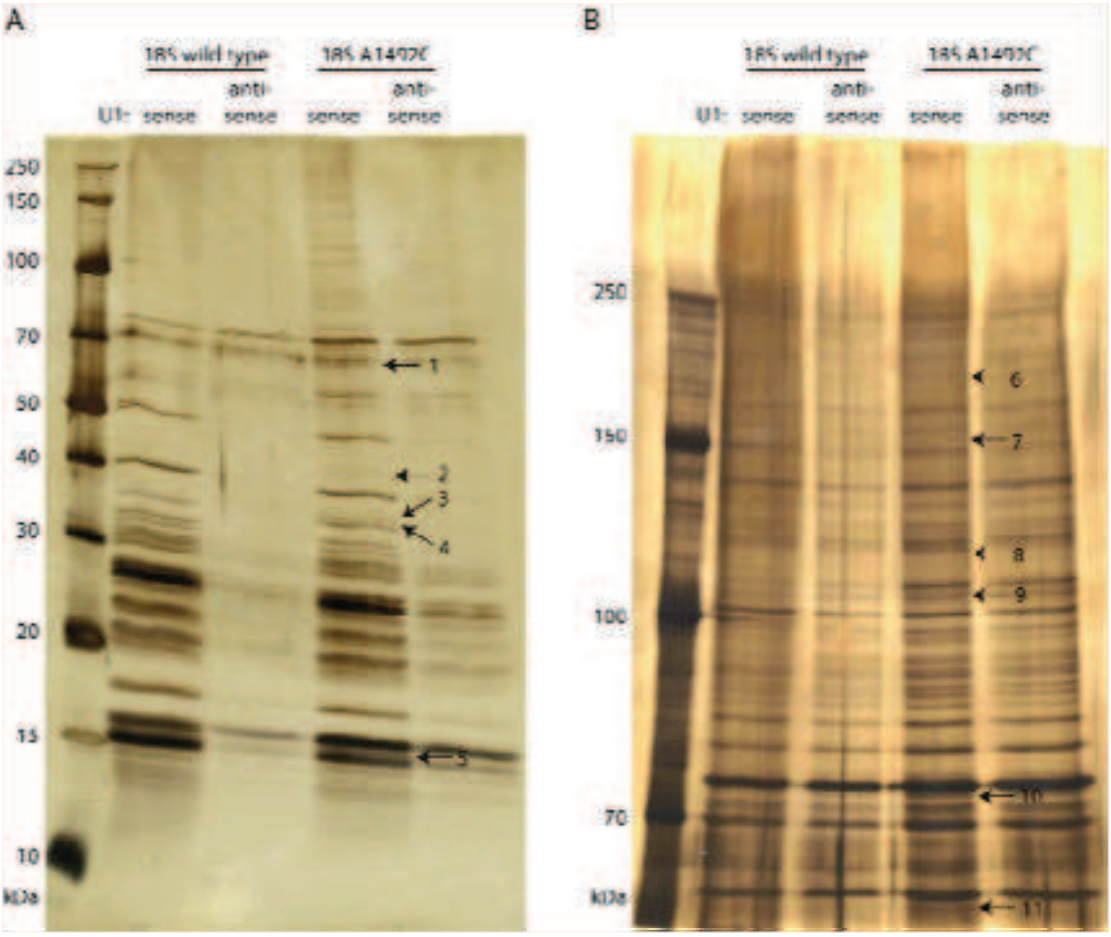

Figure 42 Purification of wild type and mutant ribosomes via U1 stem loop and U1A-TAP.
A tandem affinity purification was performed on lysate from yeast expressing 18S-U1 rRNA (wild type or mutant, sense or antisense) and U1A-TAP, grown in presence of 2% galactose. A: Elution fraction E2 was separated on a 10-20 % gradient SDS-PAGE and visualized by silver staining. The arrows indicate bands that were analysed by mass spectrometry. B: Elution fraction E3 was separated on a 7 % SDS-PAGE and visualized by silver staining. The arrows indicate bands that were analysed by mass spectrometry.

In conclusion, a method was developed that allows the specific purification of ribosomes containing a mutation in their 18S rRNA. However, using this method, no factors that are candidates for acting on stalled ribosomes were identified.

2.2.4 Analysis of the role of Ltn1 in peptide stability and mRNA degradation.

Ltn1 is responsible for polyubiquitination of peptides produced by ribosomes that stall on a subset of stall site containing mRNAs. This targets these peptides for degradation by the proteasome (Bengtson & Joazeiro, 2010). In rabbit reticulocyte lysates it was shown that Dom34-Hbs1 mediated dissociation of the stalled ribosomes is needed before efficient ubiquitination by Ltn1 can occur (Shao et al, 2013). Biochemical experiments indicate that ribosomes can only be dissociated by Dom34-Hbs1 if their mRNA does not extend too long downstream of the P-site (Pisareva et al, 2011; Shoemaker & Green, 2011). This suggests that the mRNA cleavage seen in NGD precedes ribosome dissociation. These observations suggest that Ltn1 acts downstream of mRNA cleavage. Although the majority of Ltn1 and its associated complex RQC is found to be associated to 60S subunits, in yeast some polyubiquitination was reported to occur on 80S ribosomes, hence before subunit dissociation (Defenouillere et al, 2013). This opens the possibility that Ltn1 and other components of the RQC may bind to stalled ribosomes before subunit dissociation, and affect mRNA cleavage and/or subunit splitting. I studied whether the absence of Ltn1 has an effect on the efficiency of mRNA cleavage.

To study this question, first it needed to be validated whether Ltn1 was required for peptide degradation in our yeast strain. A set of reporters was prepared that contained various ribosomal stall sites (a stem loop (SL) or stretches of basic amino acids (K12, encoded by AAG codons, and R12)) inserted between a sequence encoding a TAP-3HA sequence and a sequence encoding GFP (see Figure 43A). Negative control reporters did not contain any stall site (two types, as the sequence in which a stem loop was inserted differed from the sequence the other stall sites were inserted in). A second type of negative control, R12FS, contained the same nucleotide sequence as the R12 stall site, but with a frame shift. This resulted in a peptide that did not contain 12 consecutive arginines but rather the peptide sequence PGDDGAAGDDGAA (one amino acid more due to insertion of 3 nucleotides to establish the frame shift). All reporters were under the control of a galactose inducible promoter. The presence of the GFP sequence downstream of the stall site allowed a clear distinction, based on a difference in size, between full length protein (50-54 kDa) and a truncated protein produced by a stalled ribosome (~24 kDa).

In Figure 43A it is shown that for most reporters, even in absence of a stall site, truncated proteins were detected in yeast that expresses Ltn1 (wild type). These might be protein

degradation products. For the reporter containing a R12 stall site deletion of *LTN1* caused the appearance of a truncated peptide (red rectangles), suggesting its Ltn1 dependent degradation. In agreement with previous observations, in which proteasome inhibition did not cause accumulation of a truncated peptide produced from a stem loop reporter (Dimitrova et al, 2009), no peptide produced from a stem loop reporter accumulated in absence of Ltn1.

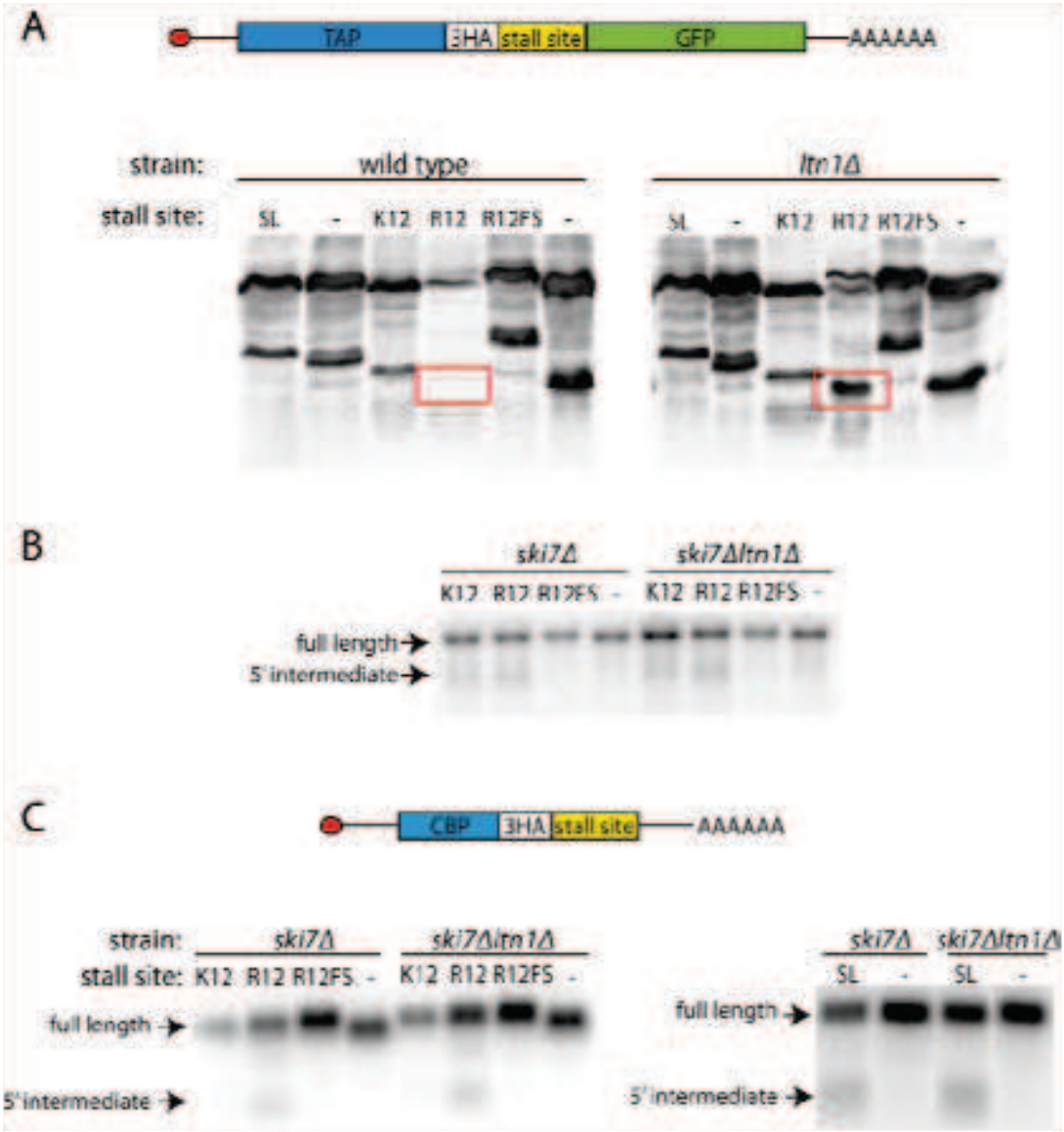

Figure 43 Effect of *LTN1* deletion on peptide stability and mRNA cleavage in NGD.
A: Steady state levels of protein produced from the depicted reporter mRNA containing the indicated stall sites. Protein was extracted from *S. cerevisiae* grown in presence of 2% galactose using a rapid protocol (Kushnirov, 2000) and was detected by western blot using PAP. B: Steady state levels of the same mRNA reporters used in A, and their degradation intermediates that accumulate in *ski7*Δ strains, in presence and absence of Ltn1. C: Steady state levels of the depicted reporter mRNA containing the indicated stall sites, and their degradation intermediates that accumulates in *ski7*Δ strains, in presence and absence of Ltn1. All RNA was analyzed by northern blot, using probe OBS4671 which hybridizes to the 3HA tag.

Surprisingly, and contrasting with previous data, no accumulation of a truncated peptide produced from a K12 reporter was observed either. Possible explanations why truncated peptides produced from reporters containing stall sites other than R12 do not accumulate are that these stall sites are less efficient in inducing stalling, or that a weak accumulation of the peptide is masked by the truncated protein signals that are also present in wild type strains.

Now that there was an indication that Ltn1 dependent degradation of stalled ribosome produced peptides occurs in our strain, at least in case of an R12 stall site, I tested whether Ltn1 had an effect on mRNA cleavage on the same mRNA reporters. For this purpose the NGD assay described in Figure 31 was used. Figure 43B shows that the absence of Ltn1 did not cause any visible reduction in the level of 5' degradation intermediate produced from K12 and R12 reporter mRNAs. Because the 5' intermediate signal from the TAP-3HA-GFP reporters was quite low, the experiment was repeated using a reporter in which a stall site was inserted downstream of a CBP-3HA encoding sequence (Figure 43C), from which the 5' intermediate accumulated at higher levels. Again Ltn1 deletion did not cause any visible reduction in the level of 5' intermediate produced from any of the reporter mRNAs. In this experiment no evidence was found supporting an effect of Ltn1 on NGD endonucleolytic cleavage.

2.2.5 Nuclease requirement for exosome-mediated No-go decay intermediate degradation

The 5' intermediate that results from mRNA cleavage in NGD is degraded by the cytoplasmic exosome. Dis3, the catalytic subunit of the cytoplasmic exosome, has both exo- and endonuclease activity (Dziembowski et al, 2007; Lebreton et al, 2008). General mRNA turnover depends on the exonuclease activity of Dis3. Meanwhile, for degradation of NSD substrates, both poly(A)+ and poly(A)-, either endonuclease or exonuclease activity is sufficient (Schaeffer & van Hoof, 2011). I examined what activity of Dis3 is required for degradation of a NGD 5' intermediate.

I tested if mutation of the Dis3 exonuclease catalytic site (D551N), mutation of the Dis3 endonuclease catalytic site (D171N) (Dziembowski et al, 2007; Lebreton et al, 2008), or mutation of both resulted in stabilization of a 5' intermediate produced from a stem loop containing CBP-3HA-SL mRNA. This NGD reporter was expressed in *S. cerevisiae* in which the essential chromosomal *DIS3* gene was controlled by a doxycycline repressible promoter

(tet-off). Dis3, wild type or mutant, was expressed from a plasmid. In presence of doxycycline, degradation by the exosome depended on the plasmid expressed Dis3.

As shown in Figure 44, mutation of endo- or exonuclease activity did not or hardly cause any stabilization of the 5' intermediate. However, when Dis3 lacks both activities, the intermediate accumulates to the same extent as in absence of the protein. These data confirm that degradation of the 5' NGD intermediate depends on the exosome. They show that either either the endo- or the exonuclease activity is sufficient for intermediate degradation. The similarity in requirement of Dis3 activity to that observed for NSD substrates supports the hypothesis that NGD and NSD are closely related, and that the 5' NGD intermediate may be functionally similar to a poly(A)- NS mRNA.

The intermediate is stabilized to higher levels a strain lacking Ski7 than in a strain in which Dis3 is repressed. This might be due to incomplete repression of chromosomal Dis3.

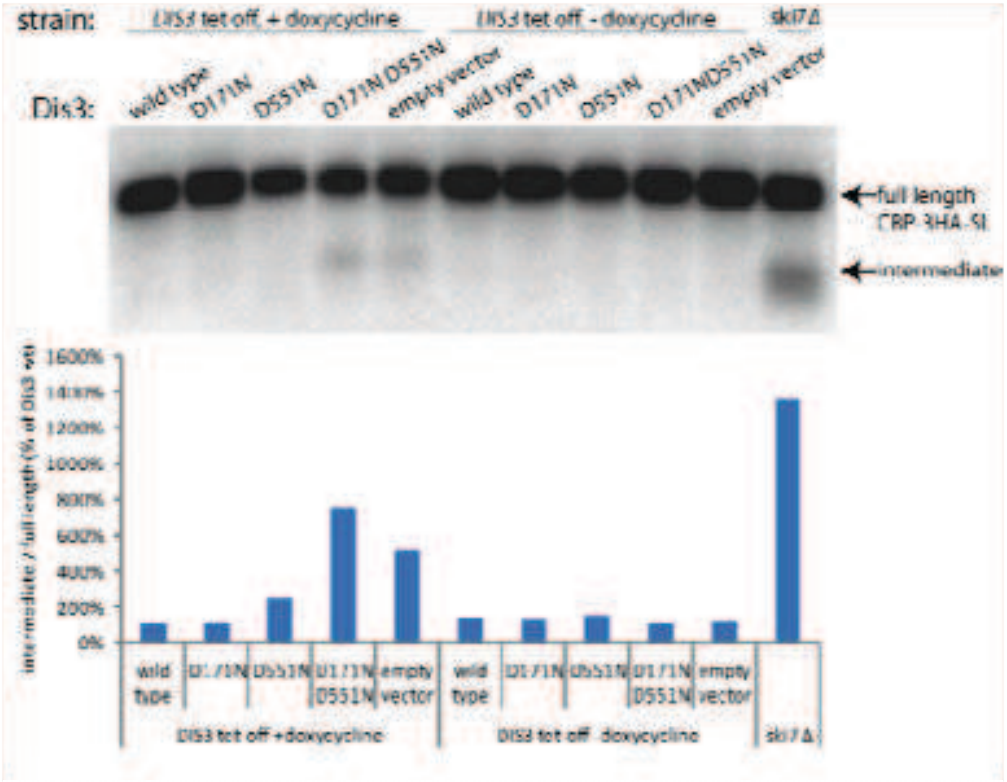

Figure 44 Requirement of exosomal endo- and exonuclease activity for NGD intermediate degradation. *S. cerevisiae* containing *DIS3* under the control of a doxycycline repressible promoter and expressing the indicated Dis3 mutants and a CBP-3HA-SL NGD reporter from a galactose inducible promoter was grown in presence of 2% galactose and, if indicated, exposed to 20 µg/ml doxycycline during 7 hours. Steady state levels of the NGD reporter mRNA and a 5' degradation intermediate produced from it were analyzed by northern blot using probe OBS4671. For each mutant the ratio of 5' intermediate over full length mRNA signal was calculated and then standardized for the ratio calculated for Dis3 wild type.

2.3 STUDY OF THE BIOLOGICAL IMPORTANCE OF DOM34-HBS1 MEDIATED RIBOSOME DISSOCIATION

The observation that Dom34 and Hbs1 (or alternative Dom34 partner aEF1α) are conserved in two domains of life suggest that they have an important function in basic cellular processes. This is supported by the embryonic lethality in mice (Adham et al, 2003) and the sterility observed in *Drosophila* lacking Dom34 (Eberhart & Wasserman, 1995). Much of the research on Dom34 and Hbs1 has focused on their role in RNA quality control. However, one could question whether Dom34-Hbs1 acting on translational complexes that stall due to accidental errors in RNA production or processing explains their high level of conservation.

The RNAs that have been used to study NGD, NSD and 18S NRD were all artificial, overexpressed and not necessarily representative of naturally occurring situations. The natural occurrence of NGD, NSD or 18S NRD substrates in a cell and the importance of Dom34-Hbs1 for removing them has not been the subject of any study so far and is therefore unknown. Especially stall sites that have been studied to induce NGD, such as large secondary structures, stretches of rare codons or of codons encoding basic amino acids, are not expected to be produced by mutations or aberrant processing with high frequency. Non-stop mRNAs may be produced more often, especially when produced as a result from the use of cryptic splice sites in the ORF. Defective ribosomes may result from aberrant rRNA production, but might also result from chemical damage. Moreover, because of their long life span, the impact of a defect in a ribosome is likely larger than that of a faulty mRNA. However, the impact of one or few ribosomes stalled on an equal number of mRNAs in a cell is not likely to have a deleterious impact. Consistently, overexpression of mRNA reporters for NSD or NGD or high-level expression of 18S NRD substrates has little impact on cell growth rate.

I was therefore interested in studying whether Dom34-Hbs1 mediated ribosome dissociation may play a role beyond RNA quality control.

2.3.1 Dom34-Hbs1 overexpression

Genetic studies in *S. cerevisiae* have mainly addressed the effect of *DOM34* or *HBS1* deletion. Although the absence of Dom34 has been reported to cause a reduced growth rate (Davis & Engebrecht, 1998), this observation was not supported by other reports (Carr-Schmid et al, 2002), see also Figure 48). Here I studied the effect of Dom34-Hbs1 overexpression on yeast growth.

Dom34 and/or Hbs1 were expressed in wild type *S. cerevisiae* from plasmid, either from their endogenous promoters or from a galactose inducible promoter. A C-terminal 3HA-tag or protein A-tag allowed the detection of Dom34 and Hbs1 respectively. It was confirmed that in presence of galactose Dom34 and Hbs1 were expressed from the galactose inducible promoters at much higher levels than from their endogenous promoters, at 30°C (Figure 45A).

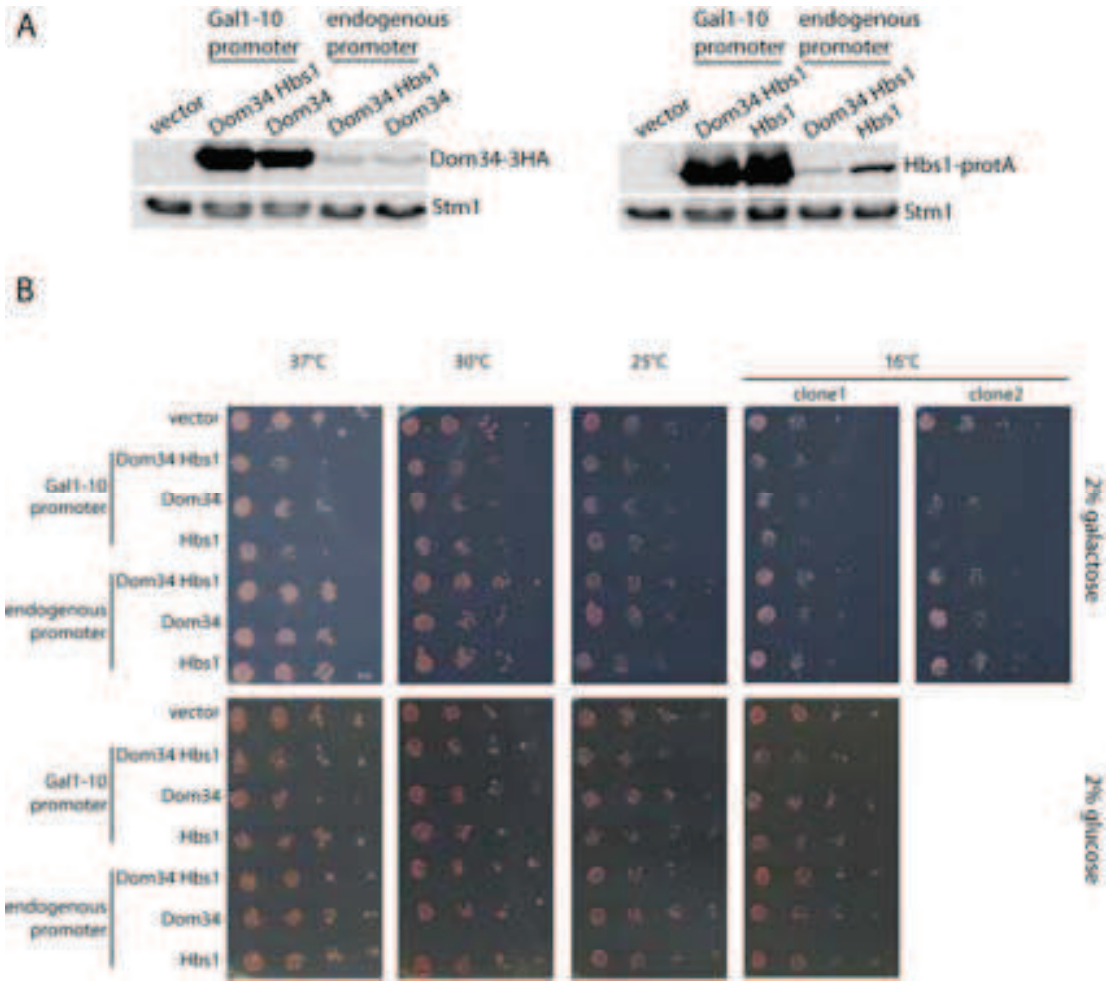

Figure 45 Effect of Dom34-Hbs1 overexpression on yeast growth.
Dom34 and/or Hbs1 was expressed from their endogenous promoter or a galactose inducible promoter in wild type *S. cerevisiae*. A: Hbs1-protein A and Dom34-3HA are overexpressed from galactose inducible *GAL1* and *GAL10* promoters respectively. Protein was extracted from yeast grown at 30°C in CSM-Leu medium containing 2% galactose using a rapid protocol (Kushnirov, 2000). Dom34-3HA and Hbs1-Protein A are detected by western analysis using anti-HA antibody and PAP respectively. Stm1 served as a loading control and was detected by antibody AbBS8. B: Yeast was grown on CSM-Leu medium containing 2% galactose or 2% glucose at the indicated temperatures. Two independent clones are represented for each strain grown at 16°C in presence of 2 % galactose.

Overexpression of Dom34 and/or Hbs1 from galactose inducible promoters did not have any effect on yeast growth at 25, 30 or 37°C (Figure 45B). At 16°C reduced growth was observed in yeast overexpressing Hbs1 and to a lesser extent also in yeast overexpressing Dom34 (Figure 45B, clone 2). However, this effect could not be reproduced with another set of independent clones grown on a second plate (Figure 45B). It was therefore concluded that Dom34-Hbs1 overexpression may reduce yeast growth only to a small extent, if any.

2.3.2 Can Dom34-Hbs1 complement the absence of eRF1-eRF3?

The eRF1-eRF3 complex and the Dom34-Hbs1 complex have in common that they bind to the ribosomal A-site and that, together with Rli1, they can induce dissociation of mRNA bound ribosomes. Whereas eRF1-eRF3 acts specifically on ribosomes with a stop codon in their A-site, Dom34-Hbs1 dissociates ribosomes with any codon in their A-site, including a stop codon (Pisareva et al, 2011; Shoemaker et al, 2010; Shoemaker & Green, 2011).

Yeast lacking eRF1 or eRF3 is inviable. The effect of their absence can be studied using thermosensitive mutants, that are inactive at 37°C. We hypothesized that overexpression of the Dom34-Hbs1 complex may rescue strains lacking functional eRF1-eRF3 complex, by releasing ribosomes that cannot terminate. Although they are paralogs, Hbs1 has been shown not to be able to complement the absence of eRF3. This is not surprising, as Hbs1 does not interact with eRF1 (Wallrapp et al, 1998), and is therefore unlikely to stimulate its activity. That does not exclude that high levels of the entire Dom34-Hbs1 complex may complement the absence of eRF1-eRF3 activity, which was tested here.

Dom34 and Hbs1 were overexpressed from galactose inducible promoters (see Figure 45A) in *S. cerevisiae* strains with thermosensitive eRF1 (sup45) and eRF3 (sup35) mutants. In Figure 46 it is shown that at 37°C, when there is no functional eRF1-eRF3 complex, overexpression of Dom34-Hbs1 complex does not rescue yeast growth. This indicates that increased Dom34-Hbs1 availability cannot replace the role of the eRF1-eRF3 complex in translation termination and recycling *in vivo*.

There can be several explanations. First, the level of overexpressed Dom34-Hbs1 complex may not be sufficient to replace eRF1-eRF3. Second, the rate of Dom34-Hbs1 mediated dissociation may be lower than that of eRF1-eRF3 induced recycling. Third, Dom34-Hbs1 may not act on ribosomes stalled on stop codons *in vivo*. Finally, an important explanation may be found in the fact the Dom34-Hbs1 complex cannot induce peptide release, as Dom34 lacks the GGQ motif required for peptidyl-tRNA hydrolysis (Graille et al, 2008; Lee et al,

2007). Importantly, peptides produced by ribosomes stalled on NS-mRNAs have later been shown to be degraded by the RQC (Brandman et al, 2012; Defenouillere et al, 2013; Verma et al, 2013). Recent reports indicate that this peptide degradation depends on Dom34-Hbs1 mediated dissociation of these stalled ribosomes (Shao et al, 2013). These observations suggest that, even if Dom34-Hbs1 dissociate ribosomes stalled on stop codons in absence of eRF1-eRF3, they may not rescue protein synthesis because all peptides are targeted for degradation.

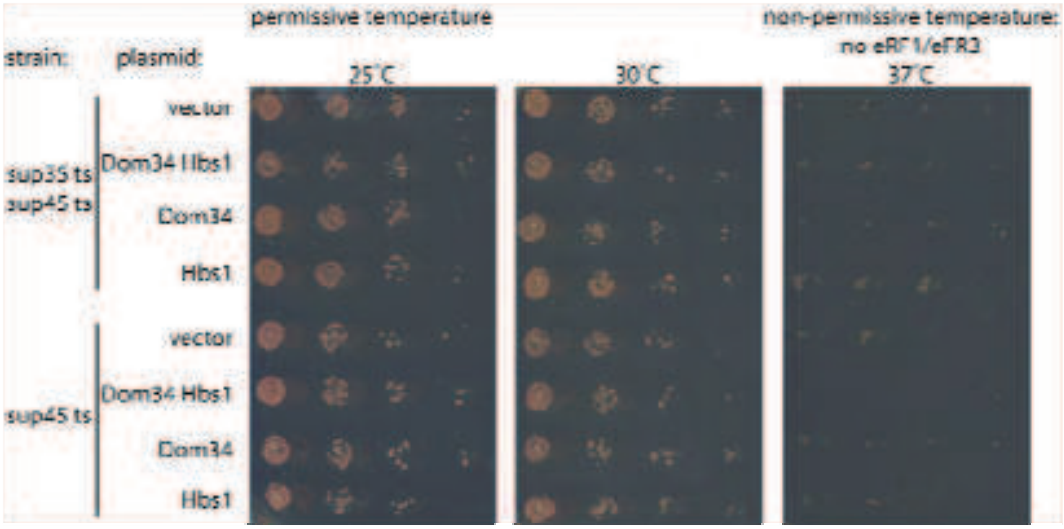

Figure 46 Dom34-Hbs1 overexpression does not rescue yeast lacking eRF1-eRF3.
In *S. cerervisiae* containing temperature sensitive mutants of eRF1 (sup45 ts) and eRF3 (sup 35 ts) Hbs1-protein A and/or Dom34-3HA were expressed from galactose inducible *GAL1* and *GAL10* promoters respectively. Yeast, in 10-fold dilution series, was grown on CSM-Leu medium containing 2 % galactose at 25°C (eRF1 and eRF3 are expressed from their mutant genes), 30°C and the non-permissive temperature 37°C (eRF1 and eRF3 are not expressed from their mutant genes).

2.3.3 Dom34-Hbs1 mediated dissociation of ribosomes bound to mRNAs that are being degraded

It has been reported that the first steps of cytoplasmic mRNA degradation, deadenylation and decapping, can occur on polysomal mRNAs (Hu et al, 2009). If the exosome and Xrn1 also act on ribosome associated mRNAs, the ribosomes may block their passage. Especially in case of exosome mediated degradation this would be problematic: at some point the exosome would digest the stop codon, making it impossible for elongating ribosomes to terminate. A mechanism would be required to remove these ribosomes, to allow efficient mRNA

degradation. I studied whether the Dom34-Hbs1 complex is needed for efficient cytoplasmic mRNA degradation.

2.3.3.1 Genetic interaction with factors involved in cytoplasmic degradation

In yeast defective for decapping, 5' to 3' mRNA decay cannot occur. General turnover is then dependent on the 3' to 5' pathway. The thermosensitive *dcp1-2* allele produces functional Dcp1 at 25°C, the permissive temperature. However, at the non-permissive temperature, 37°C, no functional Dcp1 is produced and 5' to 3' mRNA decay cannot occur (Tharun & Parker, 1999). In yeast lacking Ski7 or a component of the Ski complex, 3' to 5' mRNA decay cannot occur and general turnover depends on 5' to 3' degradation. Strains lacking both pathways are not viable (Anderson & Parker, 1998). It was examined whether in strains in which only one of the two mRNA decay pathways occurs, the presence of Dom34 is required for efficient growth.

Figure 47A shows that *dcp1-2* mutant yeast did not grow at all at non-permissive temperature (37°C). At temperatures at which the mutant strain did grow, it was observed that deletion of *DOM34* negatively affected growth in the mutant background (at 30, 32 and 34°C), but not in wild type background. A synthetic slow growth phenotype was also observed for *SKI7* and *DOM34* deletion, but only at low temperature (16°C) (Figure 47B).

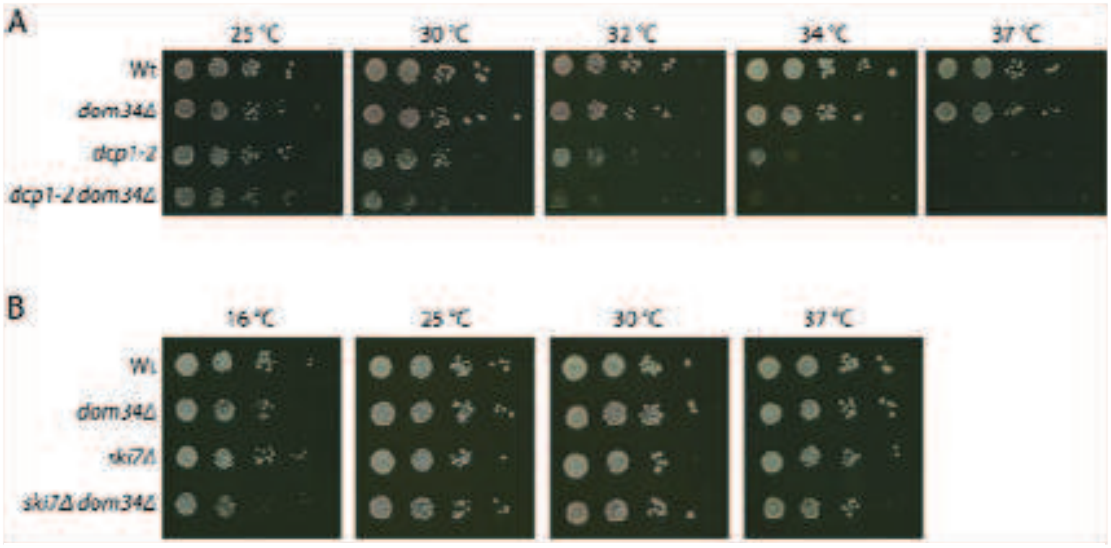

Figure 47 Genetic interaction of Dom34 with Dcp1 and Ski7.
Ten-fold dilution series of the indicated *S. cerevisiae* strains, grown on YPDA medium at the indicated temperatures.

These observations suggests that Dom34 function is needed for efficient 3' to 5' mRNA turnover by the exosome, and at low temperatures also for efficient 5' to 3' mRNA decay by Xrn1. The synthetic growth phenotype of Dom34 with Ski7 only being observed at low temperature is in agreement with the effect of *DOM34* deletion in 40S subunit deficient strains also affecting growth most at low temperatures (Bhattacharya et al, 2010; Carr-Schmid et al, 2002). An explanation may be that some energy demanding processes, e.g. ribosome dissociation or translation, occur less efficiently at low temperatures, making the need for Dom34-Hbs1 action higher. In theory, translating ribosomes may slow down Xrn1 function but should not block it completely, as translating ribosomes move in the same direction as Xrn1 and will eventually be released from the mRNA, after termination. If, at low temperatures, translation elongation, termination or recycling proceeds less efficiently, Dom34-Hbs1 mediated ribosome dissociation may be required for Xrn1 to proceed efficiently.

To test whether the genetic interaction between Dcp1 and Dom34 is caused by Dom34 being required for efficient 3' to 5' degradation, the stability of reporter mRNAs was determined in *dcp1-2* and *dcp1-2dom34*Δ yeast. As the reporters used, MFA2 and PGK1, were expressed from plasmids and under the control of galactose inducible promoters, this experiment required growing the mutant strains in media different from the ones used in Figure 47. It was therefore first confirmed that in CSM media containing either 2% galactose or 2% glucose absence of Dom34 also had a negative effect on growth of *dcp1-2* mutant yeast at 34°C (Figure 48A).

Yeast strains expressing MFA2 or PGK1 reporters were grown at 25°C, at which functional Dcp1 is produced, in presence of 2% galactose. Then they were shifted to 37°C for one hour, to inhibit Dcp1 activity, followed by resuspension in medium containing 4 % glucose at 37°C, to switch off reporter gene transcription. Reporter gene levels were then followed over time. As our hypothesis was that in absence of Dom34 translating ribosomes may block passage of the exosome, one would not expect stabilization of the entire mRNA in the *dcp1-2dom34*Δ strain, but rather of a fragment containing the 3'UTR and large part of the ORF. Such a fragment should be well separated from full length mRNA in case of the relatively short MFA2 mRNA, which was separated on a 6 % acrylamide urea gel. However, no truncated mRNA fragment was detected for either MFA2 or PGK1 (Figure 48B and C).

A truncated mRNA produced from the longer PGK1 reporter may not be well separated from the full length mRNA on the 1,5 % agarose formaldehyde gel used. Therefore the half life of

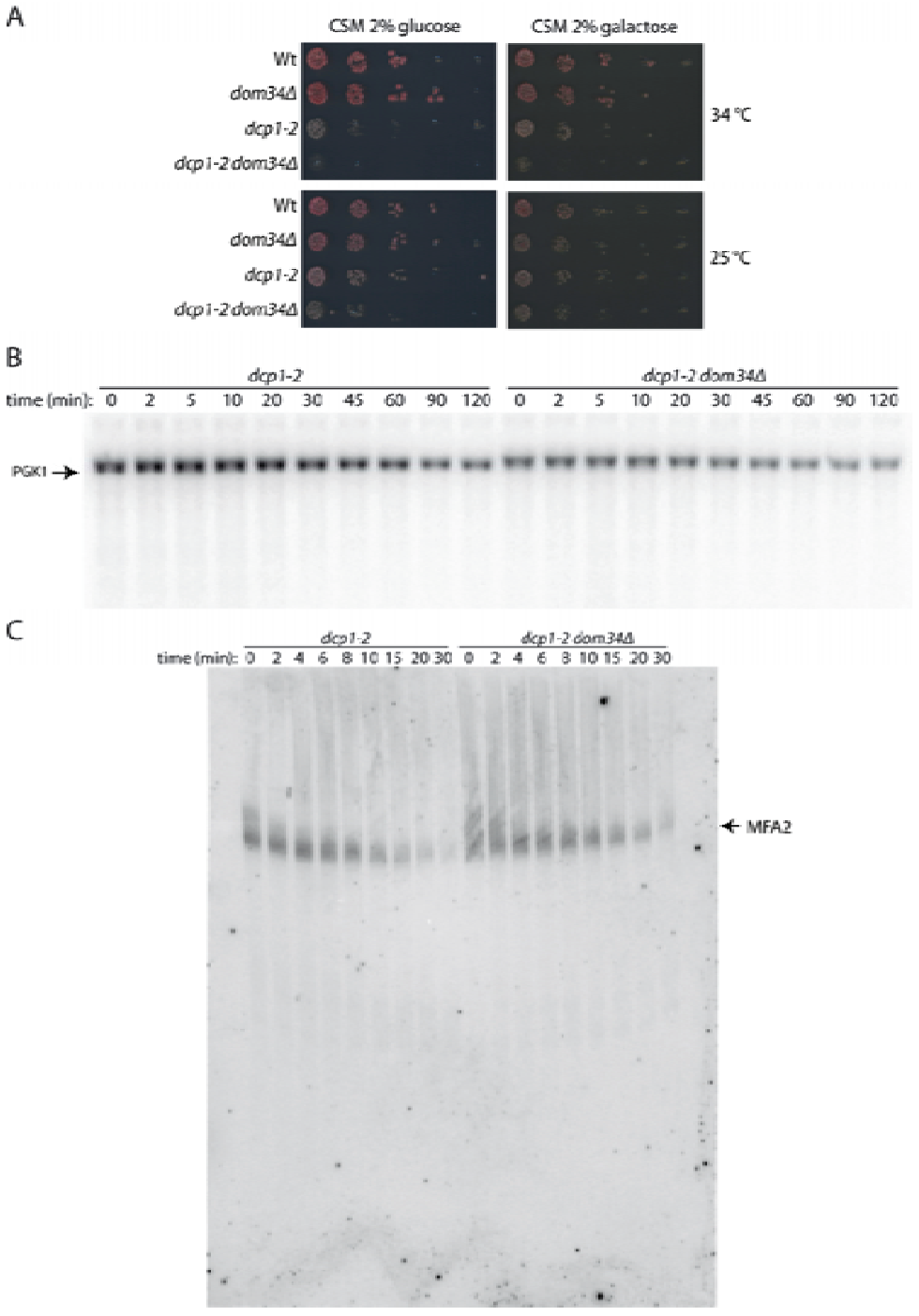

Figure 48 Effect of Dom34 on exosome mediated mRNA degradation.

A: Ten-fold dilution series of the indicated *S. cerevisiae* strains, grown on CSM medium containing 2% glucose or galactose at the indicated temperatures. B and C: Chase experiment to determine the stability of a galactose inducible PGK1 (B) of MFA2 (C) reporter mRNA in the indicated strains. Yeast was grown in CSM-Ura containing 2% galactose. Upon resuspension in CSM-Ura containing 2% glucose, thereby switching off reporter mRNA transcription, PGK1 and MFA2 mRNA levels were followed over time. mRNA was detected by Northern analysis using probes OBS5598 (for PGK1) and OBS1160 (for MFA2).

full length PGK1 was determined for *dcp1-2* and *dcp1-2dom34*Δ strains, being 67 minutes and 61 minutes respectively.

In summary no indications for a need for Dom34 in exosome mediated mRNA turnover were found. However, this does not exclude the requirement for Dom34 in regular 3' to 5' mRNA turnover. mRNAs other than the reporters used may require Dom34-Hbs1 action for efficient 3' to 5' degradation. Even the reporters used may require the complex. They both contain a poly(G) tract in their 5'UTR, which is known to partially block exosome progression (Anderson & Parker, 1998). For the PGK1 mRNA it is possible that a truncated mRNA stabilized due to the presence of this poly(G) tract was not separated from the full length mRNA on gel. One explanation why no stabilizing effect of *DOM34* deletion was observed could be that it was masked by the stabilizing effect of the poly(G) tract.

2.3.3.2 Is dissociation of ribosomes on Nonsense mediated decay targets needed for degradation?

Besides "normal" mRNAs, mRNAs containing a premature stop codon that are therefore targets of the NMD pathway have also been shown to be decapped while still polysome associated (Hu et al, 2010). I examined whether efficient mRNA degradation in NMD requires Dom34-Hbs1 action.

A reporter PGK1 mRNA containing a premature stop codon was expressed from a galactose inducible promoter. Steady state levels of the full length NMD substrate and degradation intermediates were compared between wild type and *dom34*Δ yeast, by northern analysis using a probe that hybridizes to a poly(G) sequence in the 3' UTR. No differences were observed (Figure 49).

Although I did not find any indication of Dom34-Hbs1 facilitating mRNA degradation by the exosome or Xrn1, this does not mean that it does not occur. Especially if the exosome degrades ribosome associated mRNAs, digestion of the stop codon may cause ribosomes to get stuck on the mRNA. However, in *S. cerevisiae* the major pathway for general mRNA turnover is the 5' to 3' pathway. To find a biologically significant role for the Dom34-Hbs1 complex facilitating mRNA degradation, it would therefore make sense to look more specifically into mRNAs that are known to depend mainly on the exosome for degradation. In yeast, the principal cytoplasmic exosome substrates characterized so far are NS mRNAs, with or without poly(A) tail. As recent evidence strongly indicates that degradation of these mRNAs is indeed stimuted by Dom34-Hbs1 mediated ribosome dissociation (Tsuboi et al, 2012), this line of research was not further continued.

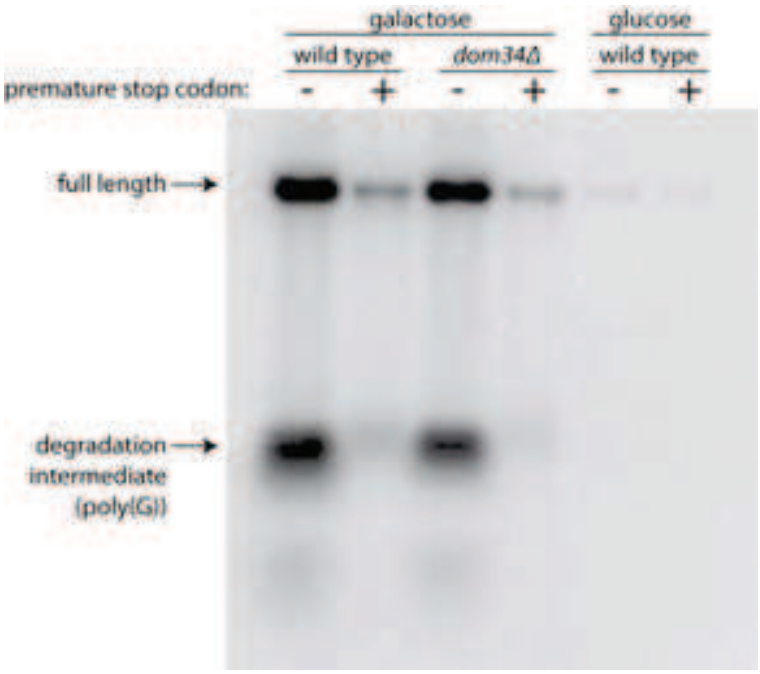

Figure 49 Effect of Dom34 on the degradation of NMD substrates.
Steady state levels of wild type and *dom34*Δ *S. cerervisiae* expressing a reporter PGK1 mRNA with or without premature stop codon. The PGK1 reporter was expressed from a galactose inducible promoter and yeast was grown in presence of 2% galactose. Total RNA was extracted and analyzed by northern blot, using probe OBS1298, hybridizing to the poly(G) tract.

2.3.4 Dom34-Hbs1 mediated dissociation of inactive ribosomes

Many stress conditions cause an inhibition of translation. Ribosomes accumulate in an inactive 80S form, which protects the ribosomal subunits from degradation and makes sure that there is a pool of ribosomes available for rapid restart of translation when this is required (see paragraph 1.2). Glucose depletion is an example of a translation inhibiting stress condition. The inactive 80S ribosomes that accumulate contain Stm1 in a conformation that is incompatible with translation and that clamps the ribosomal subunits together (Ben-Shem et al, 2011). When glucose is added, these inactive ribosomes are rapidly mobilized and translation restarts quickly. To become available for translation initiation, the subunits of the inactive 80S ribosomes need to be dissociated. I hypothesized that the Dom34-Hbs1 complex may dissociate the accumulated 80S ribosomes and thereby stimulate restart of translation after stress.

The study I performed resulted in a manuscript that was submitted for publication and is currently under revision. A brief summary of the work will be given here, followed by the

submitted manuscript. Supplementary data of the manuscript can be found in the supplementary information of this thesis. Finally, some additional experiments that are not in the manuscript will be presented.

By analyzing polysome profiles obtained from *S. cerevisiae* before, during and after glucose starvation stress, I found that Dom34 and Hbs1 stimulate a rapid restart of translation upon glucose addition, especially at low temperatures (16°C). This was confirmed at the level of protein production, by monitoring ^{35}S-methionine incorporation. The Stm1-bound inactive ribosomes that accumulate during glucose depletion differ from known Dom34-Hbs1 substrates. To test whether Dom34-Hbs1 dissociate Stm1-containing ribosomes, I applied for an EMBO short term fellowship to visit the lab of Dr. Rachel Green (Johns Hopkins University, USA) who had developed a biochemical ribosome dissociation assay for translating ribosomes. In collaboration with Anthony Schuller in her lab, we showed that these inactive ribosomes are indeed substrates of Dom34, Hbs1 and Rli1. That Dom34-Hbs1 and Rli1 also dissociate inactive ribosomes *in vivo* was supported by the finding that deletion of Stm1, which antagonizes ribosome dissociation, rescues the defect in translational restart upon glucose addition seen in strains lacking Dom34. Mutational analysis showed that the GTPase activity of Hbs1 was required for the Dom34-Hbs1function studied here, but that a stable interaction between the two factors was not. The N-terminal domain of Hbs1, of which the function is unknown, was not required either.

The pool of inactive ribosomes that accumulates during glucose depletion contains a large fraction of all ribosomal subunits in the cell. In growing, non-stressed cells, inactive 80S ribosomes form as well, although to a lesser extent. I hypothesized that they may be substrates of Dom34-Hbs1 as well. Supporting this, I found by polysome analysis in presence of high salt concentrations, that the increased 80S peak observed in *dom34*Δ strains is accounted for by an accumulation of inactive ribosomes. Moreover, I found that the Dom34-Hbs1 complex stimulates translation in a yeast extract.

In summary I found that the Dom34-Hbs1 complex dissociates inactive ribosomes, thereby making their subunits available for translation initiation. This is particularly important in cells recovering from stress, but my data indicate that it also occurs in non-stressed cells.

Dom34-Hbs1 mediated dissociation of inactive 80S ribosomes promotes restart of translation after stress

Antonia M.G. van den Elzen[1], Anthony Schuller[2], Rachel Green[2], and Bertrand Séraphin[1,*]

[1] Equipe Labellisée La Ligue, Institut de Génétique et de Biologie Moléculaire et Cellulaire (IGBMC), Centre National de Recherche Scientifique (CNRS) UMR 7104/Institut National de Santé et de Recherche Médicale (INSERM) U964/Université de Strasbourg, 67404 Illkirch, France

[2] Howard Hughes Medical Institute, Department of Molecular Biology and Genetics, Johns Hopkins University School of Medicine, Baltimore, Maryland, USA.

* Corresponding author: Bertrand Séraphin (seraphin@igbmc.fr)

Running title: Dom34-Hbs1 modulates ribosomal subunit availability after stress

Keywords: glucose-starvation, No-Go decay, Rli1, ribosome pool, ribosomal subunits, Stm1, translation initiation, translation termination

Abstract

Following translation termination, ribosomal subunits are dissociated to become available for subsequent rounds of protein synthesis. In many translation inhibiting stress conditions, e.g. glucose starvation in yeast, free ribosomal subunits reassociate to form a large pool of non-translating 80S ribosomes stabilized by the "clamping" Stm1 factor. The subunits of these inactive ribosomes need to be mobilized for translation restart upon stress relief. The Dom34-Hbs1 complex, together with the Rli1 ATPase, have been shown to split ribosomes that are stuck on mRNAs in the context of RNA quality control mechanisms. Here, using *in vitro* and *in vivo* methods, we report a new role for the Dom34-Hbs1 complex and Rli1 in dissociating inactive ribosomes, thereby facilitating translation restart in yeast cells recovering from glucose starvation stress. Interestingly, we found that this new role is not restricted to stress conditions, indicating that in growing yeast there is a dynamic pool of inactive ribosomes that needs to be split by Dom34-Hbs1 and Rli1 to participate in protein synthesis. We propose that this could provide a new level of translation regulation.

Introduction

The production of proteins by ribosomes can be divided into four stages that together form the translation cycle: initiation, elongation, termination and recycling {Krebs, 2011 #542}. Eukaryotic translation initiation requires separate 40S and 60S ribosomal subunits, which assemble on the initiation codons of messenger RNAs (mRNA) to form the actively translating 80S ribosome. Ribosomal subunits available for initiation result from ribosome recycling, which occurs after, and is tightly coupled to translation termination. Termination and recycling are triggered when a translating ribosome encounters a termination codon. At this point, the termination factors eRF1 and eRF3, together with the ATPase Rli1 (also known as ABCE1), catalyze peptide release and subsequent ribosome dissociation {Pisarev, 2010 #10;Shoemaker, 2011 #21}.

Many stress conditions cause a global shut down of translation, allowing cells to economically use limited metabolic resources to only produce proteins important for adaptation to the changing environment. Ribosomal subunits that are released through recycling may not engage in new rounds of protein synthesis, but instead associate to form a large pool of non-translating, inactive ribosomes. Formation of these inactive ribosomes may protect ribosomal subunits from damage and/or degradation. Moreover, upon stress relief, these inactive ribosomes can be easily and economically mobilized without a requirement for ribosome biogenesis. Upon prolonged stress, ribosomes may eventually be degraded by ribophagy to provide cells with energy and nutrients {Kraft, 2008 #395}.

In bacteria, it is well described that stress-induced factors bind to ”hibernating” ribosomes and induce the formation of ribosome dimers (70S + 70S). The binding sites of the stress-induced factors overlap with those of mRNA and transfer RNA (tRNA) thus inhibiting normal ribosome activities {Polikanov, 2012 #276}.

Eukaryotic hibernating ribosomes may in some organisms also form dimers {Krokowski, 2011 #315}, but mostly accumulate as inactive 80S monomers. This was shown for example to occur in mammalian cells upon serum-depletion {Nielsen, 1981 #506}, in yeast and mammalian cells after amino acid shortage {Krokowski, 2011 #315;Tzamarias, 1989 #483} and in yeast during osmotic stress {Uesono, 2002 #488}, lithium induced stress {Montero-Lomeli, 2002 #501}, and after exposure to fusel alcohols {Ashe, 2001 #505}. The most detailed example stems probably from the analysis of glucose starvation in the yeast *Saccharomyces cerevisiae*. This condition leads to the accumulation of 80S ribosomes {Ashe, 2000 #168} that contain the protein Stm1 in a conformation that clamps the ribosomal

subunits together {Ben-Shem, 2011 #173}. This structure is incompatible with translation as Stm1 occupies part of the mRNA channel. Consistent with this structural observation, Stm1 was identified as a ribosome-binding factor {Inada, 2002 #317;Van Dyke, 2006 #172} and has translation inhibiting activity *in vitro* {Balagopal, 2011 #169}. In addition, Stm1 was shown to enhance recovery following nutritional stress {Van Dyke, 2006 #172}, having a positive effect on the number of ribosomes preserved during nutrient deprivation {Van Dyke, 2013 #320}.

Mobilization of inactive ribosomes, which allows a rapid restart of translation upon stress relief {Ashe, 2000 #168} requires dissociation, making their subunits available for initiation. We wondered whether this process, in analogy to ribosome recycling after termination, depends on recycling factor activity.

In addition to normal termination and recycling factors that are thought to function on stop codons, recent studies in yeast and mammalian systems identified Dom34 (Pelota in humans) and the GTPase Hbs1, forming a complex structurally similar to eRF1 and eRF3 {Chen, 2010 #83;Kobayashi, 2010 #85;van den Elzen, 2010 #80}, that together with Rli1 similarly promote subunit dissociation. Interestingly, however, these factors appear to function on mRNA-bound ribosomes in a codon-independent manner {Shoemaker, 2010 #22;Shoemaker, 2011 #21} or to promote subunit splitting on completely empty ribosomes {Pisareva, 2011 #62}. Current models suggest that the Dom34-Hbs1 complex binds to the ribosomal A site, followed by GTP hydrolysis, dissociation of Hbs1 and accommodation of Dom34 in the ribosome. Rli1 then binds and induces ATP dependent subunit dissociation {Shoemaker, 2011 #21}. CryoEM structures provide clear support for eRF3/eRF1/Rli1 and Hbs1/Dom34/Rli1 playing related roles in ribosome recycling {Becker, 2011 #180;Becker, 2012 #19}.

In addition to these biochemical insights, Dom34 and Hbs1 were shown in genetic experiments to be important for RNA quality control in No-Go Decay targeting aberrant mRNAs {Doma, 2006 #91}) and in 18S NRD targeting defective or incompletely matured 40S ribosomal subunits {Cole, 2009 #117;Soudet, 2010 #540}. In NGD, the Dom34-Hbs1 complex may use its dissociation activity to release ribosomes that are stalled at the 3' end of mRNAs lacking a termination codon {Tsuboi, 2012 #67}. Recent reports also suggest that the Dom34-Hbs1 complex and Rli1 mediate dissociation of pre-40S and 60S subunits in a quality control step during ribosome maturation {Lebaron, 2012 #336;Strunk, 2012 #332}. Most of these processes involve the recognition of ribosomes stalled on an mRNA during translation.

We report here a new function for Dom34-Hbs1. We observe that Dom34-Hbs1 stimulates the dissociation of non-translating ribosomes that accumulate upon glucose starvation in yeast.

The biological relevance for this activity is seen in the dependence on these proteins of translational recovery in yeast cells after glucose deprivation. We further extended these ideas and show that Dom34-Hbs1 mediated dissociation of non-translating ribosomes can stimulate translation even in non-stressed conditions.

Results

The Dom34-Hbs1 complex stimulates restart of translation after glucose starvation

When the yeast *S. cerevisiae* is exposed to media lacking glucose for as little as 10 minutes, a change in the polysome profile occurs that is characteristic of translation inhibition: the polysome levels drop and ribosomes accumulate in a large 80S peak {Ashe, 2000 #168}. These 80S ribosomes are known to be inactive, bound by Stm1 in a conformation incompatible with translation {Ben-Shem, 2011 #173}. Glucose addition leads to a rapid recovery of translation, characterized by the reappearance of polysomes and a decrease in the 80S peak {Ashe, 2000 #168}. These observations were reproduced in our hands with strong translational recovery detectable 5 minutes after glucose addition (Figure 1A).

The process of translation initiation depends on the activities of separate ribosomal subunits. As such, the restart of translation in yeast recovering from glucose deprivation must depend on the dissociation of the large pool of inactive, Stm1-bound 80S ribosomes. Since human and yeast Dom34-Hbs1 complex with Rli1 can very effectively dissociate ribosomal subunits assembled with or without an mRNA *in vitro* {Pisareva, 2011 #62;Shoemaker, 2010 #22;Shoemaker, 2011 #21}, we hypothesized that these factors might also be needed to split Stm1-bound ribosomes *in vivo*. To test this possibility, we monitored the polysome profiles of isogenic wild type, *dom34*Δ or *hbs1*Δ strains in glucose-depleted conditions and after glucose addition. In contrast to the wild type strain, we found that in the absence of Dom34 or Hbs1, the 80S peak did not diminish and the polysomes did not increase after the addition of glucose. A small delay in recovery of translation was observed in mutant strains at 30°C (data not shown), but the effect was much more prominent at reduced temperatures (16°C, Figure 1A and B, see also Figure 4A) where ribosomal subunit dissociation is likely to be energetically more demanding.

To further evaluate the role of Dom34-Hbs1 in promoting the restart of translation after glucose starvation, we monitored overall ^{35}S-Met incorporation as a measure of protein synthesis in wild type and mutant cells. While in wild type cells, protein synthesis is equivalent in unstarved cells or cells recovering from starvation (Figure 1C), we see that protein synthesis was decreased in *dom34*Δ cells recovering from glucose starvation compared to unstarved cells (Figure 1D). These results indicate that the Dom34-Hbs1 complex is involved in the restart of translation in yeast recovering from glucose starvation.

Dom34-Hbs1 and Rli1 dissociate inactive ribosomes that accumulate in glucose-starved yeast.

Because of its ribosome dissociating activity *in vitro* {Pisareva, 2011 #62;Shoemaker, 2010 #22;Shoemaker, 2011 #21} it is likely that Dom34-Hbs1 stimulates restart of translation by splitting inactive 80S ribosomes that accumulate during glucose starvation. These inactive ribosomes differ from known Dom34-Hbs1 substrates in that they contain the protein Stm1 in a conformation that clamps the subunits together {Ben-Shem, 2011 #173}. We performed biochemical recycling assays to test whether the Dom34-Hbs1 complex could act on these Stm1-bound inactive ribosomes.

In *in vitro* recycling assays, ribosomes are radioactively labeled and then incubated with various factors (Dom34, Hbs1, Rli1). The complexes are then analyzed on sucrose gradients or on native gels to determine the level of "splitting" {Shoemaker, 2010 #22;Shoemaker, 2011 #21}. The protein Tif6, an initiation factor that binds to the subunit interface on the 60S subunit, is included in all experiments to trap ribosomes that undergo stimulated dissociation. For the experiments described here, ribosomes were non-specifically radiolabeled using casein kinase II {Shoemaker, 2010 #22}.

In a first experiment, "inactive" ribosomes isolated from glucose-starved yeast were incubated with various combinations of Dom34, Hbs1 and Rli1 (in addition to Tif6) and the samples were analyzed on a sucrose gradient. We see that after 15 minutes of incubation, all 80S ribosomes were dissociated into separate subunits when all three factors were added (Figure 2A, red curve). The elimination of either Rli1 or Dom34 significantly diminished the amount of dissociation observed, though not completely (Figure 2A).

In order to more precisely define the efficiencies of these splitting reactions, we used native gel electrophoresis (Supplementary Figure 1) to analyze equivalent experimental samples over time to determine relative rate constants. The rates that we measure for Dom34/Hbs1/Rli1-mediated splitting of Stm1-bound ribosome's is ~1.2 min^{-1} which is similar to the rate we previously observed (~1.6 min^{-1}) for elongating ribosomes bound to mRNA and peptidyl-tRNA {Shoemaker, 2011 #21}. In the absence of Rli1, the rate of dissociation decreased by 15 fold, close to earlier reports of a ~ 10 fold contribution {Shoemaker, 2011 #21}. In absence of *in vivo* data indicating that Rli1 is involved in dissociating inactive ribosomes (*RLI1* is an essential gene involved in other important processes) these results strongly support its participation in this process. Similar to the results of the sucrose gradient analysis (data not shown) and previous studies {Pisareva, 2011 #62;Shoemaker, 2011 #21}, elimination of Hbs1 had little effect on the observed rate of the

splitting reaction, though blocking Hbs1 GTPase activity by the inclusion of a non-hydrolyzable GTP analog (GDPNP) diminished the rate of splitting by 3 fold (Figure 2B).
Overall, these data demonstrate that Stm1-bound 80S ribosomes from glucose-starved yeast are good substrates for Dom34/Hbs1/Rli1-mediated subunit splitting *in vitro*. Indeed, while these samples were prepared at different times from different yeast cultures, the similarity in these values with earlier measurements for related but distinct complexes suggests that these ribosome complexes are equivalent targets for Dom34/Hbs1/Rli1 mediated recycling. We note that because the rates are measured with saturating amounts of Dom34/Hbs1/Rli1, the measured values are rate constants, thus allowing more readily for longitudinal comparisons to be made.

Deletion of STM1 suppresses the requirement for Dom34-Hbs1 to restart translation in vivo.
We reasoned that if the Dom34-Hbs1 complex stimulates restart of translation by dissociating Stm1-bound 80S ribosomes, weakening subunit interactions might reduce the requirement for the Dom34-Hbs1 complex. We tested this hypothesis by comparing the translation recovery of strains following glucose starvation and the re-addition of glucose in *stm1*Δ and *stm1*Δ*dom34*Δ strains. In Figure 3B, we see that deletion of *STM1* rescued the *dom34*Δ recovery deficient phenotype (Figure 3B). Importantly, deletion of *STM1* alone had no effect on translation inhibition or translation recovery (compare Figure 3A and Figure 1A).
The observation that the weakening of ribosomal subunit interactions reduces the requirement for Dom34 for recovery from starvation supports a model where Dom34/Hbs1/Rli1 promotes the dissociation of ribosomes in vivo.

Functional requirements of Dom34-Hbs1 for translational reactivation.
Our biochemical assay indicated that Hbs1 was not essential for the dissociation of inactive, Stm1-bound ribosomes *in vitro* (Figure 2B). To test the role of Hbs1 *in vivo*, we compared polysome profiles from a *hbs1*Δ mutant strain carrying the wild type *HBS1* gene on a plasmid or an empty vector. Analysis of polysomes at different time points during a glucose starvation/recovery experiment indicated that Hbs1, like Dom34, is required for optimal translational restart (Figure 4A).
We next explored the requirement of several functional regions of the Dom34-Hbs1 complex for this process. Hbs1 is a GTPase belonging to the eEF-1α-like family of GTPases {Atkinson, 2008 #144;Wallrapp, 1998 #337}, which includes the termination factor eRF3 and the elongation factor eEF-1α. Both of these factors function essentially to deliver their cargo,

eRF1 and aminoacyl-tRNA, respectively, to the ribosomal A site. We asked whether the GTPase activity of Hbs1 is required for efficient restart of translation in vivo and found that the GTP-binding defective Hbs1 mutant V176G {van den Elzen, 2010 #80} did not promote effective recovery from glucose starvation (Figure 4A).

We next probed the importance of the interaction between Dom34 and Hbs1 for the recovery from glucose starvation. The interface of these two proteins is comprised of contacts between several different regions in multiple domains of each protein {Chen, 2010 #83;Kobayashi, 2010 #85;van den Elzen, 2010 #80} where interaction defective mutants have been previously characterized {van den Elzen, 2010 #80}. The Hbs1 R517E mutant was shown by two-hybrid analysis to bind poorly to Dom34 {van den Elzen, 2010 #80}. Interestingly, this mutation did not affect the restart of translation following glucose starvation, indicating that a stable Dom34-Hbs1 interaction is not needed for this function (Figure 4A). In parallel, we used the Dom34 E361R mutant that similarly blocks formation of the Dom34-Hbs1 complex {van den Elzen, 2010 #80}, but in this case, the mutation diminished the recovery of cells from glucose starvation (Figure 4B). This asymmetric requirement for the interaction surfaces of Hbs1 and Dom34 suggests that Dom34 E361 may be important for other functions in addition to its interaction with Hbs1 (see discussion).

Members of the family of eEF1α-like GTPases are highly similar with regard to their C-terminal domains, but differ in their N-terminal length and amino acid sequence {Inagaki, 2000 #271}; the function of the N-terminus of Hbs1 is not known. Cryo-EM analysis of the Dom34-Hbs1 complex bound to an 80S ribosome revealed that it is located proximal to the mRNA entry channel {Becker, 2011 #180}. When this cryoEM structure was aligned with the high-resolution crystal structure of the ribosome from glucose-depleted yeast {Ben-Shem, 2011 #173}, we found that the N-terminus of Hbs1 would be in close contact with a portion of Stm1 located in the mRNA channel (Supplementary Figure 2). We therefore asked whether the N-terminus of Hbs1 plays a role in stimulating translation recovery after glucose depletion. Deletion of N-terminal amino acids 2-149 (mutant Hbs1 ΔN-ter) did not reduce the efficiency of translation re-initiation (Figure 4A).

The Dom34-Hbs1 complex stimulates translation in non stress-related conditions.

In non-stressed conditions, the polysome profiles of yeast lacking functional Dom34 or Hbs1 show elevated 80S peaks, which, especially at low temperatures, are combined with reduced levels of polysomes (Compare the polysome profiles on the left in Figures 1A, B and 4A, B, see also {Bhattacharya, 2010 #234;Carr-Schmid, 2002 #131}. This observation suggests that

even in non-stressed conditions, there may be inactive 80S ribosomes that depend on Dom34-Hbs1 and Rli1-mediated dissociation for their subunits to become available for translation initiation. The higher 80S peak could due to some amount of Stm1-bound ribosomes, of empty ribosomes lacking Stm1, or of mRNA-bound ribosomes that result, for example, from a Dom34-Hbs1 dependent defect in late translation initiation or early elongation. To distinguish between these possibilities, we analyzed the polysome profiles of wild type and *dom34*Δ strains in high and low salt sucrose gradients. High salt treatment is known to dissociate non-translating but not mRNA-bound 80S ribosomes {Martin, 1970 #342;Zylber, 1970 #348}. As we see in Figure 5A, in low salt conditions the 80S peak was higher for the *dom34*Δ strain compared to wild type (Figure 5A), while the 80S peaks were small and equivalent for the wild type and *dom34*Δ strains when analyzed in high salt conditions (Figure 5B). These data indicate that in the absence of Dom34, primarily non-mRNA-bound 80S ribosomes accumulate.

This observation supports a potential role for Dom34-Hbs1 and Rli1 in dissociating mRNA-free 80S ribosomes even in actively growing cells. If this is true, then the Dom34-Hbs1 complex would likely stimulate translation even in non-stressed conditions. To test this hypothesis, we used an *in vitro* translation assay where a synthetic mRNA encoding the firefly luciferase was incubated in cellular extract from a *dom34*Δ*hbs1*Δ strain, and varying amounts of recombinant Dom34 and Hbs1 were added. Luciferase activity measurements were used to monitor translation. We see that the addition of increasing concentrations of the Dom34-Hbs1 complex stimulated the translation of a firefly luciferase reporter mRNA up to 3-fold, whereas addition of Hbs1 alone did not (Figure 5C).

Together these results support the idea that the Dom34-Hbs1 complex generally stimulates translation in cells, stressed or non-stressed, by facilitating the dissociation of mRNA-free 80S ribosomes into their constituent 40S and 60S subunits.

Discussion

Currently the Dom34-Hbs1 complex is considered a central player in co-translational quality control on RNAs that cause inefficient translation {Graille, 2012 #390;Shoemaker, 2012 #352}. Dom34-Hbs1 stimulates degradation of such mRNAs and rRNAs {Cole, 2009 #117;Doma, 2006 #91}, most likely by facilitating the removal of stalled ribosomes from mRNAs {Tsuboi, 2012 #67}. Here we show that the Dom34-Hbs1 complex is a key player in the quick recovery of cells from stress and also stimulates translation under non-stress conditions. These observations expand the biochemical and physiological roles of Dom34-Hbs1 in the cell because every inactive 80S ribosome becomes a potential substrate for this complex.

Dom34-Hbs1 dissociates inactive ribosomes, promoting recovery after stress.

Our data show that the Dom34-Hbs1 complex is critical for the restart of translation in yeast recovering from glucose starvation. Two independent lines of evidence provide support for the idea that this stimulation depends on Dom34-Hbs1 dissociating inactive ribosomes, liberating subunits for new rounds of translation initiation. First, we showed that inactive ribosomes from glucose-depleted yeast are biochemical substrates of the complex (Figure 2). Second, deletion of Stm1, that stabilizes ribosomal subunit interaction {Ben-Shem, 2011 #173;Correia, 2004 #330} and therefore antagonizes dissociation, abolishes the need for the Dom34-Hbs1 complex for recovery.

The GTPase activity of Hbs1 was previously shown to be important for all of the protein's identified functions including RNA quality control {Kobayashi, 2010 #85;van den Elzen, 2010 #80}, complementation of a growth defect in a *rps30a*Δ*hbs1*Δ or a *rps28a*Δ*hbs1*Δ strain {Carr-Schmid, 2002 #131;van den Elzen, 2010 #80} and Dom34-Hbs1-Rli1 mediated dissociation of ribosomes {Pisareva, 2011 #62;Shoemaker, 2010 #22;Shoemaker, 2011 #21}. Our data here are consistent with these earlier observations. First, GTPase defective Hbs1 variants were unable to function in the recovery of cells from glucose starvation. Second, the substitution of GDPNP for GTP in the in vitro subunit splitting assays resulted in an overall inhibition of the reaction. Interestingly, as previously reported for other ribosomal substrates {Pisareva, 2011 #62;Shoemaker, 2011 #21}, Hbs1 did not increase the rate of splitting in the in vitro reactions, despite beings required in vivo for translational restart. Since the principle role of Hbs1 is likely to be in the loading of Dom34 into the ribosome, the high concentrations of Dom34 supplied in the in vitro reactions may minimize the contribution of

Hbs1. Because the cellular concentrations of Dom34 and Rli1 are much lower, the stimulatory effect of Hbs1 could be more relevant for dissociation of inactive ribosomes in the cell.

We further tested the importance of the interface between Dom34 and Hbs1 for promoting glucose starvation recovery. Here, we were somewhat surprised to see that mutation of the interface of Hbs1 had little impact on the in vivo phenotype while the Dom34 interface was critical to its function. Hbs1 being required for ribosome dissociation in vivo, these data suggest that Dom34 and Hbs1 could bind the ribosome independently, their mutual interaction being stabilized by the ribosomal context. The greater importance of the Dom34 interface may be rationalized by the fact that Dom34 must interact with Rli1 and changes conformation while bound to the ribosome {Becker, 2012 #19}. Dom34 E361 may at some stage during recycling interact with Rli1 or the ribosomes. We note that mutation of the Dom34-Hbs1 interaction surface had a similar asymmetric impact on 18S NRD {van den Elzen, 2010 #80}. However, we cannot definitively exclude that the mutation on the Hbs1 interface less effectively diminishes interactions with Dom34 than the chosen Dom34 mutation.

A general role of Dom34 –Hbs1 in modulating translation by controlling ribosomal subunit availability

Beyond its role in stress recovery, we observed that Dom34-Hbs1 mediated dissociation of inactive ribosomes can more broadly function to stimulate translation initiation. In the absence of Dom34 and/or Hbs1, polysome profiles generally have elevated 80S peaks (compare leftmost polysome profiles in Figures 1A, 1B and 4A; see also {Bhattacharya, 2010 #234;Carr-Schmid, 2002 #131}, due to accumulation of inactive ribosomes not bound to mRNA templates (Figure 5A and B). We show here that even in non-stressed conditions, Dom34-Hbs1 appears to broadly stimulate translation efficiency by making subunits available for new rounds of protein synthesis (Figure 5). This observation is consistent with the fact that depletion of orthologs of Rli1 - which acts together with Dom34-Hbs1 to dissociate inactive ribosomes – similarly results in accumulation of 80S ribosomes and decreased levels of polysomes in yeast, human and *Drosophila* cells {Andersen, 2007 #257;Chen, 2006 #261;Dong, 2004 #260}. Additionally, in a strain with impaired initiation (inhibition of eIF2), deletion of Dom34 or Hbs1 results in a synthetic growth defect {Carr-Schmid, 2002 #131} that might suggest that these factors work in a common pathway. Finally, both Dom34 and Hbs1 are important for normal growth of yeast strains with reduced amounts of 40S subunits

{Bhattacharya, 2010 #234;Carr-Schmid, 2002 #131;van den Elzen, 2010 #80} likely because these double mutant strains have too few ribosomes available to function.

During glucose deprivation, inactive ribosomes contain Stm1 in a conformation that inhibits translation and stabilizes subunit interaction {Ben-Shem, 2011 #173}. It is not clear whether this mechanism of ribosome inhibition is broadly used in response to stress, or whether it is used in a wide variety of physiological conditions. Our results show that in non-stressed conditions, deletion of Stm1 reduces the elevated 80S peak that forms in the absence of Dom34 to almost wild type levels (compare leftmost polysome profiles in Figure 1B and figure 3B). This suggests that the translation inhibiting conformation of Stm1 is present in a large fraction of inactive 80S ribosomes, even in non-stressed cells. A role for Stm1 in antagonizing Dom34-Hbs1 mediated dissociation of inactive 80S ribosomes likely explains why overexpression of Stm1 in *dom34*Δ yeast causes a growth defect {Balagopal, 2011 #169}.

Conclusion

Our work shows that Dom34-Hbs1-mediated subunit dissociation is critical in the recovery of yeast cells from glucose starvation. Our data further suggest that Dom34-Hbs1 plays a similar role in non-stressed cells, dissociating unproductive empty 80S ribosomes so that normal translation initiation can occur. These observations provide insights into a novel general mechanism for the control of translation wherein ribosomes are stored in an unproductive state (either with Stm1 bound or simply not containing an mRNA) that is readily reversed by the activities of Dom34, Hbs1 and Rli1.

We emphasize that this mechanism is likely widely used by cells to dissociate various ribosome complexes to maintain an active supply of ribosomal subunits. Indeed, a general shut down of translation is a hallmark of a cell's response to many stress conditions including nutrient depletion, temperature shock, hypoxia and DNA damage {Spriggs, 2010 #152}. Moreover, Dom34 and Hbs1 are conserved proteins: Dom34 has orthologs in eukaryotes and archaea {Eberhart, 1995 #537;Ragan, 1996 #338}. And, whereas Hbs1 has orthologs only in eukaryotes {Inagaki, 2000 #271;Wallrapp, 1998 #337}, the function is filled even in archaea by the related protein aEF1α {Kobayashi, 2010 #85;Saito, 2010 #112}.

Material and Methods

Yeast strains, media and plasmids

Yeast strains and plasmids are listed in Supplementary Table 1. Yeast strains, derivatives of of BMA64, were constructed by standard methods. The plasmid pBS4415 was constructed by inverse PCR on a pBS3614 template {van den Elzen, 2010 #80} using oligonucleotides 5'-ATATCATGAGGTTTCTTTGGTTTCATCTCGATAGTCAATAGTTGTCG-3' and 5'-CCAAAGAAACCTCATGATATTTCTGCATTTGTTAAATCTGCCTTAC-3' and was verified by sequencing.

Glucose rich and glucose depleted media were YPDA and YPA (for strains without plasmids) or CSM-Ura 2% glucose and CSM-Ura without glucose (for strains containing Dom34 or Hbs1 encoding plasmids) respectively.

Glucose starvation and repletion

Yeast was grown at 30°C at 170 rpm to an OD_{600} of 0.6, then shifted to 16°C for 2 hours. The culture was then split into multiple 100 ml cultures that were pelleted at 5400 x g for 6 min at 16°C, resuspended in 100 ml of media (precooled at 16°C) without or with 2% glucose and incubated at 16°C for 10 minutes at 170 rpm. Cells were pelleted, resuspended in 100 ml media with glucose and incubated at 16°C at 170 rpm for the indicated times.

Polysome analysis

At the indicated times after glucose depletion or glucose addition cycloheximide was added (100 μg/ml final concentration) and cells were pelleted at 5400 x g for 6 min at 4°C. Cells were washed and then lysed at 4°C in lysis buffer (10 mM Tris-Cl pH 7.5; 100 mM KCl; 5 mM $MgCl_2$; 6 mM β-mercaptoethanol; 100 μg/ml cycloheximide) or in lysis buffer containing 400 mM KCl (Figure 4B) containing glass beads by 5 cycles of 1 minute vortexing followed by 1 minute on ice, in presence of glass beads. 9 OD_{260} units of lysate were loaded on a 7-47% sucrose gradient in lysis buffer, or lysis buffer containing 400 mM KCl (Figure 4B). After a 14 h spin at 16.9 krpm in an SW41 rotor (Beckman Coulter), absorbance (254 nm) was measured on a ISCO Teledyne Foxy Jr. fraction collector.

^{35}S-Methionine incorporation

Yeast was grown in CSM-Met containing 2% glucose, shifted to 16°C, split into 8 ml cultures and resuspended in 8 ml CSM-Met with or without 2% glucose for 10 minutes as described

above. Then cells were resuspended in 8 ml CSM-Met 2% glucose (16°C) containing 4 µl ^{35}S-Methionine (1175 Ci/mmol, 5 mCi/0,49 ml, Perkin Elmer) and incubated at 16°C. At the indicated time points 1 ml samples were taken and ^{35}S-Methionine incorporation was measured as described {Ashe, 2000 #168}.

In vitro ribosome dissociation

80S ribosomes purified from glucose-depleted yeast were kindly provided by S. Melnikov and Dr. Marat Yusupov. 100 pmol ribosomes were ^{32}P-labeled using 500 U casein kinase II (NEB) and ^{32}P γ-ATP in the manufacturer's recommended buffer, then pelleted through a 600 µl 1.1 M sucrose cushion in buffer E (20 mM Tris-Cl pH 7.5, 2.5 mM $Mg(OAc)_2$, 100 mM KOAc pH7.6, 2 mM DTT, 0.25 mM spermidine) at 75000 rpm 1 h 4°C in a MLA-130 rotor followed by resuspension in buffer E. 6,25 pmol ribosomes were incubated in 25 µl buffer E containing 1 mM GTP or GDPNP and 1 mM ATP at 26°C for 15 minutes with 50 pmol Dom34, 50 pmol Hbs1, 50 pmol Rli1 and 625 pmol Tif6 - purified as described previously {Shoemaker, 2010 #22;Shoemaker, 2011 #21}. Dissociation was analyzed by centrifugation through a 10-30% sucrose gradient in buffer E at 38500 rpm for 3,5 h at 4°C in a SW41 rotor. Fractions were counted in Bio Safe II scintillation fluid. Kinetic analysis was performed by loading 2 µl fractions of the reactions on a 3% acrylamide gel in THEM buffer (34 mM Tris base, 57 mM Hepes, 0.1 mM EDTA, 2.5 mM $MgCl_2$) {Acker, 2007 #476} at indicated time points, running the gel in THEM buffer at 12W at 4°C. Gels were dried and quantified using a Typhoon 9410 phosphoimager and ImageQuantTL (GE Healthcare Life Sciences). The fraction of dissociated ribosomes was plotted against time and, using KaleidaGraph for curve fitting, rate constants were determined.

In vitro translation

Translational extracts were prepared from a *dom34*Δ*hbs1*Δ strain (BSY2550) essentially as described {Tuite, 1986 #255}. A synthetic firefly luciferase-A(50) mRNA {Gallie, 1991 #273} was incubated in this extract supplemented, or not, with recombinant Dom34-Hbs1 purified as described previously {Collinet, 2011 #331} and luciferase activity was assayed. Translation conditions have been described by Tharun et al. {Tarun, 1995 #256} (see Supplementary data for details).

Acknowledgements

Authors are grateful to S. Melnikov and M. Yusupov for purified ribosomes and discussions, F. Wyers and F. Lacroute for the *stm1*Δ strain, M. Gas Lopez for the *hbs1*Δ*N-ter (2-149)-PROTEIN A* construct, and our team members as well as A. Ben-Shem for discussions. We thank the IGBMC mass-spectrometry platforms for their help in the early part of this project and IGBMC (Institut de Génétique et de Biologie Moléculaire et Cellulaire) for assistance. This work was supported by grants from the CERBM-IGBMC, the Ligue Contre le Cancer (Equipe Labellisée 2011), the CNRS and the Agence Nationale de la Recherche (ANR 11 BSV8 009 02) to BS. A.M.G.v.d.E. was supported by predoctoral fellowships from Université de Strasbourg, the Fondation pour la Recherche Médicale and an EMBO short-term fellowship.

Author Contribution

AMGvdE performed all the *in vivo* experiments, as well as the in vitro translation, with input from BS. In vitro analyses of ribosome dissociation were performed by AS and AMGvdE with input from RG and BS. BS supervised the project. AMGvdE, AS, RG and BS wrote the manuscript.

Conflict of Interest

The authors declare that they have no conflict of interest.

References

Acker MG, Kolitz SE, Mitchell SF, Nanda JS, Lorsch JR (2007) Reconstitution of yeast translation initiation. *Methods Enzymol* **430:** 111-145

Andersen DS, Leevers SJ (2007) The essential Drosophila ATP-binding cassette domain protein, pixie, binds the 40 S ribosome in an ATP-dependent manner and is required for translation initiation. *J Biol Chem* **282:** 14752-14760

Ashe MP, De Long SK, Sachs AB (2000) Glucose depletion rapidly inhibits translation initiation in yeast. *Mol Biol Cell* **11:** 833-848

Ashe MP, Slaven JW, De Long SK, Ibrahimo S, Sachs AB (2001) A novel eIF2B-dependent mechanism of translational control in yeast as a response to fusel alcohols. *EMBO J* **20:** 6464-6474

Atkinson GC, Baldauf SL, Hauryliuk V (2008) Evolution of nonstop, no-go and nonsense mediated mRNA decay and their termination factor-derived components. *BMC Evol Biol* **8:** 290

Balagopal V, Parker R (2011) Stm1 modulates translation after 80S formation in Saccharomyces cerevisiae. *RNA* **17:** 835-842

Becker T, Armache JP, Jarasch A, Anger AM, Villa E, Sieber H, Motaal BA, Mielke T, Berninghausen O, Beckmann R (2011) Structure of the no-go mRNA decay complex Dom34-Hbs1 bound to a stalled 80S ribosome. *Nat Struct Mol Biol* **18:** 715-720

Becker T, Franckenberg S, Wickles S, Shoemaker CJ, Anger AM, Armache JP, Sieber H, Ungewickell C, Berninghausen O, Daberkow I, Karcher A, Thomm M, Hopfner KP, Green R, Beckmann R (2012) Structural basis of highly conserved ribosome recycling in eukaryotes and archaea. *Nature* **482:** 501-506

Ben-Shem A, Garreau de Loubresse N, Melnikov S, Jenner L, Yusupova G, Yusupov M (2011) The structure of the eukaryotic ribosome at 3.0 A resolution. *Science* **334:** 1524-1529

Bhattacharya A, McIntosh KB, Willis IM, Warner JR (2010) Why Dom34 stimulates growth of cells with defects of 40S ribosomal subunit biosynthesis. *Mol Cell Biol* **30:** 5562-5571

Carr-Schmid A, Pfund C, Craig EA, Kinzy TG (2002) Novel G-protein complex whose requirement is linked to the translational status of the cell. *Mol Cell Biol* **22:** 2564-2574

Chen L, Muhlrad D, Hauryliuk V, Cheng Z, Lim MK, Shyp V, Parker R, Song H (2010) Structure of the Dom34-Hbs1 complex and implications for no-go decay. *Nat Struct Mol Biol* **17:** 1233-1240

Chen ZQ, Dong J, Ishimura A, Daar I, Hinnebusch AG, Dean M (2006) The essential vertebrate ABCE1 protein interacts with eukaryotic initiation factors. *J Biol Chem* **281:** 7452-7457

Cole SE, LaRiviere FJ, Merrikh CN, Moore MJ (2009) A convergence of rRNA and mRNA quality control pathways revealed by mechanistic analysis of nonfunctional rRNA decay. *Cell* **34:** 440-450

Collinet B, Friberg A, Brooks MA, van den Elzen T, Henriot V, Dziembowski A, Graille M, Durand D, Leulliot N, Saint Andre C, Lazar N, Sattler M, Seraphin B, van Tilbeurgh H (2011) Strategies for the structural analysis of multi-protein complexes: lessons from the 3D Repertoire project. *J Struct Biol* **175:** 147-158

Correia H, Medina R, Hernandez A, Bustamante E, Chakraburtty K, Herrera F (2004) Similarity between the association factor of ribosomal subunits and the protein Stm1p from Saccharomyces cerevisiae. *Mem Inst Oswaldo Cruz* **99:** 733-737

Doma MK, Parker R (2006) Endonucleolytic cleavage of eukaryotic mRNAs with stalls in translation elongation. *Nature* **440:** 561-564

Dong J, Lai R, Nielsen K, Fekete CA, Qiu H, Hinnebusch AG (2004) The essential ATP binding
cassette protein RLI1 functions in translation by promoting preinitiation complex assembly. *J Biol Chem* **279:** 42157-42168

Eberhart CG, Wasserman SA (1995) The pelota locus encodes a protein required for meiotic cell division: an analysis of G2/M arrest in Drosophila spermatogenesis. *Development* **121:** 3477-3486

Gallie DR, Feder JN, Schimke RT, Walbot V (1991) Post-transcriptional regulation in higher eukaryotes: the role of the reporter gene in controlling expression. *Mol Gen Genet* **228:** 258-264

Graille M, Seraphin B (2012) Surveillance pathways rescuing eukaryotic ribosomes lost in translation. *Nat Rev Mol Cell Biol* **13:** 727-735

Inada T, Winstall E, Tarun SZ, Jr., Yates JR, 3rd, Schieltz D, Sachs AB (2002) One-step affinity purification of the yeast ribosome and its associated proteins and mRNAs. *RNA* **8:** 948-958

Inagaki Y, Ford Doolittle W (2000) Evolution of the eukaryotic translation termination system: origins of release factors. *Mol Biol Evol* **17:** 882-889

Kobayashi K, Kikuno I, Kuroha K, Saito K, Ito K, Ishitani R, Inada T, Nureki O (2010) Structural basis for mRNA surveillance by archaeal Pelota and GTP-bound EF1alpha complex. *Proc Natl Acad Sci U S A* **107:** 17575-17579

Kraft C, Deplazes A, Sohrmann M, Peter M (2008) Mature ribosomes are selectively degraded upon starvation by an autophagy pathway requiring the Ubp3p/Bre5p ubiquitin protease. *Nat Cell Biol* **10:** 602-610

Krebs JE, Goldstein ES, Kilpatrick ST (2011) *Lewin's Genes X*, Sudbury, MA.: Jones and Barlett Publishers. Krokowski D, Gaccioli F, Majumder M, Mullins MR, Yuan CL,

Papadopoulou B, Merrick WC, Komar AA, Taylor D, Hatzoglou M (2011) Characterization of hibernating ribosomes in mammalian cells. *Cell Cycle* **10:** 2691-2702

Lebaron S, Schneider C, van Nues RW, Swiatkowska A, Walsh D, Bottcher B, Granneman S, Watkins NJ, Tollervey D (2012) Proofreading of pre-40S ribosome maturation by a translation initiation factor and 60S subunits. *Nat Struct Mol Biol* **19:** 744-753

Martin TE, Hartwell LH (1970) Resistance of active yeast ribosomes to dissociation by KCl. *J Biol Chem* **245:** 1504-1506

Montero-Lomeli M, Morais BL, Figueiredo DL, Neto DC, Martins JR, Masuda CA (2002) The initiation factor eIF4A is involved in the response to lithium stress in Saccharomyces cerevisiae. *J Biol Chem* **277:** 21542-21548

Nielsen PJ, Duncan R, McConkey EH (1981) Phosphorylation of ribosomal protein S6. Relationship to protein synthesis in HeLa cells. *Eur J Biochem* **120:** 523-527

Pisarev AV, Skabkin MA, Pisareva VP, Skabkina OV, Rakotondrafara AM, Hentze MW, Hellen CU, Pestova TV (2010) The role of ABCE1 in eukaryotic posttermination ribosomal recycling. *Mol Cell* **37:** 196-210

Pisareva VP, Skabkin MA, Hellen CU, Pestova TV, Pisarev AV (2011) Dissociation by Pelota, Hbs1 and ABCE1 of mammalian vacant 80S ribosomes and stalled elongation complexes. *EMBO J* **30:** 1804-1817

Polikanov YS, Blaha GM, Steitz TA (2012) How hibernation factors RMF, HPF, and YfiA turn off protein synthesis. *Science* **336:** 915-918

Ragan MA, Logsdon JM, Jr., Sensen CW, Charlebois RL, Doolittle WF (1996) An archaebacterial homolog of pelota, a meiotic cell division protein in eukaryotes. *FEMS Microbiol Lett* **144:** 151-155

Saito K, Kobayashi K, Wada M, Kikuno I, Takusagawa A, Mochizuki M, Uchiumi T, Ishitani R, Nureki O, Ito K (2010) Omnipotent role of archaeal elongation factor 1 alpha (EF1alpha in translational elongation and termination, and quality control of protein synthesis. *Proc Natl Acad Sci U S A* **107:** 19242-19247

Shoemaker CJ, Eyler DE, Green R (2010) Dom34:Hbs1 promotes subunit dissociation and peptidyl-tRNA drop-off to initiate no-go decay. *Science* **330:** 369-372

Shoemaker CJ, Green R (2011) Kinetic analysis reveals the ordered coupling of translation termination and ribosome recycling in yeast. *Proc Natl Acad Sci U S A* **108:** E1392-1398
Shoemaker CJ, Green R (2012) Translation drives mRNA quality control. *Nat Struct Mol Biol* **19:** 594-601

Soudet J, Gelugne JP, Belhabich-Baumas K, Caizergues-Ferrer M, Mougin A (2010) Immature small ribosomal subunits can engage in translation initiation in Saccharomyces cerevisiae. *EMBO J* **29:** 80-92

Spriggs KA, Bushell M, Willis AE (2010) Translational regulation of gene expression during conditions of cell stress. *Mol Cell* **40:** 228-237

Strunk BS, Novak MN, Young CL, Karbstein K (2012) A translation-like cycle is a quality control checkpoint for maturing 40S ribosome subunits. *Cell* **150:** 111-121

Tarun SZ, Jr., Sachs AB (1995) A common function for mRNA 5' and 3' ends in translation initiation in yeast. *Genes Dev* **9:** 2997-3007

Tsuboi T, Kuroha K, Kudo K, Makino S, Inoue E, Kashima I, Inada T (2012) Dom34:Hbs1 plays a general role in quality-control systems by dissociation of a stalled ribosome at the 3' end of aberrant mRNA. *Mol Cell* **46:** 518-529

Tuite MF, Plesset J (1986) mRNA-dependent yeast cell-free translation systems: theory and practice. *Yeast* **2:** 35-52

Tzamarias D, Roussou I, Thireos G (1989) Coupling of GCN4 mRNA translational activation with decreased rates of polypeptide chain initiation. *Cell* **57:** 947-954

Uesono Y, Toh EA (2002) Transient inhibition of translation initiation by osmotic stress. *J Biol Chem* **277:** 13848-13855

van den Elzen AM, Henri J, Lazar N, Gas ME, Durand D, Lacroute F, Nicaise M, van Tilbeurgh H, Seraphin B, Graille M (2010) Dissection of Dom34-Hbs1 reveals independent functions in two RNA quality control pathways. *Nat Struct Mol Biol* **17:** 1446-1452

Van Dyke N, Baby J, Van Dyke MW (2006) Stm1p, a ribosome-associated protein, is important for protein synthesis in Saccharomyces cerevisiae under nutritional stress conditions. *J Mol Biol* **358:** 1023-1031

Van Dyke N, Chanchorn E, Van Dyke MW (2013) The Saccharomyces cerevisiae protein Stm1p facilitates ribosome preservation during quiescence. *Biochem Biophys Res Commun* **430:** 745-750

Wallrapp C, Verrier SB, Zhouravleva G, Philippe H, Philippe M, Gress TM, Jean-Jean O (1998) The product of the mammalian orthologue of the Saccharomyces cerevisiae HBS1 gene is phylogenetically related to eukaryotic release factor 3 (eRF3) but does not carry eRF3-like activity. *FEBS Lett* **440:** 387-392

Zylber EA, Penman S (1970) The effect of high ionic strength on monomers, polyribosomes, and puromycin-treated polyribosomes. *Biochim Biophys Acta* **204:** 221-229

Figure Legends

Figure 1. Dom34 stimulates restart of translation in yeast recovering from glucose starvation stress. (A) and (B) Dom34 stimulates the rapid reappearance of polysomes in cells recovering from glucose starvation stress. Polysome profiles of wild type (A) or *dom34*Δ (B) yeast grown in glucose rich medium (left graph), after 10 minutes of glucose starvation (second graph) and 5 and 30 minutes after glucose repletion (third and fourth graph) at 16°C. (C) and (D) Dom34 stimulates protein production in cells recovering from glucose starvation stress. Wild type (C) and *dom34*Δ (D) depleted of glucose or grown in glucose rich medium for 10 minutes at 16°C was resuspended in glucose rich medium containing ^{35}S-Methionine, followed by incubation at 16°C. ^{35}S-Methionine incorporation was measured at the indicated time points. Means and SD of 3 independent experiments are shown.

Figure 2. Dom34-Hbs1 and Rli1 participate in the dissociation of inactive, Stm1-containing, 80S ribosomes.
Dom34-Hbs1 and Rli1 dissociate ribosomes from glucose-starved yeast *in vitro*. ^{32}P-labeled 80S ribosomes purified from glucose-starved yeast were incubated with the indicated proteins in presence of ATP and GTP or GDPNP. (A) After 15 minutes of incubation dissociation was monitored by sucrose density gradient centrifugation and scintillation counting of collected fractions. (B) Observed rate constants were determined by monitoring the fraction of dissociated ribosomes over time on a native gel system (see Supplementary Figure 1). Means and SD of 3 independent experiments are shown.

Figure 3. Weakening ribosome subunit interaction reduces the need for Dom34 during restart of translation after glucose starvation stress.
Polysome profiles of *stm1*Δ (A) and *dom34*Δ*stm1*Δ (B) yeast grown in glucose rich medium (left graph) exposed to glucose starvation (second graph) and 5 and 30 minutes after glucose readdition (third and fourth graphs) at 16°C.

Figure 4. Restart of translation after glucose depletion stress requires Hbs1 GTPase activity but not Dom34-Hbs1 interaction or the Hbs1 N-terminus.
Polysome profiles of *hbs1*Δ (A) or *dom34* Δ (B) yeast transformed with plasmid expressing the indicated mutants, grown in glucose rich medium (left graph), exposed to glucose starvation (middle graph) and after glucose readdition (right graph) at 16°C.

Figure 5. The Dom34-Hbs1 complex stimulates translation in non stress-related conditions.

(A) and (B) Inactive 80S ribosomes accumulate in *dom34*Δ yeast. Polysome profiles were obtained from wild type and *dom34*Δ yeast in low (100 mM KCl) (A) and high (400 mM KCl) (B) salt conditions. Yeast strains were grown at 30°C. (C) Dom34-Hbs1 stimulates translation by ribosomes that were not exposed to starvation stress. A firefly luciferase mRNA was translated for 1 hour in cell extract obtained from a *dom34*Δ *hbs1*Δ strain, after which luciferase activity was measured. Addition of increasing amounts of recombinant Dom34-Hbs1 complex, but not of Hbs1 alone, stimulated luciferase production. Means and SD of 3 independent experiments are shown.

Figure 1

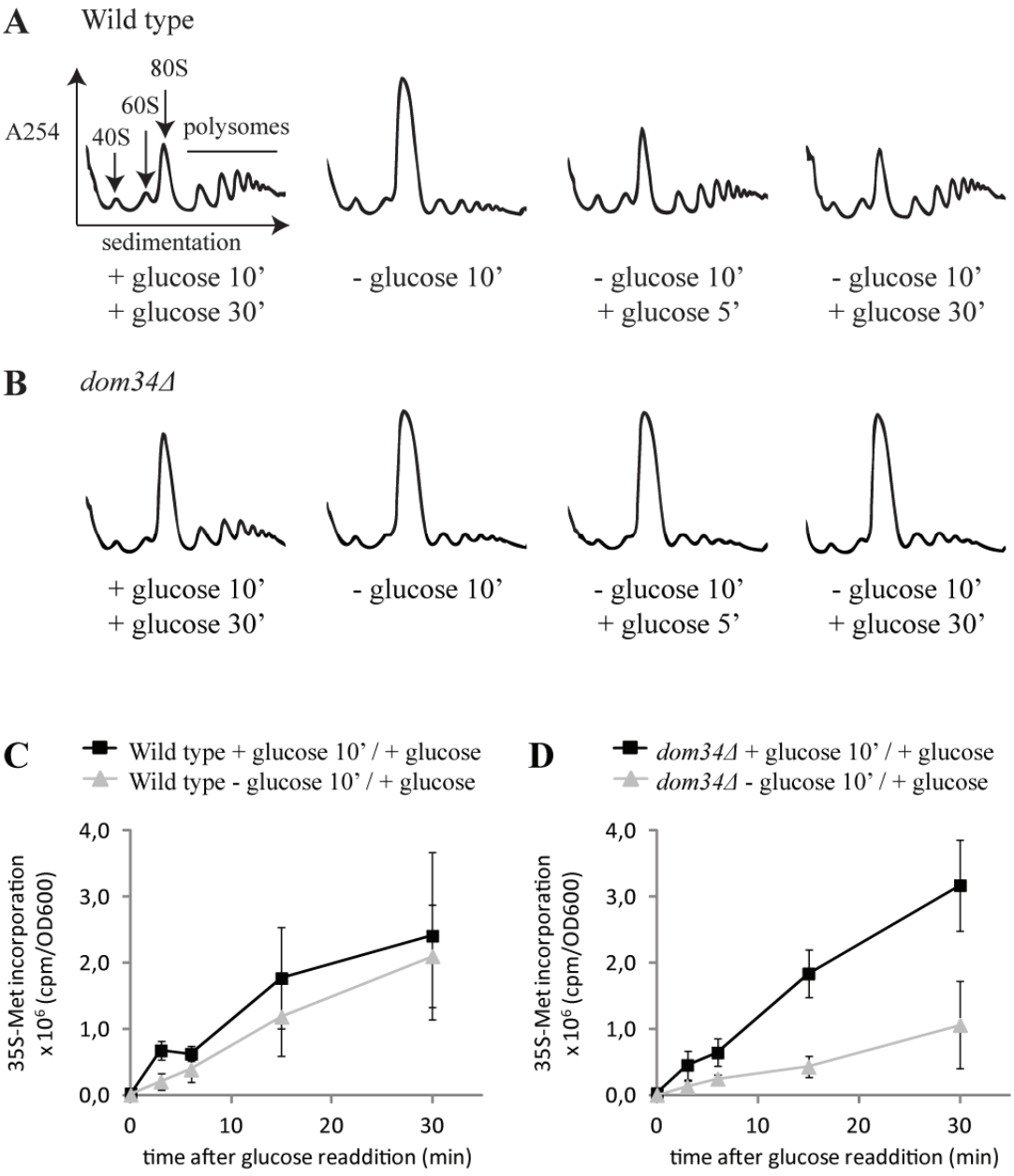
A
Wild type
80S
60S
A254
40S
polysomes
sedimentation
+ glucose 10'
+ glucose 30'
- glucose 10'
- glucose 10'
+ glucose 5'
- glucose 10'
+ glucose 30'
B
dom34Δ
+ glucose 10'
+ glucose 30'
- glucose 10'
- glucose 10'
+ glucose 5'
- glucose 10'
+ glucose 30'
C
Wild type + glucose 10' / + glucose
Wild type - glucose 10' / + glucose
35S-Met incorporation x 10⁶ (cpm/OD600)
4,0
3,0
2,0
1,0
0,0
0
10
20
30
time after glucose readdition (min)
D
dom34Δ + glucose 10' / + glucose
dom34Δ - glucose 10' / + glucose
35S-Met incorporation x 10⁶ (cpm/OD600)
4,0
3,0
2,0
1,0
0,0
0
10
20
30
time after glucose readdition (min)

Figure 2

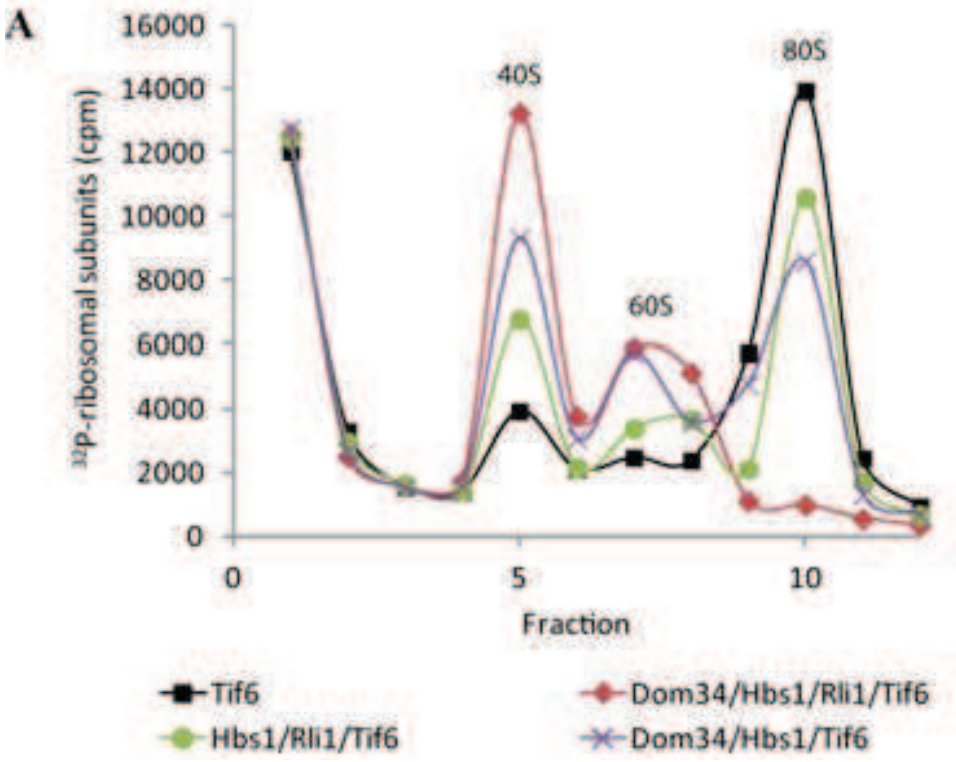
A
16000
14000
12000
10000
8000
6000
4000
2000
0
32P-ribosomal subunits (cpm)
40S
60S
80S
0
5
10
Fraction
Tif6
Hbs1/Rli1/Tif6
Dom34/Hbs1/Rli1/Tif6
Dom34/Hbs1/Tif6

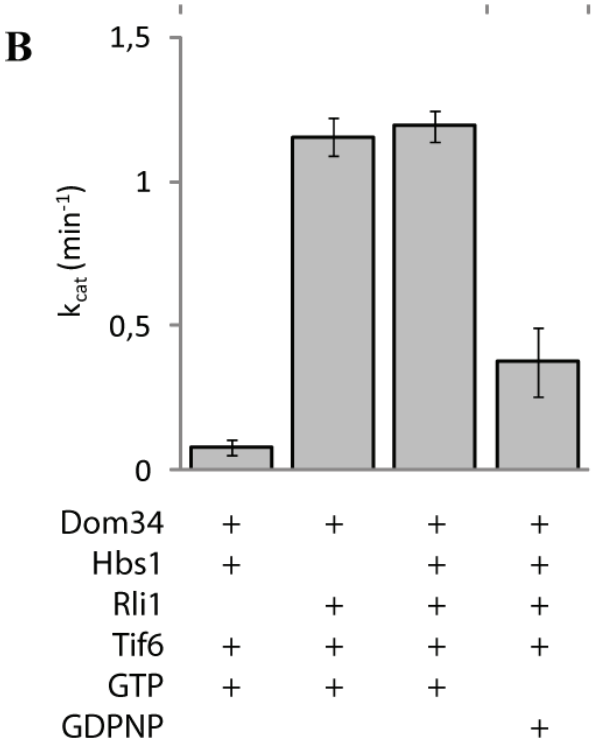
B
1,5
1
0,5
0
kcat (min-1)
Dom34 + + + +
Hbs1 + + +
Rli1 + + +
Tif6 + + + +
GTP + + +
GDPNP +

Figure 3

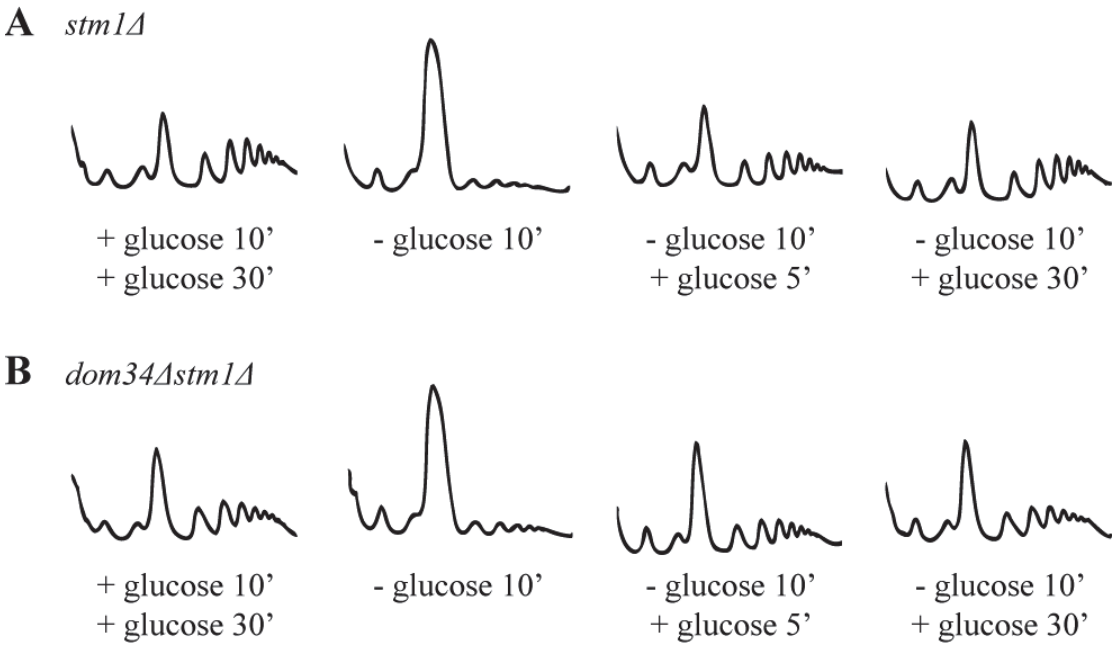
A stm1Δ
+ glucose 10’
+ glucose 30’
- glucose 10’
- glucose 10’
+ glucose 5’
- glucose 10’
+ glucose 30’
B dom34Δstm1Δ
+ glucose 10’
+ glucose 30’
- glucose 10’
- glucose 10’
+ glucose 5’
- glucose 10’
+ glucose 30’

Figure 4

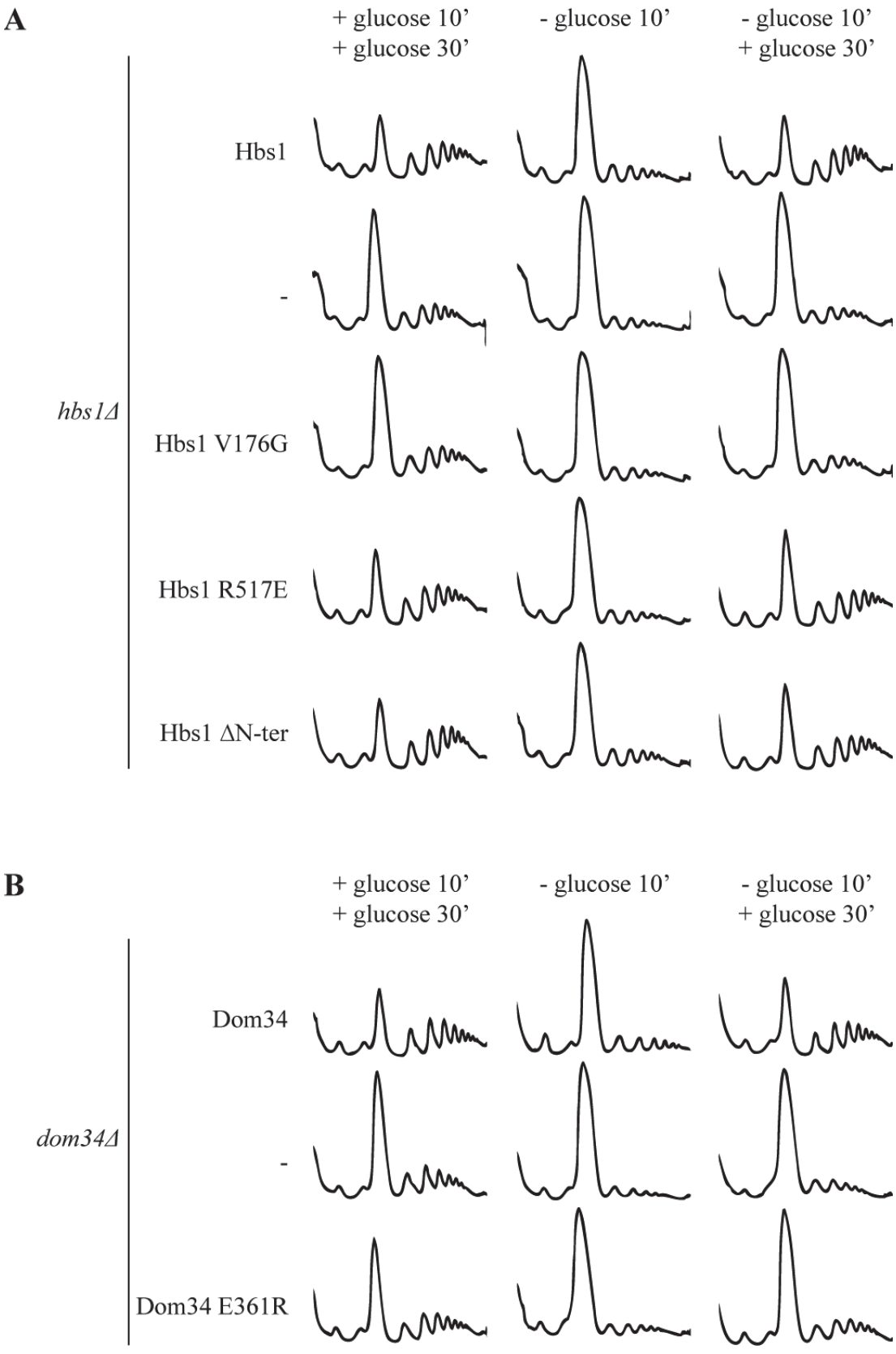
A
+ glucose 10'
+ glucose 30'
- glucose 10'
- glucose 10'
+ glucose 30'
hbs1Δ
Hbs1
-
Hbs1 V176G
Hbs1 R517E
Hbs1 ΔN-ter
B
+ glucose 10'
+ glucose 30'
- glucose 10'
- glucose 10'
+ glucose 30'
dom34Δ
Dom34
-
Dom34 E361R

Figure 5

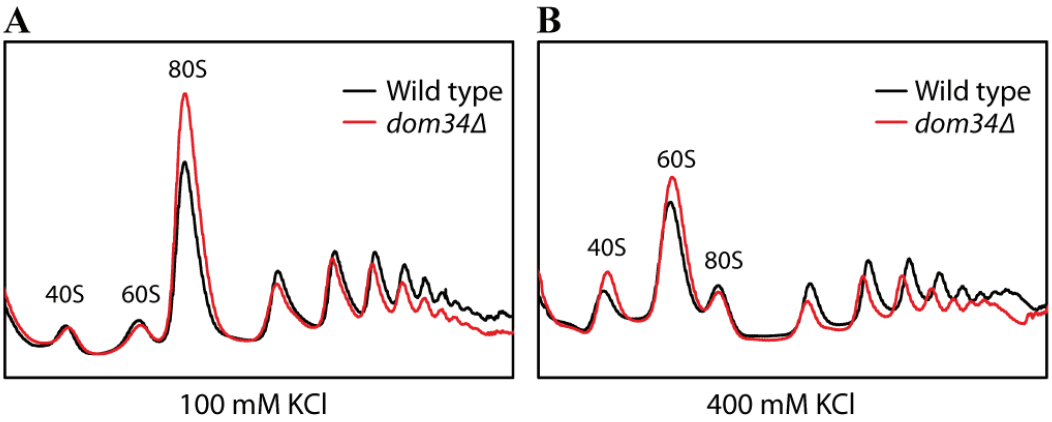
A
80S
Wild type
dom34Δ
40S
60S
100 mM KCl
B
Wild type
dom34Δ
60S
40S
80S
400 mM KCl

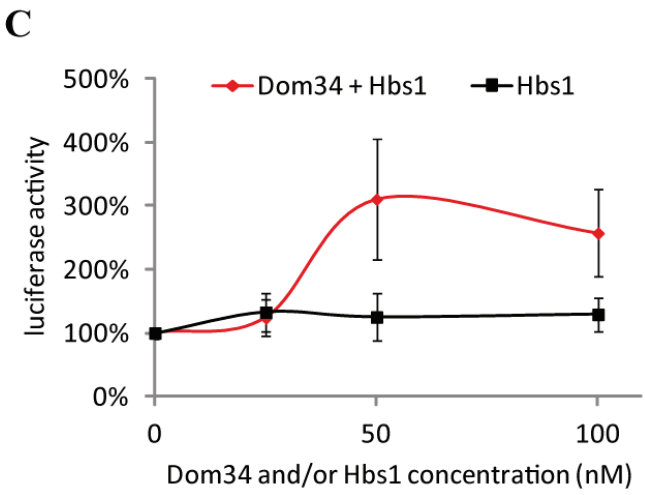
C
500%
400%
300%
200%
100%
0%
luciferase activity
Dom34 + Hbs1
Hbs1
0
50
100
Dom34 and/or Hbs1 concentration (nM)

In the manuscript it was shown that in *S. cerevisiae* lacking Dom34 translation did not recover 30 minutes after glucose addition, whereas in wild type strains in the same time window full recovery was observed, at 16°C. I studied how much time it took for *dom34*Δ yeast to reach full translational recovery after glucose starvation. In Figure 50 it is shown that this took between two and four hours.

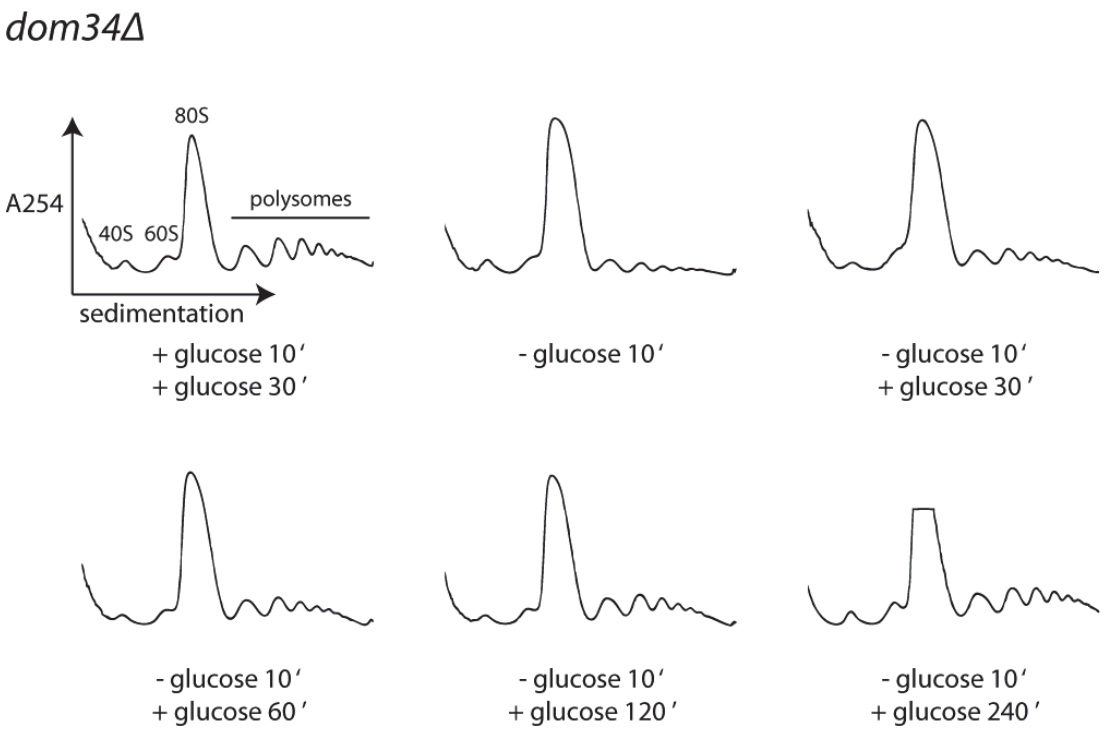

Figure 50 Recovery of translation after glucose starvation in absence of Dom34.
Translational recovery after glucose starvation takes two to four hours in absence of Dom34. Polysome profiles of *dom34*Δ *S. cerevisiae* grown in glucose rich medium (YPDA, first graph), after 10 minutes of glucose starvation in YPA (second graph) and 30, 60, 120 and 240 minutes after glucose addition (resuspension in YPDA, third to sixth graph) at 16°C. Due to a technical problem with the UV monitor the tip of the 80S peak in the 240 minute recovery graph is missing.

A failure to efficiently restart translation upon stress relief is expected to translate itself into a failure to resume cell growth and proliferation. I examined whether yeast lacking Dom34 grew more slowly than wild type strains, after exposure to glucose depletion stress.
Cell density, estimated by OD_{600} reading, was followed over time in cells that, after a brief period of glucose starvation, were grown in presence of glucose. Because the experiment was performed at 16°C, even wild type cells not exposed to stress grew slowly, making differences between the conditions very small. Consistent with the defect in translational

recovery, a *dom34*Δ strain grew more slowly in the first few hours after glucose starvation than a wild type strain (Figure 51).

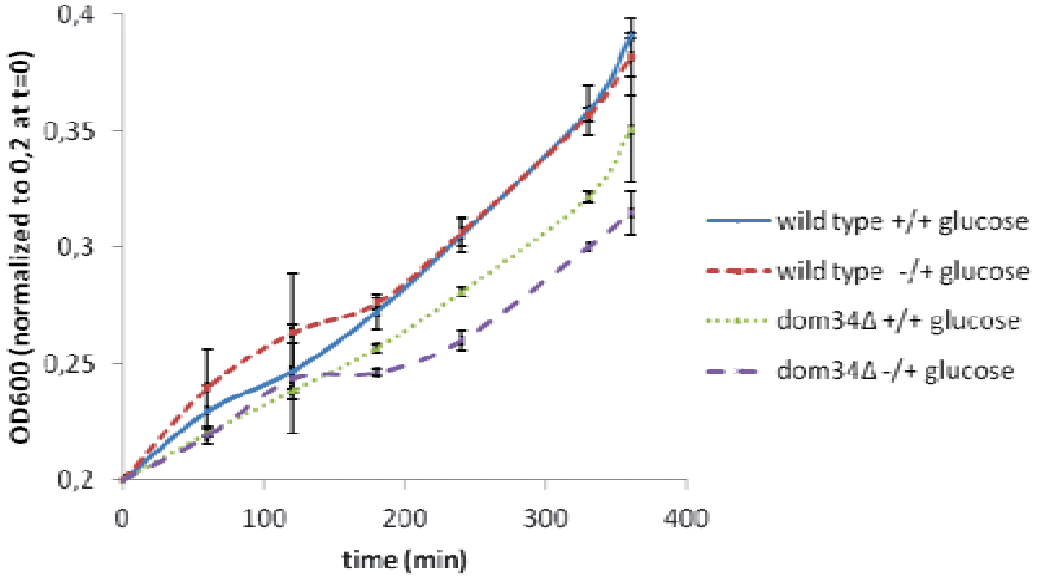

Figure 51 Recovery of growth following glucose starvation in presence and absence of Dom34.
Cell density (OD600) was monitored in *S. cerevisiae*, grown in presence of glucose (in YPDA), followed by glucose starvation or continued growth in glucose rich medium (resuspension in YPA or YPDA respectively) for 10 minutes, and then grown in presence of glucose (resuspension in YPDA) at 16°C. Timepoint 0 minutes corresponds to the moment of resuspension in YPDA.

2.4 DOM34-HBS1 INTERACTION

Not presented here were data I produced in which I show by co-purification experiments on recombinant Dom34 and Hbs1 from bacteria, that the C-terminal domain of Dom34 is essential for Dom34-Hbs1 interaction. These data were published (Collinet et al, 2011), the paper is included in the supplementary information section of this thesis.

3. DISCUSSION

In my work I identified a new role for the ribosome dissociating Dom34-Hbs1 complex. It stimulates translation, by making the subunits of inactive 80S ribosomes available for initiation. Especially in cells recovering from translation inhibiting stress, this proved to be important for translational recovery. My work also gives new insights into RNA quality control mechanisms acting on stalled translational complexes, in which the Dom34-Hbs1 complex also functions, and into how these pathways relate to each other.

3.1 RNA QUALITY CONTROL ON STALLED TRANSLATIONAL COMPLEXES

The Dom34-Hbs1 complex acts in three RNA quality control pathways that have several characteristics in common. Apart from sharing the involvement of Dom34-Hbs1, NGD, 18S NRD and NSD all target ribosomes that translate inefficiently or stall on a mRNA. In all three pathways Dom34-Hbs1 affects the degradation process of the RNAs that cause ribosomal stalling (Cole et al, 2009; Doma & Parker, 2006; Saito et al, 2013) and in NSD there are indications that the complex dissociates stalled ribosomes (Tsuboi et al, 2012). A lot of questions remain on the mechanisms of NGD, 18S NRD and NSD and how these mechanisms relate.

The endonuclease responsible for cleaving the mRNA in NGD has not been identified so far. I excluded the factors Esl1 and Esl2 as candidates. These paralogs have been predicted in the SMART database to contain a PIN domain (Bleichert et al, 2006), a domain that has been shown to have endonuclease activity in several other factors (Huntzinger et al, 2008; Lebreton et al, 2008). Yeast has several other factors that contain a PIN domain. Based on their localization and the conservation of their active sites, these factors could be tested for endonuclease activity in NGD. Another question is how the endonuclease is recruited to a mRNA with one or more stalled ribosomes. If the Dom34-Hbs1 acts upstream of the endonuclease cleavage step, the complex may play a direct role in recruiting the endonuclease. The discovery of the identity of the endonuclease will help greatly in studying the mechanism of its recruitment and in studying the sequence of events in NGD.

At the moment it is not clear whether the recruitment of the Dom34-Hbs1 complex to a ribosome stalled on a NGD substrate always causes mRNA cleavage. Biochemical experiments indicate that Dom34-Hbs1 mediated dissociation of stalled ribosomes only occurs if the mRNA extending downstream of the ribosomal P-site is of limited length

(Pisareva et al, 2011; Shoemaker & Green, 2011), suggesting that mRNA cleavage precedes ribosome dissociation. However, in theory it is possible that *in vivo* ribosome dissociation may occur without mRNA cleavage. If the identity of the endonuclease were known, *in vitro* experiments could give more insight into this. It could then be tested whether the addition of cell lysate, lacking the endonuclease, to an *in vitro* assembled translational complex stalled on a mRNA that extends far beyond the P-site results in ribosome dissociation.

In 18S NRD a defect in an 18S rRNA causes the degradation of the defective 18S rRNA, which is part of an inefficiently translating ribosome (LaRiviere et al, 2006). At the moment nothing is known about the fate of other components of the affected ribosomes. Are the associated 40S subunit proteins also degraded, or can they, or some of them, be recycled? And what happens to the 60S subunit? For the cell it would be energetically favorable to not degrade functional 60S subunits. The observation that Dom34-Hbs1 stimulates 18S rRNA degradation in 18S NRD (Cole et al, 2009) suggests that ribosome dissociation is required for rRNA degradation, possibly by making it accessible for the RNA degradation machinery. The 60S subunit may thereby be released. As discussed in paragraph 1.4.2.1 it is thought that 18S NRD is induced by inefficient translation of the affected ribosome. The question is whether the cell has mechanisms to identify what part of the ribosome causes inefficient translation and selectively degrade only this component. *In vitro* translation experiments in yeast extract, using only mutant 18S rRNA containing ribosomes, may answer the question whether a defective 18S rRNA results in destabilization of other ribosome components.

The question above can be further extended. Also NGD substrates are recognized due to an inefficiently translating ribosome. Does a cell have mechanisms to distinguish between ribosomal stalling caused by a defective ribosome and stalling caused by a stall site in a mRNA? In other words, does a stalled ribosome induce degradation of both mRNA and 18S NRD, or do NGD and 18S NRD occur separately, depending on the cause of stalling? Again, if stalling is caused by a mRNA it would be energetically favorable for the cell to not degrade the ribosome, which can be reused.
In my work I found that disrupting the interaction between Dom34-Hbs1 negatively affects accumulation of a 5' NGD intermediate in yeast deficient for cytoplasmic exosome function, but has no or much less influence on 18S NRD efficiency. This may give new information on how NGD and 18S NRD relate. The difficulty, however, is that the conclusions that can be

drawn from these observations depend on the interpretation of the role of Dom34-Hbs1 in NGD.

In NGD the Dom34-Hbs1 complex is needed for accumulation of a 5' degradation intermediate produced from some, but not all NGD substrates, in yeast deficient for cytoplasmic exosome function. Although initially interpreted as Dom34-Hbs1 stimulating mRNA cleavage, and thereby intermediate production, it can also be interpreted as Dom34-Hbs1 acting downstream of mRNA cleavage and its absence reducing intermediate stability (see paragraph 1.4.5). Comparison of the half-life of a full length NGD reporter mRNA in presence and absence of Dom34-Hbs1 would shed more light on which interpretation is correct.

The conclusions that can be drawn from my findings depend on which interpretation of the effect of Dom34-Hbs1 on NGD intermediate accumulation is used. If the hypothesis that NGD cleavage is Dom34-Hbs1 dependent is true, my data would indicate that NGD and 18S NRD can be genetically separated. It would follow from this that Dom34-Hbs1 recruitment to stalled ribosomes may not always induce the degradation of both mRNA and 18S rRNA in parallel, and that 18S rRNA degradation is not dependent on mRNA degradation.

According to the alternative hypothesis, the 5' intermediate, stabilized in *ski7*Δ, is partially destabilized in absence of functional Dom34-Hbs1, due to stalled ribosomes inducing multiple mRNA cleavages. In this context, my data would indicate that disrupting Dom34-Hbs1 interaction interferes sufficiently with the complex's function to allow stalled ribosomes to induce multiple cleavages, destabilizing the 5' mRNA intermediate in NGD. However, the complex still functions sufficiently to promote 18S NRD. This makes sense as in NGD, there would be a kinetic competition between Dom34-Hbs1 mediated ribosome dissociation and ribosome induced endonucleolytic cleavage, which is likely to be sensitive to small changes in Dom34-Hbs1 activity. On the other hand, in 18S NRD Dom34-Hbs1 has a stimulatory effect on rRNA degradation. Small changes in Dom34-Hbs1 activity will only have small changes on rRNA degradation.

The relationship between NGD and 18S NRD was further studied. My results did not indicate that a stall site in a mRNA can cause degradation of rRNA or ribosomal protein, nor did they exclude it. It would also be interesting to study whether a defect in a ribosome causes degradation of the mRNA it translates. A first indication may be obtained from *in vitro* translation experiments, using a yeast extract containing mutant 18S rRNA ribosomes only. The half-life of the mRNA that will be added to the extract can then be compared between an extract containing mutant ribosomes and an extract containing wild type ribosomes.

Apart from sharing several characteristics with 18S NRD, the NGD pathway also appears to be closely related to the NSD pathway. When ribosomes translate poly(A)+ NS mRNAs, they translate the poly(A) tail into a stretch of lysines. As discussed in paragraph 1.4.1.2, a stretch of lysines can cause a ribosome to stall and induce NGD. It is therefore tempting to speculate on poly(A)+ NSD being a form of NGD, that starts with an endonucleolytic cleavage in the poly(A) tail and subsequent degradation of the large 5' fragment (which is a poly(A)- NS mRNA) by the exosome. However, cleavage in the poly(A) tail appears unlikely, as in yeast deficient for cytoplasmic exosome activity a PGK1-NS mRNA accumulates that contains a poly(A) tail with a length similar to that of a control PGK1 mRNA (~70 nucleotides) (van Hoof et al, 2002).

The 5' mRNA cleavage product produced in NGD may be functionally identical to a poly(A)- NS mRNA. Both are capped mRNAs that lack a stop codon and a poly(A) tail and that are associated with translating ribosomes. In addition my data show that their rapid degradation depends on the same nuclease requirement of the exosome: in both cases Dis3 endo- or exonuclease activity is sufficient. If poly(A)+ NSD would start with an endonucleolytic cleavage in the poly(A) tail, the resulting 5' intermediate would therefore be expected to be degraded in a manner similar to a poly(A)- NS mRNA. However, poly(A)+ NSD and poly(A)- NSD differ mechanistically in that degradation of poly(A)+ NS mRNAs requires Ski7 N- and C-terminus, whereas the degradation of a poly(A)- NS mRNAs requires only the Ski7 N-terminus (Schaeffer & van Hoof, 2011). If poly(A)+ NSD is a form of NGD, this would suggest that the C-terminal domain of Ski7 has a function upstream of the processive, Ski7 N-terminus dependent 3' to 5' degradation of the major part of the NS mRNA.

Finally, a very important question concerns the biological relevance of NGD, 18S NRD, NSD and the role Dom34-Hbs1 plays in these pathways. The frequency and impact of accidental defects in mRNAs or ribosomes that cause ribosomal stalling, or the importance of Dom34-Hbs1 in dealing with them, have not been studied so far. There is the possibility that these mechanisms exist not only to deal with faulty RNAs, but also as a part of regulatory mechanisms. An example could be the regulated use of an alternative poly(A) signal, resulting in a NS mRNA which is consequently degraded. Genome wide data analysis, e.g. from ribosome profiling experiments, comparing strains with and without functional Dom34-Hbs1 may give new insights. Analysis of different environmental conditions or, in case of higher eukaryotes, of different cell types or developmental stages may prove important.

3.2 FUNCTIONAL IMPORTANCE OF HBS1 GTPASE ACTIVITY AND DOM34-HBS1 INTERACTION

I studied the importance of GTP binding by Hbs1 and the interaction between Dom34 and Hbs1 for several functions of the Dom34-Hbs1. Similarly to previous reports (Carr-Schmid et al, 2002; Kobayashi et al, 2010) I found that the binding and hydrolysis of GTP by Hbs1 is important for intermediate accumulation in NGD and for growth in 40S subunit deficient yeast. It also turned out to be required for efficient 18S NRD and for dissociation of inactive ribosomes in yeast recovering from stress. The latter finding parallels the requirement of Hbs1 GTPase activity for the *in vitro* dissociation of ribosomes that are stalled on a mRNA, or vacant ribosomes (Pisareva et al, 2011; Shoemaker et al, 2010; Shoemaker & Green, 2011). GTP hydrolysis is required for Hbs1 dissociation from the ribosome and is thought to induce accommodation of Dom34 in the ribosomal A-site (Shoemaker & Green, 2011), thereby promoting binding of Rli1 and subsequent ribosome dissociation or any other function of Dom34.

The interaction between Dom34 and Hbs1 is mediated by multiple domains of both proteins. The precise details of which residues in what domains participate in the interaction differ between different reports (Chen et al, 2010; Kobayashi et al, 2010). Our structural model of the Dom34-Hbs1 complex indicates that, apart from the interaction between C-terminal domain of Dom34 with domain III of Hbs1, there is an additional interface between the central domain of Dom34 and the G domain of Hbs1. Indeed, mutating conserved residues on both interfaces disrupted Dom34-Hbs1 interaction, as measured by yeast two hybrid analysis. Interestingly I found that disrupting the interaction by mutating Hbs1 did not affect 18S NRD efficiency, growth in 40S subunit deficient strains or dissociation of inactive ribosomes in yeast recovering from stress. On the other hand, the accumulation of a NGD intermediate in yeast deficient for cytoplasmic exosome function was dependent on Dom34-Hbs1 interaction. As described above, this may either reflect different functional requirements for Dom34-Hbs1 induced mRNA cleavage, or the kinetic competition between Dom34-Hbs1 mediated ribosome dissociation and mRNA cleavage.

It may seem surprising that both Dom34 and Hbs1 are required but their stable interaction is not for many of the complex's functions. There are several explanations. Dom34 and Hbs1 may be recruited to a ribosome independently as efficiently as in a complex. Their interaction

may then be stabilized in the ribosomal context. This explanation would suggest that the function of Hbs1 is not merely delivering Dom34 to the A-site, otherwise disrupting the interaction should give the same phenotype as absence of Hbs1. Its presence on the ribosome may change the conformation of Dom34. Alternatively, a third, unknown factor may stabilize the interaction between Dom34-Hbs1 outside the ribosome.

Interestingly, disrupting the interaction between Dom34 and Hbs1 by mutating Dom34 does interfere with 18S NRD, growth in a 40S subunit deficient strain and dissociation of inactive ribosomes. This may be explained from the fact that Dom34 does not only interact with Hbs1, but also with Rli1. Alternatively, after conformational changes of Dom34 on the ribosome, some of these residues may interact with the ribosome itself.

3.3 DOM34-HBS1 STIMULATES TRANSLATION BY MAKING SUBUNITS AVAILABLE FROM INACTIVE RIBOSOMES

Addressing the biological relevance of Dom34-Hbs1, I identified a new role of the complex. It was found to dissociate inactive ribosomes that accumulate during translation inhibiting glucose starvation stress. Making ribosomal subunits available, the complex thereby stimulates rapid recovery of translation after stress relief. This finding expands the number of potential substrates of the Dom34-Hbs1 complex from a small fraction of ribosomes, stalled during translation, to a large fraction of all ribosomes in the cell, which form inactive ribosomes during stress.

Dom34 and Hbs1, or alternatively aEF1α, are conserved in two domains of life (Eberhart & Wasserman, 1995; Inagaki & Ford Doolittle, 2000; Ragan et al, 1996; Saito et al, 2010; Wallrapp et al, 1998). The role of the complex in dissociating inactive ribosomes is therefore likely to be relevant in a wide range of organisms. Moreover, translation inhibition occurs in a variety of stress conditions (Spriggs et al, 2010). It would be reasonable to expect that Dom34-Hbs1 dependent stimulation of translation may be observed in many stress-related conditions. It will be important to verify these hypotheses, and test whether the Dom34-Hbs1 complex stimulates restart of translation in a variety of cells from different organisms, that recover from different types of translation inhibiting stress.

3.4 A NEW MECHANISM TO REGULATE TRANSLATION RATES?

My data indicate that the role of Dom34-Hbs1 dissociating inactive ribosomes is not restricted to cells recovering from stress. In exponentially growing, non-stressed yeast, inactive

ribosomes are also present, although to a much lesser extent than in stressed cells. In yeast lacking functional Dom34-Hbs1 complex, inactive ribosomes accumulate, strongly suggesting that Dom34-Hbs1 are responsible for their dissociation. Moreover, in yeast extract Dom34-Hbs1 complex stimulates translation. These observations suggest that Dom34-Hbs1 function may optimize translation efficiency, having a positive effect on ribosomal subunit availability for translation initiation.

This hypothesis is supported by several earlier reports. Depletion of Rli1, which most probably acts with Dom34-Hbs1 to dissociate inactive ribosomes, results in accumulation of 80S ribosomes and decreased levels of polysomes in yeast, human and *Drosophila* cells, similar to *dom34*Δ and *hbs1*Δ phenotypes (Andersen & Leevers, 2007; Chen et al, 2006; Dong et al, 2004), suggesting accumulation of inactive ribosomes. In yeast it was observed that deletion of *DOM34* or *HBS1* caused growth defects in strains in which translation initiation was limited by constitutive eIF2α phosporylation. This suggests that the absence of Dom34-Hbs1 may further reduce the rate of translation (Carr-Schmid et al, 2002). The hypothesis may also explain the growth defect caused by *DOM34* or *HBS1* deletion in 40S subunit deficient strains (Bhattacharya et al, 2010; Carr-Schmid et al, 2002). In these double mutant strains 40S subunit availability for translation initiation may decrease further by their sequestration in inactive 80S ribosomes. This idea is supported by the observation that in the slowly growing 40S subunit deficient *rps6a*Δ*dom34*Δ strain, additional deletion *RPL4A*, encoding a 60S ribosomal subunit protein, partly restores growth (Bhattacharya et al, 2010). The decrease in 60S subunits should reduce 40S subunit sequestration.

My data strongly indicate that Stm1, in its ribosomal subunit clamping conformation, antagonizes Dom34-Hbs1 mediated dissociation of inactive ribosomes in stressed cells. Up till now, there was no information on whether this translation inhibiting conformation of Stm1 is specific for ribosomes in stressed cells, or whether it may occur in inactive ribosomes in a variety of conditions. When comparing Figures 1B and 3B of the manuscript, it can be seen that in non-stressed cells (leftmost polysome profiles), deletion of *STM1* prevents the increase in 80S ribosomes caused by absence of Dom34. As I showed that this increase in 80S ribosomes is due to an increase in inactive ribosomes, this suggests that Stm1 antagonizes Dom34-Hbs1 mediated dissociation of inactive ribosomes in non-stressed cells as well. In other words, my data support that the ribosomal subunit clamping and translation inhibiting conformation of Stm1 is not specific for stress conditions, but also occurs in inactive ribosomes in non-stressed cells. This may explain why overexpression of Stm1 in *dom34*Δ

yeast causes a growth defect (Balagopal & Parker, 2011). Absence of Dom34 and overexpression of Stm1 both having a stabilizing effect on inactive ribosomes, this condition may lead to a reduced availability of ribosomal subunits for translation initiation and therefore suboptimal translation rates.

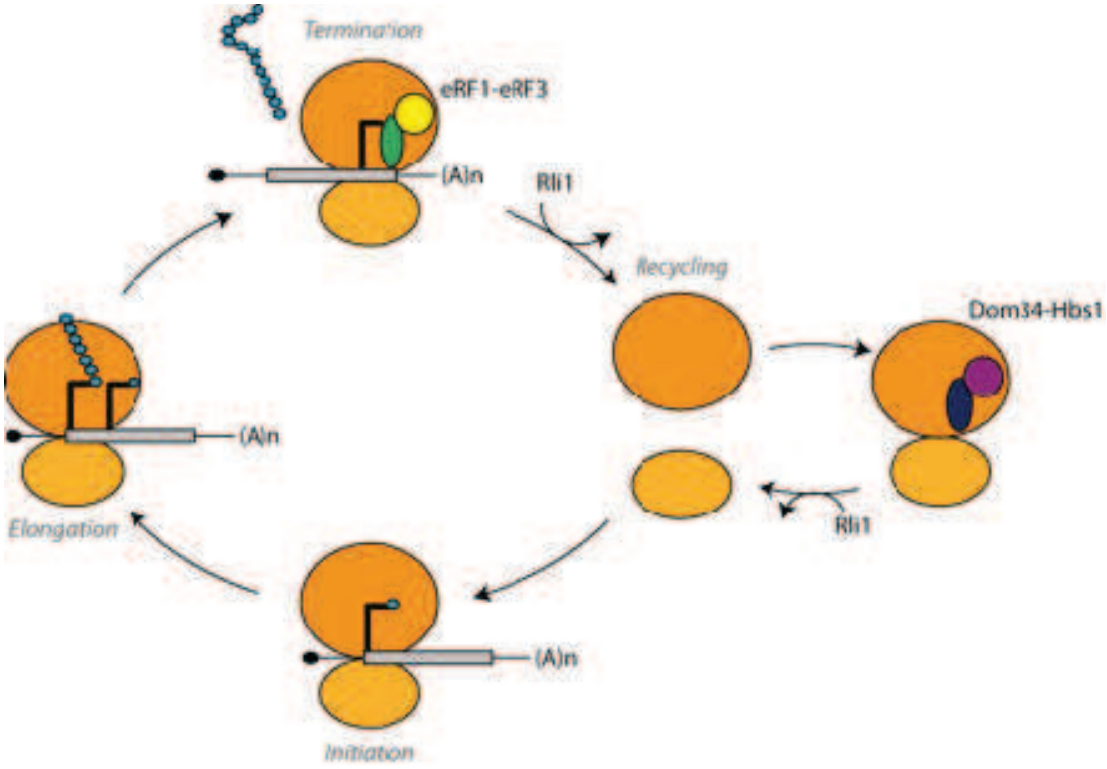

Figure52 Model for the Dom34-Hbs1 complex affecting subunit availability in the translation cycle
After termination and recycling, ribosomal subunits do not always engage immediately in a new round of translation. Instead they can associate to form inactive 80S ribosomes, not associated with a mRNA. Dissociation of these non-translating ribosomes, which depends on Dom34-Hbs1 and Rli1, is required to make their subunits available for new rounds of translation. Regulation of this dissociation process may form a new level of regulating translation initiation.

My findings add a new component to the translation cycle as it is currently viewed (Figure52). In the recycling stage of the translation cycle, dissociation of terminated ribosomes results in a 40S subunit still bound to mRNA and tRNA. The release of both RNAs is mediated by initiation factors eIF1, eIF1A, eIF3 and eIF3j (Pisarev et al, 2010). The requirement of these factors binding to a 40S subunit during translation initiation suggests that they directly connect ribosome recycling with a new round of translation (Aitken & Lorsch, 2012; Jackson et al, 2010; Nurenberg & Tampe, 2013). My data emphasize that instead, ribosomal subunits that result from recycling may associate to form inactive

ribosomes. The Dom34-Hbs1 complex, and very probably Rli, are required for their dissociation, which allows the ribosomal subunits to re-enter the translation cycle (seeFigure52). This process may provide a new level of regulation of translation, by controlling ribosomal subunit availability. That such regulation may have an important effect on translation rates is supported by a recent report, in which it was predicted from a computational model that protein production in healthy yeast cells is typically limited by the availability of free ribosomes (Shah et al, 2013).

An important question to address is whether ribosomal subunit availability may be regulated by changing Dom34-Hbs1 levels or activity. In other words: are Dom34 and Hbs1 regulated? One may expect that Dom34 and Hbs1 will be upregulated during stress conditions to allow cells to rapidly recover translation when conditions change for the better. Regulation of Dom34 and Hbs1 expression may occur on the level of mRNA (e.g. by transcriptional regulation or a change in mRNA stability) or protein abundancy (e.g. by regulation of mRNA specific translation or protein activity). Alternatively, post-translational modification may change protein activity.

It will be very interesting to see whether mRNA or protein levels of Dom34 and Hbs1 change during stress. A search in the Yeastract database (Abdulrehman et al, 2011; Monteiro et al, 2008; Teixeira et al, 2006), which reports direct or indirect regulatory associations between transcription factors and target genes in *S. cerevisiae*, implicates several stress related transcription factors in controlling Dom34 and Hbs1 transcriptional expression. These include Gcn4 (Moxley et al, 2009), Sfp1 which is involved in regulating the response to nutrient stress (Cipollina et al, 2008), Pho4 which plays a role in phosphate limited conditions, Gat1 which is upregulated during nitrogen starvation, Msn2 and Msn4 which are upregulated during stress, Rtg1 and Rtg3, which are activated during glutamine starvation (Harbison et al, 2004) and Leu3 which acts as an activator during leucine depletion (Tang et al, 2006), These transcription factors have been found by genome wide experiments to either bind directly to the *DOM34* or *HBS1* promoter region or indirectly affect their expression.

Post-translational modifications may play a role in the regulation of Dom34-Hbs1 activity. Large scale mass spectrometric analyses identified *S. cerevisae* Hbs1 to contain a phosphoserine (Albuquerque et al, 2008; Li et al, 2007). It would also be interesting to examine whether Dom34 or Hbs1 in different organisms have motifs predicting conserved phosphorylation sites. To get an indication about whether posttranslational modifications play

a role in regulating Dom34-Hbs1 activity, it could then be tested whether mutating these sites affects recovery of translation after stress or the levels of inactive ribosomes.

In higher eukaryotes Dom34-Hbs1 mediated regulation of ribosomal subunit availability may not only play a role in stress conditions, but also in developmental processes. During embryonic development, as well as in the maturation of certain cell types from stem cells into differentiated cells in mature organisms, translation rates will need to increase in stages of rapid proliferation. Strikingly, in higher eukaryotes absence of Dom34 causes defects in mitotic and meiotic cell division, leading to defective proliferation of the blastocyst inner cell mass and embryonic lethality in mice (Adham et al, 2003) and defects in spermatogenesis in *Drosophila* (Eberhart & Wasserman, 1995). It may be very interesting to examine whether these defects are accompanied by a failure of ribosomal subunits to redistribute from inactive 80S ribosomes to the translating pool.

4. MATERIALS AND METHODS

4.1 STRAINS AND MEDIA

4.1.1 Bacterial media

E. coli was grown in the following media :

- LB: 10 g/l tryptone, 5 g/l yeast extract, 5 g/l NaCl (Sigma L3022).
- Autoinduction medium: 12 g/l tryptone, 24 g/l yeast extract, 3.3 g/l $(NH_4)_2SO_4$, 6.8 g/l KH_2PO_4, 7.1 g/l Na_2HPO_4, 0.5 g/l glucose, 2.0 g/l α-lactose, 0.15 g/l $MgSO_4$, 0.03 g/l trace elements (Formedium AIMTB0210).

Depending on the selection marker of the plasmid the bacterial strain was transformed with, the following antibiotics were added to the medium: ampicillin (50 µg/ml), kanamycin (50 µg/ml), chloramphenicol (25 µg/ml).

4.1.2 Bacterial strains and plasmids

The MH1 (*araD39, lacX74Δ, gal E, gal K, hsr, rpsL*) *E. coli* strain was used for cloning and plasmid storage. For protein expression the following *E. coli* strains were used.

- BL21 (DE3) (*fhuA2 [lon] ompT gal (λ DE3) [dcm] ΔhsdS , λ DE3 = λ sBamHIo ΔEcoRI-B int::(lacI::PlacUV5::T7 gene1) i21 Δnin5*)
- BL21 CodonPlus-RIL (F– *ompT hsdS*(rB– mB–) *dcm*+ Tetr *gal endA* Hte [*argU ileY leuW* CamR])

Table 1 lists all plasmids used in *E. coli*.

Bacteria were grown at 37°C, unless indicated otherwise, and shaken at 170 rpm in liquid culture.

Table 1 List of *E. coli* plasmids.

Plasmid	Vector	Insert	Selection marker	Reference / comment
pBS3410	pET28	*HBS1-6HIS*	*KanR*	gift from M. Graille
pBS3438	pACYC LIC+	*DOM34-STREP*	*cat* (chloramphenicol resistance)	
pBS4612	pUC19	*T7-5'UTR (PGK1)-TAP-3HA-GFP-3'UTR (PGK1)-(A)50*	*AmpR*	
pBS4613	pUC19	*T7 -5'UTR (PGK1)-TAP-3HA-SL-GFP-3'UTR (PGK1)-(A)50*	*AmpR*	
pT7-LUC-A50	pBluescript	*T7-LUC-(A)50*	*AmpR*	(Gallie et al, 1991)

4.1.3 Yeast media

Yeast was either grown in rich media or in synthetic defined drop out media, lacking one or several amino acids to select for yeast containing a plasmid with a selection marker that allows the synthesis of this particular amino acid. Both types of media were used with and without 2% glucose. Synthetic defined media containing 2% galactose were also used. In the chase experiment to determine mRNA half-life 4% glucose was used.

Rich media:

- YPDA (yeast peptone dextrose adenine) (Formedium CCM1010): 10 g/l yeast extract, 30 g/l bacto peptone, 20 g/l glucose, 40 mg/l adenine sulfate.
- YPA (yeast peptone adenine): 10 g/l bacto yeast extract (BD), 30 g/l bacto peptone (BD), 40 mg/l adenine sulfate.

Synthetic defined drop out media:

- Complete supplement mixture (CSM) – amino acid (MP) (quantity defined by the manufacturer), 6.7 g/l difco yeast nitrogen base without amino acids (BD), 20 g/l (or 40 g/l or 0 g/l) glucose or galactose, 50 ml Sorensen's phosphate buffer (20x)[1].

When media were prepared in solid form, they contained 2% bacto agar (BD). Yeast was grown at 30°C, unless indicated otherwise, and shaken at 170 rpm in liquid culture.

4.1.4 Yeast strains and plasmids

S. cerevisiae strains used in this work are listed in

Table 2. All strains, except Y190, were derived from BMA64 (*ade 2-1 his3-11,15 leu2-3,112 trp1Δ ura3-1 can1-100*). Table 3 lists all yeast plasmids used in this work.

Table 2 Yeast strains.

Yeast strain	Genotype	Reference / comment
BMA64	*MAT α*	(Baudin-Baillieu et al, 1997)
BSY1486	*MAT a esl1Δ::TAP::KanR*	constructed by C. Faux
BSY1624	*MAT α dcp1-2*	constructed by C. Faux
BSY1699	*MAT α ski7Δ::Kan*	constructed by C. Faux
BSY1883	*MAT a KanMX:TetOFF-DIS3*	(Lebreton et al, 2008)
BSY1970	*MAT α dom34Δ::HIS3*	constructed by D. Lebert
BSY2029	*MAT a dom34Δ::HIS3 ski7Δ::Kan R*	constructed by C. Faux
BSY2051	*MAT a dom34Δ::HIS3 rps28AΔ::Kan R*	constructed by C. Faux
BSY2145	*MAT a hbs1Δ::KanR*	constructed by C. Faux

[1] The compositions of all buffers used are listed in paragraph 4.6.

BSY2204	*MAT a ski7Δ::KanR hbs1Δ::KanR*	
BSY2218	*MAT a rps28AΔ::KanR hbs1Δ::KanR*	
BSY2219	*MAT a sup45ts*	Gift from F. Lacroute
BSY2221	*MAT a sup35ts sup45ts*	Gift from F. Lacroute
BSY2550	*MAT a dom34Δ::HIS3 hbs1Δ::KanR*	
BSY2553	*MAT α ski7Δ::Kan esl1Δ::Kan*	
BSY2554	*MAT a ltn1Δ::His3*	
BSY2555	*MAT α ski7Δ::Kan ltn1Δ::His3*	
BSY2556	*MAT a esl2Δ::His3*	
BSY2557	*MAT α ski7Δ::Kan esl2Δ::His3*	
BSY2625	*MAT α dcp1-2 dom34 Δ::His3*	
BSY2626	*MAT a stm1Δ::TRP1 dom34Δ::HIS3*	
N20T20	*MAT a stm1Δ::TRP1*	Gift from F. Lacroute and F. Wyers
Y190	*MAT a gal4 gal80 his3 trpl-901 ade2-101 ura3-52 leu2-3, 112 + URA3::GAL-IacZ, LYS2::GAL(UAS)-HIS3 cyh r*	(Bai & Elledge, 1996)

Table 3 Yeast plasmids.

Plasmid	Vector	Insert	Selection marker	Reference / comment
pACTII			*TRP1*	(Bai & Elledge, 1996)
pAS2			*LEU2*	(Bai & Elledge, 1996)
pBS2284	pRS416	*GALp-PGK1pG*	*URA3*	(Finoux & Seraphin, 2006)
pBS3161	pRS416	*GALp-PGK1pG*-premature stop codon	*URA3*	derived from pBS2284, constructed by D. Rispal
pBS3217	pRS415	*DOM34* + 313 nucleotides upstream	*LEU2*	
pBS3269	pFL36	*lys2:DIS3-TEV-PROTEIN A*	*LEU2*	(Lebreton et al, 2008)
pBS3270	pFL36	*lys2:DIS3 D551N -TEV-PROTEIN A*	*LEU2*	(Lebreton et al, 2008)
pBS3277	pFL36	*lys2:DIS3 D171N D551N -TEV-PROTEIN A*	*LEU2*	(Lebreton et al, 2008)
pBS3278	pFL36	*lys2:DIS3 D171N -TEV-PROTEIN A*	*LEU2*	(Lebreton et al, 2008)
pBS3611	pRS415	*HBS1* + 204 nucleotides upstream and 234 nucleotides downstream	*LEU2*	constructed by M.E. Gas Lopez
pBS3614	pRS415	*HBS1-PROTEIN A*	*LEU2*	derived from pBS3611, constructed by M.E. Gas Lopez
pBS3675	pRS415	*hbs1 V176G-PROTEIN A*	*LEU2*	derived from pBS3614
pBS3676	pRS415	*hbs1 H255E-PROTEIN A*	*LEU2*	derived from pBS3614
pBS3677	pRS415	*hbs1* ^{256}*RDF*^{258}*→AAA -PROTEIN A*	*LEU2*	derived from pBS3614
pBS3678	pRS415	*hbs1 R517E-PROTEIN A*	*LEU2*	derived from pBS3614
pBS3679	pRS415	*hbs1 R557A H558A-PROTEIN A +*	*LEU2*	derived from pBS3614
pBS3680	pRS415	*hbs1 L520R-PROTEIN A*	*LEU2*	derived from pBS3614
pBS3685	pRS415	*DOM34-3HA*	*LEU2*	derived from pBS3217
pBS3699	pRS415	*hbs1 K180A-PROTEIN A*	*LEU2*	derived from pBS3614
pBS3701	pRS415	*dom34 E361R-3HA*	*LEU2*	derived from pBS3685
pBS3702	pRS415	*dom34 E361A Q364A-3HA*	*LEU2*	derived from pBS3685
pBS3703	pRS415	*dom34* ^{174}*KKKR*^{177}*→AAAA -3HA*	*LEU2*	derived from pBS3685

pBS3705	pRS415	*dom34* ^{212}*SPGF*^{215}*→ AAAA -3HA*	*LEU2*	derived from pBS3685
pBS3706	pRS415	*dom34 Y300A E361A-3HA*	*LEU2*	derived from pBS3685
pBS4104	pRS426	*GAL1p-CBP-3HA-SL-3'UTR (PGK1)*	*URA3*	
pBS4113	pRS426	*GAL1p-CBP-3HA-3'UTR (PGK1)*	*URA3*	negative control for pBS4104
pBS4197	pRS426	*GAL1p-CBP-3HA-K12-3'UTR (PGK1)*	*URA3*	
pBS4199	pRS426	*GAL1p-CBP-3HA-R12-3'UTR (PGK1)*	*URA3*	
pBS4201	pRS426	*GAL1p-CBP-3HA-R12FS-3'UTR (PGK1)*	*URA3*	
pBS4203	pRS426	*GAL1p-CBP-3HA-3'UTR (PGK1)*	*URA3*	negative control for pBS4197 and pBS4199
pBS4213	pRS415	*DOM34-3HA* (on negative strand)-*GAL1-10p-HBS1-PROTEIN A*	*LEU2*	
pBS4214	pRS415	*GAL10p-DOM34-3HA*	*LEU2*	
pBS4215	pRS415	*GAL1p-HBS1-PROTEIN A*	*LEU2*	
pBS4290	2µ	*GAL7p-35S rDNA :18S U1 stemloop in h39*	*TRP1*	derived from pWL160-2
pBS4291	2µ	*GAL7p-35S rDNA :18S U1 stemloop antisense in h39*	*TRP1*	derived from pWL160-2
pBS4292	2µ	*GAL7p-35S rDNA :18S U1 stemloop in h44*	*TRP1*	derived from pWL160-2
pBS4293	2µ	*GAL7p-35S rDNA :18S U1 stemloop antisense in h44*	*TRP1*	derived from pWL160-2
pBS4294	2µ	*GAL7p-35S rDNA :18S A1492C, U1 stemloop in h39*	*TRP1*	derived from pWL160-A1492C
pBS4295	2µ	*GAL7p-35S rDNA :18S A1492C, U1 stemloop antisense in h39*	*TRP1*	derived from pWL160-A1492C
pBS4298	pRS416	*TPIp - U1A(1-120) - TAP*	*URA3*	
pBS4372	pRS426	*GAL1p-TAP-3HA-SL-GFP-3'UTR(PGK1)*	*URA3*	
pBS4374	pRS426	*GAL1p-TAP-3HA-GFP-3'UTR(PGK1)*	*URA3*	negative control for pBS4372
pBS4375	pRS426	*GAL1p-TAP-3HA-K12-GFP-3'UTR(PGK1)*	*URA3*	
pBS4376	pRS426	*GAL1p-TAP-3HA-R12-GFP-3'UTR(PGK1)*	*URA3*	
pBS4377	pRS426	*GAL1p-TAP-3HA-R12FS-GFP-3'UTR(PGK1)*	*URA3*	
pBS4378	pRS426	*GAL1p-TAP-3HA-GFP-3'UTR(PGK1)*	*URA3*	negative control for pBS4375 and pBS4376
pBS4415	pRS415	*hbs1ΔN-ter (2-149)-PROTEIN A*	*LEU2*	derived from pBS3614
pFL36			*LEU2*	(Bonneaud et al, 1991)
pRP469		*GAL1p-PGK1pG*	*URA3*	(Doma & Parker, 2006)
pRP1251		*GAL1p-PGK1pG-SL*	*URA3*	(Doma & Parker, 2006)
pRS415				(Sikorski & Hieter, 1989)
pRP485		*GAL1 promoter-MFA2pG*	*URA3*	(Decker & Parker, 1993)
pWL160-2	2µ	*GAL7p-35S rDNA*	*TRP1*	(LaRiviere et al, 2006)
pWL160-A1492C	2µ	*GAL7p -35S rDNA 18S:A1492C*	*TRP1*	(LaRiviere et al, 2006)

4.1.5 Gene deletion

The selection marker to be used was amplified in a polymerase chain reaction (PCR), using Taq DNA polymerase and Thermopol buffer (New England Biolabs M0267), following the manufacturers recommendations and instructions. The primers used contained a 40-60 nucleotides sequence upstream of the sequence used to amplify the cassette, that corresponded to sequences upstream and downstream of the gene to be deleted (recombination sites). The PCR product was verified on a TBE agarose 0.1% EtBr gel. The DNA product was then purified by adding 1 volume of phenol:chloroform:isoamyl alcohol 25:24:1 (PCI), vortexing during 1 minute and centrifugation at 14000 rpm for 5 minutes. DNA in the upper phase was precipitated by addition of 1/10 volume of 3M NaAc pH 5.2, 2.5 volume of 100% ethanol (-20°C) and 10 µg glycogen, followed by incubation at -20°C. Following centrifugation at 14000 rpm for 25 minutes at 4°C, the pellet was washed in 70% ethanol (-20°C) and spun at 14000 rpm for 10 minutes at 4°C. The PCR product was dissolved in 10 µL H_2O. It was then used to transform the yeast strain of interest, as described in paragraph 4.1.7.

Some of the resulting colonies DNA were grown in liquid YPDA and their genomic DNA was extracted as described in paragraph 4.1.6.1.2. Gene deletion was verified by PCRs that span the 5' and 3' recombination sites respectively, using Taq DNA polymerase. PCR products were analyzed on TBE agarose 0.1% EtBr gel.

4.1.6 Cloning

4.1.6.1 DNA isolation

4.1.6.1.1 Isolation of plasmid DNA from E. coli

Plasmids were purified from *E. coli* by NucleoSpin Plasmid kit (Macherey Nagel 740588.50) (miniprep) or NucleoBond Xtra Midi kit (Macherey Nagel 740410.10) (midiprep) following the manufacturer's instructions. Plasmids were dissolved in 50 µl H_2O.

4.1.6.1.2 Isolation of yeast genomic DNA

1 ml of saturated yeast culture was pelleted at 14000 rpm for 5 minutes, resuspended in 100 µl yeast lysisbuffer and shaken at 1400 rpm for 15 minutes. Addition of 500 µl H_2O and 700 µl PCI to the lysate was followed by vortexing for 1 minute and centrifugation at 14000 rpm for

5 minutes. The DNA in the upper phase underwent an additional round of PCI extraction followed by ethanol precipitation as described in paragraph 4.1.5, and was dissolved in H_2O. If DNA was extracted for verification of a gene deletion, DNA was dissolved in a 200 µl H_2O of which 1 µL was used for a 20 µL PCR.

4.1.6.2 PCR and digestion

PCRs for cloning were performed using Phusion High-fidelity DNA polymerase and HF buffer (Finnzymes F-530) or PfuUltra II fusion HS DNA polymerase and the recommended buffer (Agilent 600670), following the manufacturer's recommendations and instructions. PCR product and 1 µg of the vector in which the PCR product was to be inserted were then digested in 50 µl reactions by various restriction enzymes (New England Biolabs, Fermentas), following the manufacturer's instructions.

4.1.6.3 In gel ligation

Digested plasmids and PCR products were separated on low melting agarose-TA gels run in TA buffer at 4°C. For fragments larger than 1 kb SeaPlaque® GTG® agarose (Lonza 50110) was used, for fragments smaller than 1 kb NuSieve agarose (Lonza 50084) was used. After staining in 0.5% EtBr in TA, bands were cut, melted at 68°C for 10 minutes and then kept at 42°C. Approximately equal molarities of vector and PCR product were mixed in a 10 µl volume, then 10 µl T4 DNA ligase 20 U/µl in 2x T4 DNA ligase buffer (New England Biolabs M0202) was added followed by incubation at 16°C over night. Reactions were melted at 68°C, then kept at 42°C. 50 µl 50 mM $CaCl_2$ was added and the reactions were cooled on ice.

4.1.6.4 Bacterial transformation

100 µl competent *E. coli* cells were added to 1-5 µl plasmid or the cooled ligation products as described above, followed by incubation on ice for 20 minutes. Cells were heat shocked at 42°C for 90 seconds, then put back on ice. After addition of 1 ml LB, cells were incubated at 37°C for 45 minutes. A fraction or the entire transformation (concentrated by a brief centrifugation step) was plated on solid LB medium, containing the appropriate antibiotic. For cloning MH1 cells were used.

4.1.6.5 Verification

A number of the resulting colonies were grown in LB containing the appropriate antibiotic. Plasmids were purified by miniprep (see paragraph 4.1.6.1.1). Correct insertion of the PCR product was verified by digestion at sites that differentiate between empty vector (or the plasmid started from) and final cloning product. Digestion products were analyzed on TBE agarose 0.1% EtBr gel. Plasmids were sequenced at GATC Biotech.

4.1.6.6 Insertion stem loop

pBS4104 was generated by replacing a sequence inserted in a precursor plasmid between SpeI and NheI, the digestion of which generates compatible sticky ends, by a stem loop. The result is a plasmid that differs from pBS4113 only by the presence of the stem loop. The precursor plasmid (2 µg) was digested with SpeI and NheI (New England Biolabs) in a 100 µl reaction following the manufacturer's instructions, followed by dephosphorylation of the resulting ends by adding 10 U calf intestinal alkaline phosphatase (New England Biolabs M0290) and incubation at 37°C for 30 minutes. The digested vector was PCI extracted, ethanol precipitated and dissolved in H_2O. Oligonucleotide OBS4533 (CTAGCGATATCCCGTGGA GGGGCGCGTGGTGGCGGCTGCAGCCGCCACCACGCGCCCCTCCACGGGATATCG) is complementary to itself and annealing of two copies generates ends that are compatible with SpeI and NheI generated sticky ends. 7 µg OBS4533 was phosporylated at its 5' end using T4 polynucleotide kinase and reaction buffer A (Fermentas EK0032) in a 50 µl reaction, then PCI extracted, ethanol precipitated and resuspended in H_2O. 200 ng vector and 47 ng OBS4533 were ligated using T4 DNA ligase at 16°C for 2 hours. This was followed by addition of 50 µl 50 mM $CaCl_2$ and transformation of competent MH1 cells.

4.1.6.7 Site directed mutagenesis

Point mutations were generated by site directed mutagenesis. Primers were designed to anneal to the exact same sequence in the plasmid on opposite strands. They contained the desired mutation flanked on each side by 15-25 nucleotides. The plasmid was linearly amplified, using 40 nM of each primer, 200 ng plasmid, 0.2 mM dNTPs, PfuUltra II fusion HS DNA polymerase and the corresponding buffer in a 50 µl reaction. The reaction went through 18 cycles of 95°C 50 seconds, 60°C 50 seconds and 68°C for approximately 1.5 x the plasmid size (kb) in minutes, preceded by a step of 60 seconds at 95°C and followed by a step of 7 minutes at 68°C. Then 20 U DpnI (New England Biolabs) was added to the reaction followed

by incubation at 37°C for 1 hour, to remove the original plasmid. The product was PCI extracted, ethanol precipitated, resuspended in H_2O and then used for MH1 transformation.

4.1.7 Yeast transformation

50 ml yeast culture in YPDA at OD_{600} 0.8-1 was pelleted at 4500 x g, resuspended in 50 ml 10 mM Tris pH 7.5 and immediately pelleted again as above. Yeast was then resuspended in LiT containing 10 mM DTT, followed by incubation at room temperature for 40 minutes. Yeast was pelleted as above and resuspended in 750 µl LiT containing 10 mM DTT. 100 µl competent yeast was then added to 1-5 µl plasmid DNA, 5 µl denatured carrier DNA (10 mg/ml) and 50 µl LiT, followed by incubation at room temperature for 10 minutes. 300 µl PEG4000 in LiT (1g dissolved in 1 ml LiT) was added to each transformation, followed by 10 more minutes at room temperature and 15 minutes at 42°C. Cells were pelleted at 14000 rpm for 10 seconds, resuspended in 1 ml YPDA and incubated at 30°C for 1 hour. Temperature sensitive strains (*dcp1-2*) were incubated at 25°C. Cells were pelleted at 14000 rpm for 60 seconds, resuspended in 100 µl 10 mM Tris pH 7.5 and plated on the appropriate synthetic defined drop out medium.

4.2 YEAST GROWTH

4.2.1 Glucose starvation and addition

Yeast was grown at 30°C to an OD_{600} of 0.6, then shifted to 16°C for 2 hours. The culture was then split into multiple 100 ml cultures that were pelleted at 5400 x g for 6 min at 16°C, resuspended in 100 ml media (precooled at 16°C) without or with 2% glucose and incubated at 16°C for 10 minutes. Cells were pelleted, resuspended in 100 ml media with glucose and incubated at 16°C for the indicated times.

4.2.2 Drop assay

Yeast was grown to mid-log phase in YPDA or in the synthetic defined drop out medium indicated. It was then diluted to OD_{600} 0.1, then a 10-fold dilution series was made, diluting in growth medium. 2 µl of each dilution was spotted on the solid medium corresponding to the liquid medium the yeast was grown in.

4.2.3 Growth curve

Yeast was grown to OD_{600} 0.6 at 30°C in YPDA, then shifted to 16°C for 2 hours. Yeast then underwent glucose starvation and glucose addition basically as described in paragraph 4.2.1. Each culture was split in 2, pelleted at 4500 x g for 10 minutes at 16°C, resuspended in 10 ml YPA (glucose starvation) or YPDA (no starvation) followed by 10 minutes incubation at 16°C. Cells were pelleted at 4500 x g for 10 minutes at 16°C, resuspended in 10 ml YPDA and immediately diluted 4-fold to OD_{600} ~ 0.2 in 10 ml final volume YPDA. This was time point 0 minutes. The OD_{600} was measured immediately and at the indicated time points. Time point 0 minutes was normalized to OD_{600} 0.2 for all cultures. All measurements corresponding to the same culture were corrected with the same factor.

4.3 RNA ANALYSIS

4.3.1 RNA extraction

For analysis of steady state RNA levels, 10 ml of yeast culture at OD_{600} ~ 0.8 was pelleted at 4500 x g, resuspended in 750 µl H_20, transferred to an eppendorf and pelleted in a micro spin centrifuge for 15 minutes. The pellet was frozen in liquid nitrogen and stored at -80°C.

RNA was isolated by hot phenol extraction. After addition of 450 µl phenol (pH 4.5-5) to the frozen pellet it was shaken at 1400 rpm at 65°C during 30 seconds, then 450 µl TES buffer was added followed by incubation at 65°C for 30 minutes. These 30 minutes contained 1 minute episodes of shaking at 1400 rpm separated by 5 minute intervals. Incubation at 4°C for 10 minutes was followed by centrifugation at 14000 rpm for 5 minutes at room temperature. To the upper phase 450 µl phenol was added followed by manual shaking, incubation at 4°C for 5 minutes and centrifugation at 14000 rpm for 5 minutes. To the upper phase 400 µl chloroform was added, followed by manual shaking and centrifugation at 14000 rpm for 5 minutes. To 250 µl of the resulting upper phase 625 µl ethanol (-20°C) and 25 µl 3 M NaAc pH 5.2 were added followed by centrifugation at 14000 rpm for 15 minutes at 4°C. The pellet was washed with 700 µl 70% ethanol (-20°C) and spun at 14000 rpm for 5 minutes at room temperature. The pellet was resuspended in 40 µl H_2O.

4.3.2 Northern analysis

4.3.2.1 Using an agarose-formaldehyde gel

Northern analysis was performed basically as described in (Sambrook et al, 1989). 10 µg or 15 µg (PGK1-SL) mRNA was mixed with 2 µl RNA loading dye, 2 µl 10x MOPS buffer, 3.5 µl formaldehyde and 10 µl formamide, heated at 65°C for 15 minutes then cooled on ice for 10 minutes, then loaded on an agarose-formaldehyde (6.7%) gel in MOPS buffer. All CBP-3HA and TAP-3HA-GFP mRNAs were separated on gels containing 2% agarose, PGK1 mRNAs on gels containing 1.25% agarose and all other RNAs on gels containing 1.5% agarose. 18x18 cm gels were run at 100 V, 10x10 cm gels at 50 V in MOPS buffer. All mRNAs containing a stem loop were separated on gels with bridges of Whatman paper separating gel from running buffer. The gel was washed in 10x SSC for 10 minutes (Invitrogen 15557-036). RNAs were transferred to a Hybond-XL membrane (GE Healthcare, RPN 203S) in 10x SSC by capillary elution over night. RNAs were cross linked to the

membrane by exposure to 240 mJ UV light. The membrane was stained in 0.1% methylene blue 0.5 M NaAc pH 5.2, then washed in H_2O.

The membrane was pre-hybridized in Church buffer, followed by hybridization in fresh, probe-containing Church buffer over night. For hybridization temperatures see Table 4. Membranes were washed at hybridization temperature in 2x SSC 0.5% SDS (1 quick wash, 2x 15 minutes wash) and 0.1x SSC 0.5% SDS (1x 15 minutes wash). Signals were visualized with a Typhoon 8600 Variable Mode Imager and quantified using ImageQuant 5.2 software (Molecular Dynamics).

4.3.2.2 Using a formaldehyde-urea gel

4 µl of RNA was mixed with 5 µl loading dye, heated at 65°C for 15 minutes, then cooled on ice. A ~ 20 cm x 20 cm 6% polyacrylamide urea gel (for composition see paragraph 4.6) was pre-run at 3 W for 15 minutes. RNA was loaded and the gel was run in TBE at 15 W. RNA was transferred to a Hybond-XL membrane in a wet/tank electroblotting system at 200 mA, 1.5 hour at 4°C. Membrane staining and hybridization as in paragraph 4.3.2.1.

4.3.2.3 Probe labeling

All probes used are listed in Table 4. They were labeled by incubating 15 pmol probe with 10 pmol γ-^{32}P ATP and 10 U T4 polynucleotide kinase in the enzyme's buffer A in a 30 µl reaction for 45 minutes. The reaction was stopped by adding 2 µl 0.5 M EDTA. After addition of 30 µL H_2O the unincorporated nucleotides were removed by passage through a pre-spun Micro Bio-Spin 6 column (Biorad 732-6221) at 3000 rpm for 1 minute.

Table 4 Probes used for northern analysis

Probe	Sequence	Hybridization temperature	Reference
OBS1160	GGCTTGTGTGGAAGCAGTGGTGATCGG	55°C	
OBS1298	ATTCCCCCCCCCCCCCCCCCCA	55°C	
FL125	CGAGGATCCAGGCTTT	40°C	(LaRiviere et al, 2006)
OBS4814	GTGCGGCCCAGAACGTCT	50°C	
OBS5408	CCGCACTCCTCGCCACAC	50°C	
OBS4671	GCCCGCATAGTCAGGAAC	49°C	
OBS5598	GATCAATTCGTCGTCGTCGAATAAAGAAGACAAG	55°C	

PGK1-SL and scR1 were detected by probes resulting from random priming of PCR product, using α-^{32}P dCTP and the NEBlot (New England Biolabs N1500L) , following the manufacturer's instructions. PCR products were obtained using Taq DNA polymerase and

primers OBS1884 (GTGGGATGGGATACGTTGAG) and OBS1885 (ATGGTTCAGGACACACTCCA) on genomic DNA for scR1 and primers OBS4139 (AAGTCCAAATCTTGGACAGAGATCAATTCG) and OBS4164 (CTAATTCGTAGTTTTTCAAGTTCTTAGATGC) on pBS3158 for PGK1. Hybridization at 55°C (scR1) and 65°C (PGK1).

4.3.3 Determine mRNA half-life

150 ml yeast cultures were grown at 25°C in synthetic defined drop out medium containing 2% galactose, which allowed expression or the galactose inducible reporter mRNA. At OD_{600} ~ 0.6, the culture was transferred to 37°C for 1 hour, to inhibit Dcp1 activity in dcp1-2 strains. Cells were pelleted at 4500 x g for 10 minutes at 37°C and resuspended in 15 ml of the same medium that now contained 4% glucose instead of galactose, causing the transcription of the reporter mRNA to switch off. Yeast was divided into 1 ml aliquots in eppendorf tubes, which were shaken at 1400 rpm at 37°C. Aliquots were pelleted for 15 seconds in a micro spin centrifuge and immediately frozen in liquid nitrogen. The time of freezing corresponds to the time points indicated in the result section. RNA was isolated by hot phenol extraction, as described in paragraph 4.3.1, and dissolved in 40 µl H_2O. 4 µl (MFA2) or 5µl (PGK1) of each sample was analyzed by northern blot.

4.4 PROTEIN ANALYSIS

4.4.1 Rapid protein extraction

This protocol was based on (Kushnirov, 2000). Yeast was grown to OD_{600} ~ 1, then 1 ml of culture was pelleted at 14000 rpm for 1 minute and resuspended in 100 µl H_2O. 100 µl 0.2 M NaOH was added, followed by 5 minutes of incubation at room temperature. After centrifugation at 14000 rpm for 5 minutes the pellet was resuspended in 50 µl protein loading dye.

4.4.2 Protein gel

4.4.2.1 SDS-PAGE

Samples to be analyzed on protein gel were mixed with 3x protein loading dye. Before loading on gel, they were heated at 99°C for 5 minutes, then spun at 14000 rpm for 5 minutes. For western blot small, 8.5 cm x 6 cm SDS polyacrylamide gels (SDS-PAGE) were used, for analysis of the elutions of ribosome purifications large 16 cm x 20 cm SDS-PAGE were used. All gels were run in Laemmli buffer. The composition of the gel is described in paragraph 4.6. Small gels were run at 120 V, large gels at 200 V. Proteins were stained using Coomassie staining followed by destaining in 20% ethanol 10% acetic acid, or by silver staining using a SilverQuest kit (Invitrogen LC6070) following the manufacturer's instructions.

4.4.2.2 Mass spectrometry

Bands cut from the silver stained gels depicted in Figures 41 and 42 were analyzed by mass spectrometry. Bands were destained by incubating them for 15 minutes in a 1:1 mixture of solutions A and B from the SilverQuest kit, while shaking at 14000 rpm. The mixture was removed, then 200 µl H_2O was added followed by shaking during 10 minutes. H_2O was removed and the bands were incubed with 200 µl acetonitril while shaking for 20 minutes. The bands were analyzed by nanoLC-MS/MS at the Proteomics platform at the IGBMC.

4.4.2.3 Western analysis

Proteins were transferred from SDS-PAGE to a Protran nitrocellulose membrane (Whatman 10401180) in a wet/tank electroblotting system in transfer buffer at 100 V during 1 hour at 4°C. The membrane was washed in water and blocked in 5% milk in PBS-Tween. It was then

incubated with a primary antibody in 5% milk-PBS-Tween for 1 hour at room temperature or over night at 4 °C. Following 4 washes (1 quick, 3 x 10 minutes) in PBS-Tween the membrane was incubated with a secondary antibody for 1 hour at room temperature. After 4 additional washes as above, the membrane was incubated with ECL (GE Healthcare), Luminata Crescendo (Millipore) or SuperSignal West Femto (Thermo Scientific) chemiluminescent reagent. Signals were visualized using a Image Quant LAS 4000 (GE Healthcare Life Sciences). All antibodies used are listed in Table 5.

Table 5 Antibodies used for western analysis

Name	Against	Source	Concentration
AbBS6	Rpl1A	Rabbit, polyclonal	1 : 10000
AbBS8	Stm1	Rabbit, polyclonal	1 : 2000
HA.11 Clone 16B12 Monoclonal Antibody, Purified	HA-tag	Mouse, monoclonal Covance MMS-101P	1 :1000
Goat anti-Rabbit IgG (H+L) Secondary Antibody, HRP conjugate	rabbit IgG + IgM secondary antibody	polyclonal Pierce 31460	1 : 10000
Peroxidase-AffiniPure Goat Anti-Mouse IgG + IgM (H+L)	mouse IgG + IgM secondary antibody	Jackson 115-035-068	1 :5000
Peroxidase anti-peroxidase	binds to protein A	Sigma P1291	3:10000

4.4.3 Purification of ribosomes by TAP method

The protocol that will be described here was used for purification of wild type ribosomes. For purification of mutant tagged ribosomes all quantities were doubled. Yeast was grown in 2 liter cultures in CSM-Trp-Ura synthetic defined medium containing 2% galactose, to OD_{600} 0.8-1.0. Cells were pelleted at 4000 x g for 20 minutes at 4°C, resuspended in 20 ml H_2O, transferred to a 50 ml falcon tube and pelleted at 4500 x g for 15 minutes at 4°C. The pellet was weighed and frozen in liquid nitrogen. All of the following steps were performed at 4°C unless otherwise indicated. The following day cells were thawed and resuspended in 1.6 ml of buffer A per gram of cell pellet, then transferred to round bottomed 35 ml tubes containing 3 g glass beads per gram of cell pellet. Cells were lysed by 5 cycles of 1 minute vortexing / 1 minute on ice. Beads were pelleted at 4343 x g for 6 minutes at 4°C and supernatant was further cleared at 30883 x g for 30 minutes at 4 °C. To the supernatant 50 µl 2 M Tris pH8.0, 200 µl NaCl 5 M and 100 µl 10% Igepal were added and it was then rotated with 200 µl IgG Sepharose (GE Healthcare), prewashed with 5 ml buffer IPP100, in a closed 10 ml column for

2 hours. The column was drained by gravity flow, then washed with 30 ml IPP100 and 10 ml TEV cleavage buffer. The IgG sepharose was incubated with 100 U TEV enzyme (Invitrogen 12575-015) in 1 ml TEV cleavage buffer for 2 hours at 16°C in a closed column. Eluate was collected, the dead volume was eluted by another 200 µl TEV cleavage buffer. To the eluate 3 volumes of IPP100 calmodulin binding buffer and 0.0030 volumes of 1 M $CaCl_2$ were added. It was then rotated with 200 µl calmodulin affinity resin (Agilent 214303), prewashed with 5 ml buffer IPP100 calmodulin binding buffer, in a closed 10 ml column for 1 hour. The column was drained by gravity flow and washed with 30 ml IPP100 calmodulin binding buffer. Proteins were eluted by adding 200 µl calmodulin elution buffer to the resin, this was repeated 5 times. To verify if any protein was left bound to the IgG sepharose or calmodulin affinity resin, additional elutions were performed using 200 µl 1% SDS. Protein loading dye (3x) was added to samples taken from cleared lysate, resuspended pellet, flow through, both washes and all elutions. Equal fractions of all stages were analyzed by western blot. The final elutions were concentrated by lyophilization and analyzed on a large SDS-PAGE.

4.4.4 Purification of recombinant factors

Hbs1 containing a C-terminal 6His-tag was expressed from plasmid pBS3410 in BL21 CodonPlus-RIL. It was also co-expressed with Dom34 containing a C-terminal strep-tag (expressed from plasmid pBS3438) in BL21 (DE3). Bacteria were grown in 500 ml autoinduction medium at 37°C to OD_{600} 0.5, were then transferred to 25°C and grown further over night. Cells were pelleted at 4000 x g for 10 minutes at 4°C, resuspended in 40 ml H_2O, transferred to a 50 ml falcon tube and pelleted at 4500 x g for 8 minutes at 4°C. All of the following steps were performed at 4°C or on ice.

4.4.4.1 His-purification

Cells were resuspended in 20 ml lysis buffer H and disrupted in a Cell Disruptor (Constant Systems) at 1.55 kbar, followed by rinsing with 10 ml buffer W. The resulting 30 ml cell lysates were cleared at 12000 rpm 30 min 4 °C. The supernatant was passed through a 0.20 µm filter and rotated with 400 µl Ni-NTA agarose (Qiagen), prewashed 3x in lysis buffer H, in a 50 ml falcon tube for 1 hour at 4°C. Then the lysate and agarose were transferred to a 10 ml column which was drained by gravity flow. The column was washed with 10 ml wash buffer H. The agarose was then incubated for 5 minutes with elution buffer H, then elution fraction 1 was collected. This was repeated to collect elution fraction 2. The elution fractions

were pooled and injected into a Superdex 75 10/300 GL column (GE Healthcare) and eluted with 1 column volume buffer SE. The resulting 500 µl elution fractions were analyzed by SDS-PAGE. Fractions containing Hbs1 were pooled and further concentrated using an Amicon Ultra-4 50K centrifugal filter.

4.4.4.2 Strep purification

Strep purification on bacteria co-expressing Dom34 and Hbs1 was performed basically as in paragraph 4.4.4.1, but with different resin and buffers. The proteins were purified on streptactin sepharose (IBA 2-1201) on a 10 ml column to which the lysate was gradually applied, without incubation in a closed column. Cells were lysed and the column was washed in buffer W (IBA 2-1003) and protein was eluted with buffer E (IBA 2-1000). After further purification by gel filtration, the protein complex was concentrated using an Amicon Ultra-0.5 ml 50 centrifugal filter.

4.4.5 Yeast two hybrid analysis

Two-hybrid Dom34 and Hbs1 (wild type and mutant) constructs were prepared as described before (Carr-Schmid et al, 2002), except that Dom34 was cloned into pAS2 and Hbs1 into pACTII. Y190 containing these plasmids was grown to mid-log phase, 750 µl was pelleted, resuspended in 500 µl buffer Z and 200 µl water saturated ether, spun for 1 minute, left to let ether evaporate for 10 min and incubated at 30°C for 5 minutes. Then 100 µl ONPG (4mg/ml in buffer Z) was added and the reactions were incubated at 30 °C untill their colour changed into bright yellow. The reaction was then stopped by addition of 250 µl 1M Na_2CO_3, reactions were spun for 5 minutes and OD_{420} was measured. The following formula was used to calculate ß-galactosidase activity:

Activity = 1000 x OD420 / (OD600 x culture volume x reaction time).

4.5 STUDYING TRANSLATION

4.5.1 Polysome analysis

100 ml yeast cultures grown to OD_{600} ~ 0.8, or yeast exposed to glucose depletion and readdition (see paragraph 4.2.1) were pelleted at 5400 x g for 6 minutes at 4°C immediately after cycloheximide addition (100 µg/ml final concentration). At 4°C, cells were washed in 10 ml polysome lysis buffer (PLB), pelleted at 5400 x g for 6 minutes, transferred to 15 ml corex tubes in 3 ml PLB, pelleted at 4343 x g for 6 minutes and resuspended in 500 µl PLB or PLB containing 400 mM KCl (manuscript, Figure 4B). 450 µl cold glass beads were added and cells were lysed at 4°C by 5 cycles of 1 minute vortexing followed by 1 minute on ice. Glass beads were pelleted at 4343 x g for 6 minutes at 4°C and the supernatant was transferred to eppendorfs and cleared in two centrifugation steps at 14000 rpm for 10 minutes at 4°C. OD_{260} was measured by nanodrop and 9 OD_{260} units of lysate were loaded on a 7-47% sucrose gradient in PLB, or PLB containing 400 mM KCl. After a 14 h spin at 16.9 krpm in an SW41 rotor (Beckman Coulter), absorbance (254 nm) was measured and 1 ml fractions were collected on a ISCO Teledyne Foxy Jr. fraction collector. From each fraction, a 40 µl sample was taken for protein analysis, to which 20 µl 3x loading dye was added. 5 µl of each fraction was used for western analysis. From each fraction, a 500 µl sample was taken for RNA analysis. The sample was stored at -20°C after addition of 1.5 ml ethanol. After pelleting at 14000 rpm for 25 minutes at 4°C, RNA was extracted by two subsequent PCI extractions, followed by ethanol precipation. RNA was resuspended in 20 µl H_2O and 5 µl was used for northern analysis.

4.5.2 In vitro ribosome dissociation

80S ribosomes purified from glucose-depleted yeast were kindly provided by S. Melnikov and Dr. Marat Yusupov and were purified as described in (Ben-Shem et al, 2011). 100 pmol ribosomes were ^{32}P-labeled using 500 U casein kinase II (NEB) and ^{32}P γ-ATP in the manufacturer's recommended buffer, then pelleted through a 600 µl 1.1 M sucrose cushion in buffer E at 75000 rpm for 1 hour at 4°C in a MLA-130 rotor followed by resuspension in buffer E. 6,25 pmol ribosomes were incubated in 25 µl buffer E containing 1 mM GTP or GDPNP and 1 mM ATP at 26°C for 15 minutes with 50 pmol Dom34, 50 pmol Hbs1, 50 pmol Rli1 and 625 pmol Tif6, all purified by C. Shoemaker (Shoemaker et al, 2010; Shoemaker & Green, 2011). Dissociation was analyzed by centrifugation through a 10-30%

sucrose gradient in buffer E at 38500 rpm for 3.5 hours at 4°C in a SW41 rotor. Fractions were counted in Bio Safe II scintillation fluid.

4.5.3 ^{35}S-methionine incorporation

Yeast was grown in CSM-Met containing 2% glucoseto OD_{600} 0.6, shifted to 16°C for 2 hours, split into 8 ml cultures and resuspended in 8 ml CSM-Met with or without 2% glucose for 10 minutes comparable to what is described in paragraph 4.2.1. Then cells were resuspended in 8 ml CSM-Met 2% glucose (16°C) containing 4 µl ^{35}S-Methionine (1175 Ci/mmol, 5 mCi/0,49 ml, Perkin Elmer) and incubated at 16°C. At the indicated time points 1 ml samples were taken and ^{35}S-Methionine incorporation was measured basically as described (Ashe et al, 2000). The 1 ml sample was added to 1 ml 20% trichloroacetic acid in a 50 ml falcon tube on ice, incubated at 95°C for 20 minutes and put back on ice. The precipitate was collected on 2.4 cm glass microfiber filter GF/C (Whatman 1822 024), using a holder for the filter on top of a vacuum flask. The filters were then washed with 10 ml 10% trichloroacetic acid and 10 ml ethanol, dried on air and counted in a scintillation counter in Ready Safe scintillation fluid (Beckman 141349).

4.5.4 *In vitro* translation

4.5.4.1 Preparation yeast extract

Translational extracts were prepared essentially as described (Tuite & Plesset, 1986). 4 l of culture at OD_{600} 1 was washed in 200 ml cold water, incubated in 100 ml β-mercaptoethanol 10mM; EDTA 2 mM for 30 minutes at room temperature, washed in 100 ml cold sorbitol 1M and resuspended in 1M sorbitol at room temperature at a concentration of 10 ml/g cells, spinning at 2000 x g for 5 minutes at 4°C in between. Zymolyase (Nacalai Tesque 07665-55) was added at 4 µg/ml final concentration. Spheroplast conversion was followed by comparing the OD_{600} of 15 µl yeast resuspended in 1 ml 1% SDS to that of 15 µl yeast resuspended in 1 ml 1 M sorbitol. The reaction was stopped by pelleting the resulting spheroplast at 1000 x g for 10 minutes at room temperature when 75% of cells had converted to spheroplasts. Spheroplasts were washed in 200 ml sorbitol 1.2 M and incubated in 500 ml YPDA-sorbitol 1M at 25°C 40 rpm. Spheroplasts were harvested at 1000 x g for 10 minutes at 4°C and lysed using glass beads (0.5 ml/g cells) in lysis buffer T (1 ml/g cells) in 5 cycles of shaking vigorously at 2 Hz for 20 seconds with 1 minute intervals on ice. Lysates were cleared

spinning at 30 000 x g for 15 minutes at 4°C, then 100 000 x g for 30 minutes at 4°C. Glycerol was added at 10% final concentration for storage at -80°C.

4.5.4.2 *In vitro* transcription

Before *in vitro* transcription, a plasmid was cleaved at a site immediately downstream of the sequence to be transcribed, to allow termination of transcription. 10 µg pT7-Luc-A50 was digested by 50 U DraI (New England Biolabs) in a 500 µl reaction in the recommended buffer at 37°C for 90 minutes. 6.5 µg pBS4612 and pBS4613 were digested by 32.5 U BsmBI (New England Biolabs) in a 325 µl reaction in the recommended buffer at 55°C for 90 minutes. The digested plasmids were PCI extracted, ethanol precipitated and dissolved in H_2O. In vitro transcription was performed using the mMessage mMachine T7 kit (Ambion M1344), following the manufacturer's instructions, to generate capped mRNAs. DNA was removed using TURBO DNase, following the kit's instructions, and mRNAs were PCI extracted, ethanol precipitated and dissolved in H_2O.

4.5.4.3 *In vitro* translation

In vitro translation was performed basically as described in (Tarun & Sachs, 1995). Translational extracts were incubated with 1500 gel units/ml (corresponds to approximately 150 Kunitz units/ml) micrococcal nuclease (New England Biolabs M0247) in presence of 480 µM $CaCl_2$ for the indicated time at 26°C. The reaction was stopped by adding 2 mM EGTA on ice. 7.5 µl extract was added to a 7.5 µl mix containing 0,1 µl RNasin (Promega N2515), 1 µl mRNA (500 ng firefly luciferase-A(50) mRNA (Gallie et al, 1991) or other mRNA at the indicated quantity), 1 µl 4 mg/ml creatine phosphokinase (Roche 10127566001), 5 µl 3x translation buffer and 0.4 µl H_2O. After 1 hour incubation at 26°C, luciferase activity was measured in 10 second measurements using a Lumat LB 9507 luminometer (Berthold technologies) adding 1 µl translation reaction to 50 µl luciferine mix. Alternatively, after an indicated time of translation protein content and RNA content in the translation reactions was analyzed. Translation reactions of which RNA was analyzed were stopped by addition of 15 µl 2% SDS and transfer on ice. RNA was extracted after diluting the sample in H_2O to 500 µl final volume, by PCI extraction and ethanol precipitation. RNA was dissolved in 40 µl H_2O, 5 µl of each reaction was analyzed by northern blot. Translation reactions of which protein was analyzed were stopped by addition of 7.5 µl 3x loading dye. 4µl of each reaction was analyzed by western blot.

4.6 LIST OF BUFFERS

Table 6 List of buffers

Buffer	Composition
Buffer A (ribosome purification)	10 mM Hepes-KOH pH 7.9; 10 mM KCl; 10 mM $MgCl_2$; 0.5 mM DTT; 0.5 mM PMSF; 2 mM benzamidine; 1 mM leupeptin; 2 mM pepstatin A; 4 mM chymostatin; 2.6 mM Aprotinin; 0.040 U RNasin
Buffer E	20 mM Tris-Cl pH 7.5; 2.5 mM $Mg(OAc)_2$; 100 mM KOAc pH7.6; 2 mM DTT; 0.25 mM spermidine
Buffer SE	20 mM Tris pH 7.5 ; 200 mM NaCl ; 5 mM β-mercaptoethanol ; 5% glycerol
Buffer Z	60mM Na_2HPO_4,; 40 mM NaH_2PO_4; 10 mM KCl, 1 mM $MgCl_2$; 50 mM β-mercaptoethanol
Coomassie staining	1 g/l Coomassie R-250; 45% ethanol; 10% acetic acid
Elution buffer H	50 mM Hepes-KOH pH 7.9; 500 mM NaCl; 5 mM β-mercaptoethanol; 300 mM imidazole; 10% glycerol; 2 mM $MgCl_2$
IPP100	10 mM Tris-Cl pH8.0; 100 mM NaCl; 10 mM $MgCl_2$; 0.1% Igepal
IPP100 calmodulin binding buffer	10 mM β-mercaptoethanol; 10 mM Tris-Cl pH8.0; 100 mM NaCl; 10 mM $MgCl_2$; 1 mM Mg-acetate; 1 mM imidazole; 2 mM $CaCl_2$; 0.1% igepal
IPP100 calmodulin elution buffer	10 mM β-mercaptoethanol; 10 mM Tris-Cl pH8.0; 100 mM NaCl; 10 mM $MgCl_2$; 1 mM Mg-acetate; 1 mM imidazole; 2 mM EGTA; 0.1% igepal
Laemmli buffer	0.10 % SDS; 1.44% glycine; 0.30 % Tris base
LiT	10 mM Tris pH 7.5; 100 mM LiOAc
Luciferine mix	470 µM luciferine; 530 µM ATP; 270 µM coenzyme A; 20 mM Tris-phosphate pH 7.8; 1.07 mM $MgCl_2$; 2.7 mM $MgSO_4$; 100 µM EDTA; 33.3 mM DTT
Lysis buffer H	75 mM Hepes-KOH pH 7.9; 300 mM NaCl; 5 mM β-mercaptoethanol; 1% Tween 20; 20 mM imidazole; 10% glycerol; 2 mM $MgCl_2$
Lysis buffer T	20 mM Hepes-KOH pH7.4; 100 mM KOAc; 2 mM $Mg(OAC)_2$; 2 mM DTT; 0.5 mM PMSF; protease inhibitor cocktail
Loading dye 3x (protein gel)	0.05% bromophenol blue; 50 mM Tris pH 6.8; 10% glycerol; 2% SDS
MOPS buffer	0.10 M MOPS; 40 mM NaAc; 5.0 mM EDTA; pH 7
PBS-Tween	PBS; 0.2% Tween 20
Polyacrylamide gel (RNA)	6.0% polyacrylamide; 8.0 M urea; 1x TBE; 0.060% ammonium persulfate; 0. 10% N,N,N',N'-Tetramethyl-ethylenediamine
Polysome lysis buffer	10 mM Tris-Cl pH 7.5; 100 mM KCl; 5.0 mM $MgCl_2$; 6.0 mM β-mercaptoethanol; 100 µg/ml cycloheximide
RNA loading dye (agarose gel)	0.25% bromophenol blue; 0.25% xylene cyanol; 50% glycerol; 1.0 mM EDTA
RNA loading dye (polyacrylamide gel)	bromophenol blue; xylene cyanol; 95% formamide; 18 mM EDTA; 0.025% SDS
SDS-PAGE	% acrylamide: bis acrylamide 37,5 :1 as indicated ; 378 mM Tris pH 8.8 ; 0.1% SDS ; 0.1% ammonium persulfate ; 0.1% N,N,N',N'-Tetramethyl-ethylenediamine
Sorensen's phosphate buffer (20x)	0.20 M Na2HPO4; 0.80 M KH2PO4; pH 6.25
Stacking gel	5% acrylamide: bis acrylamide 37,5 :1 ; 126 mM Tris pH 6.8 ; 0.1% SDS ; 0.1% ammonium persulfate ; 0.1% N,N,N',N'-Tetramethyl-ethylenediamine
TA	40 mM Tris base; 1.14% acetic acid
TBE	8.9 mM Tris base; 8.9 mM boric acid; 2.0 mM EDTA
TES buffer	10 mM Tris pH 7.5; 10 mM EDTA; 0.50% SDS

TEV cleavage buffer	10 mM Tris-Cl pH8.0; 100 mM NaCl; 10 mM $MgCl_2$; 0.1% Igepal; 0.5 mM EDTA; 1 mM DTT
Transfer buffer (western)	3 g/l Tris base; 3 g/l glycine; 0.05% SDS; 20% ethanol
Translation buffer	22 mM Hepes-KOH pH 7.4; 120 mM KOAc; 2 mM MgOAc; 750 µM ATP; 100 µM GTP; 25 mM creatine phosphate; 40 µM amino acid mixture (Promega L4461); 1.7 mM DTT
Wash buffer H	50 mM Hepes-KOH pH 7.9; 500 mM NaCl; 5 mM β-mercaptoethanol; 20 mM imidazole; 10% glycerol; 2 mM $MgCl_2$
Yeast lysis buffer for DNA purification	10 mM Tris pH 7.5; 1 mM EDTA; 3.0% SDS

REFERENCES

Abdulrehman D, Monteiro PT, Teixeira MC, Mira NP, Lourenco AB, dos Santos SC, Cabrito TR, Francisco AP, Madeira SC, Aires RS, Oliveira AL, Sa-Correia I, Freitas AT (2011) YEASTRACT: providing a programmatic access to curated transcriptional regulatory associations in Saccharomyces cerevisiae through a web services interface. *Nucleic Acids Res* **39**(Database issue)**:** D136-140

Adham IM, Sallam MA, Steding G, Korabiowska M, Brinck U, Hoyer-Fender S, Oh C, Engel W (2003) Disruption of the pelota gene causes early embryonic lethality and defects in cell cycle progression. *Mol Cell Biol* **23**(4)**:** 1470-1476

Agafonov DE, Kolb VA, Nazimov IV, Spirin AS (1999) A protein residing at the subunit interface of the bacterial ribosome. *Proc Natl Acad Sci U S A* **96**(22)**:** 12345-12349

Aitken CE, Lorsch JR (2012) A mechanistic overview of translation initiation in eukaryotes. *Nat Struct Mol Biol* **19**(6)**:** 568-576

Akimitsu N, Tanaka J, Pelletier J (2007) Translation of nonSTOP mRNA is repressed post-initiation in mammalian cells. *EMBO J* **26**(9)**:** 2327-2338

Alberts B, Johnson A, Lewis J, Raff M, Roberts K, Walter P (2008) *Molecular Biology of the Cell: Reference Edition*, 5 edn. New York: Garland Science.

Albuquerque CP, Smolka MB, Payne SH, Bafna V, Eng J, Zhou H (2008) A multidimensional chromatography technology for in-depth phosphoproteome analysis. *Mol Cell Proteomics* **7**(7)**:** 1389-1396

Alkalaeva EZ, Pisarev AV, Frolova LY, Kisselev LL, Pestova TV (2006) In vitro reconstitution of eukaryotic translation reveals cooperativity between release factors eRF1 and eRF3. *Cell* **125**(6)**:** 1125-1136

Andersen DS, Leevers SJ (2007) The essential Drosophila ATP-binding cassette domain protein, pixie, binds the 40 S ribosome in an ATP-dependent manner and is required for translation initiation. *J Biol Chem* **282**(20)**:** 14752-14760

Anderson JS, Parker RP (1998) The 3' to 5' degradation of yeast mRNAs is a general mechanism for mRNA turnover that requires the SKI2 DEVH box protein and 3' to 5' exonucleases of the exosome complex. *EMBO J* **17**(5)**:** 1497-1506

Anderson P, Kedersha N (2008) Stress granules: the Tao of RNA triage. *Trends Biochem Sci* **33**(3)**:** 141-150

Anger AM, Armache JP, Berninghausen O, Habeck M, Subklewe M, Wilson DN, Beckmann R (2013) Structures of the human and Drosophila 80S ribosome. *Nature* **497**(7447)**:** 80-85

Araki Y, Takahashi S, Kobayashi T, Kajiho H, Hoshino S, Katada T (2001) Ski7p G protein interacts with the exosome and the Ski complex for 3'-to-5' mRNA decay in yeast. *EMBO J* **20**(17)**:** 4684-4693

Arribere JA, Doudna JA, Gilbert WV (2011) Reconsidering movement of eukaryotic mRNAs between polysomes and P bodies. *Mol Cell* **44**(5)**:** 745-758

Asano K, Clayton J, Shalev A, Hinnebusch AG (2000) A multifactor complex of eukaryotic initiation factors, eIF1, eIF2, eIF3, eIF5, and initiator tRNA(Met) is an important translation initiation intermediate in vivo. *Genes Dev* **14**(19)**:** 2534-2546

Ashe MP, De Long SK, Sachs AB (2000) Glucose depletion rapidly inhibits translation initiation in yeast. *Mol Biol Cell* **11**(3)**:** 833-848

Ashe MP, Slaven JW, De Long SK, Ibrahimo S, Sachs AB (2001) A novel eIF2B-dependent mechanism of translational control in yeast as a response to fusel alcohols. *EMBO J* **20**(22)**:** 6464-6474

Atkinson GC, Baldauf SL, Hauryliuk V (2008) Evolution of nonstop, no-go and nonsense-mediated mRNA decay and their termination factor-derived components. *BMC Evol Biol* **8:** 290

Balagopal V, Parker R (2011) Stm1 modulates translation after 80S formation in Saccharomyces cerevisiae. *RNA* **17**(5)**:** 835-842

Barthelme D, Dinkelaker S, Albers SV, Londei P, Ermler U, Tampe R (2011) Ribosome recycling depends on a mechanistic link between the FeS cluster domain and a conformational switch of the twin-ATPase ABCE1. *Proc Natl Acad Sci U S A* **108**(8)**:** 3228-3233

Barthelme D, Scheele U, Dinkelaker S, Janoschka A, Macmillan F, Albers SV, Driessen AJ, Stagni MS, Bill E, Meyer-Klaucke W, Schunemann V, Tampe R (2007) Structural organization of essential iron-sulfur clusters in the evolutionarily highly conserved ATP-binding cassette protein ABCE1. *J Biol Chem* **282**(19)**:** 14598-14607

Baudin-Baillieu A, Guillemet E, Cullin C, Lacroute F (1997) Construction of a yeast strain deleted for the TRP1 promoter and coding region that enhances the efficiency of the polymerase chain reaction-disruption method. *Yeast* **13**(4)**:** 353-356

Becker T, Armache JP, Jarasch A, Anger AM, Villa E, Sieber H, Motaal BA, Mielke T, Berninghausen O, Beckmann R (2011) Structure of the no-go mRNA decay complex Dom34-Hbs1 bound to a stalled 80S ribosome. *Nat Struct Mol Biol* **18**(6)**:** 715-720

Becker T, Franckenberg S, Wickles S, Shoemaker CJ, Anger AM, Armache JP, Sieber H, Ungewickell C, Berninghausen O, Daberkow I, Karcher A, Thomm M, Hopfner KP, Green R, Beckmann R (2012) Structural basis of highly conserved ribosome recycling in eukaryotes and archaea. *Nature* **482**(7386)**:** 501-506

Ben-Shem A, Garreau de Loubresse N, Melnikov S, Jenner L, Yusupova G, Yusupov M (2011) The structure of the eukaryotic ribosome at 3.0 A resolution. *Science* **334**(6062)**:** 1524-1529

Ben-Shem A, Jenner L, Yusupova G, Yusupov M (2010) Crystal structure of the eukaryotic ribosome. *Science* **330**(6008)**:** 1203-1209

Bengtson MH, Joazeiro CA (2010) Role of a ribosome-associated E3 ubiquitin ligase in protein quality control. *Nature* **467**(7314)**:** 470-473

Bhattacharya A, McIntosh KB, Willis IM, Warner JR (2010) Why Dom34 stimulates growth of cells with defects of 40S ribosomal subunit biosynthesis. *Mol Cell Biol* **30**(23)**:** 5562-5571

Bleichert F, Granneman S, Osheim YN, Beyer AL, Baserga SJ (2006) The PINc domain protein Utp24, a putative nuclease, is required for the early cleavage steps in 18S rRNA maturation. *Proc Natl Acad Sci U S A* **103**(25)**:** 9464-9469

Boeck R, Tarun S, Jr., Rieger M, Deardorff JA, Muller-Auer S, Sachs AB (1996) The yeast Pan2 protein is required for poly(A)-binding protein-stimulated poly(A)-nuclease activity. *J Biol Chem* **271**(1)**:** 432-438

Bonneau F, Basquin J, Ebert J, Lorentzen E, Conti E (2009) The yeast exosome functions as a macromolecular cage to channel RNA substrates for degradation. *Cell* **139**(3)**:** 547-559

Bonneaud N, Ozier-Kalogeropoulos O, Li GY, Labouesse M, Minvielle-Sebastia L, Lacroute F (1991) A family of low and high copy replicative, integrative and single-stranded S. cerevisiae/E. coli shuttle vectors. *Yeast* **7**(6)**:** 609-615

Borja MS, Piotukh K, Freund C, Gross JD (2011) Dcp1 links coactivators of mRNA decapping to Dcp2 by proline recognition. *RNA* **17**(2)**:** 278-290

Brandman O, Stewart-Ornstein J, Wong D, Larson A, Williams CC, Li GW, Zhou S, King D, Shen PS, Weibezahn J, Dunn JG, Rouskin S, Inada T, Frost A, Weissman JS (2012) A ribosome-bound quality control complex triggers degradation of nascent peptides and signals translation stress. *Cell* **151**(5)**:** 1042-1054

Braunstein S, Badura ML, Xi Q, Formenti SC, Schneider RJ (2009) Regulation of protein synthesis by ionizing radiation. *Mol Cell Biol* **29**(21)**:** 5645-5656

Brengues M, Teixeira D, Parker R (2005) Movement of eukaryotic mRNAs between polysomes and cytoplasmic processing bodies. *Science* **310**(5747)**:** 486-489

Brown CE, Sachs AB (1998) Poly(A) tail length control in Saccharomyces cerevisiae occurs by message-specific deadenylation. *Mol Cell Biol* **18**(11)**:** 6548-6559

Brown JT, Bai X, Johnson AW (2000) The yeast antiviral proteins Ski2p, Ski3p, and Ski8p exist as a complex in vivo. *RNA* **6**(3)**:** 449-457

Buchan JR, Muhlrad D, Parker R (2008) P bodies promote stress granule assembly in Saccharomyces cerevisiae. *J Cell Biol* **183**(3)**:** 441-455

Burnicka-Turek O, Kata A, Buyandelger B, Ebermann L, Kramann N, Burfeind P, Hoyer-Fender S, Engel W, Adham IM (2010) Pelota interacts with HAX1, EIF3G and SRPX and the resulting protein complexes are associated with the actin cytoskeleton. *BMC Cell Biol* **11:** 28

Carr-Schmid A, Pfund C, Craig EA, Kinzy TG (2002) Novel G-protein complex whose requirement is linked to the translational status of the cell. *Mol Cell Biol* **22**(8)**:** 2564-2574

Castelli LM, Lui J, Campbell SG, Rowe W, Zeef LA, Holmes LE, Hoyle NP, Bone J, Selley JN, Sims PF, Ashe MP (2011) Glucose depletion inhibits translation initiation via eIF4A loss and subsequent 48S preinitiation complex accumulation, while the pentose phosphate pathway is coordinately up-regulated. *Mol Biol Cell* **22**(18)**:** 3379-3393

Charneski CA, Hurst LD (2013) Positively charged residues are the major determinants of ribosomal velocity. *PLoS Biol* **11**(3)**:** e1001508

Chatr-Aryamontri A, Angelini M, Garelli E, Tchernia G, Ramenghi U, Dianzani I, Loreni F (2004) Nonsense-mediated and nonstop decay of ribosomal protein S19 mRNA in Diamond-Blackfan anemia. *Hum Mutat* **24**(6)**:** 526-533

Chavatte L, Seit-Nebi A, Dubovaya V, Favre A (2002) The invariant uridine of stop codons contacts the conserved NIKSR loop of human eRF1 in the ribosome. *EMBO J* **21**(19)**:** 5302-5311

Chen L, Muhlrad D, Hauryliuk V, Cheng Z, Lim MK, Shyp V, Parker R, Song H (2010) Structure of the Dom34-Hbs1 complex and implications for no-go decay. *Nat Struct Mol Biol* **17**(10)**:** 1233-1240

Chen ZQ, Dong J, Ishimura A, Daar I, Hinnebusch AG, Dean M (2006) The essential vertebrate ABCE1 protein interacts with eukaryotic initiation factors. *J Biol Chem* **281**(11)**:** 7452-7457

Cheng Z, Saito K, Pisarev AV, Wada M, Pisareva VP, Pestova TV, Gajda M, Round A, Kong C, Lim M, Nakamura Y, Svergun DI, Ito K, Song H (2009) Structural insights into eRF3 and stop codon recognition by eRF1. *Genes Dev* **23**(9)**:** 1106-1118

Cipollina C, van den Brink J, Daran-Lapujade P, Pronk JT, Vai M, de Winde JH (2008) Revisiting the role of yeast Sfp1 in ribosome biogenesis and cell size control: a chemostat study. *Microbiology* **154**(Pt 1)**:** 337-346
Cole SE, LaRiviere FJ, Merrikh CN, Moore MJ (2009) A convergence of rRNA and mRNA quality control pathways revealed by mechanistic analysis of nonfunctional rRNA decay. *Mol Cell* **34**(4)**:** 440-450
Coller J, Parker R (2005) General translational repression by activators of mRNA decapping. *Cell* **122**(6)**:** 875-886
Collinet B, Friberg A, Brooks MA, van den Elzen T, Henriot V, Dziembowski A, Graille M, Durand D, Leulliot N, Saint Andre C, Lazar N, Sattler M, Seraphin B, van Tilbeurgh H (2011) Strategies for the structural analysis of multi-protein complexes: lessons from the 3D-Repertoire project. *J Struct Biol* **175**(2)**:** 147-158
Connolly E, Braunstein S, Formenti S, Schneider RJ (2006) Hypoxia inhibits protein synthesis through a 4E-BP1 and elongation factor 2 kinase pathway controlled by mTOR and uncoupled in breast cancer cells. *Mol Cell Biol* **26**(10)**:** 3955-3965
Correia H, Medina R, Hernandez A, Bustamante E, Chakraburtty K, Herrera F (2004) Similarity between the association factor of ribosomal subunits and the protein Stm1p from Saccharomyces cerevisiae. *Mem Inst Oswaldo Cruz* **99**(7)**:** 733-737
Cougot N, Babajko S, Seraphin B (2004) Cytoplasmic foci are sites of mRNA decay in human cells. *J Cell Biol* **165**(1)**:** 31-40
Daugeron MC, Mauxion F, Seraphin B (2001) The yeast POP2 gene encodes a nuclease involved in mRNA deadenylation. *Nucleic Acids Res* **29**(12)**:** 2448-2455
Davis L, Engebrecht J (1998) Yeast dom34 mutants are defective in multiple developmental pathways and exhibit decreased levels of polyribosomes. *Genetics* **149**(1)**:** 45-56
De Filippi L, Fournier M, Cameroni E, Linder P, De Virgilio C, Foti M, Deloche O (2007) Membrane stress is coupled to a rapid translational control of gene expression in chlorpromazine-treated cells. *Curr Genet* **52**(3-4)**:** 171-185
Defenouillere Q, Yao Y, Mouaikel J, Namane A, Galopier A, Decourty L, Doyen A, Malabat C, Saveanu C, Jacquier A, Fromont-Racine M (2013) Cdc48-associated complex bound to 60S particles is required for the clearance of aberrant translation products. *Proc Natl Acad Sci U S A* **110**(13)**:** 5046-5051
Demeshkina N, Jenner L, Westhof E, Yusupov M, Yusupova G (2012) A new understanding of the decoding principle on the ribosome. *Nature* **484**(7393)**:** 256-259
Deng J, Harding HP, Raught B, Gingras AC, Berlanga JJ, Scheuner D, Kaufman RJ, Ron D, Sonenberg N (2002) Activation of GCN2 in UV-irradiated cells inhibits translation. *Curr Biol* **12**(15)**:** 1279-1286
Dever TE, Feng L, Wek RC, Cigan AM, Donahue TF, Hinnebusch AG (1992) Phosphorylation of initiation factor 2 alpha by protein kinase GCN2 mediates gene-specific translational control of GCN4 in yeast. *Cell* **68**(3)**:** 585-596
Dimitrova LN, Kuroha K, Tatematsu T, Inada T (2009) Nascent peptide-dependent translation arrest leads to Not4p-mediated protein degradation by the proteasome. *J Biol Chem* **284**(16)**:** 10343-10352
Doma MK, Parker R (2006) Endonucleolytic cleavage of eukaryotic mRNAs with stalls in translation elongation. *Nature* **440**(7083)**:** 561-564
Dong J, Lai R, Nielsen K, Fekete CA, Qiu H, Hinnebusch AG (2004) The essential ATP-binding cassette protein RLI1 functions in translation by promoting preinitiation complex assembly. *J Biol Chem* **279**(40)**:** 42157-42168
Drazkowska K, Tomecki R, Stodus K, Kowalska K, Czarnocki-Cieciura M, Dziembowski A (2013) The RNA exosome complex central channel controls both exonuclease and endonuclease Dis3 activities in vivo and in vitro. *Nucleic Acids Res* **41**(6)**:** 3845-3858
Dziembowski A, Lorentzen E, Conti E, Seraphin B (2007) A single subunit, Dis3, is essentially responsible for yeast exosome core activity. *Nat Struct Mol Biol* **14**(1)**:** 15-22
Eberhart CG, Wasserman SA (1995) The pelota locus encodes a protein required for meiotic cell division: an analysis of G2/M arrest in Drosophila spermatogenesis. *Development* **121**(10)**:** 3477-3486
Eberle AB, Lykke-Andersen S, Muhlemann O, Jensen TH (2009) SMG6 promotes endonucleolytic cleavage of nonsense mRNA in human cells. *Nat Struct Mol Biol* **16**(1)**:** 49-55
Ebihara K, Nakamura Y (1999) C-terminal interaction of translational release factors eRF1 and eRF3 of fission yeast: G-domain uncoupled binding and the role of conserved amino acids. *RNA* **5**(6)**:** 739-750
Eulalio A, Behm-Ansmant I, Izaurralde E (2007) P bodies: at the crossroads of post-transcriptional pathways. *Nat Rev Mol Cell Biol* **8**(1)**:** 9-22
Finoux A. (2006) Etude des facteurs impliqués dans la dégradation des ARNm chez la levure *Saccharomyces cerevisiae* par fusion de domaines fonctionnels et études *in vitro*.
Fleischer TC, Weaver CM, McAfee KJ, Jennings JL, Link AJ (2006) Systematic identification and functional screens of uncharacterized proteins associated with eukaryotic ribosomal complexes. *Genes Dev* **20**(10)**:** 1294-1307

Frantz JD, Gilbert W (1995) A yeast gene product, G4p2, with a specific affinity for quadruplex nucleic acids. *J Biol Chem* **270**(16)**:** 9413-9419
Frischmeyer PA, van Hoof A, O'Donnell K, Guerrerio AL, Parker R, Dietz HC (2002) An mRNA surveillance mechanism that eliminates transcripts lacking termination codons. *Science* **295**(5563)**:** 2258-2261
Frolova L, Le Goff X, Zhouravleva G, Davydova E, Philippe M, Kisselev L (1996) Eukaryotic polypeptide chain release factor eRF3 is an eRF1- and ribosome-dependent guanosine triphosphatase. *RNA* **2**(4)**:** 334-341
Frolova L, Seit-Nebi A, Kisselev L (2002) Highly conserved NIKS tetrapeptide is functionally essential in eukaryotic translation termination factor eRF1. *RNA* **8**(2)**:** 129-136
Frolova LY, Tsivkovskii RY, Sivolobova GF, Oparina NY, Serpinsky OI, Blinov VM, Tatkov SI, Kisselev LL (1999) Mutations in the highly conserved GGQ motif of class 1 polypeptide release factors abolish ability of human eRF1 to trigger peptidyl-tRNA hydrolysis. *RNA* **5**(8)**:** 1014-1020
Fujii K, Kitabatake M, Sakata T, Miyata A, Ohno M (2009) A role for ubiquitin in the clearance of nonfunctional rRNAs. *Genes Dev* **23**(8)**:** 963-974
Fujii K, Kitabatake M, Sakata T, Ohno M (2012) 40S subunit dissociation and proteasome-dependent RNA degradation in nonfunctional 25S rRNA decay. *EMBO J* **31**(11)**:** 2579-2589
Gallie DR, Feder JN, Schimke RT, Walbot V (1991) Post-transcriptional regulation in higher eukaryotes: the role of the reporter gene in controlling expression. *Mol Gen Genet* **228**(1-2)**:** 258-264
Gandhi R, Manzoor M, Hudak KA (2008) Depurination of Brome mosaic virus RNA3 in vivo results in translation-dependent accelerated degradation of the viral RNA. *J Biol Chem* **283**(47)**:** 32218-32228
Gatfield D, Izaurralde E (2004) Nonsense-mediated messenger RNA decay is initiated by endonucleolytic cleavage in Drosophila. *Nature* **429**(6991)**:** 575-578
Gilbert WV, Zhou K, Butler TK, Doudna JA (2007) Cap-independent translation is required for starvation-induced differentiation in yeast. *Science* **317**(5842)**:** 1224-1227
Goossens A, Dever TE, Pascual-Ahuir A, Serrano R (2001) The protein kinase Gcn2p mediates sodium toxicity in yeast. *J Biol Chem* **276**(33)**:** 30753-30760
Graille M, Chaillet M, van Tilbeurgh H (2008) Structure of yeast Dom34: a protein related to translation termination factor Erf1 and involved in No-Go decay. *J Biol Chem* **283**(11)**:** 7145-7154
Graille M, Seraphin B (2012) Surveillance pathways rescuing eukaryotic ribosomes lost in translation. *Nat Rev Mol Cell Biol* **13**(11)**:** 727-735
Grousl T, Ivanov P, Frydlova I, Vasicova P, Janda F, Vojtova J, Malinska K, Malcova I, Novakova L, Janoskova D, Valasek L, Hasek J (2009) Robust heat shock induces eIF2alpha-phosphorylation-independent assembly of stress granules containing eIF3 and 40S ribosomal subunits in budding yeast, Saccharomyces cerevisiae. *J Cell Sci* **122**(Pt 12)**:** 2078-2088
Hamby SE, Thomas NS, Cooper DN, Chuzhanova N (2011) A meta-analysis of single base-pair substitutions in translational termination codons ('nonstop' mutations) that cause human inherited disease. *Hum Genomics* **5**(4)**:** 241-264
Harbison CT, Gordon DB, Lee TI, Rinaldi NJ, Macisaac KD, Danford TW, Hannett NM, Tagne JB, Reynolds DB, Yoo J, Jennings EG, Zeitlinger J, Pokholok DK, Kellis M, Rolfe PA, Takusagawa KT, Lander ES, Gifford DK, Fraenkel E, Young RA (2004) Transcriptional regulatory code of a eukaryotic genome. *Nature* **431**(7004)**:** 99-104
Harding HP, Novoa I, Zhang Y, Zeng H, Wek R, Schapira M, Ron D (2000) Regulated translation initiation controls stress-induced gene expression in mammalian cells. *Mol Cell* **6**(5)**:** 1099-1108
Hauryliuk V, Zavialov A, Kisselev L, Ehrenberg M (2006) Class-1 release factor eRF1 promotes GTP binding by class-2 release factor eRF3. *Biochimie* **88**(7)**:** 747-757
Hayashi N, Murakami S (2002) STM1, a gene which encodes a guanine quadruplex binding protein, interacts with CDC13 in Saccharomyces cerevisiae. *Mol Genet Genomics* **267**(6)**:** 806-813
Hilgers V, Teixeira D, Parker R (2006) Translation-independent inhibition of mRNA deadenylation during stress in Saccharomyces cerevisiae. *RNA* **12**(10)**:** 1835-1845
Hinnebusch AG (2005) Translational regulation of GCN4 and the general amino acid control of yeast. *Annu Rev Microbiol* **59:** 407-450
Hinnebusch AG, Lorsch JR (2012) The mechanism of eukaryotic translation initiation: new insights and challenges. *Cold Spring Harb Perspect Biol* **4**(10)
Holcik M, Sonenberg N (2005) Translational control in stress and apoptosis. *Nat Rev Mol Cell Biol* **6**(4)**:** 318-327
Holmes LE, Campbell SG, De Long SK, Sachs AB, Ashe MP (2004) Loss of translational control in yeast compromised for the major mRNA decay pathway. *Mol Cell Biol* **24**(7)**:** 2998-3010
Hook BA, Goldstrohm AC, Seay DJ, Wickens M (2007) Two yeast PUF proteins negatively regulate a single mRNA. *J Biol Chem* **282**(21)**:** 15430-15438
Hopfner KP, Tainer JA (2003) Rad50/SMC proteins and ABC transporters: unifying concepts from high-resolution structures. *Curr Opin Struct Biol* **13**(2)**:** 249-255

Hosoda N, Kobayashi T, Uchida N, Funakoshi Y, Kikuchi Y, Hoshino S, Katada T (2003) Translation termination factor eRF3 mediates mRNA decay through the regulation of deadenylation. *J Biol Chem* **278**(40)**:** 38287-38291

Hoyle NP, Castelli LM, Campbell SG, Holmes LE, Ashe MP (2007) Stress-dependent relocalization of translationally primed mRNPs to cytoplasmic granules that are kinetically and spatially distinct from P-bodies. *J Cell Biol* **179**(1)**:** 65-74

Hsu CL, Stevens A (1993) Yeast cells lacking 5'-->3' exoribonuclease 1 contain mRNA species that are poly(A) deficient and partially lack the 5' cap structure. *Mol Cell Biol* **13**(8)**:** 4826-4835

Hu W, Petzold C, Coller J, Baker KE (2010) Nonsense-mediated mRNA decapping occurs on polyribosomes in Saccharomyces cerevisiae. *Nat Struct Mol Biol* **17**(2)**:** 244-247

Hu W, Sweet TJ, Chamnongpol S, Baker KE, Coller J (2009) Co-translational mRNA decay in Saccharomyces cerevisiae. *Nature* **461**(7261)**:** 225-229

Huber LA (2003) Is proteomics heading in the wrong direction? *Nat Rev Mol Cell Biol* **4**(1)**:** 74-80

Huh WK, Falvo JV, Gerke LC, Carroll AS, Howson RW, Weissman JS, O'Shea EK (2003) Global analysis of protein localization in budding yeast. *Nature* **425**(6959)**:** 686-691

Huntzinger E, Kashima I, Fauser M, Sauliere J, Izaurralde E (2008) SMG6 is the catalytic endonuclease that cleaves mRNAs containing nonsense codons in metazoan. *RNA* **14**(12)**:** 2609-2617

Inada T, Aiba H (2005) Translation of aberrant mRNAs lacking a termination codon or with a shortened 3'-UTR is repressed after initiation in yeast. *EMBO J* **24**(8)**:** 1584-1595

Inada T, Winstall E, Tarun SZ, Jr., Yates JR, 3rd, Schieltz D, Sachs AB (2002) One-step affinity purification of the yeast ribosome and its associated proteins and mRNAs. *RNA* **8**(7)**:** 948-958

Inagaki Y, Ford Doolittle W (2000) Evolution of the eukaryotic translation termination system: origins of release factors. *Mol Biol Evol* **17**(6)**:** 882-889

Ito-Harashima S, Kuroha K, Tatematsu T, Inada T (2007) Translation of the poly(A) tail plays crucial roles in nonstop mRNA surveillance via translation repression and protein destabilization by proteasome in yeast. *Genes Dev* **21**(5)**:** 519-524

Ito K, Ebihara K, Nakamura Y (1998) The stretch of C-terminal acidic amino acids of translational release factor eRF1 is a primary binding site for eRF3 of fission yeast. *RNA* **4**(8)**:** 958-972

Ito K, Frolova L, Seit-Nebi A, Karamyshev A, Kisselev L, Nakamura Y (2002) Omnipotent decoding potential resides in eukaryotic translation termination factor eRF1 of variant-code organisms and is modulated by the interactions of amino acid sequences within domain 1. *Proc Natl Acad Sci U S A* **99**(13)**:** 8494-8499

Jackson RJ, Hellen CU, Pestova TV (2010) The mechanism of eukaryotic translation initiation and principles of its regulation. *Nat Rev Mol Cell Biol* **11**(2)**:** 113-127

Jackson RJ, Hellen CU, Pestova TV (2012) Termination and post-termination events in eukaryotic translation. *Adv Protein Chem Struct Biol* **86:** 45-93

Jin H, Kelley AC, Loakes D, Ramakrishnan V (2010) Structure of the 70S ribosome bound to release factor 2 and a substrate analog provides insights into catalysis of peptide release. *Proc Natl Acad Sci U S A* **107**(19)**:** 8593-8598

Jinek M, Coyle SM, Doudna JA (2011) Coupled 5' nucleotide recognition and processivity in Xrn1-mediated mRNA decay. *Mol Cell* **41**(5)**:** 600-608

Kaida D, Berg MG, Younis I, Kasim M, Singh LN, Wan L, Dreyfuss G (2010) U1 snRNP protects pre-mRNAs from premature cleavage and polyadenylation. *Nature* **468**(7324)**:** 664-668

Karcher A, Schele A, Hopfner KP (2008) X-ray structure of the complete ABC enzyme ABCE1 from Pyrococcus abyssi. *J Biol Chem* **283**(12)**:** 7962-7971

Kazemzadeh L, Cvijovic M, Petranovic D (2012) Boolean model of yeast apoptosis as a tool to study yeast and human apoptotic regulations. *Front Physiol* **3:** 446

Kedersha N, Stoecklin G, Ayodele M, Yacono P, Lykke-Andersen J, Fritzler MJ, Scheuner D, Kaufman RJ, Golan DE, Anderson P (2005) Stress granules and processing bodies are dynamically linked sites of mRNP remodeling. *J Cell Biol* **169**(6)**:** 871-884

Kervestin S, Frolova L, Kisselev L, Jean-Jean O (2001) Stop codon recognition in ciliates: Euplotes release factor does not respond to reassigned UGA codon. *EMBO Rep* **2**(8)**:** 680-684

Kervestin S, Jacobson A (2012) NMD: a multifaceted response to premature translational termination. *Nat Rev Mol Cell Biol* **13**(11)**:** 700-712

Khusial P, Plaag R, Zieve GW (2005) LSm proteins form heptameric rings that bind to RNA via repeating motifs. *Trends Biochem Sci* **30**(9)**:** 522-528

Klauer AA, van Hoof A (2012) Degradation of mRNAs that lack a stop codon: a decade of nonstop progress. *Wiley Interdiscip Rev RNA* **3**(5)**:** 649-660

Kobayashi K, Kikuno I, Kuroha K, Saito K, Ito K, Ishitani R, Inada T, Nureki O (2010) Structural basis for mRNA surveillance by archaeal Pelota and GTP-bound EF1alpha complex. *Proc Natl Acad Sci U S A* **107**(41)**:** 17575-17579

Kobayashi T, Funakoshi Y, Hoshino S, Katada T (2004) The GTP-binding release factor eRF3 as a key mediator coupling translation termination to mRNA decay. *J Biol Chem* **279**(44)**:** 45693-45700

Kong J, Liebhaber SA (2007) A cell type-restricted mRNA surveillance pathway triggered by ribosome extension into the 3' untranslated region. *Nat Struct Mol Biol* **14**(7)**:** 670-676

Kononenko AV, Mitkevich VA, Dubovaya VI, Kolosov PM, Makarov AA, Kisselev LL (2008) Role of the individual domains of translation termination factor eRF1 in GTP binding to eRF3. *Proteins* **70**(2)**:** 388-393

Koritzinsky M, Rouschop KM, van den Beucken T, Magagnin MG, Savelkouls K, Lambin P, Wouters BG (2007) Phosphorylation of eIF2alpha is required for mRNA translation inhibition and survival during moderate hypoxia. *Radiother Oncol* **83**(3)**:** 353-361

Krokowski D, Gaccioli F, Majumder M, Mullins MR, Yuan CL, Papadopoulou B, Merrick WC, Komar AA, Taylor D, Hatzoglou M (2011) Characterization of hibernating ribosomes in mammalian cells. *Cell Cycle* **10**(16)**:** 2691-2702

Kuroha K, Akamatsu M, Dimitrova L, Ito T, Kato Y, Shirahige K, Inada T (2010) Receptor for activated C kinase 1 stimulates nascent polypeptide-dependent translation arrest. *EMBO Rep* **11**(12)**:** 956-961

Kushnirov VV (2000) Rapid and reliable protein extraction from yeast. *Yeast* **16**(9)**:** 857-860

Lang B, Burger G, Doxiadis I, Thomas DY, Bandlow W, Kaudewitz F (1977) A simple method for the large-scale preparation of mitochondria from microorganisms. *Anal Biochem* **77**(1)**:** 110-121

LaRiviere FJ, Cole SE, Ferullo DJ, Moore MJ (2006) A late-acting quality control process for mature eukaryotic rRNAs. *Mol Cell* **24**(4)**:** 619-626

Le Hir H, Izaurralde E, Maquat LE, Moore MJ (2000) The spliceosome deposits multiple proteins 20-24 nucleotides upstream of mRNA exon-exon junctions. *EMBO J* **19**(24)**:** 6860-6869

Lebaron S, Schneider C, van Nues RW, Swiatkowska A, Walsh D, Bottcher B, Granneman S, Watkins NJ, Tollervey D (2012) Proofreading of pre-40S ribosome maturation by a translation initiation factor and 60S subunits. *Nat Struct Mol Biol* **19**(8)**:** 744-753

Lebreton A, Seraphin B (2008) Exosome-mediated quality control: substrate recruitment and molecular activity. *Biochim Biophys Acta* **1779**(9)**:** 558-565

Lebreton A, Tomecki R, Dziembowski A, Seraphin B (2008) Endonucleolytic RNA cleavage by a eukaryotic exosome. *Nature* **456**(7224)**:** 993-996

Lee HH, Jang JY, Yoon HJ, Kim SJ, Suh SW (2010) Crystal structures of two archaeal Pelotas reveal inter-domain structural plasticity. *Biochem Biophys Res Commun* **399**(4)**:** 600-606

Lee HH, Kim YS, Kim KH, Heo I, Kim SK, Kim O, Kim HK, Yoon JY, Kim HS, Kim do J, Lee SJ, Yoon HJ, Kim SJ, Lee BG, Song HK, Kim VN, Park CM, Suh SW (2007) Structural and functional insights into Dom34, a key component of no-go mRNA decay. *Mol Cell* **27**(6)**:** 938-950

Letzring DP, Dean KM, Grayhack EJ (2010) Control of translation efficiency in yeast by codon-anticodon interactions. *RNA* **16**(12)**:** 2516-2528

Li X, Gerber SA, Rudner AD, Beausoleil SA, Haas W, Villen J, Elias JE, Gygi SP (2007) Large-scale phosphorylation analysis of alpha-factor-arrested Saccharomyces cerevisiae. *J Proteome Res* **6**(3)**:** 1190-1197

Liang H, Wong JY, Bao Q, Cavalcanti AR, Landweber LF (2005) Decoding the decoding region: analysis of eukaryotic release factor (eRF1) stop codon-binding residues. *J Mol Evol* **60**(3)**:** 337-344

Ligr M, Velten I, Frohlich E, Madeo F, Ledig M, Frohlich KU, Wolf DH, Hilt W (2001) The proteasomal substrate Stm1 participates in apoptosis-like cell death in yeast. *Mol Biol Cell* **12**(8)**:** 2422-2432

Liu L, Wise DR, Diehl JA, Simon MC (2008) Hypoxic reactive oxygen species regulate the integrated stress response and cell survival. *J Biol Chem* **283**(45)**:** 31153-31162

Liu Q, Greimann JC, Lima CD (2006) Reconstitution, activities, and structure of the eukaryotic RNA exosome. *Cell* **127**(6)**:** 1223-1237

Lomakin IB, Kolupaeva VG, Marintchev A, Wagner G, Pestova TV (2003) Position of eukaryotic initiation factor eIF1 on the 40S ribosomal subunit determined by directed hydroxyl radical probing. *Genes Dev* **17**(22)**:** 2786-2797

Lu J, Deutsch C (2008) Electrostatics in the ribosomal tunnel modulate chain elongation rates. *J Mol Biol* **384**(1)**:** 73-86

Lu J, Kobertz WR, Deutsch C (2007) Mapping the electrostatic potential within the ribosomal exit tunnel. *J Mol Biol* **371**(5)**:** 1378-1391

Lui J, Campbell SG, Ashe MP (2010) Inhibition of translation initiation following glucose depletion in yeast facilitates a rationalization of mRNA content. *Biochem Soc Trans* **38**(4)**:** 1131-1136

Lykke-Andersen S, Tomecki R, Jensen TH, Dziembowski A (2011) The eukaryotic RNA exosome: same scaffold but variable catalytic subunits. *RNA Biol* **8**(1)**:** 61-66

Ma XM, Blenis J (2009) Molecular mechanisms of mTOR-mediated translational control. *Nat Rev Mol Cell Biol* **10**(5)**:** 307-318

Mascarenhas C, Edwards-Ingram LC, Zeef L, Shenton D, Ashe MP, Grant CM (2008) Gcn4 is required for the response to peroxide stress in the yeast Saccharomyces cerevisiae. *Mol Biol Cell* **19**(7)**:** 2995-3007
Meaux S, Van Hoof A (2006) Yeast transcripts cleaved by an internal ribozyme provide new insight into the role of the cap and poly(A) tail in translation and mRNA decay. *RNA* **12**(7)**:** 1323-1337
Meier KD, Deloche O, Kajiwara K, Funato K, Riezman H (2006) Sphingoid base is required for translation initiation during heat stress in Saccharomyces cerevisiae. *Mol Biol Cell* **17**(3)**:** 1164-1175
Melnikov S, Ben-Shem A, Garreau de Loubresse N, Jenner L, Yusupova G, Yusupov M (2012) One core, two shells: bacterial and eukaryotic ribosomes. *Nat Struct Mol Biol* **19**(6)**:** 560-567
Merkulova TI, Frolova LY, Lazar M, Camonis J, Kisselev LL (1999) C-terminal domains of human translation termination factors eRF1 and eRF3 mediate their in vivo interaction. *FEBS Lett* **443**(1)**:** 41-47
Mitchell SA, Spriggs KA, Bushell M, Evans JR, Stoneley M, Le Quesne JP, Spriggs RV, Willis AE (2005) Identification of a motif that mediates polypyrimidine tract-binding protein-dependent internal ribosome entry. *Genes Dev* **19**(13)**:** 1556-1571
Mitkevich VA, Kononenko AV, Petrushanko IY, Yanvarev DV, Makarov AA, Kisselev LL (2006) Termination of translation in eukaryotes is mediated by the quaternary eRF1*eRF3*GTP*Mg2+ complex. The biological roles of eRF3 and prokaryotic RF3 are profoundly distinct. *Nucleic Acids Res* **34**(14)**:** 3947-3954
Moen B, Janbu AO, Langsrud S, Langsrud O, Hobman JL, Constantinidou C, Kohler A, Rudi K (2009) Global responses of Escherichia coli to adverse conditions determined by microarrays and FT-IR spectroscopy. *Can J Microbiol* **55**(6)**:** 714-728
Monteiro PT, Mendes ND, Teixeira MC, d'Orey S, Tenreiro S, Mira NP, Pais H, Francisco AP, Carvalho AM, Lourenco AB, Sa-Correia I, Oliveira AL, Freitas AT (2008) YEASTRACT-DISCOVERER: new tools to improve the analysis of transcriptional regulatory associations in Saccharomyces cerevisiae. *Nucleic Acids Res* **36**(Database issue)**:** D132-136
Montero-Lomeli M, Morais BL, Figueiredo DL, Neto DC, Martins JR, Masuda CA (2002) The initiation factor eIF4A is involved in the response to lithium stress in Saccharomyces cerevisiae. *J Biol Chem* **277**(24)**:** 21542-21548
Moxley JF, Jewett MC, Antoniewicz MR, Villas-Boas SG, Alper H, Wheeler RT, Tong L, Hinnebusch AG, Ideker T, Nielsen J, Stephanopoulos G (2009) Linking high-resolution metabolic flux phenotypes and transcriptional regulation in yeast modulated by the global regulator Gcn4p. *Proc Natl Acad Sci U S A* **106**(16)**:** 6477-6482
Nagai K, Oubridge C, Ito N, Jessen TH, Avis J, Evans P (1995) Crystal structure of the U1A spliceosomal protein complexed with its cognate RNA hairpin. *Nucleic Acids Symp Ser*(34)**:** 1-2
Nelson LD, Musso M, Van Dyke MW (2000) The yeast STM1 gene encodes a purine motif triple helical DNA-binding protein. *J Biol Chem* **275**(8)**:** 5573-5581
Nelson RJ, Ziegelhoffer T, Nicolet C, Werner-Washburne M, Craig EA (1992) The translation machinery and 70 kd heat shock protein cooperate in protein synthesis. *Cell* **71**(1)**:** 97-105
Nicholson P, Muhlemann O (2010) Cutting the nonsense: the degradation of PTC-containing mRNAs. *Biochem Soc Trans* **38**(6)**:** 1615-1620
Nielsen PJ, Duncan R, McConkey EH (1981) Phosphorylation of ribosomal protein S6. Relationship to protein synthesis in HeLa cells. *Eur J Biochem* **120**(3)**:** 523-527
Nissan T, Rajyaguru P, She M, Song H, Parker R (2010) Decapping activators in Saccharomyces cerevisiae act by multiple mechanisms. *Mol Cell* **39**(5)**:** 773-783
Nurenberg E, Tampe R (2013) Tying up loose ends: ribosome recycling in eukaryotes and archaea. *Trends Biochem Sci* **38**(2)**:** 64-74
Ogle JM, Brodersen DE, Clemons WM, Jr., Tarry MJ, Carter AP, Ramakrishnan V (2001) Recognition of cognate transfer RNA by the 30S ribosomal subunit. *Science* **292**(5518)**:** 897-902
Olivas W, Parker R (2000) The Puf3 protein is a transcript-specific regulator of mRNA degradation in yeast. *EMBO J* **19**(23)**:** 6602-6611
Passos DO, Doma MK, Shoemaker CJ, Muhlrad D, Green R, Weissman J, Hollien J, Parker R (2009) Analysis of Dom34 and its function in no-go decay. *Mol Biol Cell* **20**(13)**:** 3025-3032
Paz I, Abramovitz L, Choder M (1999) Starved Saccharomyces cerevisiae cells have the capacity to support internal initiation of translation. *J Biol Chem* **274**(31)**:** 21741-21745
Petrov A, Puglisi JD (2010) Site-specific labeling of Saccharomyces cerevisiae ribosomes for single-molecule manipulations. *Nucleic Acids Res* **38**(13)**:** e143
Pisarev AV, Skabkin MA, Pisareva VP, Skabkina OV, Rakotondrafara AM, Hentze MW, Hellen CU, Pestova TV (2010) The role of ABCE1 in eukaryotic posttermination ribosomal recycling. *Mol Cell* **37**(2)**:** 196-210
Pisareva VP, Pisarev AV, Hellen CU, Rodnina MV, Pestova TV (2006) Kinetic analysis of interaction of eukaryotic release factor 3 with guanine nucleotides. *J Biol Chem* **281**(52)**:** 40224-40235
Pisareva VP, Skabkin MA, Hellen CU, Pestova TV, Pisarev AV (2011) Dissociation by Pelota, Hbs1 and ABCE1 of mammalian vacant 80S ribosomes and stalled elongation complexes. *EMBO J* **30**(9)**:** 1804-1817

Polikanov YS, Blaha GM, Steitz TA (2012) How hibernation factors RMF, HPF, and YfiA turn off protein synthesis. *Science* **336**(6083)**:** 915-918

Rabl J, Leibundgut M, Ataide SF, Haag A, Ban N (2011) Crystal structure of the eukaryotic 40S ribosomal subunit in complex with initiation factor 1. *Science* **331**(6018)**:** 730-736

Ragan MA, Logsdon JM, Jr., Sensen CW, Charlebois RL, Doolittle WF (1996) An archaebacterial homolog of pelota, a meiotic cell division protein in eukaryotes. *FEMS Microbiol Lett* **144**(2-3)**:** 151-155

Rigaut G, Shevchenko A, Rutz B, Wilm M, Mann M, Seraphin B (1999) A generic protein purification method for protein complex characterization and proteome exploration. *Nat Biotechnol* **17**(10)**:** 1030-1032

Rodnina MV (2013) The ribosome as a versatile catalyst: reactions at the peptidyl transferase center. *Curr Opin Struct Biol*

Safer B (1983) 2B or not 2B: regulation of the catalytic utilization of eIF-2. *Cell* **33**(1)**:** 7-8

Saito K, Kobayashi K, Wada M, Kikuno I, Takusagawa A, Mochizuki M, Uchiumi T, Ishitani R, Nureki O, Ito K (2010) Omnipotent role of archaeal elongation factor 1 alpha (EF1alpha in translational elongation and termination, and quality control of protein synthesis. *Proc Natl Acad Sci U S A* **107**(45)**:** 19242-19247

Saito S, Hosoda N, Hoshino SI (2013) Hbs1-Dom34 functions in non-stop mRNA decay (NSD) in mammalian cells. *J Biol Chem*

Salgado-Garrido J, Bragado-Nilsson E, Kandels-Lewis S, Seraphin B (1999) Sm and Sm-like proteins assemble in two related complexes of deep evolutionary origin. *EMBO J* **18**(12)**:** 3451-3462

Sambrook J, Fritsch EJ, Maniatis T (1989) *Molecular Cloning: A Laboratory Manual.*, Cold Spring Harbor: Cold Spring Harbor Laboratory Press.

Sauliere J, Haque N, Harms S, Barbosa I, Blanchette M, Le Hir H (2010) The exon junction complex differentially marks spliced junctions. *Nat Struct Mol Biol* **17**(10)**:** 1269-1271

Sauliere J, Murigneux V, Wang Z, Marquenet E, Barbosa I, Le Tonqueze O, Audic Y, Paillard L, Roest Crollius H, Le Hir H (2012) CLIP-seq of eIF4AIII reveals transcriptome-wide mapping of the human exon junction complex. *Nat Struct Mol Biol* **19**(11)**:** 1124-1131

Schaeffer D, van Hoof A (2011) Different nuclease requirements for exosome-mediated degradation of normal and nonstop mRNAs. *Proc Natl Acad Sci U S A* **108**(6)**:** 2366-2371

Schmeing TM, Ramakrishnan V (2009) What recent ribosome structures have revealed about the mechanism of translation. *Nature* **461**(7268)**:** 1234-1242

Schwartz DC, Parker R (1999) Mutations in translation initiation factors lead to increased rates of deadenylation and decapping of mRNAs in Saccharomyces cerevisiae. *Mol Cell Biol* **19**(8)**:** 5247-5256

Schwartz DC, Parker R (2000) mRNA decapping in yeast requires dissociation of the cap binding protein, eukaryotic translation initiation factor 4E. *Mol Cell Biol* **20**(21)**:** 7933-7942

Seit-Nebi A, Frolova L, Kisselev L (2002) Conversion of omnipotent translation termination factor eRF1 into ciliate-like UGA-only unipotent eRF1. *EMBO Rep* **3**(9)**:** 881-886

Seminara SB, Messager S, Chatzidaki EE, Thresher RR, Acierno JS, Jr., Shagoury JK, Bo-Abbas Y, Kuohung W, Schwinof KM, Hendrick AG, Zahn D, Dixon J, Kaiser UB, Slaugenhaupt SA, Gusella JF, O'Rahilly S, Carlton MB, Crowley WF, Jr., Aparicio SA, Colledge WH (2003) The GPR54 gene as a regulator of puberty. *N Engl J Med* **349**(17)**:** 1614-1627

Shah P, Ding Y, Niemczyk M, Kudla G, Plotkin JB (2013) Rate-limiting steps in yeast protein translation. *Cell* **153**(7)**:** 1589-1601

Shao S, von der Malsburg K, Hegde RS (2013) Listerin-Dependent Nascent Protein Ubiquitination Relies on Ribosome Subunit Dissociation. *Mol Cell*

She M, Decker CJ, Svergun DI, Round A, Chen N, Muhlrad D, Parker R, Song H (2008) Structural basis of dcp2 recognition and activation by dcp1. *Mol Cell* **29**(3)**:** 337-349

Shenton D, Smirnova JB, Selley JN, Carroll K, Hubbard SJ, Pavitt GD, Ashe MP, Grant CM (2006) Global translational responses to oxidative stress impact upon multiple levels of protein synthesis. *J Biol Chem* **281**(39)**:** 29011-29021

Sheth U, Parker R (2003) Decapping and decay of messenger RNA occur in cytoplasmic processing bodies. *Science* **300**(5620)**:** 805-808

Shoemaker CJ, Eyler DE, Green R (2010) Dom34:Hbs1 promotes subunit dissociation and peptidyl-tRNA drop-off to initiate no-go decay. *Science* **330**(6002)**:** 369-372

Shoemaker CJ, Green R (2011) Kinetic analysis reveals the ordered coupling of translation termination and ribosome recycling in yeast. *Proc Natl Acad Sci U S A* **108**(51)**:** E1392-1398

Simon E, Seraphin B (2007) A specific role for the C-terminal region of the Poly(A)-binding protein in mRNA decay. *Nucleic Acids Res* **35**(18)**:** 6017-6028

Simpson CE, Ashe MP (2012) Adaptation to stress in yeast: to translate or not? *Biochem Soc Trans* **40**(4)**:** 794-799

Song H, Mugnier P, Das AK, Webb HM, Evans DR, Tuite MF, Hemmings BA, Barford D (2000) The crystal structure of human eukaryotic release factor eRF1--mechanism of stop codon recognition and peptidyl-tRNA hydrolysis. *Cell* **100**(3)**:** 311-321

Soudet J, Gelugne JP, Belhabich-Baumas K, Caizergues-Ferrer M, Mougin A (2010) Immature small ribosomal subunits can engage in translation initiation in Saccharomyces cerevisiae. *EMBO J* **29**(1)**:** 80-92

Spriggs KA, Bushell M, Willis AE (2010) Translational regulation of gene expression during conditions of cell stress. *Mol Cell* **40**(2)**:** 228-237

Stolz A, Hilt W, Buchberger A, Wolf DH (2011) Cdc48: a power machine in protein degradation. *Trends Biochem Sci* **36**(10)**:** 515-523

Strunk BS, Novak MN, Young CL, Karbstein K (2012) A translation-like cycle is a quality control checkpoint for maturing 40S ribosome subunits. *Cell* **150**(1)**:** 111-121

Tang L, Liu X, Clarke ND (2006) Inferring direct regulatory targets from expression and genome location analyses: a comparison of transcription factor deletion and overexpression. *BMC Genomics* **7:** 215

Taniguchi A, Hakoda M, Yamanaka H, Terai C, Hikiji K, Kawaguchi R, Konishi N, Kashiwazaki S, Kamatani N (1998) A germline mutation abolishing the original stop codon of the human adenine phosphoribosyltransferase (APRT) gene leads to complete loss of the enzyme protein. *Hum Genet* **102**(2)**:** 197-202

Tarun SZ, Jr., Sachs AB (1995) A common function for mRNA 5' and 3' ends in translation initiation in yeast. *Genes Dev* **9**(23)**:** 2997-3007

Taylor D, Unbehaun A, Li W, Das S, Lei J, Liao HY, Grassucci RA, Pestova TV, Frank J (2012) Cryo-EM structure of the mammalian eukaryotic release factor eRF1-eRF3-associated termination complex. *Proc Natl Acad Sci U S A* **109**(45)**:** 18413-18418

Teixeira D, Sheth U, Valencia-Sanchez MA, Brengues M, Parker R (2005) Processing bodies require RNA for assembly and contain nontranslating mRNAs. *RNA* **11**(4)**:** 371-382

Teixeira MC, Monteiro P, Jain P, Tenreiro S, Fernandes AR, Mira NP, Alenquer M, Freitas AT, Oliveira AL, Sa-Correia I (2006) The YEASTRACT database: a tool for the analysis of transcription regulatory associations in Saccharomyces cerevisiae. *Nucleic Acids Res* **34**(Database issue)**:** D446-451

Tharun S, Parker R (1999) Analysis of mutations in the yeast mRNA decapping enzyme. *Genetics* **151**(4)**:** 1273-1285

Thompson SR (2012) Tricks an IRES uses to enslave ribosomes. *Trends Microbiol* **20**(11)**:** 558-566

Torres-Torronteras J, Rodriguez-Palmero A, Pinos T, Accarino A, Andreu AL, Pintos-Morell G, Martii R (2011) A novel nonstop mutation in TYMP does not induce nonstop mRNA decay in a MNGIE patient with severe neuropathy. *Hum Mutat* **32**(4)**:** E2061-2068

Tsuboi T, Kuroha K, Kudo K, Makino S, Inoue E, Kashima I, Inada T (2012) Dom34:hbs1 plays a general role in quality-control systems by dissociation of a stalled ribosome at the 3' end of aberrant mRNA. *Mol Cell* **46**(4)**:** 518-529

Tucker M, Staples RR, Valencia-Sanchez MA, Muhlrad D, Parker R (2002) Ccr4p is the catalytic subunit of a Ccr4p/Pop2p/Notp mRNA deadenylase complex in Saccharomyces cerevisiae. *EMBO J* **21**(6)**:** 1427-1436

Tucker M, Valencia-Sanchez MA, Staples RR, Chen J, Denis CL, Parker R (2001) The transcription factor associated Ccr4 and Caf1 proteins are components of the major cytoplasmic mRNA deadenylase in Saccharomyces cerevisiae. *Cell* **104**(3)**:** 377-386

Tuite MF, Plesset J (1986) mRNA-dependent yeast cell-free translation systems: theory and practice. *Yeast* **2**(1)**:** 35-52

Tzamarias D, Roussou I, Thireos G (1989) Coupling of GCN4 mRNA translational activation with decreased rates of polypeptide chain initiation. *Cell* **57**(6)**:** 947-954

Uesono Y, Toh EA (2002) Transient inhibition of translation initiation by osmotic stress. *J Biol Chem* **277**(16)**:** 13848-13855

Ueta M, Ohniwa RL, Yoshida H, Maki Y, Wada C, Wada A (2008) Role of HPF (hibernation promoting factor) in translational activity in Escherichia coli. *J Biochem* **143**(3)**:** 425-433

Underhill MF, Marchant RJ, Carden MJ, James DC, Smales CM (2006) On the effect of transient expression of mutated eIF2alpha and eIF4E eukaryotic translation initiation factors on reporter gene expression in mammalian cells upon cold-shock. *Mol Biotechnol* **34**(2)**:** 141-149

van Dijk E, Cougot N, Meyer S, Babajko S, Wahle E, Seraphin B (2002) Human Dcp2: a catalytically active mRNA decapping enzyme located in specific cytoplasmic structures. *EMBO J* **21**(24)**:** 6915-6924

Van Dyke MW, Nelson LD, Weilbaecher RG, Mehta DV (2004) Stm1p, a G4 quadruplex and purine motif triplex nucleic acid-binding protein, interacts with ribosomes and subtelomeric Y' DNA in Saccharomyces cerevisiae. *J Biol Chem* **279**(23)**:** 24323-24333

Van Dyke N, Baby J, Van Dyke MW (2006) Stm1p, a ribosome-associated protein, is important for protein synthesis in Saccharomyces cerevisiae under nutritional stress conditions. *J Mol Biol* **358**(4)**:** 1023-1031

Van Dyke N, Chanchorn E, Van Dyke MW (2013) The Saccharomyces cerevisiae protein Stm1p facilitates ribosome preservation during quiescence. *Biochem Biophys Res Commun* **430**(2)**:** 745-750

Van Dyke N, Pickering BF, Van Dyke MW (2009) Stm1p alters the ribosome association of eukaryotic elongation factor 3 and affects translation elongation. *Nucleic Acids Res* **37**(18)**:** 6116-6125

van Hoof A, Frischmeyer PA, Dietz HC, Parker R (2002) Exosome-mediated recognition and degradation of mRNAs lacking a termination codon. *Science* **295**(5563)**:** 2262-2264

van Hoof A, Staples RR, Baker RE, Parker R (2000) Function of the ski4p (Csl4p) and Ski7p proteins in 3'-to-5' degradation of mRNA. *Mol Cell Biol* **20**(21)**:** 8230-8243

Verma R, Oania RS, Kolawa NJ, Deshaies RJ (2013) Cdc48/p97 promotes degradation of aberrant nascent polypeptides bound to the ribosome. *Elife* **2:** e00308

Vetter IR, Wittinghofer A (2001) The guanine nucleotide-binding switch in three dimensions. *Science* **294**(5545)**:** 1299-1304

Vries RG, Flynn A, Patel JC, Wang X, Denton RM, Proud CG (1997) Heat shock increases the association of binding protein-1 with initiation factor 4E. *J Biol Chem* **272**(52)**:** 32779-32784

Wallrapp C, Verrier SB, Zhouravleva G, Philippe H, Philippe M, Gress TM, Jean-Jean O (1998) The product of the mammalian orthologue of the Saccharomyces cerevisiae HBS1 gene is phylogenetically related to eukaryotic release factor 3 (eRF3) but does not carry eRF3-like activity. *FEBS Lett* **440**(3)**:** 387-392

Wasmuth EV, Lima CD (2012) Exo- and endoribonucleolytic activities of yeast cytoplasmic and nuclear RNA exosomes are dependent on the noncatalytic core and central channel. *Mol Cell* **48**(1)**:** 133-144

Willmund F, del Alamo M, Pechmann S, Chen T, Albanese V, Dammer EB, Peng J, Frydman J (2013) The cotranslational function of ribosome-associated Hsp70 in eukaryotic protein homeostasis. *Cell* **152**(1-2)**:** 196-209

Wilson MA, Meaux S, van Hoof A (2007) A genomic screen in yeast reveals novel aspects of nonstop mRNA metabolism. *Genetics* **177**(2)**:** 773-784

Xi R, Doan C, Liu D, Xie T (2005) Pelota controls self-renewal of germline stem cells by repressing a Bam-independent differentiation pathway. *Development* **132**(24)**:** 5365-5374

Yamaguchi-Kabata Y, Shimada MK, Hayakawa Y, Minoshima S, Chakraborty R, Gojobori T, Imanishi T (2008) Distribution and effects of nonsense polymorphisms in human genes. *PLoS One* **3**(10)**:** e3393

Yamashita A, Chang TC, Yamashita Y, Zhu W, Zhong Z, Chen CY, Shyu AB (2005) Concerted action of poly(A) nucleases and decapping enzyme in mammalian mRNA turnover. *Nat Struct Mol Biol* **12**(12)**:** 1054-1063

5. SUPPLEMENTARY INFORMATION

Dissection of the Dom34-Hbs1 complex reveals independent functions in two cytoplasmic RNA quality control pathways

Antonia M.G. van den Elzen, Julien Henri, Noureddine Lazar, María Eugenia Gas, Dominique Durand, François Lacroute, Magali Nicaise, Herman van Tilbeurgh, Bertrand Séraphin and Marc Graille

Supplementary Information

Supplementary Material and methods

Crystallization and Structure determination. Crystals of the native protein were grown from a mixture in a 1:1 ratio of 15mg/mL protein solution in buffer A (20 mM Tris-HCl pH 7.5, 200 mM NaCl, 10 mM β-mercaptoethanol) and crystallization liquor containing 0.1 M Tris pH 8.5, 12% (w/v) PEG 6000 and 0.15 M NaCl, at 18 °C. Crystallization liquor for the Se-Met protein contained 0.1 M Hepes pH 7.0, 15% (w/v) PEG 4000 and 0.1 M $MgCl_2$. The crystals were flash cooled in liquid nitrogen after addition of 15% and 30% (v/v) of ethyleneglycol as a crytoprotectant. Native and Se-Met crystals of the apo-protein diffracted respectively to 2.5 Å and 3.2 Å resolution on beamline Proxima1 at SOLEIL synchrotron (Saint-Aubin, France) at 100 K. The crystals belong to space group $P4_22_12$ with two molecules in the asymmetric unit ($a = b = 110.6$ Å, $c = 188.1$ Å). The Se-Met crystal diffraction data were collected at the selenium edge ($\lambda = 0.9796$ Å). The structure was determined by the single wavelength anomalous dispersion (SAD) method using the anomalous signal of selenium atoms. Data were processed with the XDS package [1]. The SOLVE/RESOLVE package was used to find selenium atom sites in the 30-3.2 Å resolution range, to calculate experimental electron density maps and to improve them by NCS averaging, solvent flattening and phase extension using the 2.5 Å resolution native dataset [2,3]. The quality of the experimental phases allowed automatic building of a partial model with the program RESOLVE (Supplementary Fig. 1). This model was completed by iterative cycles of manual rebuilding using COOT followed by refinement with PHENIX.REFINE [4,5]. All residues display main chain dihedral angles that fall within allowed regions of the Ramachandran plot as defined by the program PROCHECK [6].

Nature Structural & Molecular Biology: doi:10.1038/nsmb.1963

In parallel, we have been able to obtain crystals of the HbsdN134 GDP bound form. A 2.95 Å resolution dataset was recorded from a crystal grown by mixing 0.2 µl of SeMet labelled protein (18 mg ml^{-1} and incubated with 1 mM GDP in the absence of Mg^{2+} ion as this cation affects GDP binding to Hbs1, data not shown) with an equal volume of the following crystallization condition: 12% (w/v) PEG 4,000, 20% (v/v) glycerol, 50 mM MOPS pH 7.0, 0.5 M KCl. The crystals were flash cooled in liquid nitrogen after transfer into a crystallization condition containing 30% glycerol. Data were collected on beamline Proxima1 at SOLEIL synchrotron (Saint-Aubin, France) at 100K (λ = 0.9796 Å).

The statistics for data collection and refinement are summarized in Supplementary Table 1. The atomic coordinates and structure factors have been deposited into the Brookhaven Protein Data Bank under accession number (3P26 and 3P27).

SAXS studies. The Dom34-Hbs1dN134 complex was prepared by mixing equimolar amounts of both purified Dom34 and Hbs1dN134 proteins in buffer A. SAXS experiments on the Hbs1-Dom34 complex were performed using the Nanostar instrument at IBBMC in Orsay. The X-rays were produced by a rotating anode (Cu Kα, wavelength λ = 1.54 Å), and the scattered X-rays were collected using a two-dimensional position sensitive detector (Vantec) positioned at 662 mm from the sample. The scattering vector range was $0.011 < q < 0.40$ $Å^{-1}$ where $q = 4\pi\sin\theta/\lambda$ and 2θ is the scattering angle. *Experiments on Hbs1 were performed on the beamline SWING, at the Synchrotron SOLEIL.* The incident beam energy was 12 keV, and the sample to detector (Aviex CCD) distance was set to 1843 mm. The scattering vector range was $0.008 < q < 0.5$ $Å^{-1}$. Several successive frames (typically 20) of 4 s each were recorded for both sample and pure solvent. We checked that X rays did not cause irradiation damage by comparing the successive frames, before calculating the average intensity and experimental error. In both cases scattering from the buffer was measured and subtracted from the corresponding protein spectra. Intensities were scaled using the scattering of water. For each protein, a range of concentrations was explored. For the Hbs1-Dom34 complex the concentration of the solution was maintained above 3 g l^{-1} to avoid dissociation. No significant effect of the concentration was observed. Calculations of the molar mass of each protein from the intensity extrapolated to $q \rightarrow 0$ gave values that were within 15% of the theoretical mass.

Scattering patterns from crystal structures were calculated using the program CRYSOL [7]. The relative position of some domains (see Supplementary Results) was refined using the rigid-body modelling program SASREF [8], which uses simulated annealing to find an optimal configuration of the domains by fitting the SAXS curve. An ultimate adjustment was performed using the program CRYSOL. The goodness of fit was characterized by the following parameter,

$$\chi^2 = \frac{1}{N-1}\sum_j \left[\frac{I_{\exp}(q_j) - cI_{calc}(q_j)}{\sigma(q_j)}\right]^2$$

Nature Structural & Molecular Biology: doi:10.1038/nsmb.1963

where N is the number of experimental points, c is a scaling factor, and $I_{calc}(q_j)$ and $\sigma(q_j)$ are the calculated intensity and the experimental error at the scattering vector q_j, respectively.

Isothermal titration calorimetry. Isothermal titration microcalorimetry (ITC) was carried out using a Microcal ITC-200 calorimeter at 20°C, with full length Hbs1 protein solutions prepared as described previously [9] and stored in 20 mM Tris pH7.5, 200 mM NaCl, 10 mM β-mercaptoethanol. The interaction of wild type and mutants (V176G, K180A and H255E) Hbs1 proteins (20 µM) with GTP/GDP (250 µM) was titrated through a series of 20 injections of 2 µl, at an interval of 3 min. A theoretical titration curve was fitted to the experimental data using the ORIGIN® software (Microcal). This software uses the relationship between the heat generated by each injection and ΔH (enthalpy change), K_a (association binding constant), n (the number of binding sites per monomer), total GTP/GDP concentration, and the free and total Hbs1 concentrations. The best fit to experimental data was obtained for a binding curve corresponding to a one binding site model and a stoechiometry of 0.7, consistent with the 1:1 Hbs1:GDP ratio observed in the crystal.

$$\Delta C_p(T) = \frac{K_d(T)\,\Delta H_{cal}\,\Delta H_{vH}}{[1+K_d(T)]^2\,RT^2}$$

Differential Scanning Calorimetry. Thermal stability was studied by differential scanning calorimetry (DSC) on a MicroCal model VP-DSC with Hbs1 and Dom34 proteins in 20mM Na-Phosphate pH 7.5; 500mM NaCl, 5mM B-mercaptoethanol. Protein concentrations ranged from 11.3 to 32.6 µM for Dom 34 and from 6.4 to 24 µM for Hbs1. Each measurement was preceded by a baseline scan with the standard buffer. Scans were performed at 1K.min^{-1} between 20°C and 80°C. The heat capacity of the buffer was subtracted from that of the protein sample before analysis.

Yeast two-hybrid interaction assay. Two-hybrid Dom34 and Hbs1 (wild type and mutant) constructs were prepared as described before [10], with the exception that Hbs1 was cloned into pACTII and Dom34 into pAS2. The resulting plasmids were transformed into strain Y190. 750 µl of cultures in exponential growth phase were spun down, resuspended in 500 µl buffer Z (Na_2HPO_4 60mM, NaH_2PO_4 40 mM, KCl 10 mM, $MgCl_2$ 1 mM, β-mercaptoethanol 50 mM) and 200 µl water saturated ether, spun for 1 minute and left to let ether evaporate for 10 min. After 5 minutes at 30 °C 100 µl ONPG (4mg ml^{-1} in buffer Z) was added. Following incubation at 30 °C the reaction was stopped by addition of 250 µl Na_2CO_3 1M, reactions were spun for 5 minutes and OD420 was measured. ß-galactosidase activity was calculated as follow: Activity = 1000 x OD420 / (OD600 x culture volume x reaction time).

Nature Structural & Molecular Biology: doi:10.1038/nsmb.1963

Supplementary Data

Hbs1 overall structure.

The structure of Hbs1dN134 has been solved by SAD. Hbs1dN134 is composed of three domains, forming a triangular prism of approximately 50 Å side length and 30 Å depth. The GTPase domain adopts the classical α/β structure common to translational GTPases such as EF-Tu and eRF3. It is composed of a central six-stranded β-sheet (strands order β6, β5, β4, β1, β3 and β2, which is antiparallel to the others) flanked by 7 α-helices (α1, α2, α6 and α7 on one side of the sheet and α3-5 on the other; Fig. 1a). The GTPase domain is connected to domain II by the long helix α7 (residues 376 to 398) and domain II is linked to domain III by a short extended stretch of peptides. Both domains II and III adopt a 6-stranded β-barrel fold similar to the corresponding domains from archaeal elongation factor 1-α (aEF-1A), bacterial elongation factor (EF-Tu) and eukaryotic class II release factor Although they belong to the same SCOP superfamily, domains II and III adopt radically different topologies (strands order βA, βB, βE, βD, βC and βF for domain II and βA', βD', βC', βB', βE' and βF' for domain III).

For both the apo and GDP bound form of Hbs1dN134, the crystal asymmetric unit contains two molecules organized as a non crystallographic dimer, yielding to 4 sets of coordinates for this Hbs1 monomer. These 4 copies are virtually identical (rmsd ≈ 0.4-0.5 Å over 430 residues) except for the switch regions that adopt different conformations. Despite the presence of 2 copies per asymmetric unit, both size exclusion chromatography coupled online to a triple detection array and small-angle X-ray scattering (SAXS) indicated that the protein is monomeric in solution. Among these four copies of Hbs1dN134, the switch II region is disordered in one GDP bound copy and adopts 3 different conformations in the others.

Hbs1 conformation.

Several structures of GTPases involved in translation have now been solved, revealing important differences in the orientation of the GTPase domain relative to domains II-III. In the structures of bacterial EF-Tu, the GTPase domain undergoes a substantial rotation with respect to domains II-III depending on the bound nucleotide (GDP or the GTP non-hydrolyzable analog GDPNP [11-14]). On the opposite, the structures of archaeal SelB elongation factor obtained in the absence of nucleotide or in the presence of GDP or GDPNP by co-crystallization, are virtually the same and correspond to the conformation adopted by EF-Tu in the presence of GTP [15]. Finally, the conformation observed in the crystal structure of *S. pombe* class II release factor eRF3 is radically different from that of EF-Tu-GTP and nucleotide (GDP or GDPNP) binding does not affect its conformation [16] (Supplementary Fig. 2a). Whether this reflects a functional property of eRF3 remains to be determined.

To investigate the conformation adopted by Hbs1dN134 in solution, we have performed small-angle X-ray scattering analysis on this fragment in the absence of nucleotide. As a first approach, we have

Nature Structural & Molecular Biology: doi:10.1038/nsmb.1963

compared the diffusion curves calculated from two different Hbs1dN134 conformations to the final experimental scattering pattern. The first conformation corresponds to that observed in the crystal while the second is based on the conformation of *S. pombe* eRF3. As shown in Supplementary Fig. 2b, the best fit is observed for the conformation corresponding to the Hbs1 crystal structure (χ value of 2.8 compared to 18.5 for the eRF3 based model). However, there is some discrepancy at q values of 0.15-0.2 $Å^{-1}$ with the final experimental scattering pattern. As in our crystal structure of Hbs1dN134, most of the switch I region was missing due to intrinsic disorder, we have first modelled this region using the coordinates of the corresponding region of eEF1A in the structure of the eEF1A-eEF1Bα complex [17]. The location of this switch I region was further adjusted by superimposing residues 35-73 from eEF1A switch I region onto helices α2 and α2' from the Hbs1-GDP complex to yield the model used to calculate the initial diffusion curve. As switch I region from G proteins is known to be highly flexible in the absence of nucleotide, we decided to move this switch I region (residues 176 to 235) as a rigid body group using the SASREF program [8]. Movement of this switch I region by 10 Å is sufficient to obtain a model with an excellent agreement with the SAXS curve (Supplementary Fig. 2b, χ value of 1.6).

Altogether, these experiments performed in solution show that the Hbs1dN134 conformation trapped in the crystal is similar to that in solution and radically different from the conformation observed for eRF3 [16].

Generation of Dom34-Hbs1 models for SAXS.

To obtain more information on the Dom34-Hbs1 complex from *S. cerevisiae*, we have performed SAXS measurements on this complex and compared diffusion curves calculated from different models to the experimental one. To build these models, we used the known crystal structures of isolated yeast and archaeal Dom34 and yeast Hbs1dN134 and of the complex between eRF1 and an eRF3 fragment lacking the GTPase domain [9,18,19]. In these models, Dom34 C-terminal domain and Hbs1 domain III were superimposed onto the corresponding domains from human eRF1 and eRF3, respectively [18]. Due to the absence of the eRF3 GTPase domain in the crystal structure of eRF1-eRF3 complex, we assumed that Hbs1 conformation in the complex is similar to that of the protein alone in the crystal and in solution. This is further supported by site directed mutagenesis experiments on eRF3 that identified residues from domain III (His582, Arg642, Arg646, Val654 and Lys656 from *S. pombe* eRF3 corresponding to Phe528, Arg591, Arg595, Ala603 and Lys605 from Hbs1, respectively) as critical for cell growth [16]. In the Hbs1 structure, these highly conserved residues are located at the interface between domain III and the GTPase domain, this strongly suggest that the integrity of this domain interface is essential for eRF3, and by inference Hbs1, activities. In addition, the substitution by Ala of two eRF3 residues from domain III (Arg642 and Arg646) results in loss of complementation of eRF3 deletion in *S. pombe* and substantially weaker eRF1 binding activity [16]. These residues are located outside eRF1-eRF3 interface [18] and would directly interact with the eRF3 GTPase domain in a

so-called eRF3 "close" conformation that would be similar to EF-Tu and Hbs1 structures. This implies that this "close" conformation is necessary for correct function of eRF3 and by extension to members of the eEF-1A family. We therefore used the coordinates of the Hbs1dN134 fragment previously determined by combining the Hbs1dN134 crystal structure and modelling of the switch I region with SASREF. As a consequence, the only difference between these models is the position of Dom34 domains relative to each other. We have previously observed that *S. cerevisiae* and archaeal Pelota proteins adopt radically different configuration with rotation by roughly 20° and 70° relative to C-terminal domain for N-terminal and central domains, respectively [9]. This allowed us to build two models based on either yeast Dom34 conformation (yeast-like model, Supplementary Fig. 4a) or archaeal Pelota conformation (archaeal-like model, Supplementary Fig. 4b).

From the comparison of the scattering curves calculated from both models with the SAXS curve (Fig. 4a), it turned out that the archaeal-like model gave the best agreement and could serve as a starting point model for further improvement using SASREF. In this archaeal-like model, the conserved and positively charged loop C from Dom34 (residues 174-176) that has been shown to be important for NGD in yeast [20] is located within the central domain and is in close proximity of the Hbs1 GTP binding site. This loop could hence contact the GTP γ-phosphate and be responsible for the higher affinity of Hbs1 for GTP in the presence of Dom34. During the rigid body refinement process using SASREF, we therefore decided to move only the N-terminal and central domains from Dom34 as the comparison of yeast Dom34 and archaeal Pelota crystal structures clearly highlighted intrinsic flexibility of these domains [9]. However, as we anticipate that Dom34 loop C may play an active role in the increase of Hbs1 affinity for GTP in the presence of Dom34, we forced the Cα atom from residues 174-177 of this loop to be within less than 15 Å away from the Cα atoms of Val176 and His255 from Hbs1. We obtain a set of models providing calculated scattering curves compatible with the experimental curve ($\chi \leq 1.7$). All these models have similar conformations differing mainly in the position of Dom34 N-terminal domain, which can rotate on itself. The SAXS measurements cannot discriminate the different positions adopted by this domain.

Nature Structural & Molecular Biology: doi:10.1038/nsmb.1963

Supplementary Table 1: Strains and plasmids

Strain or plamid name	**Description** (genotype for strains; vector/insert/marker for plasmids)	**Rererence**
BMA64	*MAT α, ura3-1, trp1Δ, ade2-1, leu2-3,112, his3-11,15*	This study
BSY1970	*MAT α, ura3-1, trp1Δ, ade2-1, leu2-3,112, his3-11,15, dom34Δ::HIS3*	This study
BSY2029	*MAT a, ura3-1, trp1Δ, ade2-1, leu2-3,112, his3-11,15, dom34Δ::HIS3 ski7Δ::Kan R*	This study
BSY2051	*MAT a, ura3-1, trp1Δ, ade2-1, leu2-3,112, his3-11,15, dom34Δ::HIS3 rps28AΔ::Kan R*	This study
BSY2145	*MAT a, ura3-1, trp1Δ, ade 2-1, leu2-3,112, his3-11,15, hbs1Δ::KanR*	This study
BSY2204	*MAT a, ura3-1, trp1Δ, ade2-1, leu2-3, 112, his3-11, 15, ski7Δ::KanR, hbs1Δ::KanR*	This study
BSY2218	*MAT a, ura3-1, trp1Δ, ade2-1, leu2-3,112, his3-11,15, rps28AΔ::KanR, hbs1Δ::KanR*	This study
Y190	*MAT a gal4 gal80 his3 trp1-901 ade2-101 ura3-52 leu2-3,-112 URA3::GAL-->lacZ, LYS2::GAL(UAS)-->HIS3cyhR*	Bai *et al*, 1996 [21]
pRP1251	*/GAL1-PGK1-SL/URA3*	Doma *et al.*, 2006 [22]
pWL160-A1492C	*/GAL7-rDNA 18S:A1492C/TRP1*	LaRiviere *et al.*, 2006 [23]
pBS3217	pRS415/*DOM34* + promoter/*LEU2*	This work
pBS3611	pRS415/ *HBS1* + promoter/*LEU2*	This work
pBS3614	pRS415/ *HBS1-PROTEIN A* + promoter/*LEU2*	This work
pBS3685	pRS415/ *DOM34-3HA* + promoter/*LEU2*	This work
pACTII	pACTII/two-hybrid vector/*LEU2*	Bai *et al*, 1996 [21]
pAS2	pAS2/two-hybrid vector/*TRP1*	Bai *et al*, 1996 [21]

Nature Structural & Molecular Biology: doi:10.1038/nsmb.1963

Supplementary Figure 1: Experimental electron density map.

Stereo view representation of the experimental electron density map obtained by phasing at 3.2 Å resolution followed by phase extension up to 2.5 Å resolution. The map is contoured at 1σ. The final model fitted into the electron density map is represented as sticks.

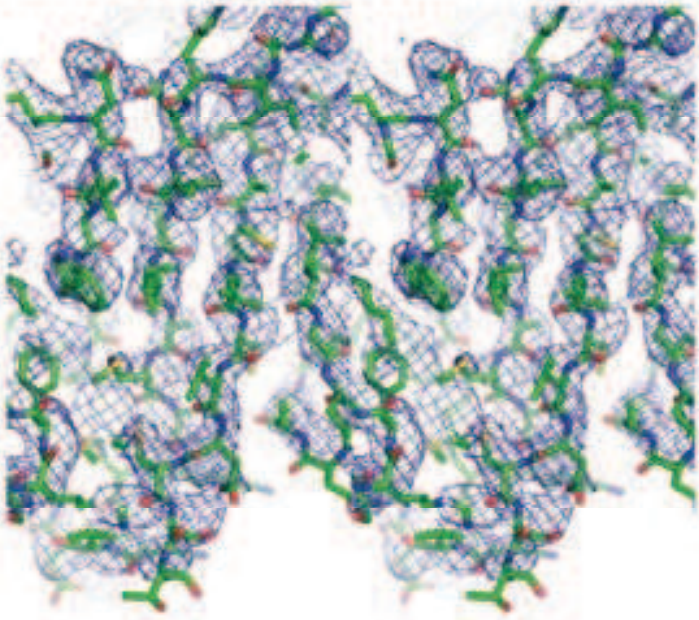

Nature Structural & Molecular Biology: doi:10.1038/nsmb.1963

Supplementary Figure 2: Conformation of Hbs1dN134 in solution.

(**a**) Stereo view of the superimposition of Hbs1dN134 (grey) onto bacterial EF-Tu (salmon) and *S. pombe* eRF3 (green). (**b**) Comparison of the scattering curves calculated from the coordinates of the Hbs1 X-ray structure (green), from a conformation based on the eRF3 structure (blue) and from the model obtained after rigid body movement of the switch I region using the program SASREF (red) with the experimental SAXS curve obtained in the absence of nucleotide (black). (**c**) Distance distribution function P(r) derived from the intensity curve I(q) using the program GNOM [24]. The maximal extension of the protein D_{max} and the radius of gyration R_g are found to be equal to 85 ± 5 Å and 25.9 ± 0.2 Å respectively.

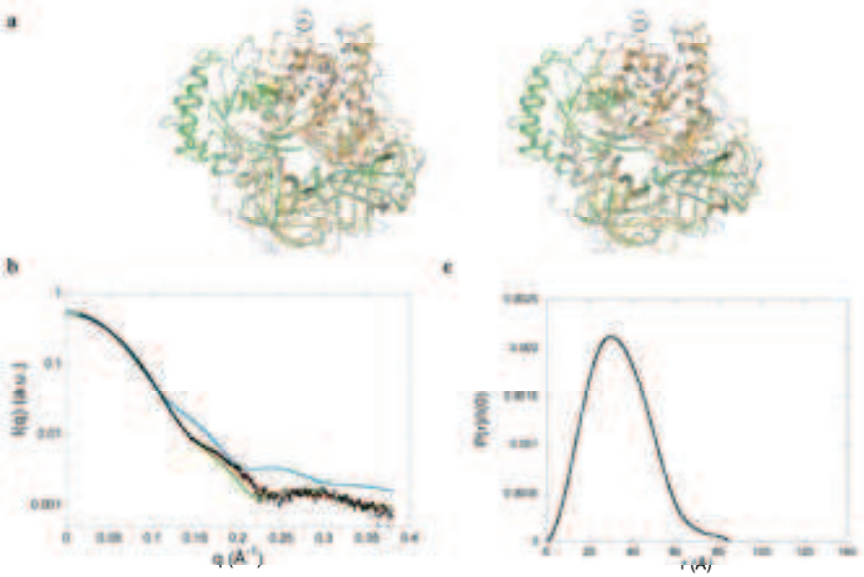

Nature Structural & Molecular Biology: doi:10.1038/nsmb.1963

Supplementary Figure 3. Microcalorimetric measurements

(a, b) Guanine nucleotide binding to Hbs1 mutants. ITC titration curves (upper part) and binding isotherms (lower part) for Hbs1 wild type (a) or Hbs1 K180A mutant (b) interaction with GDP at 20 °C. The curves obtained for interaction of Hbs1 V176G and H255E with both GDP and GTP were comparable to right panel, indicating the absence of binding and are not depicted. Kd and n (the number of binding sites per monomer) are indicated when appropriate. **(c, d)** Heat denaturation profiles of Hbs1 (c) and Dom34 (d) variants obtained by DSC.

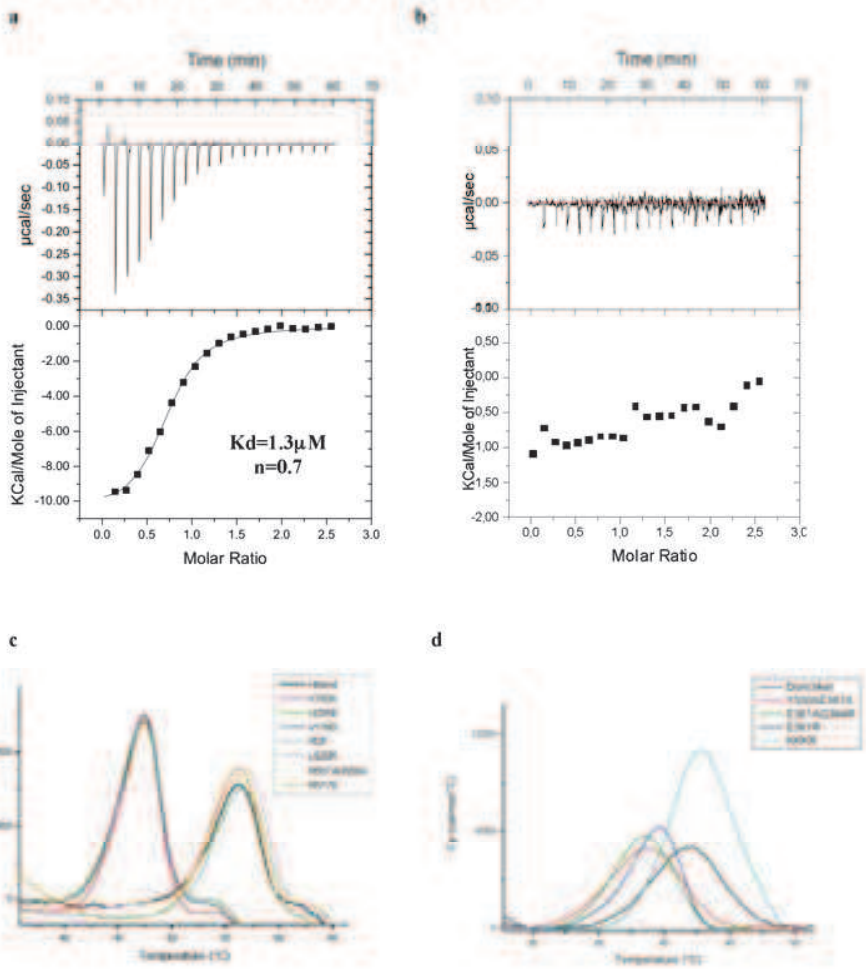

Nature Structural & Molecular Biology: doi:10.1038/nsmb.1963

Supplementary Figure 4: Building SAXS models of Dom34-Hbs1

(**a**) Dom34-Hbs1 initial models: distance distribution function P(r) derived from the intensity curve I(q) using the program GNOM [24]. The curve yields values of D_{max} = 130 ± 5 Å and 37.3 ± 0.5 Å. (**b**) Initial model based on yeast Dom34 conformation. Dom34 N-terminal, central and C-terminal domains are coloured in light green, green and dark green, respectively. Hbs1 GTPase, II and III domains are coloured in light blue, cyan and dark blue, respectively. Loops A, B and C from Dom34 that have been shown to be functionally important in NGD are indicated in red [20]. (**c**) Initial model based on archaeal Pelota conformation with colouring as in panel b. (**d**) Ribbon representation of the optimized Dom34-Hbs1dN134 model. Colouring as in panel b except that loops A, B and C from Dom34 that have been shown to be functionally important in NGD [20], are indicated in yellow, orange and red, respectively. (**e**) Surface representation of the same model using the same color code and orientation as panel d. (**f**) Representation of residue conservation mapped at the surface of this model (same orientation as panel e). Coloring is from blue (highly conserved) to grey (low conservation). (**g**) Close-up view of the contact region between Hbs1 GTPase domain and Dom34 central domain. The Dom34 SPGF and Hbs1 HRDF motifs as well as GTP molecule are shown as sticks. The same color code as in panel d is used.

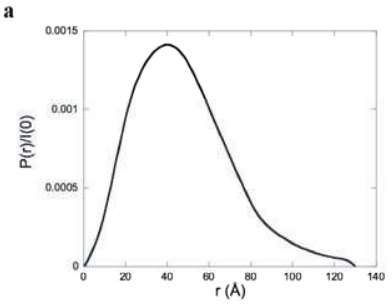

Nature Structural & Molecular Biology: doi:10.1038/nsmb.1963

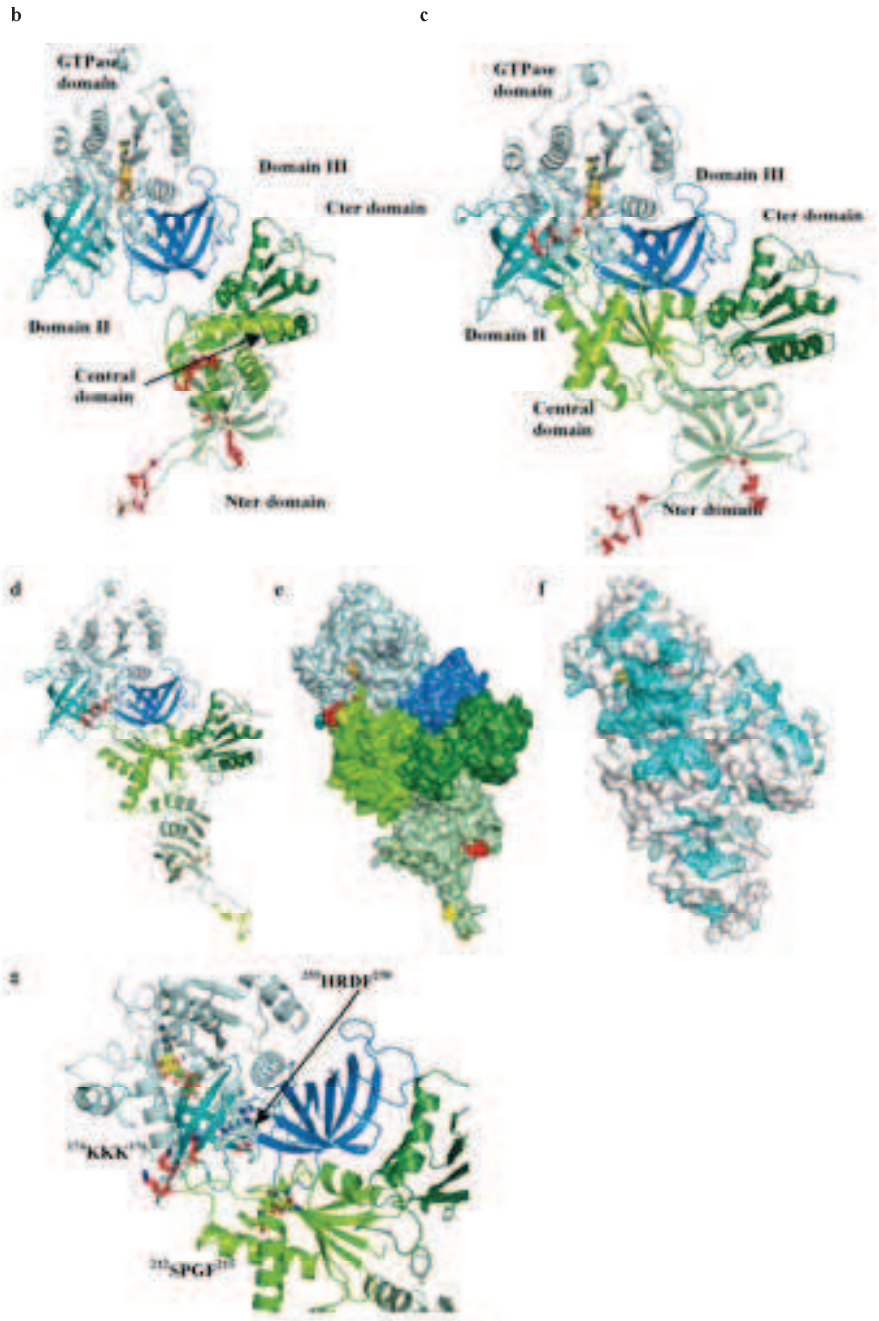

Nature Structural & Molecular Biology doi:10.1038/nsmb.1963

Supplementary Figure 5: Stability and interaction of Dom34 and Hbs1 mutants.

(**a**) Expression and stability of the mutant protein was verified by western analysis on protein extract [23] from the strains used for the analysis of the effect of mutants on NRD. Dom34-3HA and its mutants were detected with anti-HA antibody (Covance MMS-101P) and a secondary goat-anti-mouse IgG antibody (Jackson 115-035-068). Hbs1-protein A and its mutants were detected with PAP (Sigma P1291). As a loading control Stm1 was detected by a polyclonal anti-Stm1 antibody and a secondary goat-anti-rabbit IgG antibody (Pierce 31460). (**b**) Effect of Dom34 and Hbs1 interaction surface mutations on Dom34-Hbs1 interaction. Gal4 activation domain (AD)-Hbs1 and Gal4 DNA binding domain (DBD)-Dom34 fusion proteins, wild type and indicated mutants were assayed for interaction in two-hybrid reporter strain Y190 by measuring β-galactosidase activity. Average activity and SD were calculated for two biological replicas per condition, with two technical replicas per biological replica. (**c**) Expression of Gal4 AD-Hbs1 and Gal4 DBD-Dom34 fusion proteins in Y190 was verified by western analysis on protein extract [23] from the strains used for two-hybrid analysis. Both constructs were detected with anti-Gal4 antibody and a secondary goat-anti-mouse IgG antibody (Jackson 115-035-068). Stm1 served as a loading control.

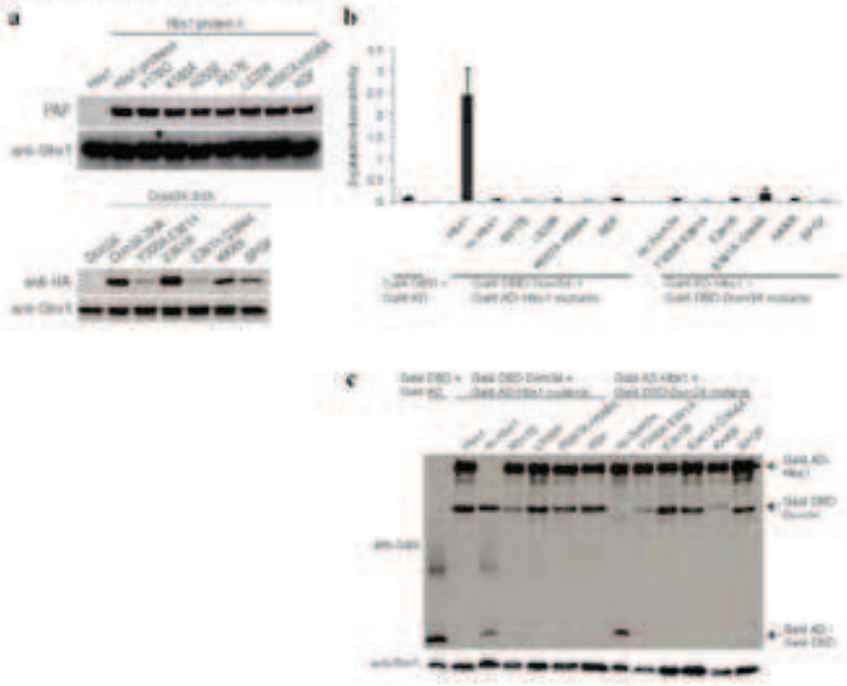

Nature Structural & Molecular Biology: doi:10.1038/nsmb.1963

Supplementary references

1. Kabsch, W. Automatic processing of rotation diffraction data from crystals of initially unknown symmetry and cell constants. *J. Appl. Cryst.* **26**, 795-800 (1993).
2. Terwilliger, T.C. Reciprocal-space solvent flattening. *Acta Crystallogr D Biol Crystallogr* **55**, 1863-71 (1999).
3. Terwilliger, T.C. & Berendzen., J. Automated MAD and MIR structure solution *Acta Cryst. D* **55**, 849-861 (1999).
4. Adams, P.D. et al. PHENIX: building new software for automated crystallographic structure determination. *Acta Crystallogr D Biol Crystallogr* **58**, 1948-54 (2002).
5. Emsley, P. & Cowtan, K. Coot: model-building tools for molecular graphics. *Acta Crystallogr D Biol Crystallogr* **60**, 2126-32 (2004).
6. Laskowski, R.A., MacArthur, M.W., Moss, D.S. & Thornton, J.M. PROCHECK: a program to check the stereochemical quality of protein structures. *J. Appl. Crystallogr.* **26**, 283-91 (1993).
7. Svergun, D.I., Barberato, C. & Koch, M.H.J. CRYSOL - a program to evaluate X-ray solution scattering of biological macromolecules from atomic coordinates. *J. Appl. Crystallogr.* **28**, 768-773 (1995).
8. Petoukhov, M.V. & Svergun, D.I. Global rigid body modelling of macromolecular complexes against small-angle scattering data. *Biophys J* (2005).
9. Graille, M., Chaillet, M. & van Tilbeurgh, H. Structure of yeast Dom34: a protein related to translation termination factor Erf1 and involved in No-Go decay. *J Biol Chem* **283**, 7145-54 (2008).
10. Carr-Schmid, A., Pfund, C., Craig, E.A. & Kinzy, T.G. Novel G-protein complex whose requirement is linked to the translational status of the cell. *Mol Cell Biol* **22**, 2564-74 (2002).
11. Andersen, G.R., Nissen, P. & Nyborg, J. Elongation factors in protein biosynthesis. *Trends Biochem Sci* **28**, 434-41 (2003).
12. Kjeldgaard, M., Nissen, P., Thirup, S. & Nyborg, J. The crystal structure of elongation factor EF-Tu from Thermus aquaticus in the GTP conformation. *Structure* **1**, 35-50 (1993).
13. Noble, C.G. & Song, H. Structural studies of elongation and release factors. *Cell Mol Life Sci* **65**, 1335-46 (2008).
14. Song, H., Parsons, M.R., Rowsell, S., Leonard, G. & Phillips, S.E. Crystal structure of intact elongation factor EF-Tu from Escherichia coli in GDP conformation at 2.05 A resolution. *J Mol Biol* **285**, 1245-56 (1999).
15. Leibundgut, M., Frick, C., Thanbichler, M., Bock, A. & Ban, N. Selenocysteine tRNA-specific elongation factor SelB is a structural chimaera of elongation and initiation factors. *Embo J* **24**, 11-22 (2005).
16. Kong, C. et al. Crystal structure and functional analysis of the eukaryotic class II release factor eRF3 from S. pombe. *Mol Cell* **14**, 233-45 (2004).
17. Andersen, G.R., Valente, L., Pedersen, L., Kinzy, T.G. & Nyborg, J. Crystal structures of nucleotide exchange intermediates in the eEF1A-eEF1Balpha complex. *Nat Struct Biol* **8**, 531-4 (2001).
18. Cheng, Z. et al. Structural insights into eRF3 and stop codon recognition by eRF1. *Genes Dev* **23**, 1106-18 (2009).
19. Lee, H.H. et al. Structural and functional insights into Dom34, a key component of No-Go mRNA decay. *Mol Cell* **27**, 938-50 (2007).
20. Passos, D.O. et al. Analysis of Dom34 and Its Function in No-Go Decay. *Mol Biol Cell* (2009).
21. Bai, C. & Elledge, S.J. Gene identification using the yeast two-hybrid system. *Methods Enzymol* **273**, 331-47 (1996).
22. Doma, M.K. & Parker, R. Endonucleolytic cleavage of eukaryotic mRNAs with stalls in translation elongation. *Nature* **440**, 561-4 (2006).
23. LaRiviere, F.J., Cole, S.E., Ferullo, D.J. & Moore, M.J. A late-acting quality control process for mature eukaryotic rRNAs. *Mol Cell* **24**, 619-26 (2006).
24. Svergun, D.I. Determination of the regularization parameter in indirect transform methods

Nature Structural & Molecular Biology: doi:10.1038/nsmb.1963

using perceptual criteria. *J. Appl. Crystallogr.* **25**, 495 - 503 (1992).
25. Kushnirov, V.V. Rapid and reliable protein extraction from yeast. *Yeast* **16**, 857-60 (2000).

Nature Structural & Molecular Biology: doi:10.1038/nsmb.1963

Supplementary information for:

Dom34-Hbs1 mediated dissociation of inactive 80S ribosomes promotes restart of translation after stress.

Antonia M.G. van den Elzen[1], Anthony Schuller[2], Rachel Green[2], and Bertrand Séraphin[1,*]

[1] Equipe Labellisée La Ligue, Institut de Génétique et de Biologie Moléculaire et Cellulaire (IGBMC), Centre National de Recherche Scientifique (CNRS) UMR 7104/Institut National de Santé et de Recherche Médicale (INSERM) U964/Université de Strasbourg, 67404 Illkirch, France

[2] Howard Hughes Medical Institute, Department of Molecular Biology and Genetics, Johns Hopkins University School of Medicine, Baltimore, Maryland, USA.

* Corresponding author: Bertrand Séraphin (seraphin@igbmc.fr)

Running title: Dom34-Hbs1 modulates ribosomal subunit availability after stress

Supplementary Material and Methods

In vitro translation

Translational extracts {Tuite, 1986 #255} were prepared from a *dom34*Δ*hbs1*Δ strain (BSY2550) as follows. 4 L of culture at OD_{600} = 1 was washed in 200 ml cold water, incubated in 100 ml β-mercaptoethanol 10mM; EDTA 2 mM for 30 minutes at room temperature, washed in 100 ml cold sorbitol 1M and resuspended in 1M sorbitol at room temperature at a concentration of 10 ml/g cells, spinning at 2000 x g for 5 min at 4°C in between. Zymolyase was added at 4 µg/ml final concentration and the reaction was stopped by pelleting the resulting spheroplast at 1000 x g for 10 min at room temperature when 75% of cells had converted to spheroplasts. Spheroplasts were washed in 200 ml sorbitol 1.2 M and incubated in 500 ml YPDA-sorbitol 1M at 25°C 40 rpm. Spheroplasts were harvested at 1000 x g for 10 min at 4°C and lysed using glass beads (0.5 ml/g cells) in lysis buffer (20 mM Hepes-KOH pH7.4; 100 mM KOAc; 2 mM $Mg(OAC)_2$; 2 mM DTT; 0.5 mM PMSF; protease inhibitor cocktail) (1 ml/g cells) in 5 cycles of shaking vigorously at 2 Hz for 20 seconds with

1 minute intervals on ice. Lysates were cleared spinning 30 000 x g for 15 min at 4°C, then 100 000 x g for 30 min at 4°C. Glycerol was added at 10% final concentration for storage at -80°C.

In vitro translation was performed basically as described in {Tarun, 1995 #256}. Translational extracts were incubated with 150 U/ml micrococcal nuclease (New England Biolabs) in presence of 480 µM $CaCl_2$ for 5 minutes at 26°C, before adding 2 mM EGTA on ice. 7.5 µl extract was added to 7.5 µl translation mix containing 0,1 µl RNasin (Promega), 500 ng firefly luciferase-A(50) mRNA {Gallie, 1991 #273} and 4 µg creatine phosphokinase (Roche) in 22 mM Hepes-KOH pH 7.4; 120 mM KOAc; 2 mM MgOAc; 750 µM ATP; 100 µM GTP; 25 mM creatine phosphate; 40 µM amino acid mixture (Promega); 1.7 mM DTT. After 1 h incubation at 26°C luciferase activity was measured in 10 s measurements using a Lumat LB 9507 luminometer (Berthold technologies) adding 1 µl translation reaction to 50 µl luciferine mix (470 µM luciferine; 530 µM ATP; 270 µM coenzyme A; 20 mM Tris-phosphate pH 7.8; 1.07 mM $MgCl_2$; 2.7 mM $MgSO_4$; 100 µM EDTA; 33.3 mM DTT).

The Dom34-Hbs1 complex added to the translation reaction was purified as described in {Collinet, 2011 #331}. Hbs1 alone was purified from BL21 codon+ cells expressing C-terminally 6xHis-tagged Hbs1 grown in Autoinduction media Terrific Broth Base including Trace elements (Formedium) over Ni-NTA agarose (Qiagen) after cell lysis in a Cell Disruptor (Constant Systems) at 1.55 kbar, using lysis buffer (75 mM Hepes pH 7.9, 300 mM NaCl, 5 mM β-mercaptoethanol, 1% Tween, 20 mM imidazole, 10% glycerol, 2 mM $MgCl_2$), wash buffer (50 mM Hepes pH 7.9, 500 mM NaCl, 5 mM β-mercaptoethanol, 20 mM imidazole, 10% glycerol, 2 mM $MgCl_2$) and elution buffer (50 mM Hepes pH 7.9, 500 mM NaCl, 5 mM β-mercaptoethanol, 300 mM imidazole, 10% glycerol, 2 mM $MgCl_2$). Both Hbs1 and the Dom34-Hbs1 complex were further purified over a Superdex 75 10/300 GL column (GE Healthcare) in 20mM Tris-Cl pH 7.5, 200mM NaCl, 5mM β-mercaptoethanol, 5% glycerol.

Supplementary table 1: Strains and plasmids

Strain or plasmid name	Description (genotype for strains; vector/insert/marker for plasmids)	Reference
BMA64	*MAT α, ura31, trp1Δ, ade21, leu23,112, his311,15*	{Baudin-Baillieu, 1997 #471}

BSY1970	*MAT α, ura31, trp1Δ, ade21, leu23,112, his311,15, dom34Δ::HIS3*	{van den Elzen, 2010 #80}
BSY2145	*MAT a, ura31, trp1Δ, ade 21, leu23,112, his311,15, hbs1Δ::KanR*	{van den Elzen, 2010 #80}
BSY2550	*MAT a, ade 2-1 his3-11,15, leu2-3,112, trp1delta ura3-1, dom34Δ::HIS3, hbs1Δ::KanR*	This study
N20T20	*MAT a, ura3-1, trp1Δ, ade2-1, leu2-3,112, his3-11,15, stm1Δ::TRP1*	Gift from F. Lacroute and F. Wyers
BSY2626	*MAT a, ura3-1, trp1Δ, ade2-1, leu2-3,112, his3-11,15, stm1Δ::TRP1, dom34Δ::HIS3*	This study
pBS3614	pRS415/ *HBS1-PROTEIN A* + promoter/*LEU2*	{van den Elzen, 2010 #80}
pBS3675	pRS415/ *hbs1 V176G-PROTEIN A* + promoter/*LEU2*	{van den Elzen, 2010 #80}
pBS3685	pRS415/ *DOM34-3HA* + promoter/*LEU2*	{van den Elzen, 2010 #80}
pBS3701	pRS415/ *dom34 E361R-3HA* + promoter/*LEU2*	{van den Elzen, 2010 #80}
pBS4415	pRS415/ *hbs1ΔN-ter (2-149)-PROTEIN A* + promoter/*LEU2*	This study

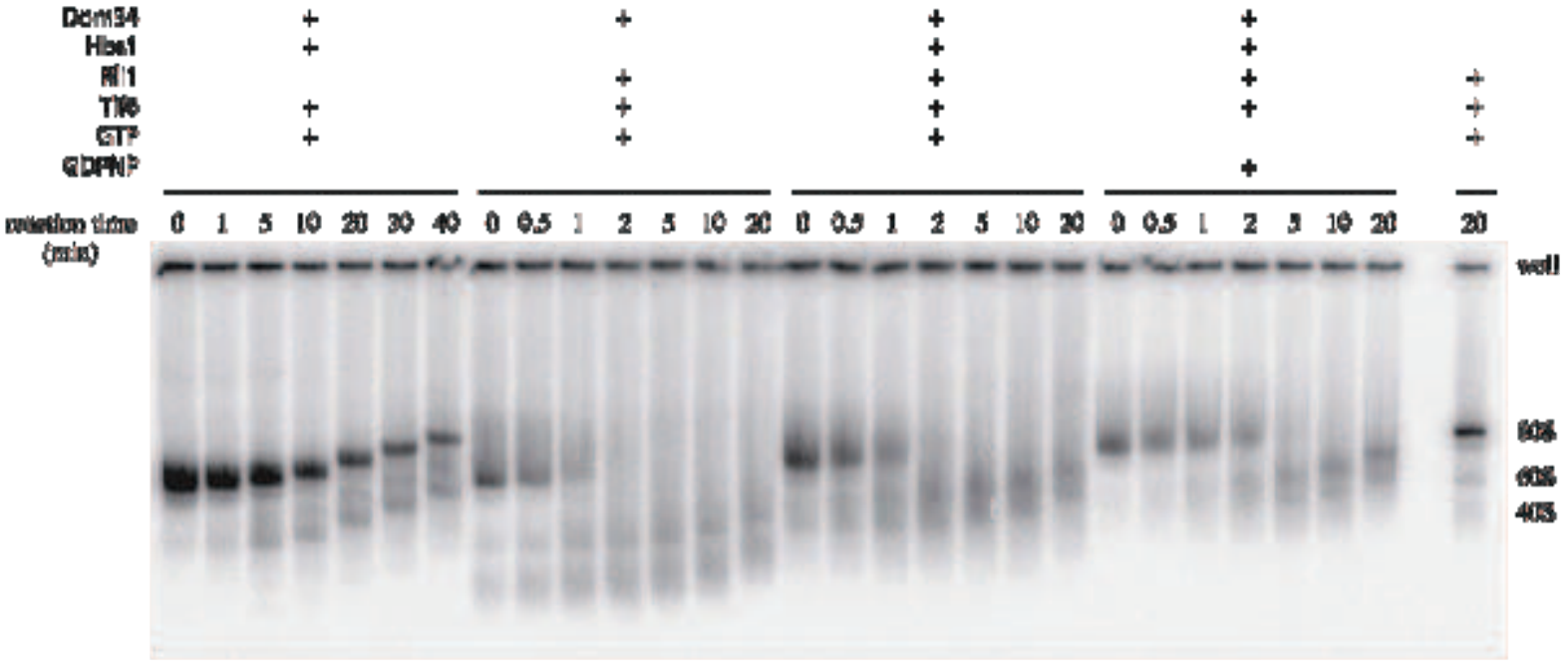

Supplementary Figure 1. Kinetic analysis of Dom34, Hbs1 and Rli1 mediated dissociation of inactive ribosomes from glucose starved yeast.

Dom34-Hbs1 and Rli1 dissociate ribosomes from glucose-starved yeast *in vitro*. ^{32}P-labeled 80S ribosomes purified from glucose-starved yeast were incubated with the indicated proteins in presence of ATP and GTP or GDPNP. At the indicated time points fractions of the reactions were analyzed on a 3% native acrylamide gel {Shoemaker, 2010 #22}. This figure shows one of the gels from which the rate constants in Figure 2B were determined.

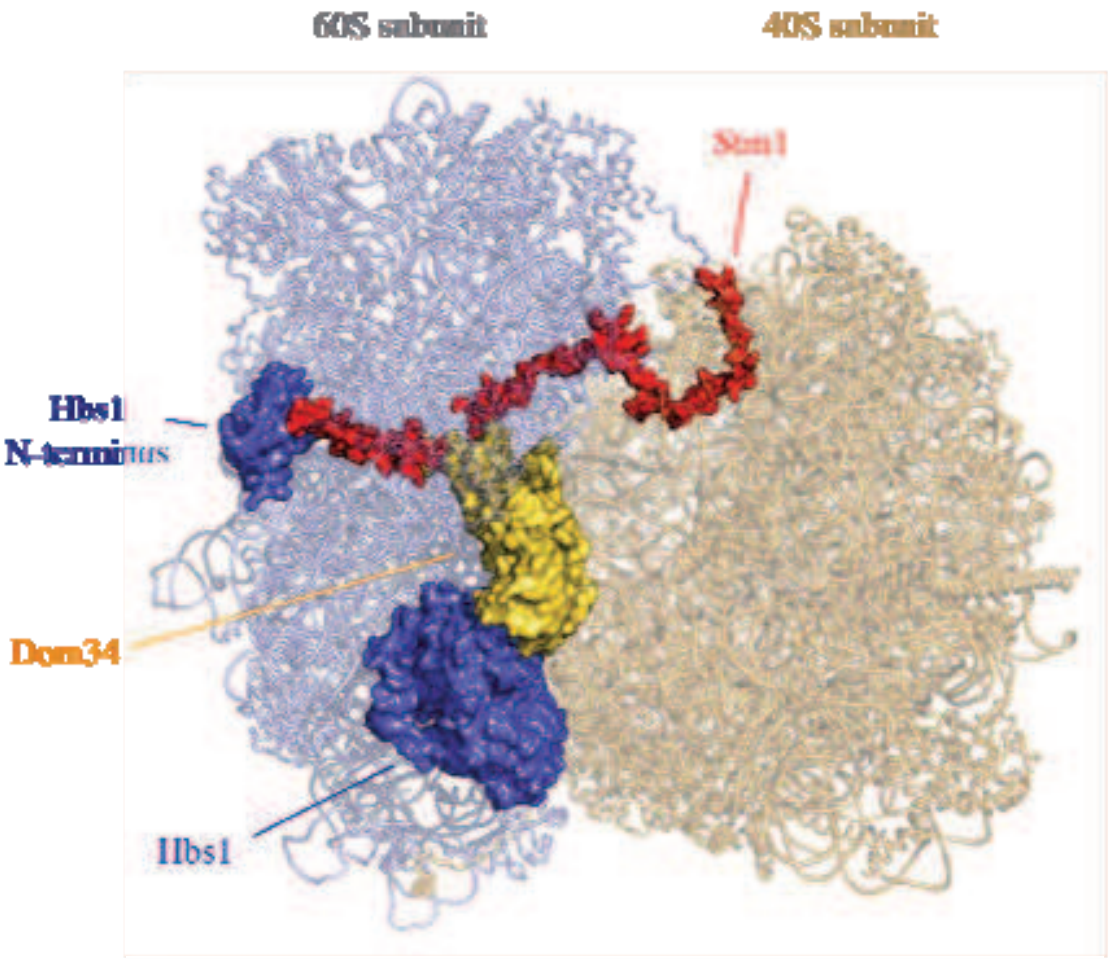

Supplementary Figure 2. Localization of the Dom34-Hbs1 complex and Stm1 in a model of the 80S ribosome.

Alignment of a high resolution structure of an 80S ribosome from glucose depleted yeast containing Stm1 (PDB 3u5b, 3u5c, 3u5d and 3u5e) {Ben-Shem, 2011 #173} and a cryo-EM structure of the Dom34-Hbs1 complex bound to an 80S ribosome (PDB 3IZQ) {Becker, 2011 #180}.

Supplementary References

Baudin-Baillieu A, Guillemet E, Cullin C, Lacroute F (1997) Construction of a yeast strain deleted for the TRP1 promoter and coding region that enhances the efficiency of the polymerase chain reaction-disruption method. *Yeast* **13:** 353-356

Becker T, Armache JP, Jarasch A, Anger AM, Villa E, Sieber H, Motaal BA, Mielke T, Berninghausen O, Beckmann R (2011) Structure of the no-go mRNA decay complex Dom34-Hbs1 bound to a stalled 80S ribosome. *Nat Struct Mol Biol* **18:** 715-720

Ben-Shem A, Garreau de Loubresse N, Melnikov S, Jenner L, Yusupova G, Yusupov M (2011) The structure of the eukaryotic ribosome at 3.0 A resolution. *Science* **334:** 1524-1529

Collinet B, Friberg A, Brooks MA, van den Elzen T, Henriot V, Dziembowski A, Graille M, Durand D, Leulliot N, Saint Andre C, Lazar N, Sattler M, Seraphin B, van Tilbeurgh H (2011) Strategies for the structural analysis of multi-protein complexes: lessons from the 3D Repertoire project. *J Struct Biol* **175:** 147-158

Gallie DR, Feder JN, Schimke RT, Walbot V (1991) Post-transcriptional regulation in higher eukaryotes: the role of the reporter gene in controlling expression. *Mol Gen Genet* **228:** 258-264

Tarun SZ, Jr., Sachs AB (1995) A common function for mRNA 5' and 3' ends in translation initiation in yeast. *Genes Dev* **9:** 2997-3007

Tuite MF, Plesset J (1986) mRNA-dependent yeast cell-free translation systems: theory and practice. *Yeast* **2:** 35-52

van den Elzen AM, Henri J, Lazar N, Gas ME, Durand D, Lacroute F, Nicaise M, van Tilbeurgh H, Seraphin B, Graille M (2010) Dissection of Dom34-Hbs1 reveals independent functions in two RNA quality control pathways. *Nat Struct Mol Biol* **17:** 1446-1452

Journal of Structural Biology 175 (2011) 147–158

Contents lists available at ScienceDirect

Journal of Structural Biology

journal homepage: www.elsevier.com/locate/yjsbi

Strategies for the structural analysis of multi-protein complexes: Lessons from the 3D-Repertoire project

B. Collinet [a,f], A. Friberg [b,c], M.A. Brooks [a,4], T. van den Elzen [d,e], V. Henriot [d,1], A. Dziembowski [e,2], M. Graille [a], D. Durand [a], N. Leulliot [a,3], C. Saint André [a], N. Lazar [a], M. Sattler [b,c], B. Séraphin [d,e,*], H. van Tilbeurgh [a,*]

[a] IBBMC-CNRS UMR8619, IFR 115, Bât. 430, Université Paris-Sud, 91405 Orsay, France
[b] Institute of Structural Biology, Helmholtz Zentrum München, 85764 Neuherberg, Germany
[c] Biomolecular NMR and Munich Center for Integrated Protein Science, Department Chemie, Technische Universität München, 85747 Garching, Germany
[d] Equipe Labellisée La Ligue, Institut de Génétique et de Biologie Moléculaire et Cellulaire (IGBMC), Institut National de Santé et de Recherche Médicale (INSERM), U964/Centre National de Recherche Scientifique (CNRS), UMR 7104/Université de Strasbourg, 67404 Illkirch, France
[e] Centre de Génétique Moléculaire (CGM), CNRS 1 Avenue de la Terrasse, 91198 Gif-sur-Yvette Cedex, France
[f] UPMC Univ. Paris 06, UFR 927 Sciences de la vie, F-75005 Paris, France

ARTICLE INFO

Article history:
Received 17 January 2011
Received in revised form 18 March 2011
Accepted 19 March 2011
Available online 2 April 2011

Keywords:
Protein complex validation for structural biology
Limited proteolysis
Crystallography
NMR
SAXS
KEOPS/EKC
MAK
RES complex
Dom34
Hbs1
Trm8
Trm81
Trm112

ABSTRACT

Structural studies of multi-protein complexes, whether by X-ray diffraction, scattering, NMR spectroscopy or electron microscopy, require stringent quality control of the component samples. The inability to produce 'keystone' subunits in a soluble and correctly folded form is a serious impediment to the reconstitution of the complexes. Co-expression of the components offers a valuable alternative to the expression of single proteins as a route to obtain sufficient amounts of the sample of interest. Even in cases where milligram-scale quantities of purified complex of interest become available, there is still no guarantee that good quality crystals can be obtained. At this step, protein engineering of one or more components of the complex is frequently required to improve solubility, yield or the ability to crystallize the sample. Subsequent characterization of these constructs may be performed by solution techniques such as Small Angle X-ray Scattering and Nuclear Magnetic Resonance to identify 'well behaved' complexes. Herein, we recount our experiences gained at protein production and complex assembly during the European 3D Repertoire project (3DR). The goal of this consortium was to obtain structural information on multi-protein complexes from yeast by combining crystallography, electron microscopy, NMR and *in silico* modeling methods. We present here representative set case studies of complexes that were produced and analyzed within the 3DR project. Our experience provides useful insight into strategies that are more generally applicable for structural analysis of protein complexes.

1. Introduction

Proteins rarely act alone in cells. Instead, they are usually part of assemblies with other macromolecules, such as proteins and nucleic acids. The integrity of these complexes is generally essential for cellular survival (Robinson et al., 2007). Many protein–protein complexes in particular are ubiquitous and are central to biological pathways. A variety of biochemical and proteomic technologies have provided crucial information on the composition of multi-protein assemblies, especially when performed in an high-throughput manner (Gavin and Superti-Furga, 2003; Gavin et al., 2002; Krogan et al., 2006). Of these techniques, the now widely used Tandem Affinity Purification technology (TAP tagging, (Puig et al., 2001; Rigaut et al., 1999) has been successfully applied during the course of large-scale proteomic studies and has led to the identification of many protein complexes.

Complexes which can be purified from their host organism in large quantities are immediately seen to be more tractable than those which cannot, and impressive results have been obtained

* Corresponding authors.
E-mail addresses: seraphin@igbmc.fr (B. Séraphin), Herman.Van-Tilbeurgh@u-psud.fr (H. van Tilbeurgh).
[1] Present address: LEBS, CNRS, Avenue de la Terrasse, 91198 Gif-sur-Yvette Cedex, France.
[2] Present address: Institute of Biochemistry and Biophysics, Polish Academy of Sciences, University of Warsaw, 02-106 Warsaw, Poland.
[3] Present address: Laboratoire de Cristallographie et RMN Biologiques, Université Paris Descartes, CNRS-UMR8015 Paris Cedex, France.
[4] Present address: Evotec (UK) Ltd., 114 Milton Park, Abingdon, Oxon OX14 4SA, UK.

1047-8477/$ - see front matter © 2011 Elsevier Inc. All rights reserved.
doi:10.1016/j.jsb.2011.03.018

in certain cases when nature has facilitated the task of protein production (*e.g.* globins, proteasomes and ribosomes) (Ban et al., 2000; Clemons et al., 1999; Groll et al., 1997; Perutz et al., 1960). However, most multi-protein complexes are present at low abundance in cells and therefore it is difficult to obtain the sufficiently high yields that are needed for structural studies. Hence, the vast majority of complexes must be produced by recombinant cloning and expression technologies. Two major strategies are used for the production of complexes. The first consists of the *in vitro* reconstitution of the complex by mixing of individually purified protein components, usually followed by additional purification of the reconstituted complex. The second strategy comprises co-expression of the various protein components. This can be performed effectively by transforming the expression host with poly-cistronic vectors that encode all components of the complex. An alternative approach consists of introducing in the expression host multiple plasmids encoding the individual subunits and carrying different selection genes.

Structural genomics programs have yielded tremendous advances in structure determination of single proteins. Vast improvements in protein expression and purification have provided strategies for the preparation of high quality samples for structural studies, mainly by NMR spectroscopy and X-ray crystallography. However, most of the structural genomics programs have concentrated on structure determination of single proteins or domains, the main drive being the discovery of new protein folds and the completion of protein structure space (Stevens et al., 2001). In Europe, structural genomics took another turn and targeted protein complexes. Two European Integrated Research projects have concentrated on multi-protein complexes. The Spine 2 project endeavored to perform the structural analysis of complexes involved in human health (http://www.spine2.eu/SPINE2/). In parallel the European 6th framework program 3D Repertoire originated from a systematic proteomics study that used tandem-affinity purification (TAP) and mass spectrometry in a large-scale approach to characterize multiprotein complexes in *Saccharomyces cerevisiae* (http://www.3drepertoire.org/). The main goal of this project was to solve the structures of all amenable protein complexes from the budding yeast *S. cerevisiae* at the best feasible resolution, by electron microscopy, X-ray crystallography, NMR, small angle X-ray scattering (SAXS) and *in silico* methods.

In this manuscript, we present some strategies that were successfully applied within the 3D Repertoire project for obtaining high quantities of multi-protein complexes. We also discuss methodologies for obtaining good quality crystals of complexes. Although X-ray crystallography remains the method of choice for the high-resolution structure determination of multi-protein complexes, complementary techniques can be very helpful for providing crucial structural information. We illustrate here a number of case studies for which SAXS was decisive in providing testable structural models for complexes that could not be crystallized but for which structures of the individual components were known. NMR spectroscopy is also useful for the optimization of constructs for structural analysis, as well as for providing information on the folding and assembly of a complex, and one case in point is described herein.

2. Material and methods

2.1. Expression and purification of the KEOPS/EKC complex and subcomplexes

We introduced a T7 promoter and terminator sequences (similar to those found in pET-family vectors) respectively at the 5′ and 3′ ends of the polycistronic gene operon. The lac-operator sequence was placed downstream of the T7 promoter sequence in order to subclone the polycistronic sequence in an expression vector containing the LacI gene. We then introduced the sequences of the target open reading frames (ORFs), each having its own RBS (ribosome binding site), AUG start codon as well as stop codon sequences. We also included specific restriction sites allowing cloning of sub-complexes into other expression vectors. The synthetic 3.5 kb gene was purchased to DNA 2.0 (Menlo Park, USA) and was cloned into a pUC derivative vector (pJ241_KEOPS/EKC-WT). The expression of this large polycistronic mRNA was by virtue of the T7 RNA polymerase system. As every ORF has its own RBS sequence, start and stop codon, every mRNA molecule can be translated by more than one ribosome.

The co-expression of the five KEOPS/EKC proteins was achieved by transforming BL21-AI *Escherichia coli* (Invitrogen, Carlsbad USA) with the vector pJ241_KEOPS/EKC-WT. Cultures were grown at 37 °C until the OD_{600nm} reached 0.4–0.5 and were then shifted to 15 °C for at least 45 min and expression was triggered by adding 2 g/L of L-arabinose and 1 mM IPTG and incubating overnight at 15 °C. Following centrifugation of the cultures at 6000g for 20 min, bacterial pellets were suspended in 35 mL of lysis buffer (Tris–HCl 25 mM pH 7.5 + 150 mM NaCl + 5 mM 2-mercaptoethanol). Bacterial lysates were then centrifuged and the supernatants applied onto Ni-IDA (Macherey Nagel, Düren, Germany) resin. Protein complex retained on the resin was eluted using imidazole. Fractions containing 10–40 mM imidazole were pooled and further purified by size exclusion chromatography using a Superdex 200 16/60 column (GE Healthcare). KEOPS/EKC complex was purified by a final step of ion exchange chromatography (Mono Q column equilibrated with lysis buffer devoid of NaCl).

2.2. Expression and purification of the Mtq2-Trm112 complex

The construction used to over-express the Mtq2 and Trm112 proteins from *E. cuniculi* was designed on the same model as for the KEOPS complex. Briefly, a synthetic DNA sequence containing the coding sequences for Trm112 (flanked by the *Nde* I and *Not* I restriction sites at the 5′ and 3′ ends, respectively) and Mtq2 (flanked by the *Nco* I and *Xho* I restriction sites at the 5′ and 3′ ends, respectively and containing an hexa-histidine tag at the C-terminal extremity of the protein), separated by a RBS sequence (containing an enhancer sequence and the Shine-Dalgarno sequence) was purchased (GenScript Corporation, Piscataway, NJ, USA). This fragment was further sub-cloned into pET21-a vector between *Nde* I and *Xho* I sites. Expression of the His-tagged Mtq2-Trm112 complex was performed using the *E. coli* strain BL21(DE3) Gold (Novagen). 800 ml of culture in 2xYT medium (BIO101 Inc.) containing ampicillin at 50 μg/ml were incubated at 37 °C until an OD600 of about 0.6–0.8 and induced with IPTG 0.5 mM final at 28 °C for 4 h. Cell were harvested by centrifugation, suspended in 40 ml of 20 mM Tris–HCl pH 7.5, 200 mM NaCl, 5 mM 2-mercaptoethanol (buffer A), and stored at −20 °C. Cell lysis was achieved by sonication. His-tagged complex was purified on a nickel-nitrilotriacetic acid (Ni^{2+}–NTA) column (Qiagen Inc.) followed by gel filtration on a Superdex 75 (16/60) column (GE Healthcare) equilibrated in buffer A.

2.3. Mak complex expression

The Mak3 coding sequence was amplified by PCR with oligonucleotides OBS1451 (5′ GATTCTAGAT AAGGAGGATA TATATGCATC ACCATCACCA TCACATGGAA ATAGTGTACA AGCCATT 3′) and OBS1452 (5′ CAATCCGGAT TATGTGGCCA GCCGGCCAT 3′) and the Phusion polymerase (Finnzymes). OBS1451 contained a Ribosome Binding site and 6His tag coding sequence. The product was digested with *Xba* I and *Bsp*EI and inserted in the pBS2454 expression vector generating pBS2870. In parallel, the Mak10 and Mak31 coding sequences were amplified by PCR using the Phusion polymerase (Finnzymes) and, respectively, oligonucleotides OBS1453

(5′ GTCCGGATCA TAAGGAGGAT ATATATGGAA GTAGACAGTA TATTA 3′), OBS1454 (5′ GGTCCGGATT ATTTATAGCG GTCTTGCT 3′), OBS1455 (5′ GTCCGGATCA TAAGGAGGAT ATATATGGAC ATCTTG AAAC TGTCA 3′), OBS1456 (5′ GGTCCGGACT AAACAATATT AGCC ATCAA 3′). PCR fragments were cloned using the Topo Blunt kit (Invitrogen) generating pBS2856 and pBS2851. The absence of unwanted mutations was ascertained by sequencing the whole inserts. Then, the Mak10 coding sequence was inserted as a *Bsp*EI fragment in pBS2870, generating pBS2880. Finally, the Mak31 coding sequence was transferred as a *Bsp*EI fragment in pBS2880, generating pBS2886. pBS2870, pBS2880 and pBS2886 were transformed in BL21(DE3)LysS cells and protein expression induced by addition of IPTG or growth in autoinducing media. Cells expressing operon constructs were broken with a Cell Disruptor (Constant systems). Purifications were performed on Ni^{2+}–NTA in batches in 20 mM Tris–Cl pH8.0, 10 mM imidazole, 500 mM NaCl, 2 mM 2-mercaptoethanol, 0.2% NP40. After several washes, proteins were eluted with the same buffer adjusted to 200 mM imidazole. Samples corresponding to the eluted fractions, and in some cases to soluble proteins isolated from the cell extract, were mixed with SDS-containing loading buffer before fractionation on denaturing gels. Proteins were detected by Coomassie staining.

2.4. Hbs1-Dom34 expression and purification

Dom34Δdomain1 (aminoacids 1–136 deleted), Dom34Δdomain2 (amino acids 141–275 replaced by $(Gly)_4$) and Dom34Δdomain3 (aminoacids 276–386 deleted) deletion mutants were produced by fusion PCR and inserted in yeast expression vector (AMGvdE and BS, unpublished) generating pBS3453, pBS3454 and pBS3455, respectively. The Dom34 domain deletion mutants were then amplified with the introduction of a C-terminal strep-tag using OBS3440 (5′ GGCTCCCATA TGGAGTATAA ATCAGACACC GC 3′) and OBS3171 (5′ acaggtacct tatttttcga actgcgggtg gctccactcc tcaccatcgt cttcatc 3′) (Dom34Δdomain1), OBS3170 (5′ GGCtcccata tgaaggttat tagtctgaaa aagg 3′) and OBS3171 (Dom34Δdomain2) or OBS3170 and OBS3443 (5′ ACAGGTACCT TATTTTTCGA ACTGCGGGTG GCTCCAAGTA TCTTGCAGCT TTGAAGC 3′) (Dom34Δdomain3), digested with *Nde* I and *Kpn* I and cloned into a pACYC-LIC + vector generating pBS3507, pBS3508 and pBS3509, respectively. All constructs were verified by sequencing.

BL21(DE3) cells containing C-terminally Strep-tagged Dom34 and/or C-terminally His-tagged Hbs1 expressing plasmid were grown in 200 ml ZYM-5052 (Studier, 2005) containing chloramphenicol 25 μg/ml and/or kanamycin 50 μg/ml at 37 °C for 7 h, then at 25 °C for 14 h. Cells were harvested by spinning at 6000*g* 10 min 4 °C, washed in 20 ml PBS (4 °C) followed by centrifugation at 5000 rpm 8 min 4 °C, and then suspended in 10 ml buffer W (100 mM Tris pH 8; 1 mM EDTA; 150 mM NaCl). Cells were lysed by passing them through a Cell Disruptor (Constant Systems) at 1.55 kbar, followed by rinsing with 5 ml buffer W. The resulting 15 ml cell lysates were centrifuged at 12000 rpm 30 min 4 °C. Strep-purification was performed on the supernatant with the Strep-tag®/Strep-tactin® affinity purification kit (IBA Biotechnology), following the manufacturer's instructions and using a 200 μl column volume. Samples from induced culture, supernatant and pellet after cell lysis and flowthrough (1:40000 of total volume) and of elution fraction E3 and E4 (1:560 of total elution volume) were analyzed on 12% SDS–PAGE and visualized by Coomassie staining.

2.5. Sample preparation for NMR measurements

Plasmids for the production of recombinant proteins were prepared using standard cloning techniques using pET-derived vectors (Novagen). $Snu17^{1-148}$, $Snu17^{1-113}$, $Bud13^{60\text{-mer}}$ and $Bud13^{40\text{-mer}}$ were expressed fused to histidine-tag to facilitate purification with Ni^{2+}–NTA resin (Qiagen). Lysogeny broth (LB) medium was used to prepare unlabeled samples. For $^{15}N/^{13}C$ and ^{15}N isotope-labeled NMR samples M9 minimal medium with ^{13}C-glucose and/or $^{15}NH_4Cl$ as the sole carbon and nitrogen sources, respectively, were utilized. Details on the cloning and purification of Bud13 constructs were previously described (Brooks et al., 2009). Snu17 proteins were obtained using similar procedures. Additionally, a shorter $Bud13^{22\text{-mer}}$ was purchased from Peptide Specialty Laboratories (Heidelberg, Germany), and extensively dialyzed before usage. Proteins and peptides were kept in a standard NMR buffer (20 mM sodium phosphate pH 6.9, 150 mM NaCl and 1 mM DTT, 0.02% NaN_3).

2.6. NMR

NMR data were acquired on a 600 MHz instrument (Bruker) equipped with pulse field gradients and with a cryo-cooled probe head. For the backbone assignment of free $Snu17^{1-113}$, the following standard experiments were recorded at 298 K: $^1H,^{15}N$ HSQC, HNCA, HNCACB, CBCA(CO)NH and $^1H,^{15}N$ HSQC-NOESY (Sattler et al., 1999). The recorded data were processed with NMRPipe/NMRDraw (Delaglio et al., 1995) and visualized as well as analyzed in NMRView (v5.0.4) (Johnson and Blevins, 1994). Spectra for figures were exported directly from Topspin v2.1 (Bruker). For backbone assignment and peptide titrations, the NMR buffer was supplemented with 10% DMSO. Hydrogen/Deuterium-exchange was recorded after lyophilization of the $Snu17^{1-113}$, with and without $Bud13^{40\text{-mer}}$, and the subsequent addition of ^2H_2O.

2.7. Isothermal titration calorimetry

Isothermal titration calorimetry (ITC) was used to measure the affinity between $Snu17^{1-113}$ and different Bud13 constructs. Measurements were performed with a VP-ITC (MicroCal Inc.) at 25 °C using proteins in NMR buffer. The concentration of $Snu17^{1-113}$ in the cell (1440 μL) varied between 30-70 μM, while the syringe (300 μL) contained the ligands at concentrations ranging from 0.6 to 1.1 mM. Normally 40–80 injections were performed over a period of 3–4 h. To estimate the heat of dilution, the ligands were also injected into buffer. The result was then subtracted from the original measurement. The analysis of the ITC data was done in Origin v7, according to the manufacturer's recommendations.

2.8. Thermofluor assay

A thermofluor assay was used to characterize the stability of $Snu17^{1-113}$ with and without $Bud13^{40\text{-mer}}$ (Ericsson et al., 2006). In brief, the emission spectrum of a fluorophore, which is added to the sample, is altered upon interaction with hydrophobic residues that are exposed upon thermal unfolding the hydrophobic core of the protein. This process can be followed with a real-time PCR machine (Stratagene M × 3005P, Agilent Technologies Inc.). 50 μL reactions contained: 20 μM $Snu17^{1-113}$, 80uM $Bud13^{40\text{-mer}}$, 5x of SYPRO-orange (5000x stock; Sigma-Aldrich). The samples were heated with 3 °C/min, starting from 25 °C.

2.9. Analysis of SAXS data

SAXS data were collected on a commercially available small-angle X-ray camera (Nanostar, Brucker AXS) adapted to a rotating anode X-ray source (CuKα, $\lambda = 1.54$ Å). Data analysis confirmed the presence of a heterodimer in solution for the Trm8-Trm82 complex and of a heterotrimer for the Trm8-Trm82-tRNA complex (Leulliot et al., 2008). Missing parts in the crystal structure, either because of proteolysis or because of their high mobility, contribute

to scattering in solution by the intact ternary complex. Their precise conformation, which is likely not unique, is not a critical issue, and certainly not when it comes to determining their contribution to the SAXS pattern, *i.e.* at low resolution. They were therefore modeled in a conformation exposed to the solvent. Six "docked models" of the ternary complex were obtained that differed by the position of the tRNA with respect to the Trm8-Trm82 complex. For each "docked model", the location of the three larger modeled fragments, namely the 22 N-ter residues of Trm8, the 14 C-ter residues of Trm82 and the 50 residues between blades B1 and B2 of Trm82 were refined in a final modeling stage using the rigid-body modeling program SASREF (Petoukhov and Svergun, 2005). The discrepancy between the calculated and the experimental scattering curves was minimized while keeping the crystal structures fixed in the docked position.

3. Results

3.1. The use of multi-cistronic constructs and multi-plasmid strategies for the production of multi-protein complexes

Two extreme strategies can be proposed to co-express recombinant complexes in *E. coli*. First, one can take advantage of the ability of bacteria to translate mRNAs encoding several distinct proteins to insert the coding sequences of the various subunits of the complex of interest into a single plasmid downstream of a single promoter. The coding sequences are separated by a short non-coding region containing ribosome binding sites, ensuring efficient translation of the various polypeptides. In general, a purification tag is fused to one of the subunits, but multiple tags may easily be used, to ensure that complexes containing various subunits are purified. Provided that none of the inserted sequences induce transcriptional stalling, a single mRNA will be produced and drive the production of the various subunits of the target complex. This ensures, in theory, that equal quantities of RNA sequences encoding the various subunits are present and thus similar levels of each subunit are expected. Deviation from this ideal situation is not rare and may result from degradation of the mRNA or unequal translation or stability of the various polypeptides.

Constructs for co-expression can easily be produced by the successive addition of coding sequences of interest. Additionally, expression experiments using plasmids that encode different combinations of subunits and purification of full and partial complexes may provide information about which subunits are involved in direct interaction and also offer the possibility of testing various assemblies for structural analyses. This approach is exemplified in Fig. 1A for the Mak complex. The Mak complex was identified by TAP purification as a hetero-trimeric assembly containing the Mak3 subunit, which presents similarities to acetyl transferases, the large Mak10 subunit, and Mak31, a divergent Sm protein (Rigaut et al., 1999). While these proteins were originally identified as required for maintenance of killer virus-like structures (hence their names), they were later shown to constitute one of the yeast protein N-acetyl transferases. Inserts encoding 6His-Mak3, Mak10 and Mak31 were successively inserted between a T7 promoter and a T7 terminator in the expression vector pBS2454. Proteins were purified on Ni^{2+}–NTA agarose after expression of the constructs in BL21(DE3) Codon + cells. All proteins were clearly visible in the purified fractions (Fig. 1B) and the presence of complexes was ascertained by further purification of the peak Ni^{2+}–NTA fraction by gel filtration (Fig. 1C). Interestingly, this revealed that 6His-Mak3 co-purified Mak10 indicating that these two factors interact directly. Moreover, Mak10 appeared to be partially degraded, but the extent of the degradation was reduced in the presence of Mak31 (Fig. 1B,C), suggesting that Mak31 interacts directly with Mak10 and hence protects it from attack by *E. coli* proteases.

The KEOPS/EKC complex is comprised of at least four subunits (Kae1, Bud32, Cgi121 and Pcc1) and additional subunits are found

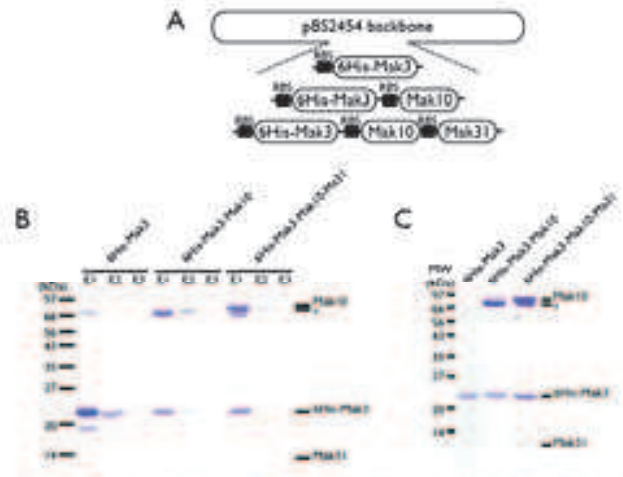

Fig. 1. Expression of the Mak complex and subcomplexes (boxed) using polycistronic vectors. (A) Structure of the 3 plasmids resulting from the successive insertion of the 6His-Mak3, Mak10 and Mak31 coding sequence in the pBS2454 backbone. A ribosome binding sequence (RBS) was inserted upstream of each ORF. (B) Coomassie stained gel showing the protein composition of three NiNTA elution fractions after expression of the three constructs depicted in A. Note that an *E. coli* contaminant corresponds also to the position of Mak10 in the construct expressing only 6His-Mak3. Position of migration of the molecular weight markers is indicated on the left. (C) Protein profile of the peaks of the gel filtration using the three constructs depicted in A. Samples purified on NiNTA as in B were fractionated on a Superdex 200 HiLoad GL column. Position of migration of the molecular weight markers is indicated on the left.

in some organisms (Gon7 in *S. cerevisiae*) (Kisseleva-Romanova et al., 2006). This complex was originally described to be required for telomere maintenance (Downey et al., 2006) and regulation of transcription (Kisseleva-Romanova et al., 2006) but its biochemical function remains unclear, which was the reason why we started structural studies of this complex. Our approach for expressing the complete yeast KEOPS/EKC complex consisted of designing a poly-cistronic bacterial expression vectors for the co-expression of all proteins of the complex (Fig. 2A). The results of the gel filtration step used during the purification process (Fig. 2B) shows that the five KEOPS/EKC proteins can be efficiently expressed in this way. As one can see, the strategy of co-expressing five proteins from one poly-cistronic vector was successful and underlies the capacity of T7 RNA polymerase to transcribe large (>3.5 kb) DNA fragments efficiently. The Gon7 protein was tagged at the C-terminus by a 6-His sequence. Using IMAC chromatography, the co-purification of the complex yielded milligram-scale quantities of protein (Fig. 2C). Crystallization trials are in progress for the whole KEOPS/EKC complex produced using this route.

Multi-cistronic constructs have the advantage of necessitating a single selection marker, thus avoiding the use of media with multiple antibiotics, often detrimental for efficient protein expression. These vectors are also compatible with a wide range of host cells. As a drawback, such constructs may become very large when the size and/or number of subunit increase(s), giving rise to problems during their construction and manipulation. However, the main limitation of multi-cistronic constructs probably resides in the additional labor required when many variants have to be tested, necessitating a new clone for each new combination of protein components in the complex. An obvious adaptation when expressing multi-protein complexes for instance, exists in permutation of the order in which the coding sequences are inserted, as this can

In order to avoid such problems, a diametrically opposed strategy may be used, in which each subunit is inserted into a different expression vector. This approach requires many vectors with different selection markers and if possible, with different replication origins to avoid interference. Constructs containing a given subunit and variants thereof are always introduced into the same vector backbone. To test expression and purification of a given set of proteins, one can then easily combine the corresponding vectors and introduce them into *E. coli*. This strategy is illustrated here with the Dom34 and Hbs1 proteins (Doma and Parker, 2006). These two factors resemble the translation termination factor, but were shown to be implicated in the degradation of mRNA and rRNA in stalled translation complexes. To define which of the three domains of Dom34 are required to interact with Hbs1, we constructed plasmids encoding either full-length Dom34 or three Dom34 variants, in each of which, one of the three domains had been deleted. Each of the Dom34 derivatives was fused to a Strep tag. These vectors were introduced into BL21(DE3) cells, together with a plasmid encoding full-length 6His-tagged Hbs1 (van den Elzen et al., 2010). Extracts were prepared after induction of protein expression and incubated with Streptactin beads. After washing, proteins bound to the beads were eluted and fractionated on denaturing gels and detected by Coomassie staining (Fig. 3). This assay was perfectly suited to the detection of the interaction of Hbs1 with Dom34, and demonstrated furthermore that the third domain of Dom34 was essential for an efficient interaction. Deletion of domain 2 reduced only slightly the interaction while deletion of domain 1 had no effect. These observations are consistent with the recent X-ray and SAXS analyses of this complex (van den Elzen et al., 2010).

As exemplified by this complex, the co-expression of different proteins encoded by different vectors offers the possibility of rapid

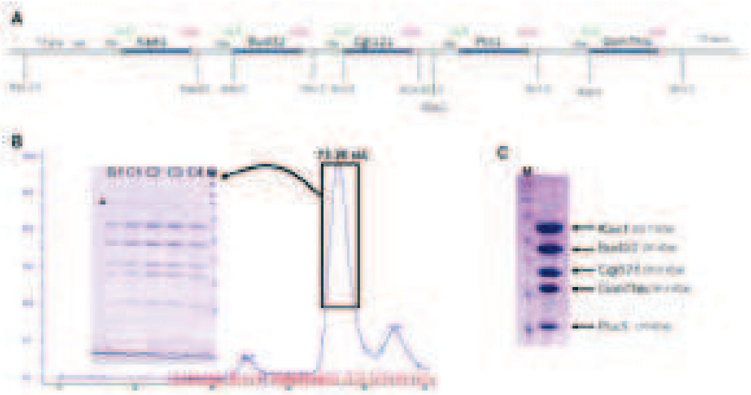

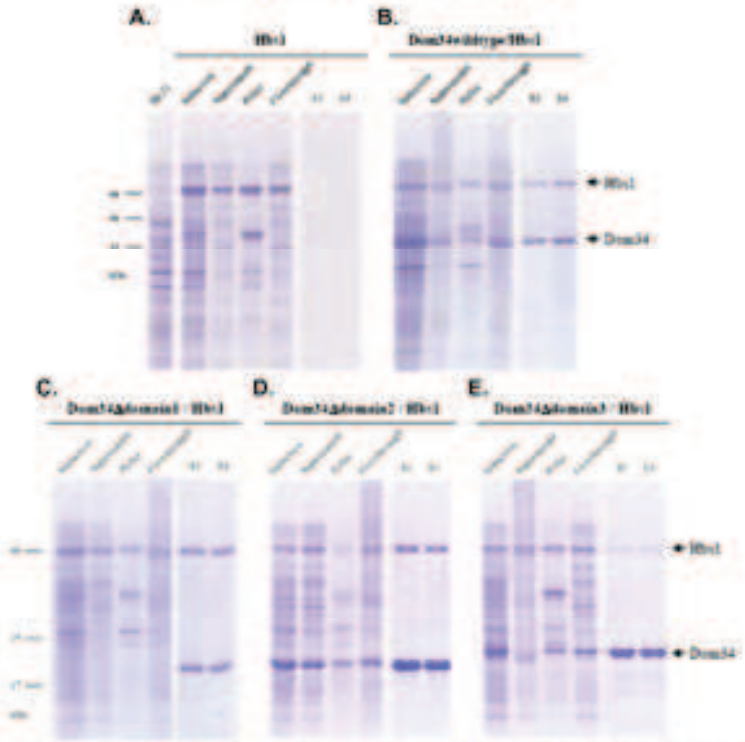

Fig. 3. Involvement of Dom34 domain in Dom34-Ilv5 interaction. C-terminally Strep-tagged Dom34, variants thereof, or as a control vector were co-expressed in BL21(DE3) cells with C-terminally His-tagged Ilv5. Protein purification with Strep-tactin Sepharose was performed on the soluble extract obtained after cell lysis. Results were analyzed on a 12% SDS-PAGE and detected by Coomassie staining.

one of the vectors encoding a complex subunit. Also, the requirement for compatible replication origins and selection markers restrict the use of this strategy to complexes containing only a limited number of subunits. Finally, given that each subunit is expressed from a different vector, it is difficult to avoid bias in the relative expression level of each protein, due to competition between promoters, or potential toxic effects of one or more of the subunits, and therefore loss of the corresponding vectors. Each of these outcomes may result in protein imbalance and thereby result in poor yield of complex at the stage of protein production.

3.2. A multi-organism approach for the production of complexes

Structural studies of multi-protein complexes using X-ray crystallography rely on the availability of diffraction quality crystals, which itself depends on several factors, such as protein solubility and stability, the presence of long flexible loops or extremities, and of surface residue distribution. Although the yeast *S. cerevisiae* is the most extensively studied eukaryotic organism, its proteins are not necessarily the most amenable to crystallogenesis, because of the comparatively long loops and extremities which are frequently found within its sequences. Hence, to obtain structural information on a biological system of interest, it is often very useful to study orthologous proteins. As the functional residues are conserved within these orthologs, their structures can serve as templates for the design of further functional and genetic studies in baker's yeast. Here, we present two examples of a multi-organism approach that proved to be successful in our hands.

In our project on the KEOPS/EKC complex we also endeavored to study individual proteins and sub-complexes. Despite extensive trials, *S. cerevisiae* Kae1 could only be recovered in the insoluble fraction following over-expression in various *E. coli* strains. Co-expression with the protein kinase Bud32, its direct partner within the KEOPS/EKC complex (Lopreiato et al., 2004), yielded soluble protein. Because the purified quantities were insufficient for structural studies, we searched for orthologous proteins in archaea and found two candidates: PAB1159, the Kae1 ortholog from *Pyrococcus abyssii* and MJ1130 from *Methanococcus jannaschii*. Interestingly, the latter is a fusion protein of Kae1 and Bud32. These two archaeal proteins could be over-expressed as soluble proteins in *E. coli* and purified in milligram-scale quantities. This allowed us to grow diffracting crystals from both proteins and to solve the crystal structures of PAB1159 and MJ1130 (Hecker et al., 2008; Hecker et al., 2007). A similar strategy was also used by Mao et al. to obtain a model of the hetero-tetrameric KEOPS/EKC core complex (Pcc1-Kae1-Bud32-Cgi121) from the structures of archa-

eal heterodimeric sub-complexes (Pcc1-Kae1; Kae1-Bud32 and Bud32-Cgi121) (Mao et al., 2008).

A second example is provided by the *S. cerevisiae* Trm112 protein that binds and activates three SAM-dependent methyltransferases (MTases) modifying translation termination factor eRF1 (Mtq2) or tRNAs (Trm9 and Trm11) (Heurgue-Hamard et al., 2006; Purushothaman et al., 2005; Studte et al., 2008). Co-expression of Trm112 with both Mtq2 and Trm9 is necessary to recover these two MTases in the soluble fraction of *E. coli* extracts (Heurgue-Hamard et al., 2006; Mazauric et al., 2010). Despite extensive efforts, we could not obtain crystals of the Mtq2-Trm112 or Trm9-Trm112 complexes from *S. cerevisiae*, human or mouse. We therefore searched for orthologs of smaller size and select those encoded by the genome of the intracellular parasite *Encephalitozoon cuniculi*. The proteins from this organism are on average 25% smaller than their orthologs from *S. cerevisiae* (Katinka et al., 2001). Using bi-cistronic vectors and non-optimized synthetic genes, we could co-express the *E. cuniculi* complexes formed by Trm112 (NP_597247.1, 125 residues *versus* 135 in yeast) with Mtq2 (NP_585817.1, 164 residues vs 221 in yeast) and Trm9 (XP_955703.1, 225 residues vs 279 in yeast). This confirmed that (i) Trm112 is needed to solubilize Mtq2 and (ii) Mtq2-Trm112 and Trm9-Trm112 interactions are also conserved in this parasite. This strategy allowed us to solve the 2.1 Å resolution crystal structure of the *E. cuniculi* Mtq2-Trm112 complex, which was then used as a model of the yeast complex for further functional experiments conducted in *S. cerevisiae* (Liger et al. 2011, Nucleic Acids Res. in press).

3.3. The use of limited proteolysis for the optimization of crystals of complexes

It has long been recognized that flexible and/or unstructured regions at the N- or C-termini can hinder the crystallization process. Therefore, a variety of methods have been developed to generate protein constructs corresponding to the minimal structured domain, including systematic domain generation coupled to solubility screening or prediction by bioinformatics. Limited proteolysis has also been widely used in order to define minimal structured domains in proteins (Quevillon-Cheruel et al., 2009; Wernimont and Edwards, 2009). The method involves incubating a purified protein with one or more of a variety of proteases in order to remove unstructured regions. SDS-PAGE, Edman sequencing and mass spectrometry can then be used to identify the boundaries of the truncated protein construct, which can then be cloned and purified. Alternatively, the limited proteolysis conditions can be scaled up, refined and an extra purification step performed to isolate the fragment of interest.

Limited proteolysis can also be used *in situ*, during the crystallization experiment (Quevillon-Cheruel et al., 2009), an idea which arose from the fact that many crystal structures present some degree of proteolysis, as confirmed by mass spectroscopy on solubilized protein crystals. In this way, it was observed that partial protein degradation had occurred naturally over time, and was probably due to the presence of trace amounts of proteases. This concept was extended by purposefully adding small amounts of proteases to samples of the purified proteins of interest. The samples are then either incubated for a certain amount of time, or used without any incubation. Either way, the sample is used directly for setting up crystallization trials, without any further purification (Wernimont and Edwards, 2009). The idea is that the proteases should still be active in the crystallization drops, and the protein will slowly be trimmed of its unstructured regions, sometimes generating over time a construct compatible with nucleation and leading to crystal growth. This technique has led to a number of successes, where all other methods failed to produce diffracting quality crystals. An important aspect of the method is that prior inspection by SDS–PAGE is not necessary, because frequently the protease will only cut within protein loops, but visualization of the denatured sample by SDS-PAGE would reveal a smear at low molecular weight fragments. This may, sometimes, become important as long unstructured loops that would otherwise prevent packing are removed, or provide additional degrees of freedom to the loop conformation necessary to form crystal contacts (Quevillon-Cheruel et al., 2009). Using limited proteolysis on protein complexes is a natural extension of this strategy, but requires additionally that the quaternary structure of the complex be preserved.

The N7-methylguanosine (m7G) modification in yeast is catalyzed by the heterodimeric complex composed of a catalytic subunit Trm8 and a non-catalytic subunit Trm82. The structure of the Trm8-Trm82 complex was solved using a combination of protein engineering and *in situ* proteolysis (Leulliot et al., 2008). Firstly, the Trm8 methylase construct had to be optimized in order to solve expression and solubility issues. Removal of the first 46 residues, which were not conserved and predicted to be unstructured, enabled a stable construct to be generated, and the protein purified and crystallized. The Trm8-Trm82 complex could then be reconstituted from the separately purified components. Crystallization trials led to polycrystalline material that resisted all optimization attempts (Fig. 4a). Trace amount of proteases (1/100 trypsin, chymotrypsin or pepsin) were then used as "additives" in the optimization stage, by incubating the complex 30 min at 21 °C, before setting up the tray. This enabled small monocrystals that diffracted to 2.4 Å resolution to be obtained (Fig. 4b). Inspection by mass spectroscopy of the species present in the crystals reveal a heterogeneous population, indicating that both proteins were extensively proteolysed at both N- and C-termini and in various loops.

3.4. Biophysical approaches for the analysis of protein complexes

3.4.1. Small angle X-ray scattering (SAXS)

X-ray crystallography is the method of choice to obtain detailed structural information of large macromolecular complexes, as testified for instance, by the structures of RNA polymerases and bacterial ribosomes (Ban et al., 2000; Ben-Shem et al., 2010; Wimberly et al., 2000; Yusupov et al., 2001). However, it is not always possible to grow diffracting crystals of complexes and alternate approaches can also bring useful information. This is indeed the case with SAXS and cryo-electron microscopy (in the latter case, for complexes of molecular weight of >200 kDa). In these cases, the knowledge of the NMR or crystal structures of isolated components of these complexes can be combined with the SAXS or cryo-EM data in order to propose a model that will need to be validated experimentally (Hura et al., 2009). SAXS also provides very useful information on the quality of the sample (aggregate formation, conformational stability etc.). Unfortunately, the access to SAXS instruments is limited and light scattering can provide a valuable alternative for the examination of the aggregation state of the sample (Senisterra and Finerty, 2009).

We have successfully used this approach for the study of both protein–protein and protein-RNA complexes. The first example concerns the Dom34-Hbs1 complex from *S. cerevisiae*, which is involved in the degradation of RNA, inducing strong translational stalls of the ribosomes (Doma and Parker, 2006). We have solved the structures of Dom34 and Hbs1 from yeast and the structure of a Dom34 archaeal ortholog was described elsewhere (Graille et al., 2008; Lee et al., 2007; van den Elzen et al., 2010). However, we could not obtain crystals for the complex. As Dom34 and Hbs1 are structurally related to translation termination factors eRF1 and eRF3, respectively (Carr-Schmid et al., 2002; Graille et al., 2008;

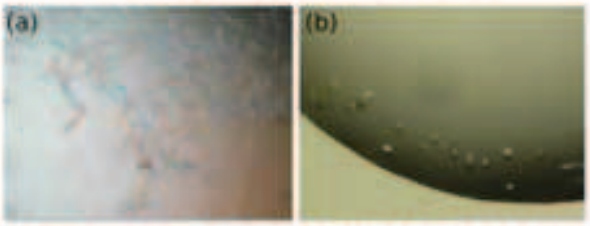

(b) Crystals of in the same condition with 0.025 mg/ml trypsin added to the protein complex sample.

Lee et al., 2007), we used the structures of human and *S. pombe* eRF1-eRF3 complexes (lacking eRF3 GTPase domain) to model the structure of *S. cerevisiae* Dom34-Hbs1 complex (Chen et al., 2010; Cheng et al., 2009). We have then superimposed the C-terminal domain from Dom34 structures onto the corresponding domain from eRF1 in the human eRF1-eRF3 complex. Similarly, we have superimposed the C-terminal domain from Hbs1 structure onto the corresponding domain from eRF3 in the human eRF1-eRF3 complex. As the crystal structures of Dom34 from yeast and archaea were dramatically different in respect to the orientation of the central domain relative to the N and C-terminal domains, this yielded two different models ("yeast-like" and "archaea-like"). To discriminate between the two models, we recorded SAXS data from the Dom34-Hbs1 complex from *S. cerevisiae*. Comparison of the scattering curves calculated from both models with the experimental one clearly showed that the "archaea-like" model fits better the solution structure of the Dom34-Hbs1 complex than the "yeast-like" complex. To further improve the "archaea-like" model, we performed rigid-body movements of two Dom34 domains against SAXS data using the program SASREF (Petoukhov et al., 2007). The final model obtained using this approach displays a strong analogy to the EF-Tu-tRNA complex that binds to the ribosomal A-site during elongation. Unexpectedly, this model predicted an interface between two highly conserved regions from Hbs1 GTPase domain (motif RDF) and Dom34 central domain (the SPGF motif). The importance of these residues for complex formation was validated using site-directed mutagenesis and the yeast two-hybrid approach (van den Elzen et al., 2010). Our model was further validated by the crystal structure of the Dom34-Hbs1-GTP complex from archeon *A. pernyx* (rmsd of 3.3 Å over 540 Cα atoms; (Kobayashi et al., 2010)), which revealed that the Hbs1 RDF motif is indeed facing the Dom34 SPGF motif.

We also used SAXS to model the structure of protein-RNA complexes, as exemplified by the structure of the Trm8-Trm82-tRNA complex. Modeling RNA protein complexes based on SAXS data is somewhat problematic, because the density of RNA is twice that of proteins. *Ab initio* modeling of the envelope of the complex can therefore be challenging due to the two phases contributing to the scattering curve. In our case, knowledge of the individual structures of the components of the complex was crucial to the success of using SAXS to obtain structural information. Indeed, the structures of Trm8 and of the binary Trm8-Trm82 complex had successfully been solved by X-ray crystallography (see above). A stable stoichoimetric trimeric Trm8-Trm82-tRNA^{Phe} could be purified by gel filtration, but did not yield any crystals. The problem could therefore reduced to docking the tRNA^{Phe} structure on the Trm8-Trm82 using SAXS scattering profile as a target. To our surprise, modeling the trimeric complex was straightforward for several reasons. First of all, the Trm8-Trm82 structure lacked several regions of the protein, which were either intrinsically unfolded, or absent in the crystal structure because of the protease treatment of the sample prior to crystallogenesis (see above). The missing Trm8 residues were therefore modeled according to the Trm8 crystal structure, the structure of bacterial homologues of Trm8 (TrmB), and by *ab initio* modeling. This structure was validated and refined with the SAXS scattering curve obtained from the Trm8-Trm82 complex. With complete atomic models of both protein and RNA partners at hand, we attempted macromolecular docking restrained by the SAXS profile. Analysis of the resulting models revealed that the solutions obtained were incoherent with the available functional and structural information. The location of the active site of Trm8 was known and confirmed by crystallization in presence of the adenosyl-methionine methyl donor. A positively charged surface patch around the active site of the protein undoubtedly contributes to its RNA binding properties. The base of the tRNA, which is modified by the Trm8-Trm82 complex, was already experimentally verified as being G46. We therefore expect that in the docked models, the guanosine at position 46 in the tRNA is located in the vicinity of the Trm8 active site. Inspection of the position of the tRNA^{Phe} in the docking results showed that the tRNA^{Phe} bound at sites distant from the predicted binding site and positioned the target guanosine too far away from the Trm8 active site. This discrepancy is thought to result from the fact that docking is performed with unbound structures, and does not account for structural rearrangements of the structures upon binding. This is especially true for the RNA moiety because G46 is involved in tertiary base pairing with the C13-G22 base pair inside the D stem. The tertiary base pair therefore has to be disrupted and that the guanine base has to flip out in order to access the small groove in the Trm8 active site. The combined errors in the model structures due to modeling of missing regions and conformational changes were large enough to drive the docking to wrong conformations, but showing very good fits to the SAXS scattering profile.

To obtain valid models of the complex, we used this knowledge in order to position the tRNA with respect to the protein. The models were generated by positioning the structure of the tRNA^{Phe} so that, upon flipping out of the tRNA^{Phe} stem, the guanosine 46 was at a distance compatible with its insertion into the Trm8 catalytic site. Next, G46 was chosen as a pivot point and many rotational orientations of the tRNA were manually generated. Three classes of orientations emerged in which the D- T- or anticodon arms were bound in the predicted Trm8 RNA binding groove (Fig. 5). Comparison of the calculated and experimental SAXS scattering curves gave a better agreement with one of the classes (goodness-of-fit indicator χ between 1.48 and 2.10) compared to the others (χ between 2.41 and 3.45).

The final structure was in good agreement with experiments measuring the methyl acceptance activities of eight truncated or mutated tRNA transcripts by both Trm8/Trm82 or by bacterial *Aquifex aeolicus* TrmB (AeTrmB) (Matsumoto et al., 2007). However,

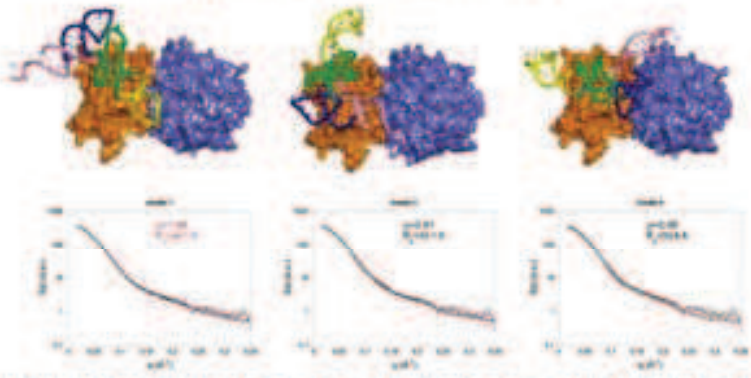

Fig. 5. SAXS curves and model of the Trm8-Trm82-tRNA complex. Representative models of the three classes of structure obtained for the Trm8-Trm82-tRNA complex. Trm8 and Trm82 are colored in orange and blue respectively. The tRNA^{Phe} is colored in anticodon, D-, T- and acceptor stem of the tRNA^{Phe} are colored pink, green, blue and yellow, the scattering curves calculated for the three models are represented below the structure in red lines, superposed to the experimentally measured curves (black dots).

no single model showed both an entirely satisfactory interaction between the protein surface and the RNA, indicating that large structural changes probably occur and involve bending of the RNA anticodon stem. While the modeling of such conformational changes requires additional efforts (Madl et al., 2011), our results confirm that predicting the structures of complexes using unbound models should be treated with extreme care and should always use additional restraints based on biochemical or functional assays.

3.4.2. Use of NMR for the biophysical dissection of the RES complex

The RES complex, a splicing factor affecting nuclear pre-mRNA retention, is composed of 3 subunits, namely Snu17, Bud13 and Pml1 (Brooks et al., 2009; Dziembowski et al., 2004; Trowitzsch et al., 2009). To obtain insights into its function, we have performed a structural investigation of this factor. Expression experiments for the structural analysis of the RES complex have taken two directions thus far: expression of the individual subunits and expression from polycistronic vectors. Single subunit expression facilitated what we consider to be one of the most important initial experiments, namely production of the full-length proteins to determine whether (i) they can be produced in a soluble form singly and (ii) whether they are folded and resistant to proteases. The expression level and solubility of the subunits provides a benchmark to which yields of truncated constructs may be compared. The results of these experiments showed that of the three subunits, Pml1 was clearly the most stable and resistant to protease digestion with trypsin and chymotrypsin. On the other hand, treatment with such proteases degraded Bud13 rapidly, without obvious protease-resistant domains. Snu17 was of intermediate stability, and was partially resistant to proteases, yielding a collection of peptides after proteolysis.

Experiments designed to produce RES from a single polycistronic vector were successful, and the complex produced in this way was stable during gel filtration (Brooks et al., 2009). However, it proved impossible to crystallize the tertiary complex, or even either of the two binary complexes. Therefore, we resorted to truncation and mutation analysis in order to delineate the minimal constructs that form binary complexes stably; attempts to do this have been published previously (Brooks et al., 2009; Trowitzsch et al., 2008; Trowitzsch et al., 2009). While the competing group used traditional cloning for this purpose, our work was based on the use of the Entranceposon transposition system (Finnzymes) to generate a library of truncated fragments of both Snu17 and Bud13. By performing a screen for loss of interaction, we were indeed able to identify stable mutants of Snu17 that still bound to Bud13 but lost interaction with Pml1 (Brooks et al., 2009). This information could then be fed back into the protein production and crystallization pipeline.

Since these attempts were again not successful in crystallization trials, we resorted to other biophysical techniques to characterize the complex, particularly in the case of the Snu17:Bud13 dimer. Nuclear magnetic resonance spectroscopy is an efficient method for characterizing biomolecular interactions and structure determination of protein complexes in solution (Madl et al., 2011; Simon et al., 2010). NMR experiments were therefore used to define the minimal region of structured polypeptide within the proteins. We were particularly intrigued by the interaction between Snu17 and Bud13, since the interaction is predicted to be generally related to the interactions between UHMs (U2AF Homology Motifs) and ULMs (UHM Ligand Motifs) (Corsini et al., 2007).

The Snu17$^{1-113}$ construct was compared to full-length Snu17 (Snu17$^{1-148}$) using $^{1}H,^{15}N$ 2D HSQC spectroscopy (Fig. 6A). The shorter of these two constructs yielded an improved spectrum, which looked promising for structural analyses. In contrast, the full-length construct gave numerous overlapped signals resonating around 8 ppm, suggesting that many residues of the C-terminus are structurally disordered and flexible. However, Snu17$^{1-113}$ precipitated during storage and NMR data acquisition, and therefore appeared to be unstable. Further evidence for the instability of Snu17 alone was provided by NMR monitored hydrogen/deuterium (H/D) exchange experiments (data not shown). These experiments demonstrated the complete exchange of amide protons within 5 min indicating that amides are not involved in strong hydrogen-bonds, as would be expected for a folded domain with stable secondary structure elements. The situation is improved significantly by the addition of a Bud13-peptide (Bud13$^{40\text{-mer}}$), which comprises a conserved tryptophan residue that is also critical for the molecular recognition of ULMs by UHM domains. In the presence of this peptide many NMR signals of Snu17$^{1-113}$ remained protonated and thus protected against H/D exchange after incubation for 15 min in deuterated water. Thermofluor assays (Ericsson et al., 2006) corroborated these results, which showed a 5 degree shift in the melting temperature upon addition of Bud13$^{40\text{-mer}}$, compared to the Snu17$^{1-113}$ protein alone (data not shown).

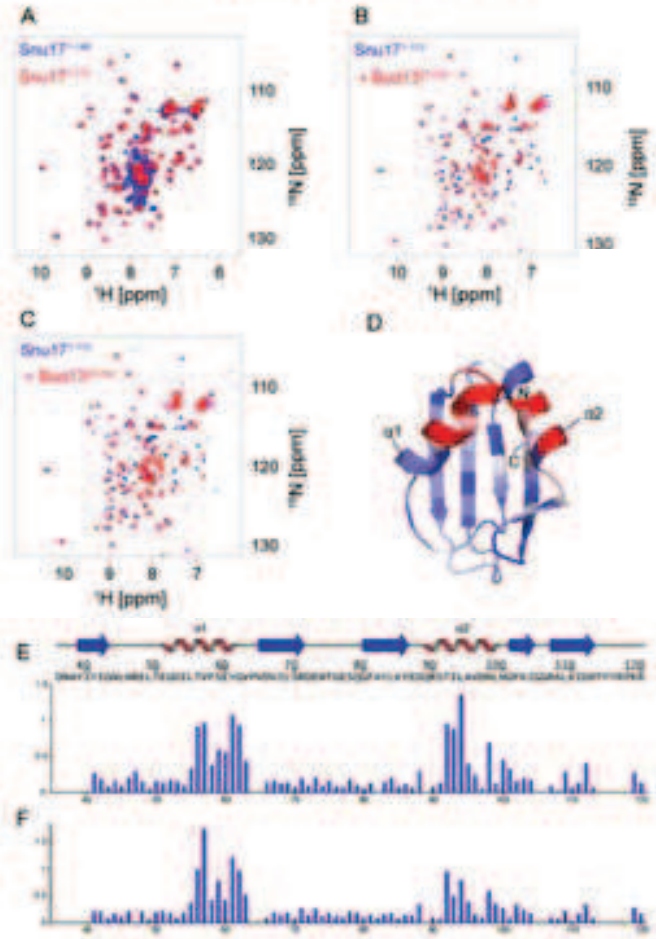

Fig. 6. Optimization of expression for structural studies using $^{1}H,^{15}N$ HSQC NMR spectroscopy. A. Comparison of $Snu17^{1-119}$ (full-length) and $Snu17^{1-107}$ using $^{1}H,^{15}N$-HSQC NMR spectroscopy. By labeling Snu17 with the isotope ^{15}N, an assessment can be made of the folding status of the construct. In the case of the full-length protein, many NMR signals overlap (Panel A, blue spectrum), suggesting that Snu17 contains regions that are structurally disordered. A panel of truncation mutants was therefore constructed and tested, of which $Snu17^{1-113}$ produced a good quality spectrum (red) with reduced signal overlap. B,C. $^{1}H,^{15}N$ HSQC NMR spectra of $Snu17^{1-113}$ alone (blue) and after addition of peptides comprising the putative ULM in Bud13 (spectra in red). A 40-residue peptide elicits similar chemical shift perturbations (red spectrum in C), but has a higher affinity (not shown) than the 22-mer (red spectrum in B). All $^{1}H,^{15}N$ HSQC spectra were recorded using samples at a concentration of 100 μM $Snu17^{1-113}$ at 300 K in (A) and 298 K in (B,C) at a 1:2 M ratio protein:ligand. (D) Induced CSPs mapped onto a homology model of the UHM domain of $Snu17^{1-113}$, illustrating that the CSPs cluster to the expected interaction site as described for other UHM-ULM complexes. Increasing CSPs (shown as a color ramp, blue through to red) are defined as: $CSP = \sqrt{\delta H[ppm]2 + 0.1 \times \delta N[ppm]^2}$. The homology model was produced using the structure of the UHM domain of human SPF45 (PDB accession code: 2PE8) as a template, using the HHpred web server (Soding et al., 2005). (E) The same CSP data as in (D) are presented in a histogram, along with the predicted secondary structure of Snu17 aligned with its amino-acid sequence. (F) Same as E but for a 22-mer peptide of Bud13. The major difference lies in the magnitude of the CSPs.

NMR titrations revealed substantial chemical shift perturbations (CSPs) in 2D $^{1}H,^{15}N$ HSQC spectra upon addition of Bud13 peptides to ^{15}N-labeled $Snu17^{1-113}$ (Fig. 6B and C). The next step was then to perform the NMR backbone resonance assignment, allowing a more thorough characterization of the effects of various Bud13 peptides on Snu17 at residue resolution. It became clear that CSPs map to the two α-helices in the putative ULM binding site of a homology model of the $Snu17^{1-113}$ UHM domain (Brooks et al., 2009). The presence of a 60-mer peptide of Bud13 yielded an almost identical $^{1}H,^{15}N$ HSQC spectrum of $Snu17^{1-113}$ as the 40-mer peptide, but the former induced aggregation of the protein (data not shown). CSPs elicited by a 22-mer Bud13 peptide were

rather similar to the 40-mer variant (Fig. 6C). However, while with both peptides a similar set of residues within helices α1 and α2 were affected, the magnitude of the CSPs with the 22-mer peptide was lower (Fig. 6E and F). The affinity of each peptide was determined by isothermal titration calorimetry (ITC). While the 22-mer could be fitted to a single site-binding model, the 40-mer could be best fitted assuming two binding sites, suggesting a bipartite mode of interaction (data not shown). Thus, the 40-mer or longer peptides are likely to provide a more complete picture of the interaction between these two splicing factors. Efforts for structure determination of this complex should therefore preferably be performed using these constructs.

In summary, the NMR data support the notion that Snu17 and Bud13 interact in a similar fashion as found in UHM-ULM complexes, exemplified by the structure of SPF45 in complex with a ULM peptide derived from SF3b155 (Corsini et al., 2007). Additionally, these results suggest that Bud13 induces an increased stability of Snu17, perhaps by induced-fit upon binding, which may also have functional consequences *in vivo*. This system provides an example of how a combination of NMR, thermofluor and ITC can be used to assist in decision-making with respect to which are the optimal constructs to use for biophysical and structural studies, and is applicable to the protein-peptide interaction paradigm in general.

4. Conclusions

Despite huge progress made over the last years in the production of proteins through technological developments in structural genomics programs (Alzari et al., 2006; Graslund et al., 2008; Stevens et al., 2001), the structural analysis of multi-protein complexes remains a challenge. Overall, there is no definitive optimal strategy for complex over-expression. Multi-cistronic constructs represent simple systems that benefit from improvement in cloning automation while multi-vector strategies facilitate the screening for optimal constructs. Obviously, these strategies may be combined. Hence, it is possible to rapidly test numerous variants of a given subunit by constructing them in a defined vector while the remaining subunits of the complex are encoded by a compatible polycistronic vector. Independent transcription units may also be inserted in a single vector to prevent problems resulting from the expression of a single large polycistronic transcript. Selection of the strategy should still currently be dictated by available information and by estimation of the steps that will be required to achieve efficient complex expression.

Multi-organism strategies for structural studies are of course not new and have been applied in many laboratories. What has changed over the recent years is the availability of a fast growing number of genome sequences, which tremendously increases the number of potential orthologs that can be tested for expression and crystallization. Organisms that survive under harsh conditions (stable proteins) or that are under selective pressure (such as occur during parasitism or when rapid replication is required) to restrict genome size, giving rise to short protein sequences, are valuable alternatives for cloning orthologous complexes. However, the use of protein sequences from more exotic organisms was until recently hampered by the difficulties of obtaining sufficient quantities of genomic or cDNA. The improved and cheaper gene synthesis facilities commercially available nowadays allow selecting and obtaining coding sequences for any protein sequence of interest that are available in the databases. As we demonstrated in the case of KEOPS/EKC, synthetic polycistronic operons can now be used for the production of complexes. The combination of an increasing number of orthologous sequences for any protein target together with the possibility of obtaining inexpensive synthetic genes coding for these orthologs will soon become a strategy of choice in structural biology and we will see the number of solved structures from proteins originating from "exotic" organisms increase.

The dominant method for high-resolution structure determination of complexes remains X-ray crystallography. Single particle electron microscopy is making steady progress and it can be expected that this technique will gain in importance, especially for complexes that are beyond reach of crystallography (Frank, 2009). Finally, complementary techniques such as NMR spectroscopy and Small Angle Scattering experiments provide important and often critical information for structural analysis of protein complexes (Hura et al., 2009; Madl et al., 2011). They have the advantage that no crystallization is required and that the complex is studied in solution, *i.e.* in a more native-like environment. If structures of individual domains are available, the structure of the complex can be obtained by using either NMR (Guttler et al., 2010), Small Angle Scattering or a combination of the two techniques (Madl et al., 2011).

Acknowledgements

The authors thank the staff at the Proxima 1 and Swing beamlines of Soleil Synchrotron, Paris. We also thank the ESRF, Grenoble for access to synchrotron radiation, as well as the macro molecular crystallography local contacts for their support. We also thank the IGBMC, Institut de Génétique et de Biologie Moléculaire et Cellulaire for assistance. This work was supported by La Ligue Contre le Cancer (Equipe Labellisée 2010) to BS, the CNRS, the Agence Nationale pour la Recherche (grants ANR-07-BLAN-0093 and ANR-06-BLAN-0075-02 to BS and HvT, respectively), the Deutsche Forschungsgemeinschaft to MS, the ESF EUROCORES RNA Quality and the EU "3D-Repertoire" program (LSHG-CT-2005-512028).

References

Alzari, P.M., Berglund, H., Berrow, N.S., Blagova, E., Busso, D., Cambillau, C., Campanacci, V., Christodoulou, E., Eiler, S., Fogg, M.J., Folkers, G., Geerlof, A., Hart, D., Haouz, A., Herman, M.D., Macieira, S., Nordlund, P., Perrakis, A., Quevillon-Cheruel, S., Tarandeau, F., van Tilbeurgh, H., Unger, T., Luna-Vargas, M.P., Velarde, M., Willmanns, M., Owens, R.J., 2006. Implementation of semi-automated cloning and prokaryotic expression screening: the impact of SPINE. Acta Crystallogr. D. Biol. Crystallogr. 62, 1103–1113.

Ban, N., Nissen, P., Hansen, J., Moore, P.B., Steitz, T.A., 2000. The complete atomic structure of the large ribosomal subunit at 2.4 A resolution. Science 289, 905–920.

Ben-Shem, A., Jenner, L., Yusupova, G., Yusupov, M., 2010. Crystal structure of the eukaryotic ribosome. Science 330, 1203–1209.

Brooks, M.A., Dziembowski, A., Quevillon-Cheruel, S., Henriot, V., Faux, C., van Tilbeurgh, H., Seraphin, B., 2009. Structure of the yeast Pml1 splicing factor and its integration into the RES complex. Nucleic Acids Res. 37, 129–143.

Carr-Schmid, A., Pfund, C., Craig, E.A., Kinzy, T.G., 2002. Novel G-protein complex whose requirement is linked to the translational status of the cell. Mol. Cell Biol. 22, 2564–2574.

Chen, L., Muhlrad, D., Hauryliuk, V., Cheng, Z., Lim, M.K., Shyp, V., Parker, R., Song, H., 2010. Structure of the Dom34-Hbs1 complex and implications for no-go decay. Nat. Struct. Mol. Biol. 17, 1233–1240.

Cheng, Z., Saito, K., Pisarev, A.V., Wada, M., Pisareva, V.P., Pestova, T.V., Gajda, M., Round, A., Kong, C., Lim, M., Nakamura, Y., Svergun, D.I., Ito, K., Song, H., 2009. Structural insights into eRF3 and stop codon recognition by eRF1. Genes Dev. 23, 1106–1118.

Clemons Jr., W.M., May, J.L., Wimberly, B.T., McCutcheon, J.P., Capel, M.S., Ramakrishnan, V., 1999. Structure of a bacterial 30S ribosomal subunit at 5.5 A resolution. Nature 400, 833–840.

Corsini, L., Bonnal, S., Basquin, J., Hothorn, M., Scheffzek, K., Valcarcel, J., Sattler, M., 2007. U2AF-homology motif interactions are required for alternative splicing regulation by SPF45. Nat. Struct. Mol. Biol. 14, 620–629.

Delaglio, F., Grzesiek, S., Vuister, G.W., Zhu, G., Zhu, P.J., Bax, A., 1995. NMRPipe: a multidimensional spectral processing system based on UNIX pipes. J. Biomol. NMR 6, 277–293.

Doma, M.K., Parker, R., 2006. Endonucleolytic cleavage of eukaryotic mRNAs with stalls in translation elongation. Nature 440, 561–564.

Downey, M., Houlsworth, R., Maringele, L., Rollie, A., Brehme, M., Galicia, S., Guillard, S., Partington, M., Zubko, M.K., Krogan, N.J., Emili, A., Greenblatt, J.F., Harrington, L., Lydall, D., Durocher, D., 2006. A genome-wide screen identifies the

evolutionarily conserved KEOPS complex as a telomere regulator. Cell 124, 1155–1168.
Dziembowski, A., Ventura, A.P., Rutz, B., Caspary, F., Faux, C., Halgand, F., Laprevote, O., Seraphin, B., 2004. Proteomic analysis identifies a new complex required for nuclear pre-mRNA retention and splicing. EMBO J. 23, 4847–4856.
Ericsson, U.B., Hallberg, B.M., Detitta, G.T., Dekker, N., Nordlund, P., 2006. Thermofluor-based high-throughput stability optimization of proteins for structural studies. Anal. Biochem. 357, 289–298.
Frank, J., 2009. Single-particle reconstruction of biological macromolecules in electron microscopy–30 years. Q. Rev. Biophys. 42, 139–158.
Gavin, A.C., Superti-Furga, G., 2003. Protein complexes and proteome organization from yeast to man. Curr. Opin. Chem. Biol. 7, 21–27.
Gavin, A.C., Bosche, M., Krause, R., Grandi, P., Marzioch, M., Bauer, A., Schultz, J., Rick, J.M., Michon, A.M., Cruciat, C.M., Remor, M., Hofert, C., Schelder, M., Brajenovic, M., Ruffner, H., Merino, A., Klein, K., Hudak, M., Dickson, D., Rudi, T., Gnau, V., Bauch, A., Bastuck, S., Huhse, B., Leutwein, C., Heurtier, M.A., Copley, R.R., Edelmann, A., Querfurth, E., Rybin, V., Drewes, G., Raida, M., Bouwmeester, T., Bork, P., Seraphin, B., Kuster, B., Neubauer, G., Superti-Furga, G., 2002. Functional organization of the yeast proteome by systematic analysis of protein complexes. Nature 415, 141–147.
Graille, M., Chaillet, M., van Tilbeurgh, H., 2008. Structure of yeast Dom34: a protein related to translation termination factor Erf1 and involved in No-Go decay. J. Biol. Chem. 283, 7145–7154.
Graslund, S., Nordlund, P., Weigelt, J., Hallberg, B.M., Bray, J., Gileadi, O., Knapp, S., Oppermann, U., Arrowsmith, C., Hui, R., Ming, J., dhe-Paganon, S., Park, H.W., Savchenko, A., Yee, A., Edwards, A., Vincentelli, R., Cambillau, C., Kim, R., Kim, S.H., Rao, Z., Shi, Y., Terwilliger, T.C., Kim, C.Y., Hung, L.W., Waldo, G.S., Peleg, Y., Albeck, S., Unger, T., Dym, O., Prilusky, J., Sussman, J.L., Stevens, R.C., Lesley, S.A., Wilson, I.A., Joachimiak, A., Collart, F., Dementieva, I., Donnelly, M.I., Eschenfeldt, W.H., Kim, Y., Stols, L., Wu, R., Zhou, M., Burley, S.K., Emtage, J.S., Sauder, J.M., Thompson, D., Bain, K., Luz, J., Gheyi, T., Zhang, F., Atwell, S., Almo, S.C., Bonanno, J.B., Fiser, A., Swaminathan, S., Studier, F.W., Chance, M.R., Sali, A., Acton, T.B., Xiao, R., Zhao, L., Ma, L.C., Hunt, J.F., Tong, L., Cunningham, K., Inouye, M., Anderson, S., Janjua, H., Shastry, R., Ho, C.K., Wang, D., Wang, H., Jiang, M., Montelione, G.T., Stuart, D.I., Owens, R.J., Daenke, S., Schutz, A., Heinemann, U., Yokoyama, S., Bussow, K., Gunsalus, K.C. 2008. Protein production and purification. Nat. Methods 5, 135–46.
Groll, M., Ditzel, L., Lowe, J., Stock, D., Bochtler, M., Bartunik, H.D., Huber, R., 1997. Structure of 20S proteasome from yeast at 2.4 A resolution. Nature 386, 463–471.
Guttler, T., Madl, T., Neumann, P., Deichsel, D., Corsini, L., Monecke, T., Ficner, R., Sattler, M., Gorlich, D., 2010. NES consensus redefined by structures of PKI-type and Rev-type nuclear export signals bound to CRM1. Nat. Struct. Mol. Biol. 17, 1367–1376.
Hecker, A., Lopreiato, R., Graille, M., Collinet, B., Forterre, P., Libri, D., van Tilbeurgh, H., 2008. Structure of the archaeal Kae1/Bud32 fusion protein MJ1130: a model for the eukaryotic EKC/KEOPS subcomplex. EMBO J. 27, 2340–2351.
Hecker, A., Leulliot, N., Gadelle, D., Graille, M., Justome, A., Dorlet, P., Brochier, C., Quevillon-Cheruel, S., Le Cam, E., van Tilbeurgh, H., Forterre, P., 2007. An archaeal orthologue of the universal protein Kae1 is an iron metalloprotein which exhibits atypical DNA-binding properties and apurinic-endonuclease activity in vitro. Nucleic Acids Res. 35, 6042–6051.
Heurgue-Hamard, V., Graille, M., Scrima, N., Ulryck, N., Champ, S., van Tilbeurgh, H., Buckingham, R.H., 2006. The zinc finger protein Ynr046w is plurifunctional and a component of the eRF1 methyltransferase in yeast. J. Biol. Chem. 281, 36140–36148.
Hura, G.L., Menon, A.L., Hammel, M., Rambo, R.P., Poole 2nd, F.L., Tsutakawa, S.E., Jenney Jr., F.E., Classen, S., Frankel, K.A., Hopkins, R.C., Yang, S.J., Scott, J.W., Dillard, B.D., Adams, M.W., Tainer, J.A., 2009. Robust, high-throughput solution structural analyses by small angle X-ray scattering (SAXS). Nat. Methods 6, 606–612.
Johnson, B.A., Blevins, R.A., 1994. NMRView: a computer program for the visualization and analysis of NMR data. J. Biomol. NMR 6, 603–614.
Katinka, M.D., Duprat, S., Cornillot, E., Metenier, G., Thomarat, F., Prensier, G., Barbe, V., Peyretaillade, E., Brottier, P., Wincker, P., Delbac, F., El Alaoui, H., Peyret, P., Saurin, W., Gouy, M., Weissenbach, J., Vivares, C.P., 2001. Genome sequence and gene compaction of the eukaryote parasite *Encephalitozoon cuniculi*. Nature 414, 450–453.
Kisseleva-Romanova, E., Lopreiato, R., Baudin-Baillieu, A., Rousselle, J.C., Ilan, L., Hofmann, K., Namane, A., Mann, C., Libri, D., 2006. Yeast homolog of a cancer-testis antigen defines a new transcription complex. EMBO J. 25, 3576–3585.
Kobayashi, K., Kikuno, I., Kuroha, K., Saito, K., Ito, K., Ishitani, R., Inada, T., Nureki, O., 2010. Structural basis for mRNA surveillance by archaeal Pelota and GTP-bound EF1alpha complex. Proc. Natl. Acad. Sci. USA 107, 17575–17579.
Krogan, N.J., Cagney, G., Yu, H., Zhong, G., Guo, X., Ignatchenko, A., Li, J., Pu, S., Datta, N., Tikuisis, A.P., Punna, T., Peregrin-Alvarez, J.M., Shales, M., Zhang, X., Davey, M., Robinson, M.D., Paccanaro, A., Bray, J.E., Sheung, A., Beattie, B., Richards, D.P., Canadien, V., Lalev, A., Mena, F., Wong, P., Starostine, A., Canete, M.M., Vlasblom, J., Wu, S., Orsi, C., Collins, S.R., Chandran, S., Haw, R., Rilstone, J.J., Gandi, K., Thompson, N.J., Musso, G., St Onge, P., Ghanny, S., Lam, M.H., Butland, G., Altaf-Ul, A.M., Kanaya, S., Shilatifard, A., O'Shea, E., Weissman, J.S., Ingles, C.J., Hughes, T.R., Parkinson, J., Gerstein, M., Wodak, S.J., Emili, A., Greenblatt, J.F., 2006. Global landscape of protein complexes in the yeast *Saccharomyces cerevisiae*. Nature 440, 637–643.
Lee, H.H., Kim, Y.S., Kim, K.H., Heo, I., Kim, S.K., Kim, O., Kim, H.K., Yoon, J.Y., Kim, H.S., Kim, J., do, J., Lee, S.J., Yoon, H.J., Kim, S.J., Lee, B.G., Song, H.K., Kim, V.N., Park, Suh, S.W., 2007. Structural and functional insights into Dom34, a key component of no-go mRNA decay. Mol. Cell. 27, 938–950.
Leulliot, N., Chaillet, M., Durand, D., Ulryck, N., Blondeau, K., van Tilbeurgh, H., 2008. Structure of the yeast tRNA m7G methylation complex. Structure 16, 52–61.
Liger D., Mora L., Lazar N., Figaro S., Henri J., Scrima N., Buckingham R.H., van Tilbeurgh H., Heurgue-Hamard V., Graille M., 2011. Mechanism of activation of methyltransferases involved in translation by the Trm112 'hub' protein. Nucleic Acids Res, in press.
Lopreiato, R., Facchin, S., Sartori, G., Arrigoni, G., Casonato, S., Ruzzene, M., Pinna, L.A., Carignani, G., 2004. Analysis of the interaction between piD261/Bud32, an evolutionarily conserved protein kinase of *Saccharomyces cerevisiae*, and the Grx4 glutaredoxin. Biochem. J. 377, 395–405.
Madl, T., Gabel, F., Sattler, M., 2011. NMR and small-angle scattering-based structural analysis of protein complexes in solution. J Struct Biol 173, 472–482.
Mao, D.Y., Neculai, D., Downey, M., Orlicky, S., Haffani, Y.Z., Ceccarelli, D.F., Ho, J.S., Szilard, R.K., Zhang, W., Ho, C.S., Wan, L., Fares, C., Rumpel, S., Kurinov, I., Arrowsmith, C.H., Durocher, D., Sicheri, F., 2008. Atomic structure of the KEOPS complex: an ancient protein kinase-containing molecular machine. Mol. Cell. 32, 259–275.
Matsumoto, K., Toyooka, T., Tomikawa, C., Ochi, A., Takano, Y., Takayanagi, N., Endo, Y., Hori, H., 2007. RNA recognition mechanism of eukaryote tRNA (m7G46) methyltransferase (Trm8-Trm82 complex). FEBS Lett. 581, 1599–1604.
Mazauric, M.H., Dirick, L., Purushothaman, S.K., Bjork, G.R., Lapeyre, B., 2010. Trm112p is a 15-kDa zinc finger protein essential for the activity of two tRNA and one protein methyltransferases in yeast. J. Biol. Chem. 285, 18505–18515.
Perutz, M.F., Rossmann, M.G., Cullis, A.F., Muirhead, H., Will, G., North, A.C., 1960. Structure of haemoglobin: a three-dimensional Fourier synthesis at 5.5-A. resolution, obtained by X-ray analysis. Nature 185, 416–422.
Petoukhov, M.V., Svergun, D.I., 2005. Global rigid body modeling of macromolecular complexes against small-angle scattering data. Biophys. J. 89, 1237–1250.
Petoukhov, M.V., Konarev, P.V., Kikhney, A.G., Svergun, D.I., 2007. TSAS 2.1 - towards automated and web-supported small-angle scattering data analysis. J. Appl. J. Appl. Cryst. 40, s223–s228.
Puig, O., Caspary, F., Rigaut, G., Rutz, B., Bouveret, E., Bragado-Nilsson, E., Wilm, M., Seraphin, B., 2001. The tandem affinity purification (TAP) method: a general procedure of protein complex purification. Methods 24, 218–229.
Purushothaman, S.K., Bujnicki, J.M., Grosjean, H., Lapeyre, B., 2005. Trm11p and Trm112p are both required for the formation of 2-methylguanosine at position 10 in yeast tRNA. Mol. Cell. Biol. 25, 4359–4370.
Quevillon-Cheruel, S., Leulliot, N., Muniz, C.A., Vincent, M., Gallay, J., Argentini, M., Cornu, D., Boccard, F., Lemaitre, B., van Tilbeurgh, H., 2009. Evf, a virulence factor produced by the Drosophila pathogen *Erwinia carotovora*, is an S-palmitoylated protein with a new fold that binds to lipid vesicles. J. Biol. Chem. 284, 3552–3562.
Rigaut, G., Shevchenko, A., Rutz, B., Wilm, M., Mann, M., Seraphin, B., 1999. A generic protein purification method for protein complex characterization and proteome exploration. Nat. Biotechnol. 17, 1030–1032.
Robinson, C.V., Sali, A., Baumeister, W., 2007. The molecular sociology of the cell. Nature 450, 973–982.
Sattler, M., Schleucher, J., Griesinge, r.C., 1999. Heteronuclear multidimensional NMR experiments for the structure determination of proteins in solution employing pulsed field gradients. Prog. NMR Spectrosc. 34, 93–158.
Senisterra, G.A., Finerty Jr., P.J., 2009. High throughput methods of assessing protein stability and aggregation. Mol. Biosyst. 5, 217–223.
Simon, B., Madl, T., Mackereth, C.D., Nilges, M., Sattler, M., 2010. An efficient protocol for NMR-spectroscopy-based structure determination of protein complexes in solution. Angew. Chem. Int. Ed. Engl. 49, 1967–1970.
Soding, J., Biegert, A., Lupas, A.N., 2005. The HHpred interactive server for protein homology detection and structure prediction. Nucleic Acids Res. 33, W244–8.
Stevens, R.C., Yokoyama, S., Wilson, I.A., 2001. Global efforts in structural genomics. Science 294, 89–92.
Studier, F.W., 2005. Protein production by auto-induction in high density shaking cultures. Protein Expr. Purif. 41, 207–234.
Studte, P., Zink, S., Jablonowski, D., Bar, C., von der Haar, T., Tuite, M.F., Schaffrath, R., 2008. TRNA and protein methylase complexes mediate zymocin toxicity in yeast. Mol. Microbiol. 69, 1266–1277.
Trowitzsch, S., Weber, G., Luhrmann, R., Wahl, M.C., 2008. An unusual RNA recognition motif acts as a scaffold for multiple proteins in the pre-mRNA retention and splicing complex. J. Biol. Chem. 283, 32317–32327.
Trowitzsch, S., Weber, G., Luhrmann, R., Wahl, M.C., 2009. Crystal structure of the Prn11p subunit of the yeast precursor mRNA retention and splicing complex. J. Mol. Biol. 385, 531–541.
van den Elzen, A.M., Henri, J., Lazar, N., Gas, M.E., Durand, D., Lacroute, F., Nicaise, M., van Tilbeurgh, H., Seraphin, B., Graille, M., 2010. Dissection of Dom34-Hbs1 reveals independent functions in two RNA quality control pathways. Nat. Struct. Mol. Biol. 17, 1446–1452.
Wernimont, A., Edwards, A., 2009. In situ proteolysis to generate crystals for structure determination: an update. PLoS ONE 4, e5094.
Wimberly, B.T., Brodersen, D.E., Clemons Jr., W.M., Morgan-Warren, R.J., Carter, A.P., Vonrhein, C., Hartsch, T., Ramakrishnan, V., 2000. Structure of the 30S ribosomal subunit. Nature 407, 327–339.
Yusupov, M.M., Yusupova, G.Z., Baucom, A., Lieberman, K., Earnest, T.N., Cate, J.H., Noller, H.F., 2001. Crystal structure of the ribosome at 5.5 A resolution. Science 292, 883–896.

Antonia VAN DEN ELZEN

Étude du complexe Dom34-Hbs1 ressemblant aux facteurs de terminaison: analyse fonctionnelle de ses rôles dans le contrôle qualité des ARN et dans la stimulation de la traduction par dissociation des ribosomes inactifs.

Résumé

Après un cycle de la production des protéines, les sous-unités des ribosomes terminés sont dissociés, afin de les rendre disponibles pour de nouveaux cycles de traduction. Si lors de la traduction le ribosome pause, il ne pourra pas terminer la traduction et être recyclé par la voie classique. Un mécanisme de recyclage alternatif a évolué pour dissocier de tels ribosomes arrêtés. Un complexe composé des facteurs Dom34 et Hbs1 induit leur dissociation. Ce complexe est aussi impliqué dans des voies de contrôle qualité qui ciblent des ARN qui causent des arrêts ribosomiques. Dans cette thèse, l'importance de plusieurs sites fonctionnels du complexe Dom34-Hbs1 pour ces voies contrôle qualité des ARNs est étudiée. De plus, la relation entre ces voies et leurs détails sont examiné. Finalement, un nouveau rôle de Dom34-Hbs1, en dissociant des ribosomes inactifs ce qui rend leurs sous-unités disponibles pour de nouveaux cycles de la traduction, est décrit.

Résumé en anglais

Protein production is a cyclic process that consists of four stages: initiation, elongation, termination and recycling. During recycling the subunits of terminated ribosomes are dissociated, to make them available for new rounds of translation. If ribosomes stall during translation, ribosomes cannot terminate properly and canonical recycling cannot occur. Cells have mechanisms to rescue these stalled ribosomes. A complex formed by the factors Dom34 and Hbs1 induces their dissociation. This compex in RNA quality control, targeting RNAs that cause ribosomal stalling. In this thesis the importance of several functional sites of the Dom34-Hbs1 complex for the degradation of these RNA sis investigated. Details of and the relationship between RNA quality control pathways in which the complex functions are further investigated. Finally, a new role of this complex, dissociating inactive ribosomes and thereby making their subunits available to re-enter the translation cycle is described.